Institute of Nutritional Science

Department of Food Science

Justus Liebig University Giessen, Germany

Development and comparison of standardized bacterial metabolite profiles
by hyphenated planar chromatography
for characterization of feed additives and probiotic feeds

Cumulative dissertation

for the degree of

***Doctor rerum naturalium* (*Dr. rer. nat.*)**

Submitted to the

Faculty of Agricultural Sciences, Nutritional Sciences,

and Environmental Management

By

Stefanie Kruse, M. Sc.

Ankum, Germany

Giessen, May 2022

Table of content

II

With permission of the Faculty of Agricultural Sciences, Ecotrophology and Environmental Management of the Justus Liebig University Giessen

Examining Committee

1st Reviewer	Prof. Dr. Gertrud Morlock
2nd Reviewer	Prof. Dr. Rolf-Alexander Düring
3rd Examiner	Prof. Dr. Wolfgang Schwack
3rd Examiner	Prof. Dr. Sylvia Schnell

IV

Declaration

I declare: this dissertation submitted is a work of my own, written without any illegitimate help by any third party and only with materials indicated in the dissertation. I have indicated in the text where I have used texts from already published sources, either word for word or in substance, and where I have made statements based on oral information given to me. At any time during the investigations carried out by me and described in the dissertation, I followed the principles of good scientific practice as defined in the "Justus Liebig University Giessen Statute for Ensuring Good Scientific Practice".

Giessen, May 2022

Stefanie Kruse

Acknowledgments

My special thanks go to Prof. Dr. Gertrud Morlock, who gave me the opportunity to do my doctorate in her research group. She always supported me in my project and I could always rely on her. Thank you very much for the nice and instructive time.

Furthermore, I would like to thank Prof. Dr. Alexander Düring for taking over the second review.

Next, I would like to thank Tamara Schreiner, Annabel Mehl, Alisa Ronzheimer, and Isabel Müller. Thank you for always being there for me. I couldn't have asked for better colleagues.

Julia Heil and Simone Cutts, you are really the good soul of the working group. Without you, something would simply be missing. Thank you for your support.

Also, I would like to thank my primary school teacher Mrs. Kempgens. I know that you have certainly contributed a lot to me getting this far.

Last but not least, I would like to thank my parents, my partner Jonas Kethorn and my best friend Sarah Gründing for their support during my studies and my PhD.

VIII

Scientific contributions

Peer-reviewed original research papers

1) Kruse, S., Pierre, F., Morlock, G. E., *J. Chromatogr. A* 2021, 1640, 461929
   Imaging high-performance thin-layer chromatography as powerful tool to visualize metabolite profiles of eight *Bacillus* candidates upon cultivation and growth behavior

2) Kruse, S., Pierre, F., Morlock, G. E., *J. Agric. Food Chem.* 2021, 69, 11272-11281
   Effects of the Probiotic Activity of *Bacillus subtilis* DSM 29784 in Cultures and Feeding Stuff

3) Kruse, S., Becker, S., Pierre, F., Morlock, G. E., 2022 — Submitted to *Anal. Bioanal. Chem.* 2022
   Metabolic profiling of bacterial co-cultures linked to predominant species identification

4) Kruse, S., Schenk, M., Pierre, F., Morlock, G. E., *Anal. Chim. Acta.* 2022 — in revision
   Bacillus subtilis spores in probiotic feed quantified via bacterial metabolite using planar chromatography

5) Kruse, S., Becker, S., Pierre, F., Morlock, G. E., 2022 — Submitted to *J. Chromatogr. A* 2022
   Strain-specific quantification of probiotic *Bacillus subtilis* DSM 29784 in feed by imaging high-performance thin-layer chromatography

X

List of figures

1. Introduction

1.1. Discovery of probiotic microorganisms

In 1908, Ilja Iljitsch Metschnikoff established the basis for the development of probiotics. He discovered the beneficial effect of lactic acid bacteria in fermented dairy products, such as yogurt, on the intestinal microbiome leading to gut heath and longer life [1]. In 1953, the term probiotic was published the first time by Werner Kollath. Probiotics were described as "active substances that are essential for a healthy development of life" [2]. In 1965, Lilly and Stillwell adopted this term to describe them as growth-promoting factors [3]. In the following decades, the definition of the term was regularly changed (Table 1), until 2002, when the Food and Agriculture Organization of the United Nations (FAO) and the World Health Organisation (WHO) classified probiotics as "live microorganisms which, when administered in adequate amounts, confer a health benefit on the host" [4]. Up to now, this classification is the most common used definition in the world.

Table 1 Definitions of probiotics over time.[5]

Author/Year	Definition
Lilly and Stillwell/ 1965	A substance secreted by one microorganism which stimulates the growth of another.[3]
Fuller/1989	Live microbial feed supplement which beneficially affects the host animal by improving microbial balance.[6]
Huis Veld and Havenaar/1991	mono- or mixed culture of live microorganisms which, applied to animals or human, affects beneficially the host by improving the properties of the indigenous microflora.[7]
Guarner and Schaafsma/1998	Living microorganisms which, upon ingestion in certain numbers, exert health benefits beyond inherent basic nutrition.[8]
Naidu, Bidlack and Clemens/1999	A microbial dietary adjuvant that beneficially affects the host physiology by modulating mucosal and systemic immunity, as well as improving nutritional and microbial balance in the intestinal tract.[9]
Schrezenmeir and de Vrese/2001	A preparation of or a product containing viable, defined microorganisms in sufficient numbers, which alter the microflora (by implantation or colonization) in a compartment of the host and by that exert beneficial health effect in this host.[10]
FAO and WHO/2002	live microorganisms which, when administered in adequate amounts, confer a health benefit on the host.[4]

INTRODUCTION

The use of probiotics in the food industry was introduced by the discoveries of Numri and Rantala in 1971. Several Finnish broiler flocks were affected by *Salmonella infantis* infection. The infection caused economic losses to the farmers, and in a few cases, the disease was transmitted to humans, causing adverse health effects. Nurmi and Rantala used the probiotic knowledge to produce effective resistance to *Salmonella* infection in hatched chicks. The gut microbiome of adult birds was inoculated into the young chicks, which led to the protection of the animals.[11] Thus, since this application, the use of probiotics has increased. To date, bacterial species of the genus *Bacillus* [12], *Streptococcus* [13], *Lactobacillus* [14], and *Enterococcus* as well as yeasts are the most commonly used probiotics.[15, 16]

1.2. Launch of probiotics in poultry industry

The application of probiotic microorganisms in poultry started with the discoveries of Nurmi and Rantala. In 1970, the European Union enacted a strict regulation about the use of feed additives (70/524/EC) [17] but the administration of probiotics was not covered by this regulation. Thus, a large number of probiotic solutions were introduced to the market, resulting in uncontrolled application of probiotics in animals. The microorganisms were administered in different concentrations, as a simple or a complex mixture, as tablets, or as powders but the probiotic efficiency was never statistically and scientifically studied. As a result, no significant probiotic effect was described in the literature, and researchers, nutritionists, and farmers rejected the probiotic theory. Therefore, the sale of probiotics in the food industry declined in the early 1990s. During the same period, the public confidence in the farming system was undermined in the European Union by a series of food safety crises such as bovine spongiform encephalitis (better known as BSE) [18], dioxin contamination [19] and hormone-laced animal feeds. The entire product chain, from animal production to consumption, needed to be revised. In 1997, the National Advisory Committee on Microbiological Criteria for Foods enacted a revision of the Hazard Analysis and Critical Control Point Systems (HACCP) [20] to provide a standardized procedure for analyzing all hazards and verifying all critical points throughout the whole production chain. Additionally, the European Food Safety Authority (EFSA) was founded in 2002 as a control measurement for food and feed safety, nutrition safety, animal health and welfare, plant protection and plant health. The first official task of the EFSA was to revise the regulations (70/524/EC) [17] from

1970. The improved regulations were enacted in the regulation 1831/2003/EC to provide the basis for the protection of human health, animal health and welfare, the environment, and user and consumer interests in relation to feed additives, which included the ban of antibiotic growth promoters (AGP) in 2006.[21] AGP are known to improve animal growth and feed conversion ratios (FCR), as well as reduce animal morbidity and mortality, but researchers have linked the increasing resistance of antibiotics in humans to the application of AGP.[22, 23] Probiotics research has increased due to the need for an effective alternative to AGP. The regulation 1831/2003/EC introduced further control measurement *i.e.* detailed rules for the application (429/2008/EC) [24] and compliance with the feed and food law and the animal health and animal welfare rules (882/2004/EC) [25]. In addition to these legal requirements, probiotic microorganisms must meet further requirements that ensure probiotic activity after the feed manufacturing process. These requirements can be classified into three different areas and are listed in Table 2.

Table 2 Requirements for probiotic microorganism.[26–28]

Safety	Functionality	Technological convenience
1. Animal origin 2. Isolation from the gastrointestinal tract of healthy individuals 3. Bile salt hydrolase 4. Absence of genes responsible for antibiotic resistance is localized in non-stable elements 5. Antimicrobial and antagonism activity against potentially pathogenic bacteria 6. Resistance against digestive enzymes and lysozyme	1. Ability to survive in the host and maintain the metabolic activity 2. Resistance to bile salts and enzymes 3. Adherence to mucus 4. Competitiveness in respect to microbial species inhabiting the intestinal ecosystem (including closely related species). 5. Ability to grow within the host organism, and survive in the gastrointestinal system.	1. Genetic stability 2. High storage survival rate in finished products 3. Resistance to bacteriophages 4. Viability and stability of the desired properties of probiotic bacteria during the production process

INTRODUCTION

1.3. Probiotics, prebiotics and synbiotics

Probiotics are classified as "live microorganisms which could confer a beneficial health status on the host"[4]. Just as the definition of probiotics, the definition of prebiotics has also changed over the years [5], but in 2008, the FAO defined prebiotics as "non-viable food components that confer a health benefit on the host associated with modulation of the microbiota" [29]. Prebiotics and probiotics are applied to balance the gut microflora and improve the health status of the host. [27] Mostly, prebiotics are used as an alternative to probiotics or in combination with them, whereby the combined application is described as synbiotics. The mode of action of prebiotics and probiotics is different. Probiotics, such as direct-fed microbials (DFM) of the genus *Bacillus*, *Streptococcus*, *Lactobacillus*, and *Enterococcus* as well as yeasts, could stabilize the gut microbiota and modulate the host immune system. Contrarily, prebiotics, mostly carbohydrates, are intended to influence the existing microbiome [30] to improve mineral absorption and enhance immune functions to support the microflora in the gut [31]. In synbiotics, prebiotics supports the survival and growth of probiotics [32], but the use of both is challenging. The beneficial effect for each individuum depends on the strain (for probiotics) and the dose (for both).[33–35] In several trial studies, the dependency of the doses [36] as well as the performance of the combination [37, 38] were tested.

1.4. Application of probiotics in poultry industry

Selection of the optimal probiotic strain requires an intensive screening process, including evaluation of all regulated requirements (Safety, Functionality, and Technological Convenience; Table 2). Adisseo and Novozymes designed a specified probiotic solution for the poultry industry and announced its launch in 2016. The selection process will be described based on this probiotic solution.
Novozymes has one of the largest microbial strain collection in the world. Over 900 potential probiotic candidates were considered for the strain screening. All candidates underwent the safety requirements to follow the main important aspects of the regulation 1831/2003/EC [21]. Microorganisms, which are potentially pathogenic, had antibiotic resistance genes or could be digested by enzymes were excluded. All safety aspects of the selected probiotic were documented.[39] The next step in the screening process was the testing of robustness. All candidates, which were stable in the gut and during the feed manufacturing met the

4

requirements and were selected for the performance test. Initially, *in vitro* tests were performed. Probiotic bacteria of the genus *Bacillus* have the advantage to sporulate. Spores are robust to high temperature, pressure, acidic pH or toxic chemicals and survive both production and intestinal processes, allowing for long storage [40]. Subsequently, the performance was tested *in vivo*. These tests included the activity of the microorganisms in the small intestine, like the germination process and gut health. The last aspect was the testing of the selected strains in *in vivo* trials. Health, body weight gain (BWG), and FCR were the most interesting aspects. The candidate with the best consistency and conviction in these aspects was selected as the probiotic (Figure 1).
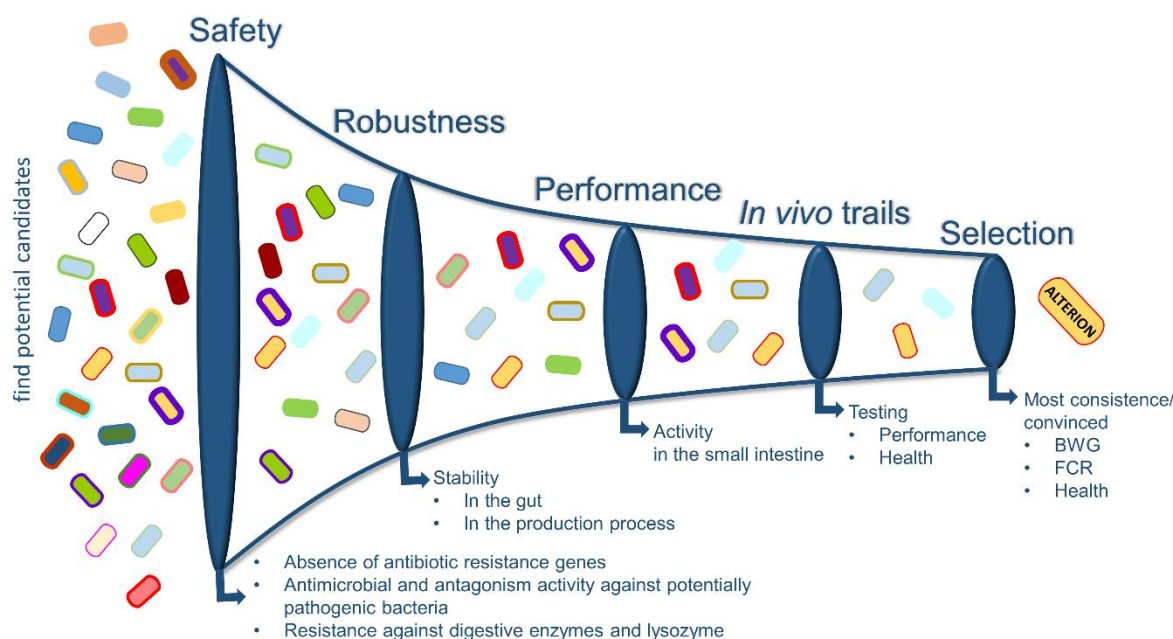
Figure 1 Selection process for the probiotic ALTERION®.

Bacillus subtilis der Deutschen Sammlung für Mikroorganismen und Zellkulturen (DSM) 29784 (*B. s.* 29784) was the finally selected strain (commercial name ALTERION®). Species of the genus *Bacillus* are mostly non-pathogenic Gram-positive firmicutes. The rod-shaped *B. s.* bacteria (about 2–3 µm long and 0.6 µm wide) has its natural habitat in the upper soil layers as well as in the rhizosphere, where it is exposed to varying nutrient supplies.[41] Normally, aerobic conditions were required for cell growth, but an anaerobic growth behavior is possible in presence of nitrate and glucose as nitrogen, carbon, or energy sources. Furthermore, *B. s.* has become a model organism in biochemistry, genetics, medicine, food and feed industry.[42] However, other species of the genus *Bacillus* were also important for the industrial sector *e.g. B. licheniformes,*

B. amyloliquefaciens, or *B. pumilus*. The production of enzymes (like α-amylases) [43], antibiotics (like surfactin) [44], fine biochemicals (like hypoxanthine) [45], or insecticides (like endotoxins) [42] defines the industrial importance of the different *Bacilli*. Additionally, the complete screening of the genome, the robust growth behavior and the heat resistance are important aspects for industrial use.[41] The selected probiotic *B. s.* 29784 was isolated from the soil and has not been genetically modified. The genome is also already known and the microorganism is registered (DSM 29784).

The safety, robustness, and performance tests were completed. To ensure that comprehensive germination of the spores in the intestine occurs, the germination process of the selected probiotic was analyzed in more detail. Performance was compared to other *Bacilli* and to potential variations in presence of different gut-like conditions and feed ingredients. The benefit of the probiotic *B. s.* 29784 was confirmed by faster germination compared to other *Bacilli.* Additionally, an influence of feed ingredients (filtered corn, soybean and wheat feed) was not detected.[46] However, the main requirement is germination in the gut of broiler chicks. To visualize this process, two genes were integrated into the genome of the probiotic strain *B. s.* 29784. The first encodes a green fluorescent protein and the second a red one. Green signals indicated spores and a change to a red signal was an indicator for the germination to vegetative cells. The identification of spores or vegetative cells by these fluorescence genes was tested *in vitro* and proved by fluorescence microscopy at different time points.

Subsequently, germination was observed *in vivo*. The ileum of broilers treated with *B. s.* 29784 supplemented feed was analyzed. Red fluorescent vegetative cells were observed in the analyzed ileum samples. This observation indicates the germination of *B. s.* 29784 in the gut of these broilers (Figure 2).[46] Approval of all aspects enabled the highest probability of probiotics efficiency in broiler chicks.
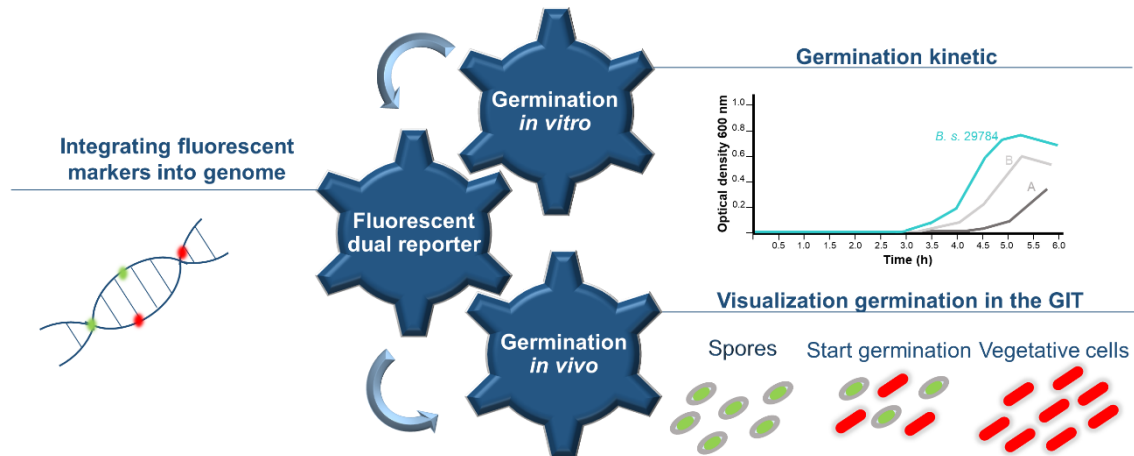
Figure 2 Comparison of germination kinetics of *B. s.* 29784 to other *Bacilli* (A, B) and the visualization of this process by two different fluorescent genes.[46]

1.4.1. *Bacilli* sporulation, germination and probiotic lifecycle

Species of the genus *Bacillus* have the important benefit of forming endospores at nutrient depletion. The soil bacterium used this process as last resort to survive changing environmental conditions, but it requires a lot of energy. This formation offers a significant advantage for industrial applications because spores are stress-resistant to temperature, pressure, pH, dryness, and toxic chemicals.[40, 47, 48] Sporulation can be divided into eight stages involving several genes and lasting up to seven hours (Figure 3).[49] In stage 0, the vegetative cells induce sporulation. The phosphorylation of a sufficient amount of the transcription factor Spo0A leads to the initiation of sporulation. In stage I the duplicated chromosomes stretch from one pole of the cell to the other (axial filamentation). The consequence is the elongation of the cell. The formation of the sporulation septum in stage II leads to an asymmetrical cell deviation, generating a forespore and a mother spore. One-third of the chromosome was present in the forespores.[49] Additionally, several sigma factors were activated to initiate the engulfment of the forespore in the mother spore.[50] The cell membrane of the mother spore grows and include the forespore so that the forespore has two membrane layers and is no longer in direct contact with the cytosol of the mother cell (stage III). The metabolic activity of the forespore is reduced.[48] In stage IV, the coat and the cortex are synthesized. The cortex is the inner shell of the spore and consists of special peptidoglycan. The main function of the two envelopes is to protect the genome, which also explains the resilience of spores.[47] The finalization and the lysis of the mother cell occur in stage V causing

the maturation of the endospore in stage VI. Stage VII is the last step in sporulation and describes the cell release of the endospore.
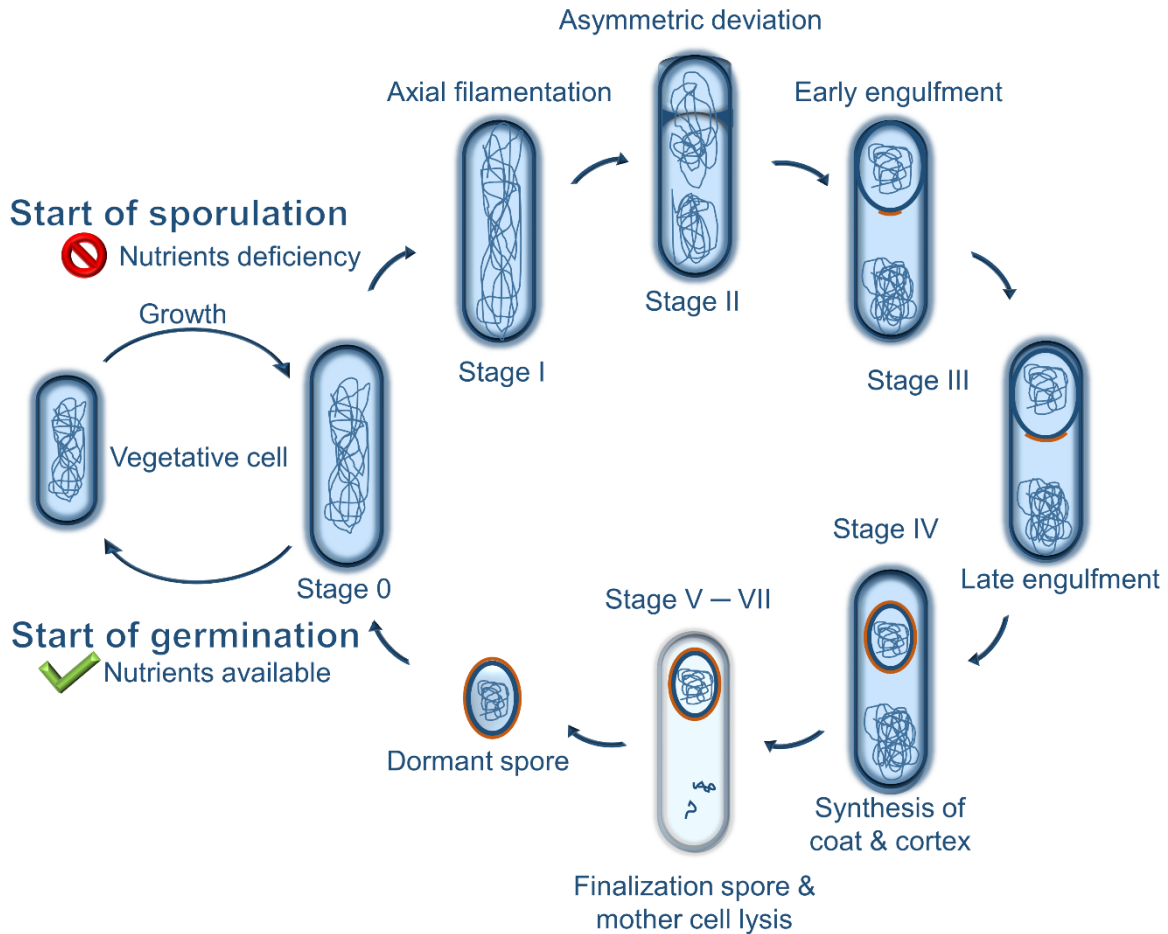

Figure 3 Stages I to VII of the sporulation process of microorganisms.

Spores are metabolically inactive, but changes in environmental conditions are sensed by germinant receptors which were embedded in the inner spore membrane.[51] The induction of germination is evoked by different agents, *e.g.*, nutrients, high pressure or dodecylamine. Several biophysical reactions were started such as the release of cations or calcium(II)dipiocolinic acid or their replacement with water (stage I of germination). The peptidoglycan cortex was hydrolyzed and subsequent hydration of the core (stage II of germination) induced enzyme activity, metabolism, and macromolecular synthesis, so that outgrowth started.[52, 53] The first cell deviation terminates the outgrowth process. The sporulation and germination processes are important benefits of probiotics from the genus *Bacillus*. The spore morphology allows the *Bacilli* to survive processing conditions such as pelleting in the production process and the low pH of the crop and stomach. However, to be metabolically active and perform positive effects in the chicken gut, the spores have to germinate fast. In the crop as well as in the

stomach the probiotics are exposed to digestive enzymes and physical stress (grinding). These conditions can trigger germination, and thus, activated spores reach the small intestine.[54, 55] In different studies, the germination of probiotic spores was also proven in the broiler crop [55], due to a variety of germination factors in the broiler gastrointestinal tract. Plate counts of gut samples, real-time quantitative polymerase chain reaction (RT-qPCR) [56], or the visualization with a fluorescent reporter gene [46] were performed to detect probiotic germinated spores in the gut. However, the intestinal physiology is slightly different in each animal [57] and may influence the germination process.

1.4.2. Commercial probiotic *B. s.* 29784

In the poultry industry, probiotics are profitably used to protect broiler chicks from pathogenic bacteria like *Salmonella enterica*, *Escherichia coli* or *Campylobacter jejuni*. The most common used probiotic bacteria are *Lactobacillus*, *Streptococcus*, *Enterococcus* and *Bacillus*.[5, 15, 16] The bacteria can be applied in different forms, *i.e.* as liquid or powder [58, 59]. The spore-forming properties of *B. s.* 29784 enabled its commercial use as feed additive. Lyophilized spores of this probiotic strain are glued onto calcium carbonate particles. For the commercial product (ALTERION® NE with 1×10^{10} colony forming units (CFU)/g; ALTERION® NE50 with 2×10^8 CFU/g), these particles were mixed with different carriers (sodium aluminosilicate, calcium carbonate and sucrose). The exact, and therefore secret, formulation of these carriers is essential for a homogeneous mixture of the active substance in the feeds. Different amounts of the commercial product are added to premixes or feeds to generate a final concentration of 1×10^8 CFU/kg in the feed. After mixing, the homogeneous feed powder is pelleted to prevent the sedimentation of constituents and to administer a homogeneous ratio of all ingredients to the animal. The spores of *B. s.* 29784 survive the high pelleting temperature up to 90 °C [60] and the high pressure up to 552 kPa [61] so that a high recovery of spores is present in the feed.

1.4.3. Characterization and enumeration of *B. s.* 29784 in feeds

Identification and detection of the microorganism in feeds or feed additives is a requirement for the launch of any probiotic.[21, 24] These requirements were followed for the probiotic *B. s.* 29784, and the approval in Europe was received in

2018.[62] Taxonomical identification was based on the analysis of 16S ribosomal ribonucleic acid (rRNA) genes by PCR and confirmed by the sequencing of the gyrB gene.[39] The genetic stability and identification of the microorganism were performed by pulsed-field gel electrophoresis (PFGE) [63]. The advantage over conventional gel electrophoresis is the significantly better resolution of deoxyribonucleic acid (DNA) fragments up to 10 Mb. The principles of normal gel electrophoresis are as follows. Molecules are moved through an agarose gel, which is placed in an electric field. The different negatively charged samples are located at the negatively charged start and passed through the gel to the positively charged end. The DNA fragments are separated, based on their different size and charge. Larger fragments are moving more slowly compared to the smaller ones. But direct genomic analysis requires large DNA fragments, which are not separated in normal gel electrophoresis.

In PFGE, the electrical field is periodically pulsed. The molecules have to reorient in a permanently changing electric field. The complete orientation depends on the size of the molecules and the time of the pulse.[64] Therefore, the pulsed field enabled the separation of larger DNA fragments. Different applications of the PFGE exist, such as field inversion gel electrophoresis, transverse alternative field electrophoresis, contour-clamped homogenous electric field, and rotation gel electrophoresis. [65] This PFGE identification method for *B. s.* 29784 was evaluated by the European Committee for Standardization (CEN) Technical Committee 327 to become a European standard.[39] The enumeration of *B. s.* 29784 is performed according to the EN 15784:2009 [66] method and is used to quantify probiotics in feed. A certain quantity of the feed is suspended in phosphate-buffered saline (PBS) and homogenized. All vegetative cells should die during the heat treatment (10 min at 80 °C). The heat-treated suspension is decimally diluted, plated on tryptic soy agar (TSA), and incubated for 16–24 h at 37 °C. The number of CFU per g is calculated from the colonies on the plate.

1.4.4. Probiotic activity of *B. s.* 29784

The probiotic activity of *B. s.* 29784 was evaluated *in vitro* and *in vivo*. The increasing growth performance of laying hens, shaver white pullets [36], broilers [67], and Tom turkeys [68] was determined in several *in vivo* trial studies. The BWG was increased by a constant or reduced feed intake, which leads to an improvement

of the FCR. Additionally, gut health has a key role in animal performance. Inflammations and digestive or gut disorders are supported by an unbalanced microbial composition. Several studies have reported the direct and indirect influence of probiotics on microbial compositions [15, 69], including under necrotic enteritis conditions [70]. *B. s.* 29784 also shows a change in the microbial composition [45, 71]. In some studies [71, 72], the content of *Firmicutes* and *Bacteroidetes* were increased by supplementing broilers with *B. s.* 29784, but in another study, the content of *Bacteroidetes* had decreased and only the content of Firmicutes increased [73]. In several human [74] and animal [75] studies, the influence of the *Firmicutes*/*Bacteroidetes* ratio on the gut was demonstrated and higher ratios were associated with fat accumulation.[76] It was assumed that lower ratios (found in lean animals/humans) indicated a better fat conversion as an energy source, however also contrary results were reported. [77] The observation of these changing results may depend on the age of the animals, antibiotic conditions, physical activity, environmental conditions, and all conditions affecting the gut microbiome [57, 78, 79] and need to be analyzed in more detail. However, an unbalanced ratio can lead to microbial dysbiosis and is individual for each animal/human. The probiotic treatment can balance the gut microbiota, which is important for maintaining health.[27, 80] Additionally, the increase of *Firmicutes* corresponds to the detection of higher butyrate concentrations in the animals.[45, 70, 71, 73] These metabolites are known for a positive effect on the host microbiome and may explain the improvement in growth performance after the application of *B. s.* 29784. Butyrate and its derivates are known as a primary energy source for enterocytes [81], as a mediator for gene expression or cellular differentiation processes [82], and lead to prolonged microvilli [73]. Furthermore, conjugated linoleic acid, known for its anti-inflammatory properties [83], was found in higher concentrations in animals treated with the probiotic [73]. *In vivo* and *in vitro* production of nicotinic acid and hypoxanthine were also reported as beneficial effects of *B. s.* 29784.[45] Nicotinic acid (vitamin B3) is an essential nutrient in animal nutrition that is associated with anti-inflammatory properties and is an important precursor of several coenzymes.[84] Anti-inflammatory effects were also reported by *Rhayat et al.*[85]. Hypoxanthine is a degradation product of adenosine nucleotide and is known to promote intestinal barrier functions [86] and reduce

antioxidative stress. The anti-oxidative capacity was also reported for *B. s.* 29784.[72]

The different studies highlighted the positive effects of probiotic *B. s.* 29784. All these aspects are indications of the mechanism of the selected probiotic, but in some cases, contrary observations were reported. This is related to the poor data situation of the studies or the fact that the results could be influenced by the circumstances of the animals or environmental conditions. For a better understanding of the probiotic effect, *B. s.* 29784 should be analyzed in more detail.

1.5. High-performance thin-layer chromatography

High-performance thin-layer chromatography (HPTLC) is an enhancement of the well-known thin-layer chromatography (TLC). More powerful adsorbents with reduced particle sizes of predominantly 5–7 µm, a narrower particle size distribution and the development of automated instrumental technology are the major improvements.[87] Compared to other chromatographic separation techniques, HPTLC offers the following advantages. Sample preparation can be reduced because matrix substances usually remain on the starting zone or are eluated to the solvent front and do not interfere with the analytes. Simultaneous analysis of different samples side-by-side for comparison under the same analytical conditions can be performed and all results are presented in one image. A visualization at white light, UV 254 nm, and FLD 366 nm as well as densitometric measurements of fluorescence, absorption (200–800 nm), and the recording of UV spectra are possible. For the detection of unknown substances, post-chromatographic derivatization could be performed using universal or specific reagents. These derivatization reagents can be applied via dipping, spraying, or vaporizing. Several chemical reagents for the detection of *e.g.* sugars (diphenylamine aniline phosphoric acid reagent), peptides (ninhydrin reagent), lipopeptides (primulin reagent), or natural products (anisaldehyde sulfuric acid reagent) are possible. Functional groups of the separated analytes are modified by the used reagent and converted into a detectable substance. Additionally, effect-directed analysis (EDA) [88] is an important detection strategy and represents the *in situ* detection of microchemical (antioxidant activity), biochemical (enzymatic inhibition/ induction) or biological active (bioassays) compounds. Quantitative evaluation is possible via densitometry [89, 90], digital image evaluation [91, 92] and mass spectrometry [93, 94]. In

addition, HPTLC is compatible with nuclear magnetic resonance (NMR) [95, 96] spectroscopy for further characterization of analytes.

1.6. Scope

Probiotics are getting more and more attention in the feed and food-producing industry, due to the European ban of AGP in 2006. Bacteria of the genus *Bacillus*, *Lactobacillus, Enterococcus,* or *Streptococcus* are commonly used as probiotics, but their positive action is not fully understood. However recent results suggest that specific metabolites are responsible for the host health benefit.

New analytical methods are needed to compare the metabolic profile of probiotic microorganisms with genetically very similar bacteria and to identify specific metabolites in the probiotic. The aim of this study is to develop a new HPTLC method with an upstream cultivation process of a probiotic bacterium and genetically similar bacteria leading to a better understanding of the probiotic effect. The supernatant or liquid extract of the supernatant will be analyzed by HPTLC. This chromatographic method offers the advantage that the metabolic profiles of different bacteria can be compared directly side-by-side on the same chromatogram. Hyphenation of HPTLC and EDA should allow the direct attribution of probiotic relevant activities to the metabolites produced, leading to a better understanding of probiotic action. Furthermore, compared to axenic bacterial cultures, co-cultures should be used to analyze the influence of bacterial interactions on the metabolic profile of the probiotic.

Following, the newly established HPTLC method will be used to quantify probiotic active spores in feeds. Up to now, cell counting has been commonly used for the determination of probiotics in feeds, but this non-specific method leads to high result deviations. For more precise and accurate quality control, HPTLC with upstream cultivation of spore-containing standard solutions should be used to quantify the added amount of probiotic active cells in the feed due to the production of metabolites of the cells themselves.

1.7. Progress achieved by imaging HPTLC

The results of the study are presented in the following sections. A new HPTLC method with an upstream cultivation process was developed to study the metabolic profile of probiotic bacteria compared to genetically similar bacteria. The new method was used to draw conclusions about the probiotic activity and to determine the influence of co-cultures on the metabolic profiles. Furthermore, the method was optimized to quantify probiotically active cells in feed based on a metabolite produced by the probiotic cells.

1.7.1. Metabolic profiles of genetical similar bacteria (Publication I)

The increasing interest in bacteria of the genus *Bacillus* is due to their presumed probiotic effect. Probiotic activity is not fully understood but it is assumed that metabolites may cause these effects.[45] Several metabolites, such as cyclic lipopeptides [97, 98] produced by most *Bacillus* species, are known to have beneficial effects, but to the best of our knowledge, the metabolite profiles of different *Bacillus* species have not yet been characterized or compared to each other. Some species have a probiotic effect, while other species of the same genus indicate no positive response. For a better understanding of these differences, the metabolite profile of the probiotic *B. s.* 29784 should be compared to other genetically similar *Bacilli*. Imaging HPTLC with upstreamed cultivation visualized the differences in metabolite profiles of multiple *Bacillus* species under the same analytical conditions.[99] The intra- and inter-species comparison of different *Bacillus* species (*B. subtilis*, *B. licheniformis*, *B. pumilus,* and *B. amyloliquefaciens*) and of *B. s.* strains with high genetic similarity (98.4–99.5%) is possible with the developed imaging technique. Small differences between the selected candidates were visible, but the results showed the significant influence of cultivation conditions such as nutrient supply, temperature, and oxygen level on the individual metabolite profile. This visualization allowed us to see the influence of cultivation conditions on the metabolic profile of the different species and thus on the probiotic effect. It was demonstrated that some candidates adapted better to harsher cultivation conditions (less nutrient and oxygen content), compared to the other *Bacilli.* Adaptation to harsh cultivation conditions is important for the selection of probiotic bacteria, as the probiotic is exposed to harsh conditions in the intestine of the animals and can thus influence the production of metabolites. Additionally, imaging HPTLC allowed an

analysis of the cultivation conditions required for the production of specific metabolites. For the application of probiotics, these results indicated the importance of constant conditions to ensure a positive and harmless application of probiotic bacteria in the animal gut. For a non-target comparison of metabolite profiles between the selected candidates, the direct use of culture supernatants for the HPTLC method is the best choice, but matrix-rich culture media could suppress the detection of secondary metabolites. Therefore, during the development of the method, different measures were evaluated to reduce the matrix content of the supernatant, *e.g.*, different solvents were tested for liquid extraction depending on the metabolites analyzed. In conclusion, the application of imaging HPTLC as a beneficial visualization technique for an intra- and inter-species comparison of metabolite profiles at different cultivation conditions, for optimization of nutrients consumption, and as quality control in cultivation processes, was established.[99]

1.7.2. Effects of the probiotic activity detected (Publication II)

Imaging HPTLC was used as a stronge feature to visualize metabolite patterns depending on cultivation conditions.[99] Subsequently, multi-imaging and the hyphenation of this technique to EDA were used to improve the understanding of the probiotic action by comparing the metabolic profile of the probiotic *B. s.* 29784 with seven other bacteria of the genus *Bacillus*. To characterize the probiotic activity, the different *Bacillus* candidates were screened for lipopeptides, antioxidants, antimicrobials, and estrogenic or androgenic substances. Furthermore, the metabolic profile of pure cell cultures was compared with the profile of a cultured feed sample (including spores of the probiotic) which should support the explanation of the probiotic effect of *B. s.* 29784.[100]

Lipopeptides

Lipopeptides (such as surfactin, iturin and fengycin) are produced from a wide range of *Bacillus* microorganisms. Beneficial effects like antifungal, antimicrobial, and surface-active properties were attributed to these non-ribosomal peptides.[101, 102] The produced amount of the biosurfactants in probiotic active microorganism was compared to that of other *Bacilli*. Imaging HPTLC enabled the detection of a faster production of surfactin in the probiotic *B. s.* 29784 compared to the other *Bacilli*. This

time-dependent production of surfactin is indicative of the benefical effect of the probiotic.

Antioxidative metabolites

Antioxidants can reduce oxidative stress[103], which is a common stress factor in poultry production. These substances have a major impact on the health status and metabolism of farm animals. Oxidative stress can impair proteins or other biological molecules, which cause structural damage or modify the functions of macromolecules.[104] Antioxidative substances donate electrons to free radicals and prevent these mechanisms.[105] A higher level of antioxidative substances and two specific antioxidants (explained by the faster growth) were detected in the probiotic strain. A two-dimensional separation technique led to the association of the antioxidants to different substance classes, like lipopeptides, glycopeptides, and glycolipopeptides. Potential oxidative stress can be minimized in the animals, which were supplemented with *B. s.* 29784, supporting their health status.

Physiologically active substances

Physiologically active substances like estradiol, progesterone and testosterone are endogenous hormones in animals. These molecules belong to the class of steroids and are the most important female and male sex hormones. These physiologically active substances could support the growth rate of farm animals [106] resulting in an increased BWG of the animals despite a constant feed intake. Imaging HPTLC indicated that bacteria were able to produce physiologically active metabolites under certain conditions. However, no estrogen or androgen-like metabolites were detected in the probiotic that could explain the increased BW of the supplemented animals.[100] The increased BWG of the animals supplemented with the *B. s.* 29784 must therefore be related to other causes, such as the production of metabolites used as essential nutrients [45].

Antimicrobial substances

Antibiotics were used in livestock to reduce the risk of infections to animals but the high use promoted the spread of antibiotic-resistant bacteria also in human health.[107] Thus, the application of antibiotics in livestock production was banned in 2006.[21] Probiotics are used as an alternative because these microorganisms can produce antimicrobial active substances, which prevent the farm animals from

infections and reduce the mortality rate. The bioautogram of the *Aliivibrio fischeri* bioassay indicated several bioactive substances in the probiotic *B. s.* 29784 but these substances were also detected in other *Bacilli*.[100] However, it has been demonstrated that the formation of these antimicrobial substances depends on the cultivation time of the active cells as well as on possible influences by the feed ingredients. Imaging HPTLC enabled to investigate these influences and improve the understanding of the probiotic effect.

Gastrointestinal digestibility

Germination of probiotic *B. s.* in the gastrointestinal tract of broiler chicks was proven in previous studies.[45, 56, 108] Vegetative cells in the gut produce metabolites, which contributed to acting beneficial for the host or are metabolized (digested) by the gastrointestinal microbiome. The metabolization of characteristic substances could also lead to beneficials. The miniaturized all-in-one nanoGIT$^{+active}$ system was developed using porcine pancreatin to simulate the human digestion system.[109] As the main digestion enzymes of the broilers intestine (trypsin, chymotrypsin, amylase, and lipase) are comparable to porcine pancreatin, nanoGIT$^{+active}$ was used to investigate the influence of digestion on the produced metabolites and the formation of potentially new analytes. A decrease of specific metabolites or the formation of new positive acting substances after digestion could contribute to the understanding of the probiotic effects of the analyzed *Bacillus*. The nanoGIT$^{+active}$ system proved that surfactin produced by *B. s.* 29784 was digested by the pancreatic enzymes. This indicated that enzymes can use surfactin as an additional nutrient for the cells. Furthermore, the produced antioxidative substances were also digested by pancreatin. Imaging HPTLC visualized the decrease of these substances and a formation of a new antioxidative metabolite after digestion [100] and thus the interaction of the digestion enzymes with antioxidants was demonstrated by comparison of digested and non-digested samples. These interactions could also take place in the gut of the animals and indicated a probiotic effect of *B. s.* 29784.

In conclusion, imaging HPTLC allows a side-by-side comparison of metabolite profiles of probiotic and non-probiotic *Bacilli* to gain a better understanding of the probiotic effect. Faster growth and the detection of higher levels of beneficial substances such as surfactin, antioxidants, and antimicrobial substances were detected. The digestibility of these substances was proven, which could have an

influence on the animals supplemented with the probiotic. Additionally, the impact of feed ingredients, and gut conditions on the probiotic cells, was demonstrated.

1.7.3. Metabolic profiling of *Bacillus* and *E. coli* co-cultures (Publication III)

In natural systems, microbes only occur in the presence of other species, so bacterial co-cultivation is becoming increasingly important. In some cases, the production of specific metabolites [110, 111] or the induction of specific effects [112, 113] is only possible, due to the interaction of different species. In the feed- and food industry, this technique has also been implemented through the application of probiotics. Probiotics (as single or as a combination of individual probiotics) can interact with the existing microbiome to generate beneficial effects for the host. Imaging HPTLC was proven as a visualization technique for screening metabolic profiles of genetically similar bacteria and therefore the method could also be used for the metabolic screening of bacterial co-cultures compared to the axenic cultures. Another major advantage of this co-culture analysis is the identification of the predominant species in the co-culture, based on the side-by-side comparison of the metabolic profiles. In conclusion, also the influence of changes in the cultivation process (temperature, rotation speed, incubation time, culture media) on the predominant species or the production of a particular metabolite in the co-cultures can be analyzed using imaging HPTLC.[114]

1.7.4. Quantification of bacterial spores in probiotic feed (Publication IV)

Quantification of probiotics in animal nutrients is challenging, due to the influence of cultivation conditions such as viable but non-culturable bacteria, the presence of other *Bacilli* with high genetic similarity, or the high matrix content of the feed. Cell counting is the most common analytical tool for counting CFU of the probiotic *Bacilli* in feeds and the requirements for the official control are described in the European standard EN 15784:2009.[66] According to this regulation, the feed was suspended in PBS, treated at 80 °C for 10 min (leading to the death of all vegetative cells), and further diluted with PBS. An aliquot was used for cultivation on tryptic soy agar plates. After incubation, the *Bacilli* colonies were counted and reported as CFU. Only plates containing more than 30 and less than 300 presumptive *Bacilli* were considered (Figure 4). This method is an excellent research tool to determine the cell number of the probiotic in the feed, but the influence of the spore germination

process, growth behavior in the presents of the feed, and changing cultivation conditions are not considered. Recent results indicate that individual metabolites are probably responsible for the probiotic effect.[45] Therefore, a method using imaging HPTLC with upstream cultivation of spore-containing standard solutions should be developed to quantify probiotics in feeds based on formed metabolites (Figure 4). For linear calibration, different amounts of the *B. s.* 29784 spores were added to the culture producing the metabolite of interest. The spore-containing standards and the diluted feed were cultured in parallel, resulting in several advantages of this new quantification technique. The cultivation conditions, the germination process, the growth behavior, and the influence of nutrient-rich feed matrix were considered by the spore-containing standard solutions. This new method was validated based on a highly selective, but non-specific metabolite of the probiotic *B. s.* 29784 concerning linearity, selectivity, limit of quantification (LOQ), precision, recovery, and robustness. A linear regression (R of 0.993, RSD 5%) was achieved. The repeatability of the method (RSD 1.9%) and the recovery (111% ± 21% in the feed additive matrix, and 96% ± 13% in a feed matrix) were excellent (all n = 3). Variation of the results (RSD 12%) is dependent on the complex germination process of the spores and fluctuating cultivation parameters during cultivation (such as temperature, humidity, and solar radiation) and the presence of other microbes in the feed. In conclusion, a new method was developed which can provide a more accurate indication of the amount of probiotic cells present in the feed. The excellent validation data proved the good performance of the streamlined method [115] and by identifying specific metabolites in the probiotic, this method could be used for species-specific quantification of the probiotic in feeds. Further advantages are the side-by-side comparison of spore standard solutions and feed samples in terms of metabolite production and nutrient consumption, to determine if the spores were affected by the feed matrix.
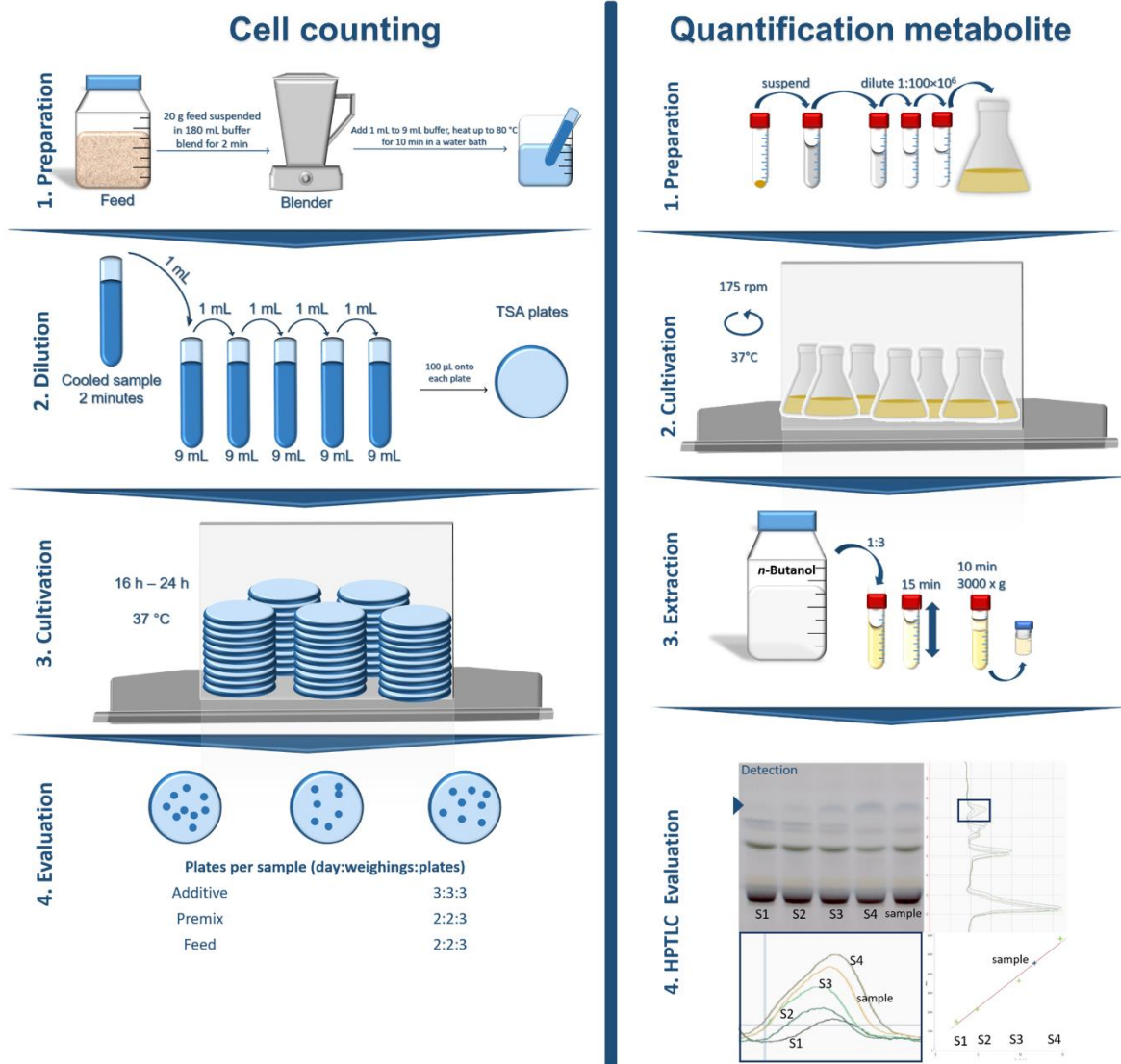
Figure 4 Quantification of probiotics in feed. Comparison of cell counting and imaging HPTLC with upstream cultivation.

1.7.5. Species - specifc quantification of *B. s.* 29784 (Publication V)

In a previous study, a method using imaging HPTLC with upstream cultivation of spore containing standard solutions was developed and validated for more accurate quantification of probiotic microorganisms in feed. The quantification is based on an unspecific metabolite of the probiotic. Thus, genetically very similar bacteria could also have produced this metabolite, which could have caused higher calculated amounts of dried spores in the feed. Therefore, the formation of a specific metabolite in the probiotic is required so that the environmental microflora does not affect the results. In the probiotic, a brown zone was detected in the chromatogram using imaging HPTLC with upstreamed two-step cultivation. The specificity of this metabolite was proven multiple times for five high genetically similar (up to 99.5%)

bacteria of the genus *Bacillus*. Multi-imaging by post-chromatographic derivatizations and EDA enabled a better characterization of this metabolite. Furthermore, the hyphenation of imaging HPTLC to reversed-phase high-performance liquid chromatography with diode array detection and mass spectrometry allowed assignment of the molecular formula $C_{35}H_{44}N_6O_2$ (580.35257 Da). The specific metabolite has antimicrobial properties and is digested by pancreatin, which may also be important for the probiotic effect. Therefore, the specific metabolite was used to quantify dried spores of *B. s.* 29784 in feed by imaging HPLC with upstream cultivation of spore standard solutions. Only the cultivation process had to be optimized to obtain a linear working range (increasing amounts of dried spores resulted in increasing cell number, with the increasing formation of the specific metabolite). The performance of the method was tested concerning selectivity, linearity, limit of quantification (LOQ), precision, and recovery in the feed matrix. The results are comparable to the validation data by using an unspecific metabolite.[116]

In conclusion, a specific metabolite was detected in the probiotic bacterium, under the given cultivation conditions and against genetical similar bacteria of the genus *Bacillus*. The cultivation process of the new quantification method was adapted to quantify the specific metabolite and the performance data were comparable to the validation of imaging HPTLC with upstreamd cultivation [115].

INTRODUCTION

2. References

1. Metchnikhoff E. The Prolongation of Life. Nature. 1908; https://doi.org/10.1038/077289b0

2. Kollath W. The increase of diseases of civilization and their prevention. Munch. Med. Wochenschr. 1953;95:1260–1262.

3. Lilly DM, Stillwell RH. Probiotics: Growth-promoting factors produced by microorganisms. Science. 1965; https://doi.org/10.1126/science.147.3659.747

4. Food and Agriculture Organization of the United Nations, World Health Organisation. Guidelines for the Evaluation of Probiotics in Food: FAO/WHO; April 30-May 2002.

5. Markowiak P, Śliżewska K. The role of probiotics, prebiotics and synbiotics in animal nutrition. Gut Pathog. 2018; https://doi.org/10.1186/s13099-018-0250-0

6. Fuller R. Probiotics in man and animals. J. Appl. Bacteriol. 1989;66:365–378.

7. Huis Veld JHJI, Havenaar R. Probiotics and health in man and animal. J. Chem. Technol. Biotechnol. 1991; https://doi.org/10.1002/jctb.280510419

8. Guarner F, Schaafsma GJ. Probiotics. Int. J. Food Microbiol. 1998; https://doi.org/10.1016/S0168-1605(97)00136-0

9. Naidu AS, Bidlack WR, Clemens RA. Probiotic spectra of lactic acid bacteria (LAB). Crit. Rev. Food Sci. Nutr. 1999; https://doi.org/10.1080/10408699991279187

10. Schrezenmeir J, Vrese M de. Probiotics, prebiotics, and synbiotics— approaching a definition. Am. J. Clin. Nutr. 2001; https://doi.org/10.1093/ajcn/73.2.361s

11. Nurmi E, Rantala M. New aspects of *Salmonella* infection in broiler production. Nature. 1973; https://doi.org/10.1038/241210a0

12. Kőrösi Molnár A, Podmaniczky B, Kürti P, Glávits R, Virág G, Szabó Z, Farkas Z. Effect of Different Concentrations of *Bacillus subtilis* on Immune Response of Broiler Chickens. Probiotics & Antimicro. Prot. 2011; https://doi.org/10.1007/s12602-011-9063-x

13. Owings WJ, Reynolds DL, Hasiak RJ, Ferket PR. Influence of dietary supplementation with *Streptococcus faecium* M-74 on broiler body weight, feed conversion, carcass characteristics, and intestinal microbial colonization. Poult. Sci. 1990; https://doi.org/10.3382/ps.0691257

REFERENCES

14. Tortuero F. Influence of the implantation of *Lactobacillus* acidophilus in chicks on the growth, feed conversion, malabsorption of fats syndrome and intestinal flora. Poult. Sci. 1973; https://doi.org/10.3382/ps.0520197

15. Mountzouris KC, Tsirtsikos P, Kalamara E, Nitsch S, Schatzmayr G, Fegeros K. Evaluation of the efficacy of a probiotic containing *Lactobacillus*, *Bifidobacterium*, *Enterococcus*, and *Pediococcus* strains in promoting broiler performance and modulating cecal microflora composition and metabolic activities. Poult. Sci. 2007; https://doi.org/10.1093/ps/86.2.309

16. Lutful Kabir SM. The role of probiotics in the poultry industry. Int. J. Mol. Sci. 2009; https://doi.org/10.3390/ijms10083531

17. The Concil Of The European Communities. Concil Directive 70/524/EEC of 23 November 1970 concerning additives in feeding-stuffs: L270/1; Novembre, 23 1970.

18. Wells GA, Hawkins SA, Green RB, Austin AR, Dexter I, Spencer YI, Chaplin MJ, Stack MJ, Dawson M. Preliminary observations on the pathogenesis of experimental bovine spongiform encephalopathy (BSE): an update. Vet. Rec. 1998; https://doi.org/10.1136/vr.142.5.103

19. Hayward DG, Nortrup D, Gardner A, Clower M. Elevated TCDD in chicken eggs and farm-raised catfish fed a diet with ball clay from a Southern United States mine. Environ. Res. 1999; https://doi.org/10.1006/enrs.1999.3976

20. National Advisory Comittee On Microbiological Criteria For Foods. Hazard analysis and critical control point principles and application guidelines. National Advisory Committee on Microbiological Criteria for Foods. J. Food. Prot. 1998;61:762–775.

21. The European Parlament And Of The Council. Regulation (EC) No 1831/2003 of the European Parlament and of the CouncilL of 22 September 2003 on additives for use in animal nutrition: L 268/29; 2003.

22. Dibner JJ, Richards JD. Antibiotic growth promoters in agriculture: history and mode of action. Poult. Sci. 2005; https://doi.org/10.1093/ps/84.4.634

23. Hershberger E, Oprea SF, Donabedian SM, Perri M, Bozigar P, Bartlett P, Zervos MJ. Epidemiology of antimicrobial resistance in enterococci of animal origin. J. Antimicrob. Chemother. 2005; https://doi.org/10.1093/jac/dkh508

24. The European Parlament And Of The Council. Commission Regulation (EC) No 429/2008 of 25 April 2008 on detailed rules for the implementation of

REFERENCES

Regulation (EC) No 1831/2003 of the EuropeanParliament and of the Council as regards the preparation and the presentation of applications and theassessment and the authorisation of feed additives: L 133/1; 2008.

25. The European Parlament And Of The Council. Regulation (EC) No 882/2004 of the European Parlament and of the Council of 29 April 2004 on official controls performed to ensure the verification of compliance with feed and food law, animal health and animal welfare rules: L 165/1; 2004.

26. Anadón A, Martínez-Larrañaga MR, Aranzazu Martínez M. Probiotics for animal nutrition in the European Union. Regulation and safety assessment. Regul. Toxicol. Pharmacol. 2006; https://doi.org/10.1016/j.yrtph.2006.02.004

27. Isolauri E, Kirjavainen PV, Salminen S. Probiotics: a role in the treatment of intestinal infection and inflammation? Gut. 2002; https://doi.org/10.1136/gut.50.suppl_3.iii54

28. Shokryazdan P, Faseleh Jahromi M, Liang JB, Ho YW. Probiotics: From Isolation to Application. J. Am. Coll. Nutr. 2017; https://doi.org/10.1080/07315724.2017.1337529

29. Pineiro M, Asp N-G, Reid G, Macfarlane S, Morelli L, Brunser O, Tuohy K. FAO Technical meeting on prebiotics. J. Clin. Gastroenterol. 2008; https://doi.org/10.1097/MCG.0b013e31817f184e

30. Kumar S, Shang Y, Kim WK. Insight Into Dynamics of Gut Microbial Community of Broilers Fed With Fructooligosaccharides Supplemented Low Calcium and Phosphorus Diets. Front. Vet. Sci. 2019; https://doi.org/10.3389/fvets.2019.00095

31. Wang Y, Zeng T, Wang S, Wang W, Wang Q, Yu H-X. Fructo-oligosaccharides enhance the mineral absorption and counteract the adverse effects of phytic acid in mice. Nutr. 2010; https://doi.org/10.1016/j.nut.2009.04.014

32. Adebola OO, Corcoran O, Morgan WA. Synbiotics: the impact of potential prebiotics inulin, lactulose and lactobionic acid on the survival and growth of lactobacilli probiotics. J. Funct. Foods. 2014; https://doi.org/10.1016/j.jff.2014.05.010

33. Chaveerach P, Lipman L, van Knapen F. Antagonistic activities of several bacteria on in vitro growth of 10 strains of Campylobacter jejuni/coli. Int. J. Food Microbiol. 2004; https://doi.org/10.1016/S0168-1605(03)00170-3

REFERENCES

34. Campana R, van Hemert S, Baffone W. Strain-specific probiotic properties of lactic acid bacteria and their interference with human intestinal pathogens invasion. Gut Pathog. 2017; https://doi.org/10.1186/s13099-017-0162-4

35. Soumeh EA, Del Cedeno ARC, Niknafs S, Bromfield J, Hoffman LC. The Efficiency of Probiotics Administrated via Different Routes and Doses in Enhancing Production Performance, Meat Quality, Gut Morphology, and Microbial Profile of Broiler Chickens. Anim. 2021; https://doi.org/10.3390/ani11123607

36. Neijat M, Shirley RB, Welsher A, Barton J, Thiery P, Kiarie E. Growth performance, apparent retention of components, and excreta dry matter content in Shaver White pullets (5 to 16 week of age) in response to dietary supplementation of graded levels of a single strain *Bacillus subtilis* probiotic. Poult. Sci. 2019; https://doi.org/10.3382/ps/pez080

37. Al-Khalaifa H, Al-Nasser A, Al-Surayee T, Al-Kandari S, Al-Enzi N, Al-Sharrah T, Ragheb G, Al-Qalaf S, Mohammed A. Effect of dietary probiotics and prebiotics on the performance of broiler chickens. Poult. Sci. 2019; https://doi.org/10.3382/ps/pez282

38. Śliżewska K, Markowiak-Kopeć P, Żbikowski A, Szeleszczuk P. The effect of synbiotic preparations on the intestinal microbiota and her metabolism in broiler chickens. Sci. Rep. 2020; https://doi.org/10.1038/s41598-020-61256-z

39. Rychen G, Aquilina G, Azimonti G, Bampidis V, Bastos MDL, Bories G, Chesson A, Cocconcelli PS, Flachowsky G, Gropp J, Kolar B, Kouba M, López-Alonso M, López Puente S, Mantovani A, Mayo B, Ramos F, Villa RE, Wallace RJ, Wester P, Brozzi R, Saarela M. Safety and efficacy of Alterion NE® (*Bacillus subtilis* DSM 29784) as a feed additive for chickens for fattening and chickens reared for laying. EFSA Journal. 2017; https://doi.org/10.2903/j.efsa.2017.4933

40. Higgins D, Dworkin J. Recent progress in *Bacillus subtilis* sporulation. FEMS Microbiol. Rev. 2012; https://doi.org/10.1111/j.1574-6976.2011.00310.x

41. Kunst F, Ogasawara N, Moszer I, Albertini AM, Alloni G, Azevedo V. The complete genome sequence of the Gram-positive bacterium *Bacillus subtilis.* Nature. 1997; https://doi.org/10.1038/36786

REFERENCES

42. Harwood CR. Bacillus subtilis and its relatives: molecular biological and industrial workhorses. Trends Biotechnol. 1992; https://doi.org/10.1016/0167-7799(92)90233-L

43. Salim AA, Grbavčić S, Šekuljica N, Stefanović A, Jakovetić Tanasković S, Luković N, Knežević-Jugović Z. Production of enzymes by a newly isolated Bacillus sp. TMF-1 in solid state fermentation on agricultural by-products: The evaluation of substrate pretreatment methods. Bioresour. Technol. 2017; https://doi.org/10.1016/j.biortech.2016.12.081

44. Ferreira WT, Hong HA, Hess M, Adams JRG, Wood H, Bakun K, Tan S, Baccigalupi L, Ferrari E, Brisson A, Ricca E, Teresa Rejas M, Meijer WJJ, Soloviev M, Cutting SM. Micellar Antibiotics of *Bacillus*. Pharmaceutics. 2021; https://doi.org/10.3390/pharmaceutics13081296

45. Choi P, Rhayat L, Pinloche E, Devillard E, Paepe E de, Vanhaecke L, Haesebrouck F, Ducatelle R, van Immerseel F, Goossens E. *Bacillus Subtilis* 29784 as a Feed Additive for Broilers Shifts the Intestinal Microbial Composition and Supports the Production of Hypoxanthine and Nicotinic Acid. Animals. 2021; https://doi.org/10.3390/ani11051335.

46. Saxena S, Devillard E, Sidelmann K. Visualizing the germination and activity of a probiotic inside birds. Asian Poultry Magazine;April 1, 2020.

47. McKenney PT, Driks A, Eichenberger P. The *Bacillus subtilis* endospore: assembly and functions of the multilayered coat. Nat. Rev. Microbiol. 2013; https://doi.org/10.1038/nrmicro2921

48. Tan IS, Ramamurthi KS. Spore formation in Bacillus subtilis. Environ. Microbiol. Rep. 2014; https://doi.org/10.1111/1758-2229.12130

49. Errington J. Regulation of endospore formation in Bacillus subtilis. Nat. Rev. Microbiol. 2003; https://doi.org/10.1038/nrmicro750

50. Hilbert DW, Piggot PJ. Compartmentalization of gene expression during *Bacillus subtilis* spore formation. Microbiol. Mol. Biol. Rev. 2004; https://doi.org/10.1128/MMBR.68.2.234–262.2004

51. Paredes-Sabja D, Setlow P, Sarker MR. Germination of spores of Bacillales and Clostridiales species: mechanisms and proteins involved. Trends Microbiol. 2011; https://doi.org/10.1016/j.tim.2010.10.004

52. Setlow P. Spore germination. Curr. Opin. Microbiol. 2003; https://doi.org/10.1016/j.mib.2003.10.001

REFERENCES

53. Delbrück AI, Zhang Y, Heydenreich R, Mathys A. *Bacillus* spore germination at moderate high pressure: A review on underlying mechanisms, influencing factors, and its comparison with nutrient germination. Compr. Rev. Food Sci. Food Saf. 2021; https://doi.org/10.1111/1541-4337.12789

54. Bernardeau M, Lehtinen MJ, Forssten SD, Nurminen P. Importance of the gastrointestinal life cycle of *Bacillus* for probiotic functionality. J. Food Sci. Technol. 2017; https://doi.org/10.1007/s13197-017-2688-3

55. Latorre JD, Hernandez-Velasco X, Kallapura G, Menconi A, Pumford NR, Morgan MJ, Layton SL, Bielke LR, Hargis BM, Téllez G. Evaluation of germination, distribution, and persistence of *Bacillus subtilis* spores through the gastrointestinal tract of chickens. Poult. Sci. 2014; https://doi.org/10.3382/ps.2013-03809

56. Cartman ST, La Ragione RM, Woodward MJ. *Bacillus subtilis* spores germinate in the chicken gastrointestinal tract. Appl. Environ. Microbiol. 2008; https://doi.org/10.1128/AEM.00580-08

57. Stanley D, Geier MS, Hughes RJ, Denman SE, Moore RJ. Highly Variable Microbiota Development in the Chicken Gastrointestinal Tract. PLoS One. 2013; https://doi.org/10.1371/journal.pone.0084290

58. Makinen K, Berger B, Bel-Rhlid R, Ananta E. Science and technology for the mastership of probiotic applications in food products. J. Biotechnol. 2012; https://doi.org/10.1016/j.jbiotec.2012.07.006

59. Tripathi MK, Giri SK. Probiotic functional foods: Survival of probiotics during processing and storage. J. Func. Foods. 2014; https://doi.org/10.1016/j.jff.2014.04.030

60. Amerah AM, Quiles A, Medel P, Sánchez J, Lehtinen MJ, Gracia MI. Effect of pelleting temperature and probiotic supplementation on growth performance and immune function of broilers fed maize/soy-based diets. Anim. Feed Sci. Technol. 2013; https://doi.org/10.1016/j.anifeedsci.2013.01.002

61. Ramlucken U, Ramchuran SO, Moonsamy G, van Jansen Rensburg C, Thantsha MS, Lalloo R. Production and stability of a multi-strain *Bacillus* based probiotic product for commercial use in poultry. Biotechnol. rep. 2021; https://doi.org/10.1016/j.btre.2020.e00575

62. The European Parlament And Of The Council. Commission Implementing Regulation (EU) 2018/328 of 5 March 2018 concerning the authorisation of the

preparation of Bacillus subtilis DSM 29784 as a feed additive for chickens for fattening and chickens reared for laying (holder of authorisation Adisseo France SAS): L63; 2018.

63. The European Parlament And Of The Council. Commission implementing Regulation (EU) 2018/1080: L 194/134; 2018.

64. Herschleb J, Ananiev G, Schwartz DC. Pulsed-field gel electrophoresis. Nat. protoc. 2007; https://doi.org/10.1038/nprot.2007.94

65. Parizad EG, Parizad EG, Valizadeh A. The Application of Pulsed Field Gel Electrophoresis in Clinical Studies. J. Clin. Diagn. Res. 2016; https://doi.org/10.7860/JCDR/2016/15718.7043

66. European Committee for Standardization. Animal feeding stuffs - Isolation and enumeration of presumptive *Bacillus spp.*: EN 15784; 2009.

67. Rhayat L, Jacquier V, Brinch KS, Nielsen P, Nelson A, Geraert P-A, Devillard E. *Bacillus subtilis* strain specificity affects performance improvement in broilers. Poult. Sci. 2017; https://doi.org/10.3382/ps/pex018

68. Mohammadigheisar M, Shirley RB, Barton J, Welsher A, Thiery P, Kiarie E. Growth performance and gastrointestinal responses in heavy Tom turkeys fed antibiotic free corn-soybean meal diets supplemented with multiple doses of a single strain *Bacillus subtilis* probiotic (DSM29784)1. Poult. Sci. 2019; https://doi.org/10.3382/ps/pez305

69. Wang Y, Sun J, Zhong H, Li N, Xu H, Zhu Q, Liu Y. Effect of probiotics on the meat flavour and gut microbiota of chicken. Sci. Rep. 2017; https://doi.org/10.1038/s41598-017-06677-z

70. Keerqin C, Rhayat L, Zhang Z-H, Gharib-Naseri K, Kheravii SK, Devillard E, Crowley TM, Wu S-B. Probiotic *Bacillus subtilis* 29,784 improved weight gain and enhanced gut health status of broilers under necrotic enteritis condition. Poult. Sci. 2021; https://doi.org/10.1016/j.psj.2021.01.004

71. Neijat M, Habtewold J, Shirley RB, Welsher A, Barton J, Thiery P, Kiarie E. *Bacillus subtilis* Strain DSM 29784 Modulates the Cecal Microbiome, Concentration of Short-Chain Fatty Acids, and Apparent Retention of Dietary Components in Shaver White Chickens during Grower, Developer, and Laying Phases. Appl. Environ. Microbiol. 2019; https://doi.org/10.1128/AEM.00402-19

72. Wang Y, Heng C, Zhou X, Cao G, Jiang L, Wang J, Li K, Wang D, Zhan X. Supplemental *Bacillus subtilis* DSM 29784 and enzymes, alone or in

REFERENCES

combination, as alternatives for antibiotics to improve growth performance, digestive enzyme activity, anti-oxidative status, immune response and the intestinal barrier of broiler chickens. Br. J. Nutr. 2021; https://doi.org/10.1017/S0007114520002755

73. Jacquier V, Nelson A, Jlali M, Rhayat L, Brinch KS, Devillard E. *Bacillus subtilis* 29784 induces a shift in broiler gut microbiome toward butyrate-producing bacteria and improves intestinal histomorphology and animal performance. Poult. Sci. 2019; https://doi.org/10.3382/ps/pey602

74. Ley RE, Turnbaugh PJ, Klein S, Gordon JI. Microbial ecology: human gut microbes associated with obesity. Nature. 2006; https://doi.org/10.1038/4441022a

75. Turnbaugh PJ, Ley RE, Mahowald MA, Magrini V, Mardis ER, Gordon JI. An obesity-associated gut microbiome with increased capacity for energy harvest. Nature. 2006; https://doi.org/10.1038/nature05414

76. Hou Q, Kwok L-Y, Zheng Y, Wang L, Guo Z, Zhang J, Huang W, Wang Y, Leng L, Li H, Zhang H. Differential fecal microbiota are retained in broiler chicken lines divergently selected for fatness traits. Sci. Rep. 2016; https://doi.org/10.1038/srep37376

77. Jumpertz R, Le DS, Turnbaugh PJ, Trinidad C, Bogardus C, Gordon JI, Krakoff J. Energy-balance studies reveal associations between gut microbes, caloric load, and nutrient absorption in humans. Am. J. Clin. Nutr. 2011; https://doi.org/10.3945/ajcn.110.010132

78. Fernandes J, Su W, Rahat-Rozenbloom S, Wolever TMS, Comelli EM. Adiposity, gut microbiota and faecal short chain fatty acids are linked in adult humans. Nut. Diabetes. 2014; https://doi.org/10.1038/nutd.2014.23

79. Mariat D, Firmesse O, Levenez F, Guimarães V, Sokol H, Doré J, Corthier G, Furet J-P. The Firmicutes/Bacteroidetes ratio of the human microbiota changes with age. BMC Microbiol. 2009; https://doi.org/10.1186/1471-2180-9-123

80. Stojanov S, Berlec A, Štrukelj B. The Influence of Probiotics on the Firmicutes/Bacteroidetes Ratio in the Treatment of Obesity and Inflammatory Bowel disease. Microorganisms. 2020; https://doi.org/10.3390/microorganisms8111715

REFERENCES

81. Donohoe DR, Garge N, Zhang X, Sun W, O'Connell TM, Bunger MK, Bultman SJ. The microbiome and butyrate regulate energy metabolism and autophagy in the mammalian colon. Cell Metab. 2011; https://doi.org/10.1016/j.cmet.2011.02.018

82. Bedford A, Gong J. Implications of butyrate and its derivatives for gut health and animal production. Anim. Nutr. 2018; https://doi.org/10.1016/j.aninu.2017.08.010

83. Stuyvesant VW, Jolley WB. Anti-inflammatory activity of d-alpha-tocopherol (vitamin E) and linoleic acid. Nature. 1967; https://doi.org/10.1038/216585a0

84. Singh N, Gurav A, Sivaprakasam S, Brady E, Padia R, Shi H, Thangaraju M, Prasad PD, Manicassamy S, Munn DH, Lee JR, Offermanns S, Ganapathy V. Activation of Gpr109a, receptor for niacin and the commensal metabolite butyrate, suppresses colonic inflammation and carcinogenesis. Immunity. 2014; https://doi.org/10.1016/j.immuni.2013.12.007

85. Rhayat L, Maresca M, Nicoletti C, Perrier J, Brinch KS, Christian S, Devillard E, Eckhardt E. Effect of *Bacillus subtilis* Strains on Intestinal Barrier Function and Inflammatory Response. Front. immunol. 2019; https://doi.org/10.3389/fimmu.2019.00564

86. Lee JS, Wang RX, Alexeev EE, Lanis JM, Battista KD, Glover LE, Colgan SP. Hypoxanthine is a checkpoint stress metabolite in colonic epithelial energy modulation and barrier function. J. Biol. Chem. 2018; https://doi.org/10.1074/jbc.RA117.000269

87. Morlock G, Schwack W. Hyphenations in planar chromatography. J. Chromatogr. A. 2010; https://doi.org/10.1016/j.chroma.2010.04.058

88. Morlock GE. Chromatography Combined with Bioassays and Other Hyphenations – The Direct Link to the Compound Indicating the Effect. In: Instrumental Methods for the Analysis and Identification of Bioactive Molecules, vol. 1185. pp. 101–121.

89. Häbe TT, Morlock GE. Challenges in quantitative high-performance thin-layer chromatography — Part 1: Influence of densitometric settings on the result. J. Chromatogr. A. 2015; https://doi.org/10.1556/1006.2015.28.6.2

90. Klingelhöfer I, Morlock GE. Challenges in quantitative high-performance thin-layer chromatography — Part 2: Influence of the application mode on the result. J. Chromatogr. A. 2017; https://doi.org/10.1556/1006.2017.30.5.11

REFERENCES

91. Fichou D, Morlock GE. quanTLC, an online open-source solution for videodensitometric quantification. J. Chromatogr. A. 2018; https://doi.org/10.1016/j.chroma.2018.05.027

92. Fichou D, Ristivojević P, Morlock GE. Proof-of-Principle of rTLC, an Open-Source Software Developed for Image Evaluation and Multivariate Analysis of Planar Chromatograms. Anal. Chem. 2016; https://doi.org/10.1021/acs.analchem.6b04017

93. Häbe TT, Morlock GE. Quantitative surface scanning by Direct Analysis in Real Time mass spectrometry. Rapid Commun Mass Sp. 2015; https://doi.org/10.1002/rcm.7127

94. Morlock GE, Brett N. Correct assignment of lipophilic dye mixtures? A case study for high-performance thin-layer chromatography-mass spectrometry and performance data for the TLC-MS Interface. J. Chromatogr. A. 2015; https://doi.org/10.1016/j.chroma.2015.02.011

95. Azadniya E, Morlock GE. Bioprofiling of Salvia miltiorrhiza via planar chromatography linked to (bio)assays, high resolution mass spectrometry and nuclear magnetic resonance spectroscopy. J. Chromatogr. A. 2018; https://doi.org/10.1016/j.chroma.2017.12.014

96. Azadniya E, Goldoni L, Bandiera T, Morlock GE. Same analytical method for both (bio)assay and zone isolation to identify/quantify bioactive compounds by quantitative nuclear magnetic resonance spectroscopy. J. Chromatogr. A. 2020; https://doi.org/10.1016/j.chroma.2020.461434

97. Jamshidi-Aidji M, Morlock GE. Fast Equivalency Estimation of Unknown Enzyme Inhibitors in Situ the Effect-Directed Fingerprint, Shown for *Bacillus* Lipopeptide Extracts. Anal. Chem. 2018; https://doi.org/10.1021/acs.analchem.8b03407

98. Jemil N, Manresa A, Rabanal F, Ben Ayed H, Hmidet N, Nasri M. Structural characterization and identification of cyclic lipopeptides produced by *Bacillus methylotrophicus* DCS1 strain. J. Chromatogr. B. 2017; https://doi.org/10.1016/j.jchromb.2017.06.013

99. Kruse S, Pierre F, Morlock G. Imaging high-performance thin-layer chromatography as powerful tool to visualize metabolite profiles of eight *Bacillus* candidates upon cultivation and growth behavior. J. Chromatogr. A. 2021; https://doi.org/10.1016/j.chroma.2021.461929

REFERENCES

100. Kruse S, Pierre F, Morlock GE. Effects of the Probiotic Activity of Bacillus subtilis DSM 29784 in Cultures and Feeding Stuff. J. Agric. Food Chem. 2021; https://doi.org/10.1021/acs.jafc.1c04811

101. Sharma D, Singh SS, Baindara P, Sharma S, Khatri N, Grover V, Patil PB, Korpole S. Surfactin Like Broad Spectrum Antimicrobial Lipopeptide Co-produced With Sublancin From *Bacillus subtilis* Strain A52: Dual Reservoir of Bioactives. Front. Microbiol. 2020; https://doi.org/10.3389/fmicb.2020.01167

102. Desmyttere H, Deweer C, Muchembled J, Sahmer K, Jacquin J, Coutte F, Jacques P. Antifungal Activities of *Bacillus subtilis* Lipopeptides to Two Venturia inaequalis Strains Possessing Different Tebuconazole Sensitivity. Front. Microbiol. 2019; https://doi.org/10.3389/fmicb.2019.02327

103. Miller JK, Brzezinska-Slebodzinska E, Madsen FC. Oxidative Stress, Antioxidants, and Animal Function. J. Dairy. Sci. 1993; https://doi.org/10.3168/jds.S0022-0302(93)77620-1

104. Zhao Y, Flowers WL, Saraiva A, Yeum K-J, Kim SW. Effect of social ranks and gestation housing systems on oxidative stress status, reproductive performance, and immune status of sows. J. Anim. Sci. 2013; https://doi.org/10.2527/jas.2013-6388

105. Lykkesfeldt J, Svendsen O. Oxidants and antioxidants in disease: oxidative stress in farm animals. Vet. J. 2007; https://doi.org/10.1016/j.tvjl.2006.06.005

106. Islam R, Sultana N, Ayman U, Islam MR, Hashem MA. Role of steroid growth promoter on growth performance and meat quality traits in broiler. Poult. Sci. 2022; https://doi.org/10.1016/j.psj.2022.101904

107. McEwen SA, Fedorka-Cray PJ. Antimicrobial use and resistance in animals. Clin. Infect. Dis. 2002; https://doi.org/10.1086/340246

108. Casula G, Cutting SM. *Bacillus* probiotics: spore germination in the gastrointestinal tract. Appl. Environ. Microbiol. 2002; https://doi.org/10.1128/AEM.68.5.2344-2352.2002

109. Morlock GE, Drotleff L, Brinkmann S. Miniaturized all-in-one nanoGIT+active system for on-surface metabolization, separation and effect imaging. Anal. Chim. Acta. 2021; https://doi.org/10.1016/j.aca.2021.338307

110. Zhang J, Luo W, Wang Z, Chen X, Lv P, Xu J. A novel strategy for D-psicose and lipase co-production using a co-culture system of engineered *Bacillus subtilis* and Escherichia coli and bioprocess analysis using

metabolomics. Bioresour. Bioprocess. 2021; https://doi.org/10.1186/s40643-021-00429-8

111. S Hifnawy M, Hassan HM, Mohammed R, M Fouda M, Sayed AM, A Hamed A, F AbouZid S, Rateb ME, Alhadrami HA, Abdelmohsen UR. Induction of Antibacterial Metabolites by Co-Cultivation of Two Red-Sea-Sponge-Associated Actinomycetes Micromonospora sp. UR56 and Actinokinespora sp. EG49. Mar. Drugs. 2020; https://doi.org/10.3390/md18050243

112. Ravikrishnan A, Blank LM, Srivastava S, Raman K. Investigating metabolic interactions in a microbial co-culture through integrated modelling and experiments. Comput. Struct. Biotechnol. J. 2020; https://doi.org/10.1016/j.csbj.2020.03.019

113. Bertrand S, Bohni N, Schnee S, Schumpp O, Gindro K, Wolfender J-L. Metabolite induction via microorganism co-culture: a potential way to enhance chemical diversity for drug discovery. Biotechnol. Adv. 2014; https://doi.org/10.1016/j.biotechadv.2014.03.001

114. Kruse S, Becker S, Pierre F, Morlock GE. Metabolic profiling of bacterial co-cultures with link to the dominant species identification. close to submission;2022.

115. Kruse S, Schenk Mareike, Pierre F, Morlock GE. *Bacillus subtilis* spores in probiotic feed quantified via bacterial metabolite using planar chromatography. Anal. Chim. Acta - in revision;2022.

116. Kruse S, Becker S, Pierre F, Morlock GE. Species-specific quantification of probiotic Bacillus subtilis DSM 29784 in feed by imaging high-performance thin-layer chromatography. close to submission;2022.

3. Publication I

Imaging high-performance thin-layer chromatography as powerful tool to visualize metabolite profiles of eight *Bacillus* candidates upon cultivation and growth behavior.

Stefanie Kruse[a], Francis Pierre[b], Gertrud E. Morlock[a,*]

[a]Chair of Food Science, Institute of Nutritional Science, and Interdisciplinary Research Centre for Biosystems, Land Use and Nutrition, Justus Liebig University Giessen, Heinrich-Buff-Ring 26-32, 35392 Giessen, Germany

[b]Adisseo France S.A.S, Immeuble Anthony Parc 2, 10 Place du Général de Gaulle, 92160 Antony, France

PUBLICATION I

Imaging high-performance thin-layer chromatography as powerful tool to visualize metabolite profiles of eight *Bacillus* candidates upon cultivation and growth behavior

Stefanie Kruse[a], Francis Pierre[b], Gertrud Morlock[a,*]

[a] *Chair of Food Science, Institute of Nutritional Science, and Interdisciplinary Research Centre for Biosystems, Land Use and Nutrition, Justus Liebig University Giessen, Heinrich-Buff-Ring 26-32, 35392 Giessen, Germany*
[b] *Adisseo France S.A.S, Immeuble Anthony Parc 2, 10 Place du Général de Gaulle, 92160 Antony, France*

ARTICLE INFO

ABSTRACT

Imaging high-performance thin-layer chromatography (HPTLC) was explored with regard to its ability to visualize changes in the metabolite profile of bacteria. *Bacillus subtilis* has become a model organism in many fields. The increasing interest in these bacteria is driven by their attributed probiotic activity. However, growth behavior and metabolism of *Bacillus* species have a considerable influence on their activity and secondary metabolite profile. On the HPTLC plate, cultivation broths of *Bacillus* species (*B. subtilis, B. licheniformis, B. pumilus* and *B. amyloliquefaciens*) and some *B. subtilis* strains of high genetic similarity up to 99.5% were applied directly and compared with their respective liquid-liquid extracts. The latter as well as the cultivation in a minimal medium reduced the matrix load and improved the zone resolution. Cultivation parameters such as nutrient supply, cultivation temperature, cultivation time and rotational speed (oxygen level) as well as medium change were shown to have a considerable influence on the growth behavior and resulting metabolite profiles. Imaging HPTLC turned out to be an efficient and affordable tool to visualize such influences of cultivation parameters on the metabolite profiles. It converts the complexity of reaction processes occurring during cell cultivation in easy-to-understand images, which are helpful to figure out factors of influence and understand activity changes. The results highlighted that optimal cultivation conditions need to be found for the intended bacterial application, and in particular, these conditions have to be kept constant. It must be ensured that small variations in cultivation parameters of bacteria do not change the specified (probiotic) effect on the health of animals and humans. The HPTLC metabolite profiles represented the cultivation conditions of specific bacteria and were found to be a proof of the activity of distinct bacteria. In addition, HPTLC can also be used to optimize and streamline the culture media. The quality control of cultivation or fermentation processes can benefit from such a powerful tool, as a picture is worth a thousand words.

1. Introduction

The metabolism of bacteria and their growth behavior change upon cultivation conditions. Nutrient supply, oxygen content, cultivation time and cultivation temperature are important parameters that have an influence [1]. *Bacillus subtilis* has become a model organism in biochemistry, biotechnology, genetics, medicine, food and feed industry [2]. This is justified by the complete sequencing of the genome [3], its heat resistance, robust growth behavior and similarity to many pathogenic endospore-forming bacteria like *B. cereus* and *B. anthracis* [4]. Most bacteria of the genus *Bacillus* are non-pathogenic Gram–positive firmicutes. The natural habitat of the rod-shaped *B. subtilis* bacteria (about 2–3 µm long and 0.6 µm wide) is in the upper soil layers as well as rhizosphere, where it is exposed to varying nutrient supplies [3]. Usually the cells grow under aerobic conditions; however, an anaerobic growth is possible in presence of nitrate and glucose as nitrogen/carbon/energy source.

High-performance thin-layer chromatography (HPTLC) enables the parallel analysis of samples with complex matrices. This allows the simultaneous analysis of different *Bacillus* species side by side and the comparison of their metabolite profiles under the same analytical conditions. Imaging HPTLC is a flexible method because different derivatization reagents or effect-directed assays can be used for multiple detection of metabolites. Such multi–imaging

of the chromatogram can detect differences between species or strains [5]. For example, selective chemical derivatization reagents [6] were used to differentiate the formed metabolites according to substance classes, *e.g.*, cyclic lipopeptides [5], or for classification of enzymes, *e.g.*, industrial enzymes [2]. The most common secondary metabolites of *Bacillus* species are such lipopeptides produced in different concentrations and compositions depending on the culture conditions [5,7,8]. The co-migration of standard solutions was used to confirm the cyclic lipopeptides found, which consist of a cyclic peptide connected to a long fatty acid chain. The latter moiety was detected by the primuline reagent, which attaches preferably to this lipophilic chain. Many other derivatization reagents can be used for the detection of further metabolites of quite different structural groups [6]. Treasured information with regard to bioactivity is obtained by the application of planar effect-directed assays (EDA) [9,10]. For example, individual antibacterial compounds can thus be detected in complex mixtures [10]. For further information, the separated analyte zones of interest can be online eluted from the HPTLC plate to high-resolution mass spectrometry (HRMS) systems [10,11]. Instead, the zone can be transferred to a vial to be further analyzed by nuclear magnetic resonance or infrared spectroscopy. A quantification of the detected metabolites is possible by densitometry [12,13] or digital image evaluation [14,15] or mass spectrometry [16,17].

In this study, it was hypothesized that imaging HPTLC could be a useful new tool for quality control in the wide field of biotechnology including fermentation technologies. To the best of our knowledge, HPTLC profiles have not been studied for quality control of cultivation or fermentation processes so far. Eight *Bacillus* candidates were selected, *i.e.* four different *Bacillus* species and four different *B. subtilis* strains of a high genetic similarity (98.4%–99.5%). HPTLC methods were developed to evaluate the expressed secondary metabolite profiles. It was explored whether differences in the HPTLC profiles of these *Bacillus* candidates were detectable when variations or changes in growing conditions occurred. If HPTLC profiles will represent the cultivation conditions of specific bacteria, quality control can benefit, as a picture is worth a thousand words.

2. Materials and methods

2.1. Chemicals and materials

Tryptic soy broth and HPTLC plates silica gel 60 (NP) or RP18 (RP) were purchased from Merck, Darmstadt, Germany. Toluene (≥99%), chloroform (≥99%) and hydrochloric acid (37%, purest) were obtained from Carl Roth, Karlsruhe, Germany. *n*–Butanol (HPLC grade) was delivered by Acros Organics, Fair Lawn, NJ, USA. Aniline (≥99.5%), diphenylamine (≥99.5%), *n*–hexane (≥99.5%), primuline (≥99%), yeast extract (for use in microbial growth medium), D–glucose (Glc, ≥99.5%), D–lactose (Lac, ≥99%), D–maltose (Mal, ≥99%), D–mannose (Man, ≥99%), D–fructose (Fru, ≥99%), glutamic acid (Glu, ≥99%), glutamine (Gln, ≥98.5%), lysogeny broth and Mueller-Hinton broth (for microbiology) were purchased from Sigma Aldrich, Steinheim, Germany. Sodium chloride, anhydrous magnesium sulphate and sodium hydroxide (all ≥99%) were obtained from Fluka, Buchs, Switzerland. Methanol and acetone (both HPLC grade) were purchased from VWR, Darmstadt, Germany. Ethyl acetate (≥99.8%) was delivered by Th. Geyer, Renningen, Germany. Bidistilled water was prepared by a Destamat Bi 18E (Heraeus, Hanau, Germany). The marine microorganism *Aliivibrio fischeri* (strain 7151) was provided by Leibniz Institute DSMZ, German Collection of Microorganisms and Cell Cultures, Berlin, Germany.

2.2. Origin of the Bacillus candidates and stock solutions

As candidates, four *B. subtilis* (**1**: DSM 29784 reference strain, **2**: MIC39 genetically similar up to 99.5%, **3**: ATCC6633 genetically similar up to 99.4% and **4**: not identified, genetically similar up to 98.4%), **5**: *B. licheniformis* SB3114, **6**: *B. pumilus* SB3839 and two *B. amyloliquefaciens* (**7**: SB3234 and **8**: SB3837) were obtained by Novozymes, Bagsværd, Denmark. Each *Bacillus* candidate was cultivated in the TSBY (3% tryptic soy broth with 0.6% yeast extract added to 1 L water adjusted to pH 6.2 with 2 M hydrochloric acid solution) at 37 °C up to an optical density (OD, measured at 660 nm) of 0.5. The cells were two times washed with 0.9% sodium chloride solution (ratio 2:3), and also resuspended in it (ratio 1:3). The stock solutions were stored dark at 5 °C.

2.3. Cultivation parameters

The bacteria were cultivated in four different culture media at 30 °C and 37 °C. The four culture media were TSBY, MH (2.3% Mueller Hinton broth added to 1 L water, adjusted to pH 7.4), LB (2% lysogeny broth added to 1 L water with 0.5% sodium chloride and 1% Glc adjusted to pH 7.0 with sodium hydroxide) and pYES (usually used for the planar yeast estrogen screen [18,19]: sterile solution of 10 g Glc and 6.8 g yeast nitrogen base without amino acids in 100 mL water added to 800 mL autoclaved double distilled water and 100 mL sterile amino acid solution). Five different saccharide/energy sources (Glc, Lac, Mal, Man and Fru) and two amino acids (Glu and Gln) were tested for the cultivation in the pYES medium. The respective medium (30 mL) was inoculated with 150 µL of the respective stock solution. The rotation speed of the orbital shaker SM-30 (Edmund Bühler, Bodelshausen, Germany) was set to 100 rpm (220 rpm for the pYES culture). The bacteria were cultivated for either a specific OD or defined period, as mentioned.

2.4. Extraction of metabolites

The explored extraction methods and solvents were listed (Table S1). After cultivation, the OD was measured with the M501 Single Beam Scanning UV/Visible Spectrophotometer (CamSpec, Garforth, UK). The culture medium was centrifuged with the centrifuge 5702 (Eppendorf, Hamburg, Germany) at 3000 × g for 10 min to separate the cells from the supernatant. A liquid-liquid extraction was performed with volume ratios of either 1:1 or 1:3 of extraction solvent to supernatant for extraction times of 15 min or 60 min with each of the five extraction solvents ethyl acetate, *n*–butanol, toluene, *n*–hexane and chloroform or combinations. For the Quick, Easy, Cheap, Efficient, Rugged and Safe (QuEChERS) extraction [20], 10 mL acetonitrile were added to each supernatant (10 mL), vortexed (highest speed, 1 min) and mixed with 4 g anhydrous magnesium sulphate as well as 1 g sodium chloride. Each mixture was shaken vigorously for 1 min and centrifuged at 3000 × g for 1 min.

2.5. HPTLC procedure

The extracts (100, 150 or 200 µL, but possible up to 800 µL) were applied on the HPTLC plate as area of 8 mm × 10 mm with the Automatic TLC Sampler 4 (ATS 4, CAMAG, Muttenz, Switzerland). For the ethyl acetate, *n*–hexane, chloroform and toluene extracts, a dosage speed of 1200 nL/s was set, whereas it was 600 nL/s for the *n*–butanol extracts. Further application parameters were listed (Table S2), also for the application of supernatants (150 µL, but possible up to 300 µL, 10 mm × 20 mm area). The syringe was rinsed twice with methanol. The applied areas were focused up to 20 mm with acetone and two times with methanol in

a twin through chamber (CAMAG) to achieve a sharp start band. If not stated otherwise in respective Figures depending on the used stationary phase and extraction method, a mobile phase of ethyl acetate – methanol – water was used at the specified ratios. For the analyses via the primuline reagent, the chamber was saturated with the mobile phase for 10 min. Each development was performed up to a migration distance of 70 mm (measured from the lower plate edge) with Automatic Development Chamber (ADC 2, CAMAG) after activation of the plate surface with magnesium chloride (33% relative humidity). Each chromatogram was dried for 5 min (ADC 2) and documented at white light illumination (Vis), UV 254 nm and FLD 366 nm (TLC Visualizer 2, CAMAG). Different derivatization reagents and bioassays were used, *e.g.*, the primuline reagent (detects lipophilic substances), diphenylamine aniline sulfuric acid reagent (detects saccharides) or the *Aliivibrio fischeri* bioassay (detects antibacterial compounds).

3. Results and discussion

3.1. Outline of the profiling

Eight *Bacillus* candidates were selected, *i.e.* four *B. subtilis* **1–4**, one *B. licheniformis* **5**, one *B. pumilus* **6**, and two *B. amyloliquefaciens* **7** and **8**. The four *B. subtilis* strains **1–4** were of high genetic similarity (98.4%–99.5%). The metabolic profiles were expected to be most similar for genetically similar *Bacillus* candidates, if compared to lower genetic similarities. Hence, it was most challenging to find any differences in similar strains of one species or in similar species. A selection of candidates was made, if not all needed to be investigated in the following experiments. The application of *Bacillus* supernatants (possible up to 300 µL) on the HPTLC plate required a larger area (10 mm× 20 mm) than the respective extracts (possible up to 800 µL, 8 mm × 10 mm). The bandwise application of the required high volumes was not or hardly possible (Table S2). High application volumes are advantageous for visualization of the low expressed metabolites. Hence, an area application was found to be precondition for a successful metabolite pro-

filing. Respective medium or solvent blanks were also applied on each plate. Different separation systems were investigated to find out and illustrate any differences in the *Bacillus* metabolite profiles obtained by changed growing conditions. Parameters such as cultivation medium composition, rotation speed (oxygen level), cultivation temperature, cultivation time and extraction methods were varied to determine the influence of the respective condition on the bacterial metabolite profile. To a certain extent, this also simulated possible variations that may occur in routine or due to a method transfer to another laboratory.

3.2. Influence of nutrient supply on growth behavior and Bacillus metabolite profile

This experiment aimed at finding out the influence of different cultivation conditions on the metabolite profile for four selected *Bacillus* candidates (**1–3** and **5**). These candidates were selected with regard to highest genetic similarity but also species difference. The cultivation was performed using different media, rotation speeds (oxygen level), temperatures and durations. The resulting metabolite profiles of the strains of the different *Bacillus* species were visualized by imaging HPTLC. Thereby, different extraction parameters and chromatographic conditions were tested to widen the perspective and to obtain comprehensive information on secondary metabolites (Fig. 1).

The selected three universal culture media, *i.e.* tryptic soy broth with yeast (TSBY, adjusted to pH 6.2) [21], Mueller Hinton broth (MH, adjusted to pH 7.4) [22] and lysogeny broth (LB, adjusted to pH 7.0) [23], differed with regard to the Glc concentration, yeast presence (only in TSBY and LB media), casein type and pH. It was assumed that longer cultivation times cause higher ODs and also a higher expression of extracellular metabolites. The growth behavior of these bacteria was investigated over a 40-h period at 37 °C and a rotation speed of 100 rpm. All experiments were performed twice. Every two hours, a 1.5-mL aliquot was taken and the OD was measured. Due to the required sampling over this long cultivation time, two cultures (150 µL stock solution in 30 mL cul-
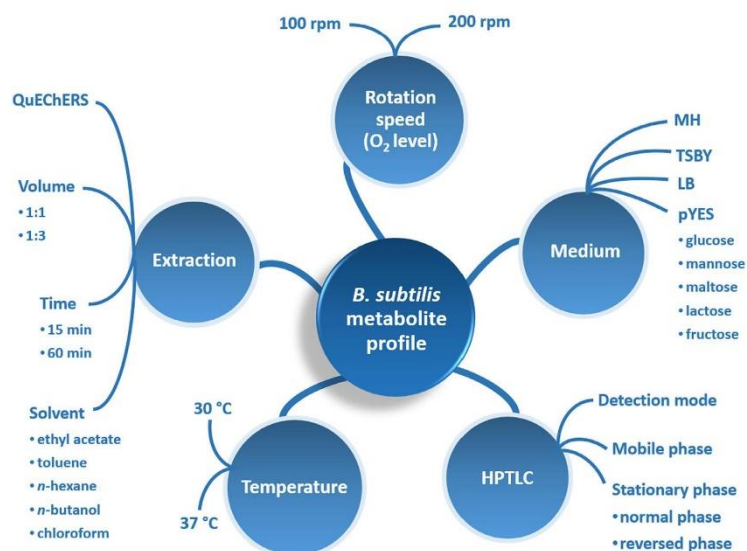

Fig. 1. Parameters investigated with influence on the *Bacillus* metabolite profile.
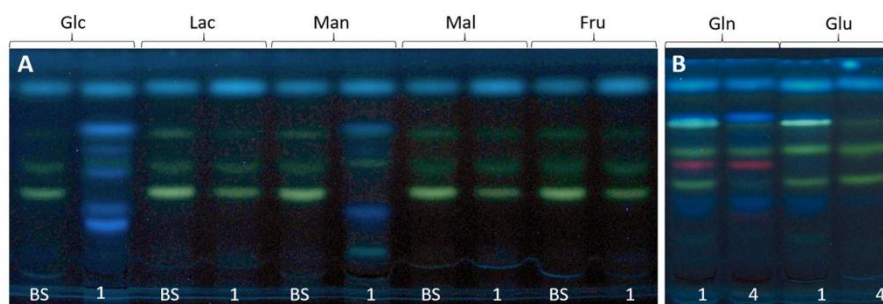
Fig. 2. HPTLC chromatograms at FLD 366 nm of blank samples (BS: pYES medium) and *n*–butanol extracts of *B. subtilis* strains **1** and **4** (200 µL/band each) cultivated in pYES medium using different saccharide energy sources (**A**; Glc, Lac, Man, Mal and Fru) or amino acid sources (**B**; Gln and Glu) at a rotation speed of 100 rpm, cultivation temperature of 37 °C and duration of 18 h (Glc, Man, Glu and Gln) or even 40 h (Lac, Mal and Fru); separation on HPTLC plates silica gel 60 with ethyl acetate – methanol – water 7.5:1.7:0.8, *V/V/V*.

ture medium) were prepared in parallel, whereby only minor deviations were observed in the OD between the two parallel cultures and the repeated set. The investigated bacteria showed a different growth behavior in the three universal media. It is known that *Bacillus* species can be triggered by the nutrient supply to grow single-stage or diauxic [24]. Cultivation in TSBY and MH showed such a two–step growth behavior for some strains (Fig. S2). For the *B. subtilis* strains **1–3**, the highest OD was achieved by cultivation in TSBY. In contrast, the highest OD of the *B. licheniformis* strain **5** was reached in the MH medium. The subsequent HPTLC analysis of all aliquots collected at the different cultivation times revealed an increase in the number of bands with increasing cultivation time. It was also observed that some metabolites were only formed at distinct cultivation times (Fig. S1), *e.g.*, metabolite bands were detected for shorter cultivations, but not for longer ones anymore. This was explained by the fact that bacteria can not only release metabolites but also convert and consume these. Imaging HPTLC revealed that the rich nutrient supply provided by the three universal culture media had only a small influence on the cell metabolism and thus metabolite profile (Fig. S1). In TSBY, more pronounced metabolite changes were detected between the samples, if compared to both other media. For longer cultivations, a cell adhesion effect was observed by microscopy (Fig. S3). The inner cells of the agglomerates were cut off from the nutrient supply, causing the cells to enter the stationary or anaerobic dying phase, and thus form cell degradation products. Hence, the different cultures were also examined for cell adhesion and cultures with agglomerated cells were excluded to limit the complexity of the experiment.

In a next experiment, the culture medium was changed to a minimal medium [18,19,25] and studied for all four species. The use of minimal media is advantageous because the co–extracted matrix and thus matrix load on the plate was less, if compared to the more complex universal media. This allowed the better differentiation of metabolites from matrix and the more sensitive detection of low metabolite amounts by application of higher extract volumes. The cell growth was slower in the pYES minimal medium than in the complex media. As the Glc concentration in the minimal medium was at least up to four-fold higher than in the complex media, a lack in other nutrients was found to cause the slow growth. Still, the complexity of the medium had a considerable influence on the extraction and chromatographic separation. With increasing complexity of the medium, more matrix components were co–extracted, whereby blurred bands can appear in the HPTLC chromatogram. In comparison, the pYES minimal medium showed more distinct metabolite bands and con-

siderably less matrix components (Fig. S4). In the pYES minimal medium, saccharides and amino acids were exchanged. The substitution of the Glc energy source by Lac or Mal or Fru had a crucial influence on the growth behavior and cell metabolism, as no growth was observed even for up to 40-h cultivations. In contrast, a growth was observed for the substitution by Man, the C2–epimere of Glc. This growth observation was confirmed via the HPTLC profiling which illustrated the preferred and selective saccharide metabolization for Glc and Man (Fig. 2A). It is also known that chemotrophic bacteria initially use only one of the available energy sources for growth. After consumption of the most accessible energy source, the cells had to adapt to the new environmental conditions [24]. Such a consumption of nutrients can also be studied and visualized by the HPTLC profiling to optimize cultivation broths. The exchange of a single amino acid like Glu by Gln had a direct influence on the metabolism, for example evident as additional red band in the HPTLC metabolite profile (Fig. 2B).

Differences in the bacterial growth behavior and metabolite profile were also observed by changing the rotation speed and cultivation temperature. The change of the rotation speed from 220 rpm to 100 rpm changed the metabolite profiles. In the HPTLC profile, significantly fewer metabolites were detected at the lower rotation speed (Fig. S5). A growth of *B. subtilis* is possible in a wide temperature range [26]. Both 30 °C and 37 °C were often described as optimal growth temperatures [27,28] and thus chosen. As expected, a longer cultivation time was needed at a lower cultivation temperature to achieve the same OD. No or hardly any metabolites were detected at a cultivation temperature of 30 °C, even for a 20-h cultivation (Fig. 3A). However, when the cultivation temperature was increased to 37 °C, metabolites were already detected in some samples (Fig 3B).

Imaging HPTLC was found to be advantageous and highly suitable for visualization of the resulting metabolite profile of the complex bacterial reaction mechanisms. Several cultivation samples were simultaneously studied under the same chromatographic conditions (separated in parallel on the same chromatogram). Influences and changes by the nutrient supply, rotation speed, cultivation temperature and duration were successfully demonstrated and documented by the respective metabolite profiles. Thus, profound information was obtained on essential cultivation parameters for the intended bacterial application purpose. The HPTLC metabolite profiles represented the cultivation conditions of specific bacteria and were found to be a proof of the activity of distinct bacteria, which is important for quality control of cultivation or fermentation processes.
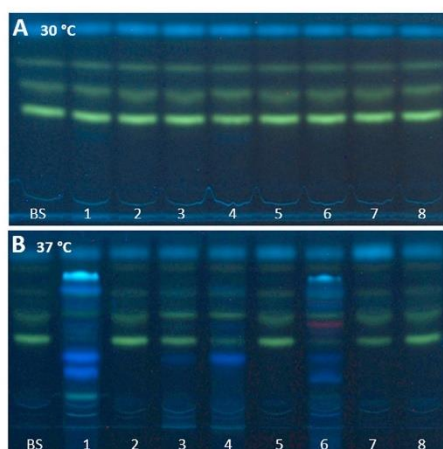
Fig. 3. HPTLC chromatogram at FLD 366 nm of the pYES medium (blank sample, BS) and the *n*–butanol extracts of *Bacillus* candidates **1–8** (200 μL/band each) after 20-h cultivation in pYES medium at a rotation speed of 100 rpm and a cultivation temperature of 30 °C (**A**) and 37 °C (**B**); separation as in Fig. 2.

3.3. Influence of extraction methods on metabolite profile

For the metabolite extraction, different liquid-liquid extractions and a modified QuEChERS method [20] were explored for a high metabolite yield. A phase separation was precondition for liquid-liquid extraction of the cultivation broth, and thus polar extraction solvents like methanol could not be used. Hence, the discovery of polar metabolites is challenging and the direct application of the culture supernatant is recommended along with a selective and sensitive detection of metabolites via derivatization reagents. This would be the best option for a non–target metabolite profiling. However, the application of volumes higher than 300 μL (as 10 mm × 20 mm area) was not possible due to the overload of the start area with medium nutrients, which impaired the subsequent zone focusing and development (Fig. S6). Thus, the direct application of matrix-rich supernatants of culture broths on the HPTLC plate was shown to be possible, but difficult to handle for the subsequent development. For application of the aqueous samples on the NP layer, a low application speed was required to avoid the spreading of the low-volatile liquid excess. The complex medium contains salts and other polar ingredients. These have an abrasive effect on the adsorbent surface, so that the layer may be damaged during spray-on application.

Comparatively easier was the analysis of non–polar metabolites. The selective extraction of mid–polar and non–polar metabolites was studied by the use of *n*-butanol, ethyl acetate, chloroform, toluene and *n*–hexane or combinations. The influence of the different extraction solvents (or a 1:1 mixture with ethyl acetate) on the metabolite profile was investigated exemplarily for the supernatant of the cultivated *B. licheniformis* strain **5**. The application parameters for the different solvents had to be optimized (regular settings were not useful) due to the high volume and individually different, heavy matrix loads. Depending on the extraction solvent, differences in the fluorescence or color intensity were already observed after area application of the extracts (Fig. 4A). These tentative differences in the sample extracts were pronounced clearly after development (Fig. 4B). The HPTLC chromatogram at FLD 366 nm revealed that the most metabolites were extracted with mid–polar solvents. Chloroform extracts showed nearly the same metabo-
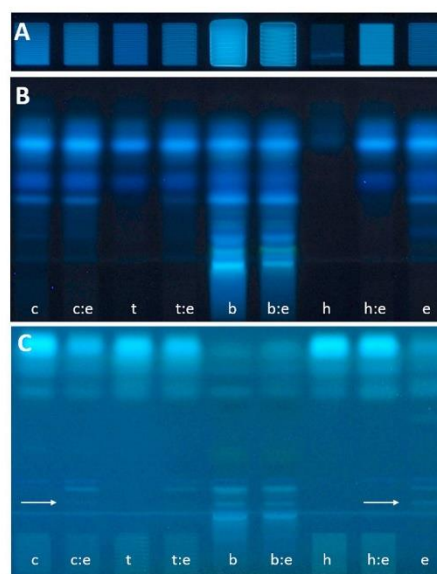
Fig. 4. Application areas (**A**) and HPTLC chromatograms of *B. licheniformis* strain **5** (100 μL/band each), cultivated in TSBY at 37 °C for 35 h and extracted with chloroform (c), ethyl acetate (e), toluene (t), *n*–butanol (b), *n*–hexane (h) or 1:1 mixtures; separation on HPTLC plates silica gel 60 with ethyl acetate – methanol – water 8.2:1.1:0.7, *V/V/V* detected at FLD 366 nm (**B**) and same via the primuline reagent (**C**).

lite profile as ethyl acetate extracts, but more polar metabolites were extracted with *n*–butanol (Figs. 4B and S7A/B). Still, less culture medium components of the TSBY were co–extracted with *n*–butanol and thus applied, if compared to the direct application of the supernatant. This allowed the application of a larger extract volume and a higher application speed. Through this comparison, the importance of selectivity testing of the extraction solvent was demonstrated. However, also multi–imaging gave further insights in the metabolite profile. After FLD detection via the primuline reagent, further apolar but also polar to mid–polar metabolites (Fig. 4C, white arrow) were detected in the ethyl acetate extracts. These results on the extraction selectivity were confirmed by further HPTLC chromatograms exploiting diverse derivatization reagents (not shown) and detection of antioxidants by the radical scavenging assay (Fig. S7C–F).

The influence of the extraction time (15 min and 60 min) and the volume ratio of culture supernatant to extraction solvent (1:1 and 1:3) were also investigated (Fig. 5). The extraction times of 15 min and 60 min did not make a difference in the metabolite profile, meaning no additional bands or a difference in band intensity were detectable (Fig. 5). The volume ratio of culture supernatant to extraction solvent can also have an influence. If the extraction solvent volume is too low, the solvent can be saturated (especially by excessively co–extracting medium nutrients); there could be a possible loss of certain low-concentrated metabolites, which can no longer accumulate in the saturated extraction solvent. Otherwise, if the volume of the extraction solvent is too high, a dilution effect may occur. Hence, two extraction solvent ratios of 1:1 and 1:3 were compared. The higher extraction solvent volume (1:1) resulted in a comparatively much weaker intensity pattern. Thus, a 1:3 volume ratio of extraction solvent to culture su-
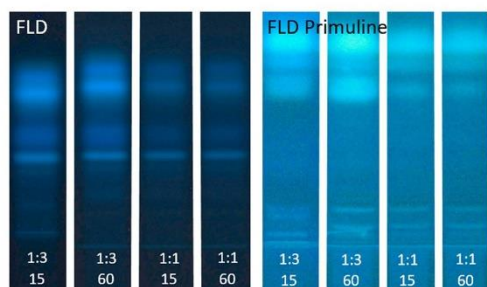
Fig. 5. HPTLC chromatograms of ethyl acetate extracts (volume ratios 1:3 or 1:1 of extraction solvent to culture supernatant, and extraction times of 15 min or 60 min) of *B. subtilis strain* **3** (100 μL/band each), cultivated in TSBY at 37 °C for 40 h, detected at FLD 366 nm (**A**) and same via the primuline reagent (**B**); separation on HPTLC plates silica gel 60 with ethyl acetate – methanol – water 8:1.1:0.7, *V*/*V*/*V*.

pernatant and an extraction time of 15 min were sufficient for metabolite extraction (Fig. 5; results for bacteria **1**, **2** and **5** in Fig. S8). For nutrient-rich cultivation media (TSBY, MH and LB) generating a very high matrix load on the HPTLC plate, the amount of interfering co–extracted matrix was reduced by this selective extraction, but also part of the very polar metabolites could be lost.

The QuEChERS extraction is mainly deployed for pesticide analysis in food and environmental samples. Such a procedure should also reduce the matrix load of nutrient-rich cultivation media and result in a more pronounced metabolite profile. However, neither an improvement nor reduction of the matrix load were achieved. Compared to the extraction with *n*–butanol or ethyl acetate, less metabolites were extracted, and at the same time, the proportion of extracted matrix components increased considerably. Unfortunately, almost exclusively matrix components were observed in the

HPTLC chromatograms (Fig. S9). Normally, the QuEChERS clean-up is tailored for the enrichment of target analytes. In our case of a non–target metabolite screening, neither an improvement in selectivity nor a reduction of the matrix load were achieved via the standard QuEChERS extraction using acetonitrile and salts. An improvement might be achieved by an extended and more dedicated protocol including solid phase extraction of the first QuEChERS extract or a dispersive QuEChERS method [20], but this workflow is too cost- and time-intensive. Especially for screening, a fast workflow is attractive.

3.4. Comprehensive information by HPTLC

The high versatility and flexibility of HPTLC was exploited with regard to application, separation and detection. Various derivatization reactions can be used to identify different metabolite substance classes. The standardized workflow enabled reproducible results. The application area and (as high as possible) application volume was adjusted to the individual sample matrix load. The stationary as well as the mobile phase were varied to study the separation of metabolites from matrix. Any differences in the metabolite profile obtained by NP versus RP separation were examined after detection via the diphenylamine aniline reagent (Fig. 6). A better separation was achieved in the NP system because some of the metabolites were not separated from bands of the blank sample medium and thus not selectively detectable on the RP plate (Fig. 6, orange arrow). On the latter plate, a lot of culture medium matrix was co–extracted, and the pattern of the blank sample compared to that of the bacteria **1**–**8** was almost the same. Only small differences were detected at FLD 366 nm in the RP-HPTLC chromatogram (Fig. 6, white arrows). After the derivatization with the diphenylamine aniline reagent and detection at white light illumination, further substances were revealed which were not visible in the respective medium extract (blank sample) but in the cell culture extract. An effect-directed detection is also advantageous for the metabolite profiling. For example via the *Aliivibrio fischeri*
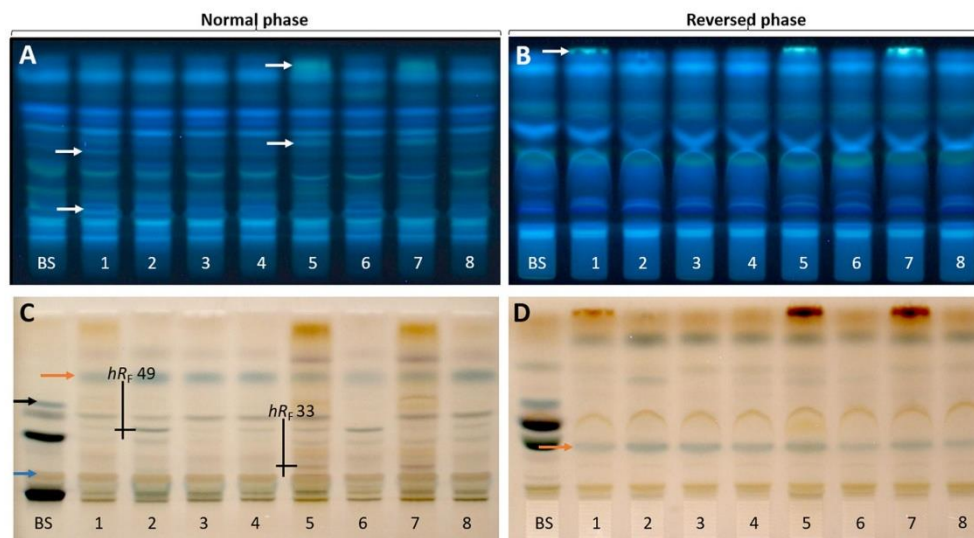
Fig. 6. HPTLC chromatograms of the TSBY medium (blank sample, BS) and the *n*–butanol extracts of *Bacillus* candidates **1**–**8** (200 μL/band each), cultivated in TSBY at 37 °C for 40 h at FLD 366 nm (**A**, **B**) and white light illumination after derivatization with the diphenylamine aniline sulfuric acid reagent (**C**, **D**); NP separation on HPTLC plates silica gel 60 (A, C) and RP separation on HPTLC plates silica gel 60 RP18 (B, D), both with ethyl acetate – methanol – water 8:1.3:0.7, *V*/*V*/*V*.

6

bioassay, differences in the detection of antimicrobial substances were observed for different cultivation times of the *B. subtilis* strain **4** (Fig. S10). Thus, the imaging HPTLC enables the temporal identification of specific antibacterial compounds which could explain a positive probiotic effect.

Both, similarities as differences in the strains of different *Bacillus* species were detected by this powerful imaging. The band at hR_F 33 was only detected in the bacteria species **5** and **7**. This band was also not present in the blank samples. Therefore, it was assumed that this metabolite was formed only in these two species, despite the high genetic similarity to the other bacteria. Hence, inter–species differences in the metabolite concentration were also detected by this imaging. The band at hR_F 49 was visible in all samples, but the intensity of this band was by a factor of five increased in bacteria species **2** and **6**. Apart from the visualization of the metabolite profile, this method can also be used to visualize the respective consumption of the nutrients by the different bacteria candidates. Selective derivatization reagents can be used for detection (*e.g.*, the diphenylamine aniline sulfuric acid reagent for detection of saccharides or the ninhydrin reagent for detection of amino acids or peptides). Some nutrients of the culture medium were completely consumed during the cultivation process, whereas others were detected at the same intensity in the chromatogram (Fig. 6C, black and blue arrow, respectively). For more details about the consumption of individual nutrients, the compound zones can be identified by HPTLC-HRMS and analyzed quantitatively. Thus, it got evident that imaging HPTLC can also be used to optimize and streamline the culture media, *e.g.*, by removal of not consumed nutrients to slim down cultivation broths.

4. Conclusions

Selected *Bacillus subtilis* bacteria strains are used by the food or feed industry due to their attributed probiotic activity. It is assumed that these bacteria can have a positive influence on the intestinal tract and thus on the health of animals or humans. By consuming these bacteria, it must be ensured that there is no harm to the consumer. The demonstrated imaging HPTLC revealed the considerable influence of cultivation parameters on the metabolite profile of strains of different *Bacillus* species. Among others, it visualized not only the intra– and inter–species behavior, but also the behavior of genetically similar strains within a species at different cultivation conditions. The comparative HPTLC screening under identical analytical conditions clearly showed the influence on the bacterial metabolism and thus expressed metabolite profile by variations in the cultivation. Of course, the metabolism in the gastrointestinal tract of animals or humans may differ from those cultured *in vitro* as growth conditions change due to anerobic conditions, influence of nutrients *etc.* among many other reasons. Nevertheless, the quality control of cultivation or fermentation processes can benefit from such a powerful multi–imaging tool, also useful to optimize and streamline culture media.

Declaration of Competing Interest

The authors declare that they have no known competing financial interests or personal relationships that could have appeared to influence the work reported in this paper.

CRediT authorship contribution statement

Stefanie Kruse: Conceptualization, Methodology, Investigation, Formal analysis, Writing - original draft. **Francis Pierre:** Resources, Writing - review & editing. **Gertrud Morlock:** Conceptualization, Methodology, Supervision, Resources, Funding acquisition, Project administration, Writing - review & editing.

References

[1] L.F. Posada-Uribe, M. Romero-Tabarez, V. Villegas-Escobar, Effect of medium components and culture conditions in *Bacillus subtilis* EA-CB0575 spore production, Bioprocess. Biosyst. Eng. 38 (2015) 1879–1888.

[2] C.R. Harwood, *Bacillus subtilis* and its relatives: molecular biological and industrial workhorses, Trends Biotechnol 10 (1992) 247–256.

[3] F. Kunst, N. Ogasawara, I. Moszer, A.M. Albertini, G. Alloni, V. Azevedo, The complete genome sequence of the Gram–positive bacterium *Bacillus subtilis*, Nature 390 (1997) 249–356.

[4] J.L. Sagripanti, M. Carrera, J. Insalaco, M. Ziemski, J. Rogers, R. Zandomeni, Virulent spores of *Bacillus anthracis* and other *Bacillus* species deposited on solid surfaces have similar sensitivity to chemical decontaminants, J. Appl. Microbiol. 102 (2007) 11–21.

[5] M. Jamshidi-Aidji, G.E. Morlock, Fast equivalency estimation of unknown enzyme inhibitors in situ the effect-directed fingerprint, shown for *Bacillus* lipopeptide extracts, Anal. Chem. 90 (2018) 14260–14268.

[6] H. Jork, T.-L. Chromatography, Reagents and Detection Methods, VCH, Weinheim, 1990.

[7] N. Jemil, A. Manresa, F. Rabanal, H. Ben Ayed, N. Hmidet, M. Nasri, Structural characterization and identification of cyclic lipopeptides produced by *Bacillus methylotrophicus* DCS1 strain, J. Chromatogr. B 1060 (2017) 374–386.

[8] C.R. Harwood, J.M. Mouillon, S. Pohl, J. Arnau, Secondary metabolite production and the safety of industrially important members of the *Bacillus subtilis* group, FEMS Microbiol. Rev. 42 (2018) 721–738.

[9] M.N. Taha, M.B. Krawinkel, G.E. Morlock, High-performance thin-layer chromatography linked with (bio)assays and mass spectrometry - a suited method for discovery and quantification of bioactive components? Exemplarily shown for turmeric and milk thistle extracts, J. Chromatogr. A 1394 (2015) 137–147.

[10] M. Jamshidi-Aidji, G.E. Morlock, Bioprofiling of unknown antibiotics in herbal extracts: Development of a streamlined direct bioautography using *Bacillus subtilis* linked to mass spectrometry, J. Chromatogr. A 1420 (2015) 110–118.

[11] T. Kowalska, T. Sajewicz, J. Sherma, Planar Chromatography - Mass Spectrometry. 10 Strategies of Coupling Planar Chromatography to HPLC-MS Eds, 1st ed., CRC Press, Boca Raton, Florida, 2015.

[12] T.T. Häbe, G.E. Morlock, Challenges in quantitative high-performance thin-layer chromatography — Part 1: Influence of densitometric settings on the result, J. Chromatogr. 28 (2015) 426–435.

[13] I. Klingelhöfer, G.E. Morlock, Challenges in quantitative high-performance thin-layer chromatography — Part 2: Influence of the application mode on the result, J. Chromatogr. 30 (2017) 411–417.

[14] D. Fichou, G.E. Morlock, quanTLC, an online open-source solution for videodensitometric quantification, J. Chromatogr. A 1560 (2018) 78–81.

[15] D. Fichou, P. Ristivojević, G.E. Morlock, Proof-of-Principle of rTLC, an open-source software developed for image evaluation and multivariate analysis of planar chromatograms, Anal. Chem. 88 (2016) 12494–12501.

[16] T.T. Häbe, G.E. Morlock, Quantitative surface scanning by direct analysis in real time mass spectrometry, Rapid Commun. Mass Spectrom. 29 (2015) 474–484.

[17] G.E. Morlock, N. Brett, Correct assignment of lipophilic dye mixtures? A case study for high-performance thin-layer chromatography-mass spectrometry and performance data for the TLC-MS Interface, J. Chromatogr. A 1390 (2015) 103–111.

[18] I. Klingelhöfer, G.E. Morlock, Sharp-bounded zones link to the effect in planar chromatography-bioassay-mass spectrometry, J. Chromatogr. A 1360 (2014) 288–295.

[19] I. Klingelhöfer, G.E. Morlock, Bioprofiling of surface/wastewater and bioquantitation of discovered endocrine-active compounds by streamlined direct bioautography, Anal. Chem. 87 (2015) 11098–11104.

[20] M. Anastassiades, S.J. Lehotay, D. Štajnbaher, F.J. Schenck, Fast and easy multiresidue method employing acetonitrile extraction/partitioning and "dispersive solid-phase extraction" for the determination of pesticide residues in produce, J. AOAC Int. 86 (2003) 412–431.

[21] Bacteriological Analytical Manual, Trypticase Soy Broth with 0.6% Yeast Extract (TSBYE), 1998. https://www.fda.gov/food/laboratory-methods-food/bam-media-m154-trypticase-tryptic-soy-broth (accessed 7 January 2021).

[22] J.H. Mueller, J. Hinton, A protein-free medium for primary isolation of the gonococcus and meningococcus, Exp. Biol. Med. 48 (1941) 330–333.

[23] G. Bertani, Studies on lysogenesis i. the mode of phage liberation by lysogenic escherichia coli, J. Bacteriol. 62 (1951) 293–300.

[24] J. Chung, H.E. Yoon, H.C. Shin, E.Y. Choi, W.H. Byeon, Induction of growth phase-specific autolysis in *Bacillus subtilis* 168 by growth inhibitors, J. Microbiol. 47 (2009) 50–59.

[25] E.J. Routledge, J.P. Sumpter, Estrogenic activity of surfactants and some of their degradation products assessed using a recombinant yeast screen, Environ. Toxicol. Chem. 15 (1996) 241–248.

[26] A.D. Warth, Relationship between the heat resistance of spores and the optimum and maximum growth temperatures of *Bacillus* species, J. Bacteriol. 134 (1978) 699–705.

[27] P. Murphy, B.C. Dowds, D.J. McConnell, K.M. Devine, Oxidative stress and growth temperature in *Bacillus subtilis*, J. Bacteriol. 169 (1987) 5766–5770.

[28] P. Graumann, T.M. Wendrich, M.H. Weber, K. Schröder, M.A. Marahiel, A family of cold shock proteins in *Bacillus subtilis* is essential for cellular growth and for efficient protein synthesis at optimal and low temperatures, Mol. Microbiol. 25 (1997) 741–756.

44

Supplementary Information

Imaging high-performance thin-layer chromatography as powerful tool to visualize metabolite profiles of eight *Bacillus* candidates upon cultivation and growth behavior

Stefanie Kruse[a], Francis Pierre[b], Gertrud Morlock[a,*]

[a]Chair of Food Science, Institute of Nutritional Science, and Interdisciplinary Research Centre for Biosystems, Land Use and Nutrition, Justus Liebig University Giessen, Heinrich-Buff-Ring 26–32,

35392 Giessen, Germany

[b]Adisseo France S.A.S, Immeuble Anthony Parc 2, 10 Place du Général de Gaulle, 92160 Antony, France

*Corresponding author: Prof. Dr. Gertrud Morlock, phone: +49-641-9939141; fax +49-641-99-39149, email: gertrud.morlock@uni-giessen.de

Table of Content

2

46

focused two times with acetone, then acetone – methanol and methanol – water (each 1:2, V/V) (B1), two times with acetone and then tetrahydrofuran (B2), both followed by plate cut, and of ethyl acetate extracts either 1 mL concentrated to 100 μL (B3) or 100 μL used directly (B4) focused with acetone and two times methanol, in comparison to the TSBY medium (blank sample, BS); NP separation with ethyl acetate – methanol – water 8.7:1:0.3, V/V/V.	
Fig. S7 HPTLC chromatograms at FLD 366 nm of the ethyl acetate (A) and *n*–butanol (B) extracts of *Bacillus* candidates **1–8** cultivated in TSBY medium (two steps cultivation: pre–culture 16 h, main culture 24 h) at 37 °C and 100 rpm, in comparison to the medium (blank sample, BS), and antioxidant detection at Vis via the DPPH$^\bullet$ assay after 4 h (C, D) and 24 h (E, F; more intense); separation on NP first up to 70 mm with ethyl acetate – methanol 8:0.5, V/V and second up to 40 mm with ethyl acetate – methanol – water 7:2:1, V/V/V.	Page S–9
Fig. S8 HPTLC chromatograms at FLD 366 nm of the different ethyl acetate extracts (100 μL/area; A, B) of selected *B. subtilis* strains **1–3** and *Bacillus licheniformis* **5** cultivated in TSBY in comparison to the medium (blank sample, BS) at 37 °C and 100 rpm for 40 h; separation on NP with ethyl acetate – methanol – water 8:1.1:0.7, V/V/V and detection by the primuline reagent (C, D).	Page S–10
Fig. S9 HPTLC chromatograms of QuEChERS *versus* ethyl acetate extracts of *B. subtilis* strain **1** (cultivated in TSBY at 37 °C at 100 rpm) in comparison to the medium (blank sample, BS) after detection by primuline, 2,2-diphenyl-1-picrylhydrazyl (DPPH$^\bullet$) and diphenylamine aniline sulfuric acid (DPA) reagents; separation on NP with ethyl acetate – methanol – water 8:1.1:0.7, V/V/V for the primuline reagent, with ethyl acetate – methanol 8:0.5, V/V up to 70 mm and then ethyl acetate – methanol – water 7:2:1, V/V/V up to 40 mm for DPPH$^\bullet$ and with ethyl acetate – methanol – water 8.7:1:0.3, V/V/V for the DPA reagent.	Page S–11
Fig. S10 HPTLC chromatogram of the ethyl acetate extracts of *B. subtilis* strain **4** cultivated in TSBY medium (at 37 °C and 100 rpm for different durations of 2–36 h) in comparison to the medium (blank sample, BS) at UV 254 nm (A), and respective bioluminescent *A. fischeri* bioautogram after 3 min (B) and 30 min (C); separation on NP with ethyl acetate – methanol 8:0.5, V/V, up to 70 mm and then ethyl acetate – methanol 8:2, V/V, up to 30 mm.	Page S–12

3

Table S1 Parameters for the liquid-liquid and QuEChERS extractions.

Method	Extraction solvent/salt and volume	Implementation
Liquid-liquid	ethyl acetate (1:1 / 1:3) *n*-hexane (1:3) *n*-butanol toluene chloroform	add extraction solvent to supernatant (1:1, 1:3), shake for 15 min or 60 min (highest speed) and centrifuge by 3.000 *g* (10 min)
QuEChERS	acetonitrile 4 g magnesium sulfate + 1 g sodium chloride	add extraction solvent to supernatant (1:1), vortex for 1 min (highest speed), add salt mixture, vortex for 1 min (highest speed) and centrifuge by 3.000 *g* (1 min)

Table S2 Application parameters for supernatants and extracts.

Application	Application parameters	Problems	Focusing parameters	Problems	Conclusions
Supernatant as area	- 300 µL - 600 nL/s - nozzle heating 60 °C - 10 mm x 20 mm	-	2 x acetone 1 x tetrahydrofuran application zone cut before development	without cut development is not possible due to high matrix load	- long-lasting - analytes lost, which cannot be focused
Extract as band	dependent on solvent (*e.g.*, EtOAc) - 100 µL, - 50 nL/s	- sample volume not always sufficient - long-lasting (slow application speed)	not necessary	-	suitable for small sample volumes
Extract as area	dependent on the solvent (*e.g.*, EtOAc) - < 800 µL, - 1200 nL/s - 8 mm x 10 mm	-	1 x acetone 2 x methanol	handling of manual focusing	- suitable for larger sample volumes - faster application
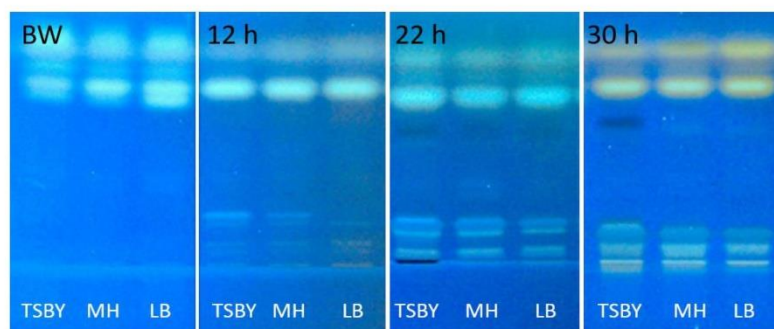
Fig. S1 Metabolite profile comparison in different universal media: HPTLC chromatograms at FLD 366 nm of *B. subtilis* strain **1** after the cultivation in TSBY, MH and LB media (cultivation temperature 37 °C; rotation speed 100 rpm) depending on the cultivation time (12 h, 22 h and 30 h) in comparison to the medium (blank sample BW); separation of the ethyl acetate extract on NP with ethyl acetate – methanol – water 8:1.1:0.7; V/V/V.
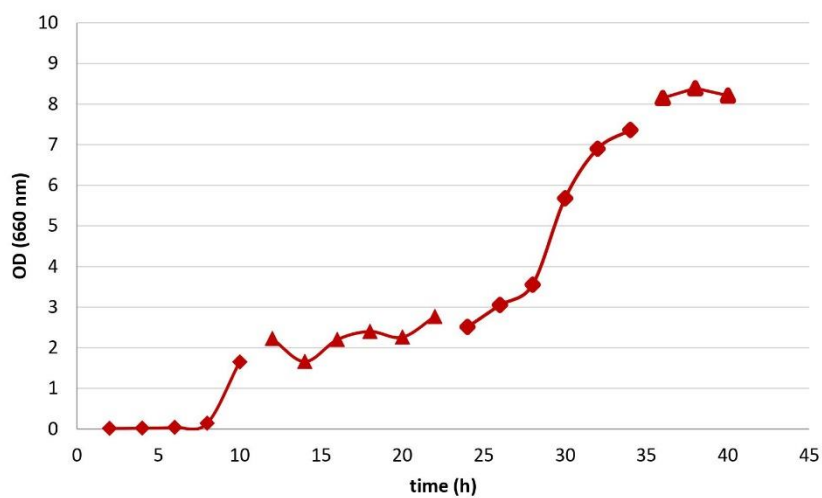
Fig. S2 Diauxic growth behavior observed in TSBY medium for *B. subtilis* strains **1–3** and *Bacillus licheniformis* **5** and in MH medium for *B. subtilis* strain **2;** here exemplarily shown for *B. subtilis* strain **2** in the TSBY medium at 37 °C and a rotation speed of 100 rpm (diamond: first cultivation**,** triangle: second cultivation).

5
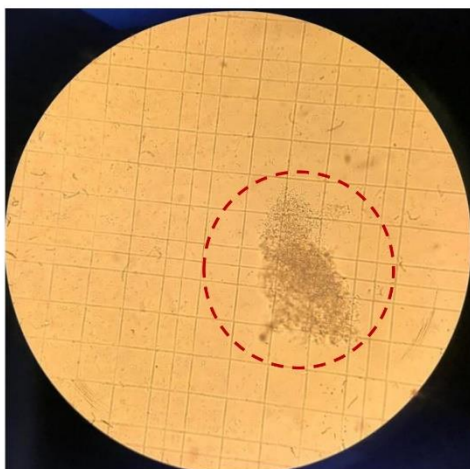
Fig. S3 Cell adhesions effect in *B. subtilis* strain **3** for the cultivation in LB medium at 37 °C and 100 rpm.
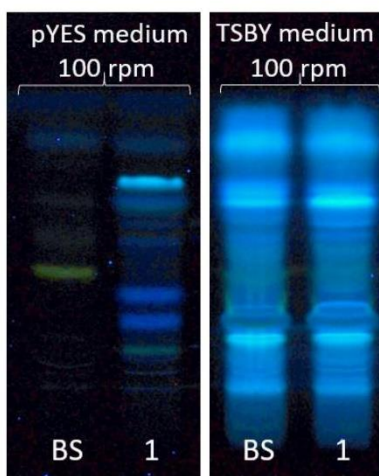
Fig. S4 HPTLC chromatograms at FLD 366 nm of the *n*–butanol extract of *B. subtilis* strain **1** cultivated in pYES or TSBY medium (cultivation temperature 37 °C; rotation speed 100 rpm) compared to the matrix load of the respective culture medium (blank sample, BS); separation on NP with ethyl acetate – methanol – water 8.7:1:0.3, V/V/V.

6
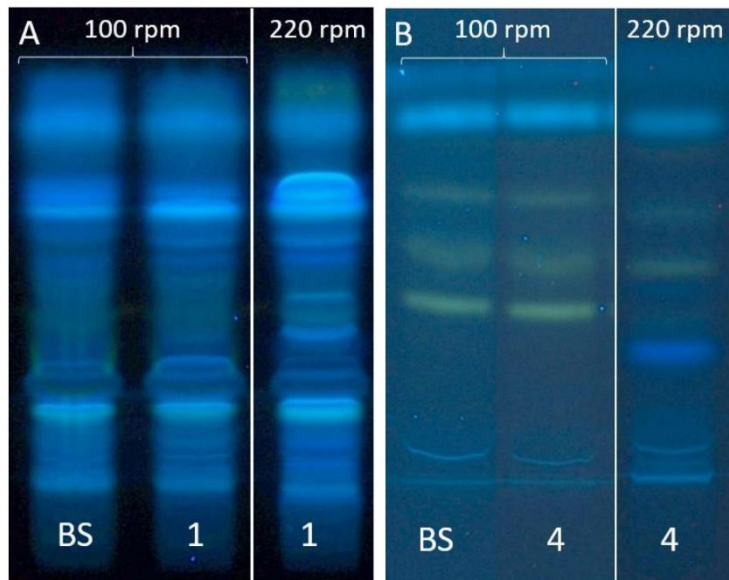
Fig. S5 HPTLC chromatograms at FLD 366 nm of the *n*–butanol extract of *B. subtilis* strain **1** cultivated in TSBY medium with different rotation speeds at 37 °C for 24 h separated on NP with ethyl acetate – methanol – water 8.7:1:0.3, V/V/V (A), and of *B. subtilis* strain **4** cultivated in pYES minimal medium with different rotation speeds at 37 °C for 16 h separated on NP with ethyl acetate – methanol – water 7.5:1.7:0.8, V/V/V (B); both in reference to the respective medium blank (blank sample, BS).

7

52
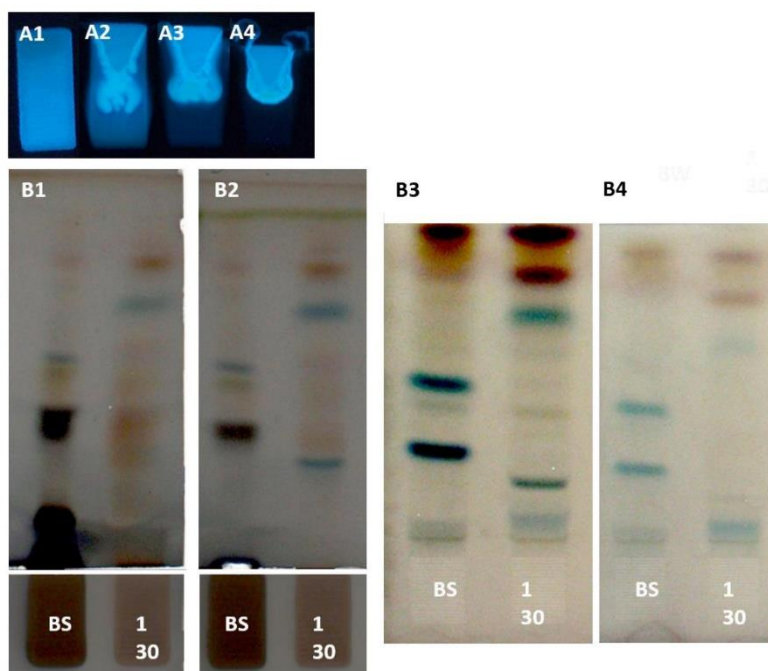
Fig. S6 Influence of the focusing of the area application (10 mm x 20 mm, 150 µL each, 600 nL/s) of *Bacillus licheniformis* **5** supernatant (A1) with acetone – NH$_4$OH (25%) – water 6.5:1.5:2.0, V/V/V (A2) or methanol – water 1:2, V/V (A3) or acetone – water 1:2, V/V (A4) as well as HPTLC chromatograms of supernatants (B1, B2) focused two times with acetone, then acetone – methanol and methanol – water (each 1:2, V/V) (B1), two times with acetone and then tetrahydrofuran (B2), both followed by plate cut, and of ethyl acetate extracts either 1 mL concentrated to 100 µL (B3) or 100 µL used directly (B4), both (8 mm x 10 mm), focused with acetone and two times methanol, in comparison to the TSBY medium (blank sample, BS); NP separation with ethyl acetate – methanol – water 8.7:1:0.3, V/V/V.

8

Fig. S7 HPTLC chromatograms at FLD 366 nm of the ethyl acetate (A) and *n*–butanol (B) extracts of *Bacillus* candidates **1–8** cultivated in TSBY medium (two steps cultivation: pre–culture 16 h, main culture 24 h) at 37 °C and 100 rpm, in comparison to the medium (blank sample, BS), and antioxidant detection at Vis via the DPPH• assay after 4 h (C, D) and 24 h (E, F; more intense); separation on NP first up to 70 mm with ethyl acetate – methanol 8:0.5, V/V and second up to 40 mm with ethyl acetate – methanol – water 7:2:1, V/V/V.

9

54

Fig. S8 HPTLC chromatograms at FLD 366 nm of the different ethyl acetate extracts (100 µL/area; A, B) of selected *B. subtilis* strains **1–3** and *Bacillus licheniformis* **5** cultivated in TSBY in comparison to the medium (blank sample, BS) at 37 °C and 100 rpm for 40 h; separation on NP with ethyl acetate – methanol – water 8:1.1:0.7, V/V/V and detection by the primuline reagent (C, D).

Fig. S9 HPTLC chromatograms of QuEChERS *versus* ethyl acetate extracts of *B. subtilis* strain **1** (cultivated in TSBY at 37 °C at 100 rpm) in comparison to the medium (blank sample, BS) after detection by primuline, 2,2-diphenyl-1-picrylhydrazyl (DPPH•) and diphenylamine aniline sulfuric acid (DPA) reagents; separation on NP with ethyl acetate – methanol – water 8:1.1:0.7, V/V/V for the primuline reagent, with ethyl acetate – methanol 8:0.5, V/V up to 70 mm and then ethyl acetate – methanol – water 7:2:1, V/V/V up to 40 mm for DPPH• and with ethyl acetate – methanol – water 8.7:1:0.3, V/V/V for the DPA reagent.

11

Fig. S10 HPTLC chromatogram of the ethyl acetate extracts of *B. subtilis* strain **4** cultivated in TSBY medium (at 37 °C and 100 rpm for different durations of 2–36 h) in comparison to the medium (blank sample, BS) at UV 254 nm (A), and respective bioluminescent *A. fischeri* bioautogram after 3 min (B) and 30 min (C); separation on NP with ethyl acetate – methanol 8:0.5, V/V, up to 70 mm and then ethyl acetate – methanol 8:2, V/V, up to 30 mm.

12

4. Publication II

Effects of the Probiotic Activity of Bacillus subtilis DSM 29784 in Cultures and Feeding Stuff.

Stefanie Kruse[a], Francis Pierre[b], Gertrud E. Morlock[a,*]

[a]Chair of Food Science, Institute of Nutritional Science, and Interdisciplinary Research Centre for Biosystems, Land Use and Nutrition, Justus Liebig University Giessen, Heinrich-Buff-Ring 26-32, 35392 Giessen, Germany

[b]Adisseo France S.A.S, Immeuble Anthony Parc 2, 10 Place du Général de Gaulle, 92160 Antony, France

PUBLICATION II

Article

Effects of the Probiotic Activity of *Bacillus subtilis* DSM 29784 in Cultures and Feeding Stuff

Stefanie Kruse, Francis Pierre, and Gertrud E. Morlock*

Cite This: https://doi.org/10.1021/acs.jafc.1c04811

Read Online

ACCESS | 📊 Metrics & More | 📄 Article Recommendations | 🔵 Supporting Information

ABSTRACT: The European Union banned the usage of antibiotic growth promoters in animal production. The probiotic microorganism of the genus *Bacillus* appeared to be an attractive candidate to replace antibiotics. The *Bacillus subtilis* DSM 29784 is one of these strains. To date, the probiotic effect has not been completely understood, but it is supposed that the effect depends on metabolites of the microorganism. Imaging high-performance thin-layer chromatography (HPTLC) is a powerful tool to visualize differences in the metabolite profile of bacteria with high genetic similarity to allow a better understanding of the probiotic effect. In comparison to other bacteria, especially these bacterial cells were more robust to harsh cultivation conditions and produced a higher level of antioxidants or bioactive substances such as surfactin. HPTLC enabled the comparison of pure cell cultures to the spore cultivation in the feed, and the results explain and support the probiotic effect.

KEYWORDS: *animal feed, probiotic, antioxidant metabolites, Bacillus spp., imaging HPTLC*

1. INTRODUCTION

Animal production is an important pillar of the food chain. To improve and increase animal production, various measures were taken, such as innovatory animal breeding techniques or practices, diet optimizations, and the use of additives (supplements, auxiliary substances, digestive enhancers, and disease-preventing agents). Animal performance is driven by gut health, which helps to prevent the risk of infectious diseases and digestive disorders.[1] For more than five decades,[2] antibiotic growth promoters were used in industrial animal husbandry to maintain the intestinal health of the animals and thus minimize infections[3] and to improve growth performance and feed efficiency.[4,5] Due to the increase of antimicrobial resistance,[6,7] the European Union banned the use of antibiotic growth promoters in 2006.[3,8] Probiotics are available as an efficacious alternative. The official classification of the Food and Agriculture Organization of the United Nations and the World Health Organization describes probiotics as "live microorganisms which when administered in adequate amounts confer a health benefit on the host".[9] In animal nutrition, the major types of microorganisms used as probiotics include *Bacilli*,[10] *Lactobacilli*,[11] *Bifidobacteria, Enterococci*,[12] and yeasts.[13] These microorganisms support the gut flora by promoting the secretion of analytes hampering the colonization by pathogens and thus improving the health status of the animals. They maintain and optimize the gastrointestinal structure and integrity to enable a full genetic potential or improve the growth. In the poultry industry, several benefits to the immune status and feed efficiency of broilers have already been noted with the use of probiotics.[14−16] The benefits are limited to certain species and even strains and may depend on their ability to tolerate bile salts, heat, and osmotic or oxidative stress in the host environment and during feed processing and storage.[17] *Bacillus* species, which form stable endospores, are

heat resistant and have the ability to survive the gastric barrier,[18] and are very attractive candidates to replace the antibiotics. Previous studies have already shown that *Bacillus* species promote the formation of antioxidants and reduce oxidative stress.[19] Oxidative stress plays an important role in the metabolism and health of farm animals. All biological molecules such as proteins can be damaged by oxidative stress, resulting in structural damage or modified function of macromolecules.[20] Antioxidants could quench oxidative stress reactions by donating electrons to free radicals and prevent oxidation.[21]

The *Bacillus subtilis* DSM 29784 (*B. s.* 29784) has been previously selected via extensive screening based on the absence of antibiotic resistance, the absence of hemolytic and cytotoxic properties, the ability to withstand pelleting and digestive conditions, and *in vitro* anti-inflammatory and anti-*Clostridium perfringens* activities. Tests were also carried out to select the strain with the most efficient germination characteristics. The stability and timely germination of *B. s.* 29784 secure its activity in the intestine. Furthermore, the performance of broilers, reared under different conditions, were increased by their supplementation.[22] Spores of this species were glued on calcium carbonate particles, which allowed a good mixing with the feeding stuff achieving a homogenous blend. A study with 1600 one-day-old Cobb 500 male broiler chicks was performed to investigate the influence of *B. s.* 29784 on the body weight gain, feed intake, feed conversion ratio,

A

mortality, microbiota composition, and intestinal architecture.[22] The results of former studies[23] were confirmed, as the body weight gain of the group treated with *B. s.* 29784 increased compared to the control group, without an increase of the feed intake. Another observation was the increase of bacterial population, which led to an increase in the production of beneficial metabolites such as butyrate and conjugated linoleic acid.[22] These metabolites indicated positive effects after necrotic enteritis[24] or on the energy status and growth performance of broiler chickens.[25]

In an initial study, factors of influence from the cultivation and the general suitability of imaging high-performance thin-layer chromatography (HPTLC) for a meaningful side-by-side metabolite profiling were successfully proven using different *Bacillus* species.[26] In this study, imaging HPTLC was used to visualize differences in the metabolite profile of the probiotic *B. s.* 29784 compared to seven other bacteria of the genus *Bacillus* with high genetic similarity. The visualization of differences in the metabolic profiles helped to understand the probiotic effects, especially with regard to antioxidative substances able to reduce oxidative stress in the gastrointestinal tract, physiologically active substances increasing the body weight, and antimicrobial substances preventing infections.

2. MATERIALS AND METHODS

2.1. Chemicals and Materials. Tryptic soy broth, normal phase (NP) HPTLC plates silica gel 60, glacial acetic acid, and citric acid (per analysis) were purchased from Merck, Darmstadt, Germany. *n*−Butanol [high-performance liquid chromatography (HPLC) grade] and diisopropyl ether (99%, extra pure, stabilized with butylhydroxytoluene) were delivered by Acros Organics, Fair Lawn, NJ, USA. Primuline (≥99%), yeast extract (for use in microbial growth medium), D−glucose (Glc, ≥99.5%), yeast nitrogen base without amino acids (for molecular biology), ninhydrin (≥99%), aniline (≥99.5%), diphenylamine (≥99%), and pancreatin from porcine pancreas (8 × USP specifications) were purchased from Sigma-Aldrich, Steinheim, Germany. Sodium chloride (≥99%) was obtained from Fluka, Buchs, Switzerland. Methanol and acetone (both HPLC grade) were purchased from VWR, Darmstadt, Germany. Hydrochloric acid (37%, purest), magnesium chloride (≥98.5%), calcium chloride (≥98%), dimethyl sulfoxide (≥99.8%), disodium hydrogen phosphate (≥99%), sodium hydroxide (≥99%), 4-anisaldehyde (≥97.5%), and 4-methylumbelliferyl-β-D-galactopyranoside (MUG) were obtained from Carl Roth, Karlsruhe, Germany. 17β-Estradiol (98.5%) was delivered by Dr. Ehrenstorfer, Augsburg, Germany, whereas testosterone (≥99%) was obtained from AppliChem, Darmstadt, Germany. Ethyl acetate (≥99.8%) and *i*-propanol were delivered by Th. Geyer, Renningen, Germany. Acetonitrile (≥99%) and starch (soluble, analytical reagent) were purchased from Honeywell, Morristown, NJ, USA. 2,2-Diphenyl-1-picrylhydrazyl (DPPH•; 95%) was purchased from Alfa Aesar, Haverhill, MA, USA. Ethanol (≥99.8%, HPLC grade) was obtained from Fisher Scientific, Hampton, NH, USA. Bidistilled water was prepared using a Destamat Bi 18E (Heraeus, Hanau, Germany). The marine microorganism *Aliivibrio fischeri* (strain 7151) was provided by Leibniz Institute DSMZ, German Collection of Microorganisms and Cell Cultures, Berlin, Germany. *Saccharomyces cerevisiae* BJ1991, equipped with the human androgen receptor (AR), was delivered by Xenometrix, Allschwil, Switzerland. *S. cerevisiae* BJ3505 (protease-deficient, MATα, pep4:HIS3, Prb1-D1.6R, his3D200, lys2Δ208, trp1-D101, and ura3ΔS2) were genetically modified by McDonnell *et al.* and used as readily prepared cryostock (−80 °C) in a growth medium supplemented with 30% glycerol.[27−29]

2.2. Origin of the *Bacillus* Candidates and Stock Solutions. As candidates, four *Bacillus subtilis* (1: *B. s.* 29784 reference strain, commercially available as ALTERION®NE, ADISSEO France SAS, France, 2: MIC39 genetically similar up to 99.5%, 3: ATCC 6633

genetically similar up to 99.4%, and 4: not identified, genetically similar up to 98.4%), 5: *Bacillus licheniformis* SB3114, 6: *Bacillus pumilus* SB3839, and two *Bacillus amyloliquefaciens* (7: SB3234 and 8: SB3837) strains were obtained from Novozymes, Bagsværd, Denmark. Each *Bacillus* candidate was cultivated in the tryptic soy broth (TSBY; 3% added to 1 L water with 0.6% yeast extract and adjusted to pH 6.2 with 2 M hydrochloric acid solution) at 37 °C up to an optical density (OD) of 0.5 measured at 660 nm (MS01 Single Beam Scanning UV/visible Spectrophotometer, CamSpec, Garforth, UK). The cells were washed two times with 0.9% sodium chloride solution (ratio 2:3, V/V), centrifuged at 2500g for 5 min (centrifuge 5702, Eppendorf, Hamburg, Germany), and then resuspended (ratio 1:3, V/V). The stock solutions were stored at 5 °C in the dark.

2.3. Cultivation. The bacteria were cultivated at 37 °C in TSBY culture medium or minimal medium (sterile solution of 10 g Glc and 6.8 g yeast nitrogen base without amino acids in 100 mL water added to 800 mL autoclaved double distilled water and 100 mL sterile amino acid solution[30,31]) usually used for the planar yeast estrogen screen (pYES). The respective medium (30 mL) was inoculated with 150 μL of the respective stock solution or with a special volume of a diluted feed sample. The rotation speed of the orbital shaker SM-30 (Edmund Bühler, Bodelshausen, Germany) was set to 200 rpm (100 rpm for the pYES culture). The bacteria were cultivated for a defined period, as mentioned.

2.4. Extraction of Metabolites. After cultivation, the OD_{660} was measured. The culture medium was centrifuged at 3000g for 10 min to separate the cells from the supernatant. Liquid−liquid extraction was performed by adding 5 mL *n*-butanol to 15 mL supernatant each (1:3, V/V) and vortexing it for 15 min. Each sample was centrifuged again at 3000g for 10 min and the upper phase was transferred to a vial for further analysis.

2.5. Prechromatographic Simulated Metabolite Digestion. The *n*-butanol extracts were applied and sharpened to bands as described in 2.6. All HPTLC instruments were from CAMAG, Muttenz, Switzerland. A starch solution (2.5 μL/band; 1 mg/mL in water; Automatic TLC Sampler ATS 4) was applied as a positive control. All the bands were oversprayed with the pancreatin solution (1 μL, 20 × 10^{-3} TAME U). A 0.1 M calcium chloride solution (6 pmol/μL) was piezoelectrically sprayed on the plate (2 mL, yellow nozzle, level 6, Derivatizer). The plate was incubated at 37 °C for 1 h in a moistened polypropylene KIS-box (26.5 × 16 × 10 cm, ABM, Wolframs-Eschenbach, Germany) and then dried for 20 min (Automatic Development Chamber ADC 2).[32] The plate part containing the digested starch solution was cut, developed separately (as proof for proper saccharide digestion) with acetonitrile−water−*i*-propanol−acetone (12:3:4:1, V/V/V/V), up to a migration distance of 70 mm (always measured from the lower plate edge), and detected under white light illumination (vis, TLC Visualizer 2) via the diphenylamine aniline *o*-phosphoric acid reagent. The digested *n*-butanol extracts were developed and detected as follows.

2.6. HPTLC Method. The *n*-butanol extracts (100−200 μL) were applied on the NP−HPTLC plate to an area of 8 × 10 mm with a dosage speed of 600 nL/s (ATS 4). The syringe was rinsed twice with methanol after each application. The applied areas were focused (front-eluted) up to 20 mm with acetone and two times with methanol in a twin-trough chamber (20 × 10 cm or 10 × 10 cm). Mostly, a mobile phase of ethyl acetate−methanol−water was used (different solvent ratios as specified). Each development (ADC 2) was performed up to 70 mm after activation of the adsorbent layer with magnesium chloride (33% relative humidity) for 10 min, followed by drying for 5 min. The chromatogram was recorded at vis, UV 254 nm and FLD 366 nm (TLC Visualizer 2).

2.7. Detection of Metabolites via Derivatization. The HPTLC chromatogram was dipped (immersion time 2 s, immersion speed 3.5 cm/s, Chromatogram Immersion Device 3) in the primuline reagent (250 mg primuline in 50 mL water and 200 mL acetone) and dried in a cold stream of air (hairdryer) for 1 min; or in the diphenylamine aniline *o*-phosphoric acid reagent (2 g diphenylamine in 100 mL *i*-propanol and 2 mL aniline in 100 mL *i*-propanol, mixed 1:1, V/V, and slowly added 20 mL *o*-phosphoric acid, 85%); or

60

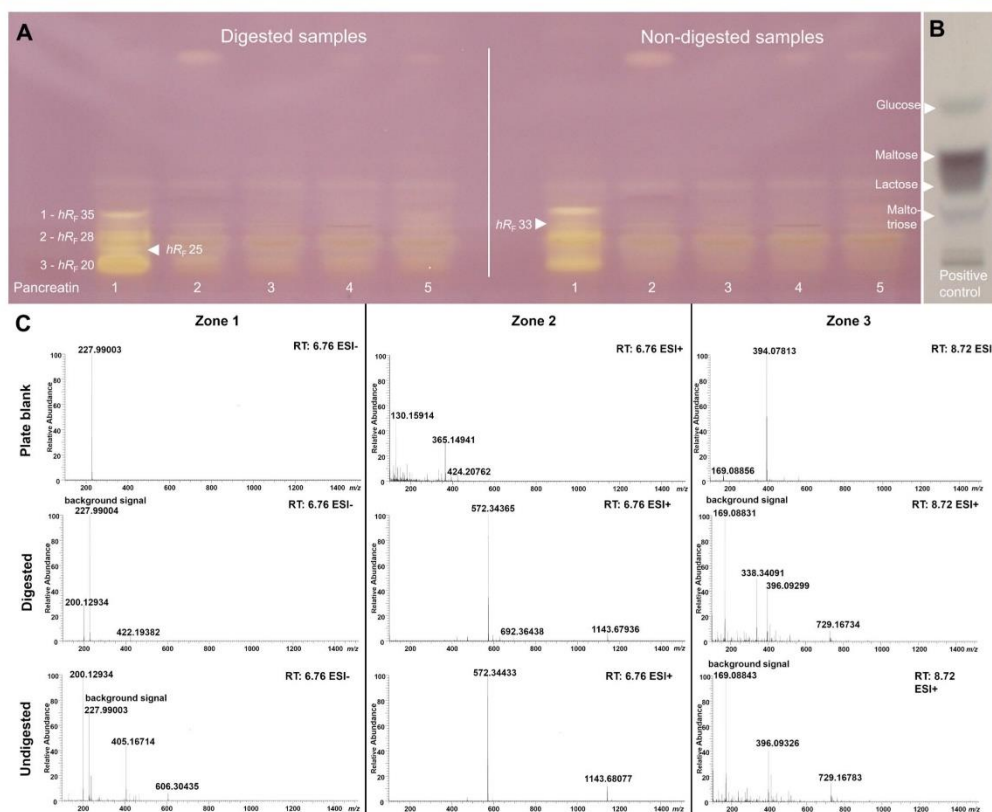**Figure 1.** HPTLC−vis chromatograms under white light illumination of the *Bacillus* candidates (**1−5**, 100 μL/area each) and the pancreatin solution (blank for digestion) after detection by the DPPH• assay: digested and non-digested samples (A) and the positive control (starch) solution after derivatization with the diphenylamine aniline *o*-phosphoric acid reagent (B). The bacteria were cultivated in TSBY at 37 °C and 100 rpm. The *n*-butanol extract was separated on NP plates with ethyl acetate−methanol (16:1, *V/V*) up to 70 mm and then ethyl acetate−methanol−water (7:2:1, *V/V/V*) up to 40 mm. The positive control was developed with acetonitrile−water−*i*-propanol−acetone (12:3:4:1, *V/V/V/V*) up to 70 mm. The negative or positive electrospray ionization HRMS spectra of a specific retention time were compared for the digested versus non-digested zones (C).

in the ninhydrin reagent (500 mg ninhydrin in 230 mL ethanol with 20 mL acetic acid); or in the anisaldehyde sulfuric acid reagent (1.5 mL 4-anisaldehyde in a mixture of 210 mL methanol, 25 mL acetic acid, and 13 mL sulfuric acid). The latter three plates were heated at 110 °C (Plate Heater 3) for approximately 10 min.

2.8. Detection of Radical-Scavenging Metabolites. The positive control gallic acid (100 ng/band; 0.1 mg/mL in methanol) was applied in the upper plate edge. The plate was dipped in the DPPH• assay solution (100 mg DPPH• in 200 mL methanol),[33] dried in a cold stream of air for 1 min, and documented at vis. On the next day, the HPTLC chromatogram was recorded again to detect additional antioxidants of slower reactivity.

2.9. Detection of Antimicrobial Metabolites Active Against *A. fischeri* Bacteria. The positive control caffeine (1 μg/band; 1 mg/mL in methanol) was applied in the upper plate edge. The *A. fischeri* bacteria suspension, overnight cultivated at 75 rpm at room temperature, was piezoelectrically sprayed (3.5 mL, red nozzle, level 6, Derivatizer) onto the plate.[34] 10 bioautograms, each with an exposure time of 100 s, were recorded over 30 min (BioLuminizer 2).

2.10. Detection of Physiologically Active Metabolites by pYES and pYAS Bioassays. The positive control for the pYES bioassay (17β-estradiol at 100 pg/band, 100 pg/μL) or for the planar yeast androgen screen (pYAS) bioassay (testosterone at 750 pg/band, 750 pg/μL) was applied in the upper plate edge. For the pYAS bioassay,[35] the *S. cerevisiae* BJ1991 cell suspension (containing the human AR expression plasmid, Xenometrix), and for the pYES bioassay,[30] the *S. cerevisiae* BJ3505 cell suspension were piezoelectrically sprayed (2.8 mL, red nozzle, level 6, Derivatizer) on the plate and incubated at 30 °C in a moistened polypropylene box either for 3 h (pYES) or 4 h (pYAS). After incubation, the plate was dried for 4 min (cold stream of air; hairdryer). The substrate solution (2 mg MUG in 100 μL dimethyl sulfoxide, diluted with 3 mL citrate phosphate buffer, *i.e.*, 6 g/L citric acid and 10 g/L disodium hydrogen phosphate) was piezoelectrically sprayed (2.3 mL, yellow ultranozzle, level 2) on the plate, which was incubated at 37 °C in a moistened polypropylene box for 1 h. After drying for 4 min, detection was performed at FLD 366 nm.[31]
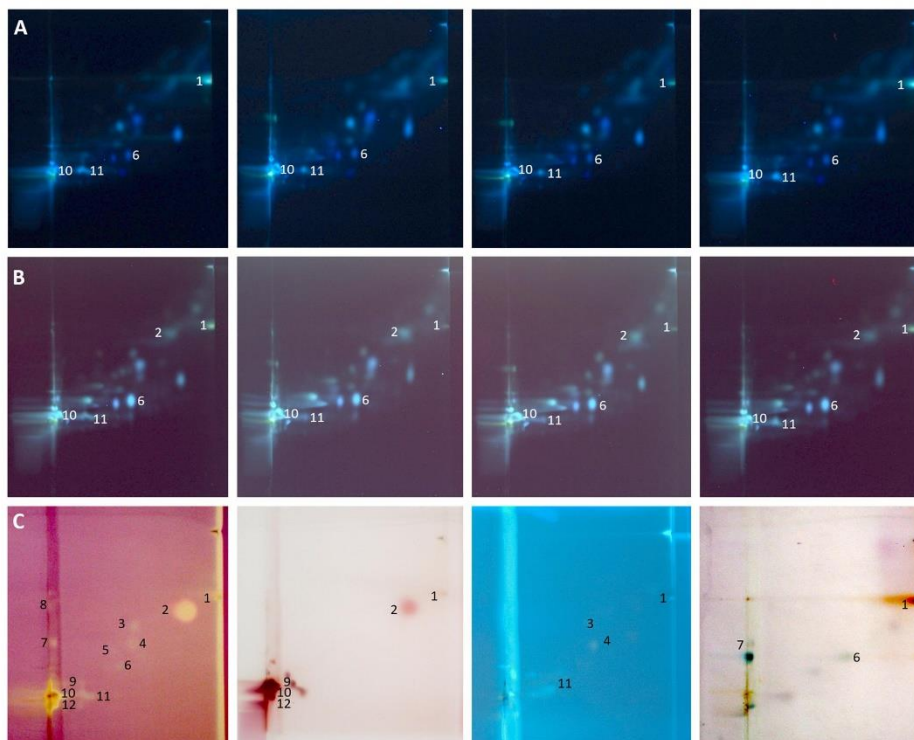
Figure 2. Four 2D-HPTLC chromatograms at FLD 366 nm (A), FLD 254 nm (B), and after derivatization with the DPPH•, ninhydrin, primuline, and diphenylamine aniline o-phosphoric acid reagents at vis/FLD (C) of the n-butanol extract of strain stock solution 1 (80 μL/area each), cultivated in TSBY in two cultivation steps at 100 rpm and 37 °C (first 150 mL stock solution in 30 mL TSBY medium; second 5 mL preculture with 25 mL fresh medium), 2D separated on NP plates with toluene−ethyl acetate−methanol−water−formic acid (12:17:8:2:1, V/V/V/V/V), and after the plate turns by 90°, with diisopropylether−n-butanol−methanol (2:2:1, V/V/V), each up to 75 mm.

2.11. NP−HPTLC−RP−UPLC−PDA−ESI−MS. The NP−HPTLC plate was connected via an elution head-based interface [TLC−MS Interface 2, CAMAG] to the ultra-HPLC−photodiode array detector−electrospray ionization (ESI) mass spectrometry system (UPLC−PDA−ESI−MS; Acquity H Class with PDA and QDa, Waters, Eschborn, Germany). A desalting device and an orthogonal reversed-phase (RP)-HPLC column (Accucore RP−MS 100 × 2.1 mm, 2.6 μm, Thermo Scientific) were installed to reduce the matrix components of the culture medium or the derivatization reagent and to prevent ion suppression of the low-concentrated metabolites.[36,37]

2.12. NP−HPTLC−RP−UHPLC−PDA− HESI−HRMS. The analogous hyphenation was performed, however, using the open-source modified autoTLC−LC−MS, which was fully automated for sequential analysis,[38] connected via a monolithic column (Chromolith Flash RP-18e, 25 × 2 mm, Merck, Darmstadt, Germany) to a high-resolution mass spectrometry (UHPLC−PDA−HESI−HRMS) system with a PDA detector and a Q Exactive Plus Hybrid Quadrupole-Orbitrap Mass Spectrometer (Thermo Fisher Scientific).[39]

3. RESULTS AND DISCUSSION

3.1. Outline of the Study. Eight different *Bacillus* candidates (four *B. subtilis* strains 1−4, one *B. licheniformis* strain 5, one *B. pumilus* strain 6, and two *B. amyloliquefaciens*

strains 7 and 8) were cultivated in two different media. The initial study has already shown that the use of different extraction solvents had an influence on the detection of these metabolites.[26] Hence, the cells were centrifuged and a liquid−liquid extraction with n-butanol as the extraction solvent was used to extract the metabolites out of the supernatant. The metabolites were analyzed by imaging HPTLC with a focus on the detection of radical-scavenging (antioxidant), physiologically active, and antimicrobial metabolites. The aim was to investigate if the metabolites produced by the probiotic *Bacillus B. s.* 29784 (strain 1) provide a better understanding of the postulated probiotic effect from animal feed supplemented with *B. s.* 29784. In particular, potential radical-scavenging metabolites, which could reduce oxidative stress in the gastrointestinal tract, potential physiologically active metabolites, which could increase the body weight, and potential antimicrobial metabolites, which could prevent infections were targeted.

3.2. Detected Metabolites Providing Evidence for Use of Strain 1 in Livestock Farming. Under different cultivation conditions, mostly the strain 1 achieved the highest OD_{660} in the shortest cultivation duration. The results of the analysis of antioxidants confirmed these rapid growth results.
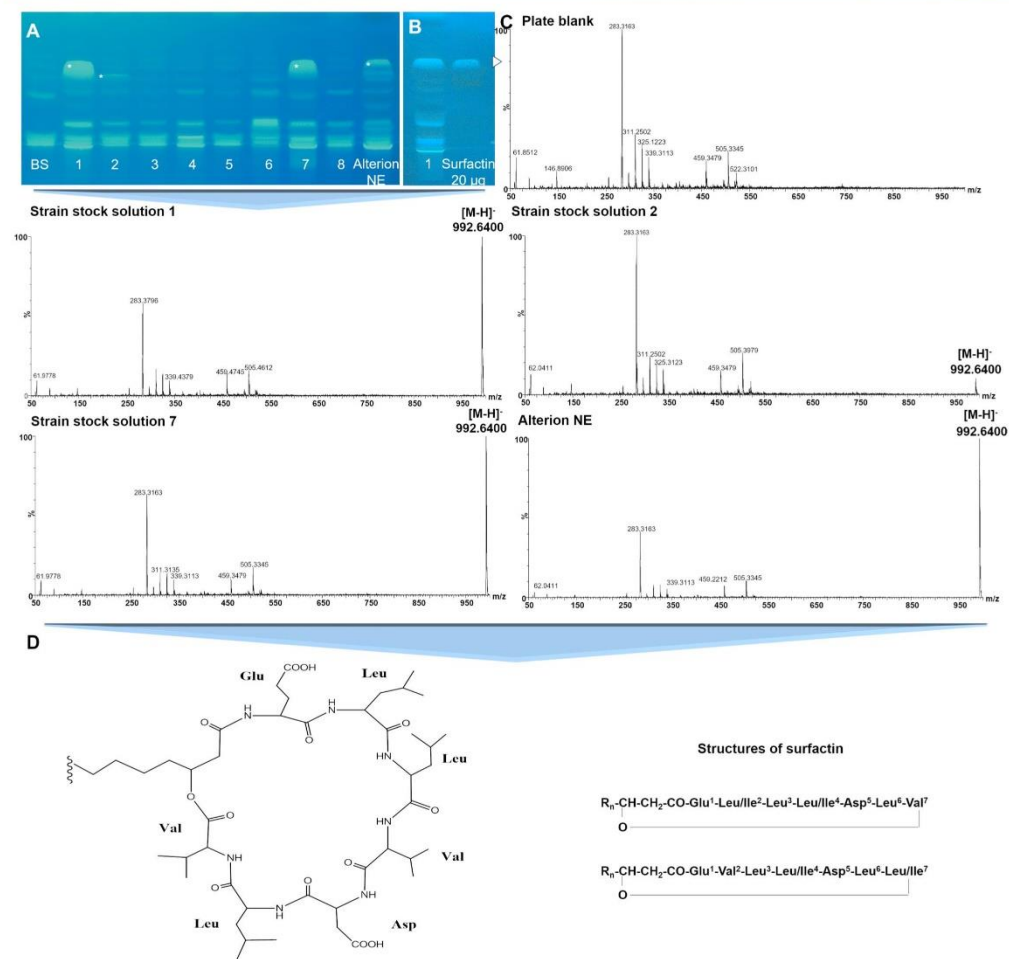
D

Figure 3. HPTLC chromatogram at FLD 366 nm of the blank sample, the eight different *Bacillus* candidates (**1**−**8**, 100 μL/area each, *n*-butanol extracts) and the feed additive sample *B. s.* 29784 after derivatization with primuline (A). The bacteria were cultivated in TSBY at 37 °C and 200 rpm for 16 h and separated on NP with ethyl acetate−methanol−water (8.3:1.2:0.5, *V/V/V*). The identification of surfactin (D) was performed in comparison to a standard solution of surfactin (B; 10 μg/μL, 20 μg/area) and by mass spectrometry (C; eluted zones marked*, plate blank at hR_F 59).

All strains produced nearly the same antioxidants (Figure 1) but the produced amount of antioxidants was much higher in the strain **1**.[26] This higher level of antioxidants could explain a positive effect on treated broilers, as the redox system is balanced so that the various macromolecules (proteins and enzymes) can perform their functions and thus contribute to the health of the chicks. For a better characterization of these polar antioxidative metabolites, the mobile phase was adjusted and several derivatization reagents were exploited. At least two zones were detected, which were only visible in stock solution of strain **1** (Figure S1A, black arrows). These specific zones could also be explained by the faster growth of this probiotic *Bacillus*. The use of different derivatization reagents indicated

that the detected antioxidants are of different structural substance classes such as lipopeptides, glycopeptides, and glycolipopeptides (Figure S1B−E). A better characterization was achieved after a two-dimensional (2D) development of the strain **1** stock solution (Figure 2), which separated the coeluting metabolites. Especially, the 2D HPTLC−DPPH• assay separation clearly pointed to three polar antioxidants in the start area (Figure 2, zones 9, 10, and 12) and another more apolar antioxidant (Figure 2, zone 2), all of which were also detected by the ninhydrin reagent indicating the presence of amino or peptide groups in the molecule.

Additionally, the intestinal digestion of the metabolites was simulated. The influence of pancreatic enzymes on these
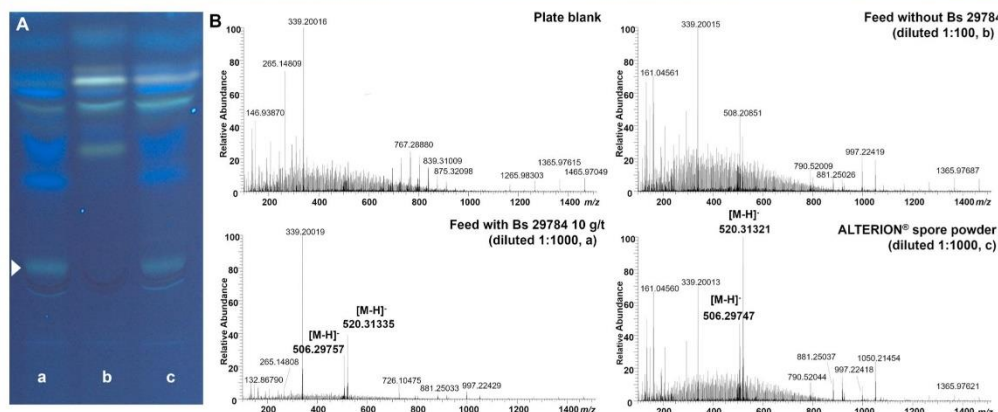
E

Figure 4. HPTLC chromatogram at FLD 366 nm of the *n*-butanol extracts (A; 100 μL/area each) from a supplemented (a) and unsupplemented (b) feed sample as well as the *B. s.* 29784 spore powder (c, diluted 1:1000 with PBS) cultivated for 16 h in the pYES minimal medium at 37 °C and a rotation speed of 100 rpm. The extracts were separated on NP plates with ethyl acetate−methanol−water (7.5:1.7:0.8, *V/V/V*) and the ESI⁻-HRMS spectra of the marked zones (B) were recorded.

antioxidants was studied, whereby starch was used as positive control. Compared to the non-digested extract of strain **1**, an additional zone at hR_F 25 and a more intense zone at hR_F 20 were recognized after the simulated intestinal on-surface digestion. Another observation was the decrease in intensity of the zone at hR_F 33 and 35. The enzymes digested these substances or used them to protect themselves from oxidative stress. These processes can also occur in the intestine of the animals. The main digestion enzymes in the intestine of broilers are trypsin, chymotrypsin, amylase, and lipase, which were also present in the used pancreatin. For a comparison of the digested with the non-digested samples, the metabolites were heart-cut eluted and transferred to a RP column for orthogonal separation and detection by HESI−HRMS. The HPLC chromatograms revealed coeluting metabolites (Figure S2). In contrast to the previous 2D HPTLC−DPPH• assay, which clearly pointed to the main antioxidants due to the effect-detection, here (via HPTLC−heart-cut HPLC−HESI−HRMS) the main antioxidants were not clear among all the peaks. The HRMS spectra of one specific retention time (Figure 1, zones 1−3) were illustrated to demonstrate the principle of digestion. The comparison of the HRMS signals of digested versus non-digested samples revealed, for example, the complete (*e.g.*, zone 1, ESI⁻, RT 6.76 min, m/z 405.16714, and m/z 606.30435) or the partial (*e.g.*, zone 2, ESI⁺, RT 6.76 min, and m/z 1143.68077) digestion of metabolites, and in contrast, the detection of newly formed substances after digestion (*e.g.*, zone 3, ESI⁺, RT 8.72 min, and m/z 338.34091). In the digested samples, a higher number of lower m/z signals and a lower number of higher m/z signals (or even their absence) were detected, if compared to the non-digested samples (Figure 1C). This provides evidence for the successful simulated digestion of the applied samples, besides the properly digested positive control.

In addition to the increased amount of antioxidants, which are partially digestible, an increased amount of the bacterial biosurfactant surfactin was detected in the *n*-butanol extracts of strains **1** and **7** (*B. amyloliquefaciens* SB3234), if compared to the other strains (Figure 3A). This lipopeptide was identified

via HRMS (deprotonated molecule [M⁻H]⁻ at m/z 992.6400,[40,41] Figures 3C and S3), physisorption to the primuline reagent (indicates the lipophilic moiety), and standard comparison by HPTLC−FLD (Figure 3B). The primuline attaches to lipophilic moieties in the structure and thus makes the molecule blue fluorescent at FLD 366 nm. After cultivation of a feed additive sample of the probiotic strain **1** (*B. s.* 29784), surfactin was also detected as a relevant bioactive molecule. The other detected HRMS signals from the surfactin zone in the strain stock solutions as well as in the feed additive sample *B. s.* 29784 were background signals, which were also detectable in the spectrum of the plate blank (Figure 3C).

With regard to the bacterial surfactin production, the two strain stock solutions **1** and **2** were comparatively investigated in more detail using two different cultivation protocols (Figure S4). After the single-step cultivation, the strain stock solution **1** already produced surfactin at a considerable amount, whereas the strain stock solution **2** produced only small amounts. It was evident that the strain **1** had an increased production of this biosurfactant compared to the other *Bacillus* candidate. After the longer-lasting two-step cultivation, the strain stock solution **2** also produced surfactin at a comparable amount to strain **1**, which produced it, however, much faster after a single cultivation step. After the longer two-step cultivation, surfactin was again degraded/digested in the strain stock solution **1**, which indicated that bacteria use surfactin for further growth. Hence, the intestinal digestion was also simulated for surfactin, and a considerable reduction of surfactin was detected on the HPTLC chromatogram after simulated intestinal on-surface digestion (Figure S5). These results indicate the conversion and the positive effect of surfactin on vegetative cells for further growth. Other beneficial effects are already known of these non-ribosomal peptides, such as antifungal,[42] antimicrobial, and surface-active properties.[43]

3.3. Specific Characteristics of Strain 1. Only small fluctuations in the metabolite profile of the different bacteria were observed under optimal cultivation conditions. However, after 20 h cultivations under more stressful conditions
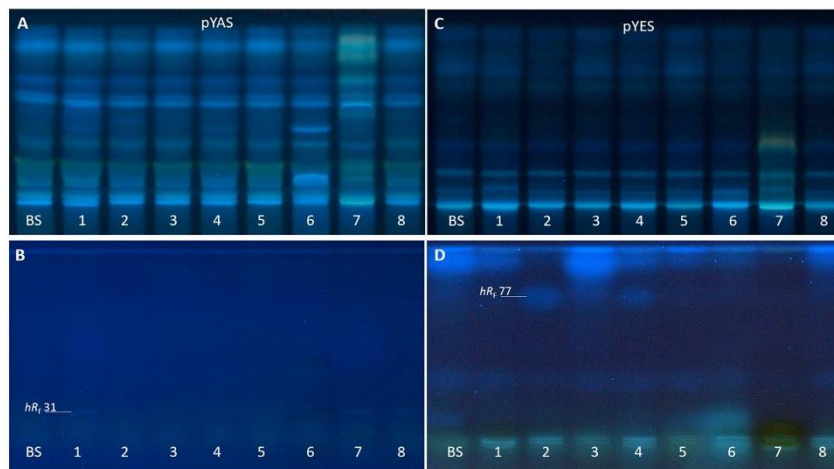
F

Figure 5. HPTLC chromatogram at FLD 366 nm before (A,C) and after the bioassay (B,D) of a blank sample (BS, TSBY) and the *Bacillus* candidates **1**−**8** cultivated in TSBY (16 h, 37 °C, 200 rpm). Their *n*-butanol extracts (100 μL/area each) were separated on NP with ethyl acetate−methanol−water (8.3:1.2:0.5, *V/V/V*) for the pYAS bioassay (B) or ethyl acetate−methanol (16:1, *V/V*) for the pYES bioassay (D) to detect 4-methylumbelliferone-blue fluorescent physiologically active substances at FLD 366 nm.

(minimal medium and a slower rotation speed), a significantly higher cell number for the strain stock solution **1** was obtained compared to the other strains. The growth conditions heavily influenced the metabolite profiles of the five *Bacillus* candidates **2**, **3**, **5**, **7**, and **8**, which stopped the production of metabolites, as evident in the HPTLC chromatogram at FLD 366 nm. Only the bands of the blank sample (pYES medium) were noticed (Figure S6). In contrast, candidate **1** produced several metabolites of highest intensity, compared to the metabolite patterns at a lower intensity of candidates **4** and **6**. The turquoise (hR_F 31) and the blue (hR_F 40) zones were only detectable in strain **1**. These specific metabolites were produced by defined cultivation parameters (a 200 rpm rotation speed and pYES minimal medium). For a prolonged cultivation, the blue zone was detected in the other bacterial stock solutions, too. Also, the turquoise zone was detected in some bacterial stock solutions. The faster growth of strain **1** stock solutions associated with the production of two specific metabolites may also explain the probiotic effect. The positive effect cannot directly be linked to the two metabolites at hR_F 31 and 40, but it highlights the robust metabolism of this probiotic strain compared to the other *Bacillus* candidates. The feed is supplemented with spores of this probiotic *Bacillus* strain (added as premix containing spores glued on calcium carbonate), which should sprout in the gastrointestinal tract of the animals, and obviously form metabolites more easily. Comparably harsh conditions exist in the gastrointestinal tract of the animals. The robustness of this strain could lead to an earlier sprout or better survival of the vegetative cells, which could influence the probiotic effect positively.

A similar robustness and metabolite profile of the strain **1** either as stock solution, or as *B. s.* 29784 spores (premix containing spores glued on calcium carbonate), or in feed supplemented with *B. s.* 29784 spores would support the probiotic effect. Feed without the probiotic strain was used as the control sample. The cultivation conditions remained unchanged. The spores in the feed were able to sprout despite the high dilutions (10 ng *B. s.* 29784 in the culture), and comparable metabolite profiles of the cultivated stock solutions and spores were observed in the HPTLC−FLD chromatogram and the corresponding mass spectra (Figure 4). The HRMS spectrum of spore powder of *B. s.* 29784 was comparable to the spectrum of the supplemented feed (Figure 4C), whereas the untreated feed (control sample) showed a different HRMS spectrum. The presence of feed ingredients had no influence on the expressed metabolite profile, that is, the detected metabolites of the stock solutions were comparable with those of the supplemented feed for the given cultivation conditions. Nevertheless, it was noticed that the feed ingredients had an influence on the extraction of the metabolites. A dilution of the feed was necessary to highlight the metabolites and to minimize the extraction of feed ingredients, which could suppress the HRMS detection of metabolites (Figure S7, with dilution reduced tailing along the track). The robustness of the probiotic bacteria to the production process as well as subsequent germination of the spores is of high importance. The results pointed to a better adaption of strain **1** to harsh cultivation conditions compared to the other bacteria. These aspects were also confirmed by the metabolite profiles of the vegetative cells in comparison to the spores in the supplemented feed.

3.4. Detection of Physiologically Active or Antimicrobial Substances. The influence on the increase of the body weight gain at constant feed intake can be caused by the presence of physiologically active substances. As reported, the supplementation with probiotics showed an effect on the concentration of growth hormones, which were produced by the animals themselves.[44] The focus was on the production of physiologically active metabolites in animals, fed with supplemented versus non-supplemented feed. However, also physiologically active substances, which were produced by the *Bacillus* species itself, could be responsible for the observed
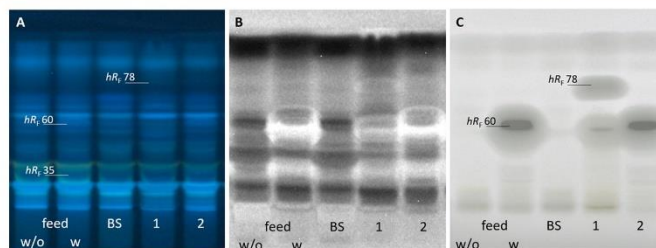
Figure 6. HPTLC chromatogram at FLD 366 nm (A), *A. fischeri* bioautogram after 9 min (B) and under white light illumination (C) of a supplemented (w) as well as unsupplemented (w/o) feed sample (diluted 1:10 with PBS) and a blank sample (BS) in comparison to the strain stock solutions 1 and 2. The feed was cultivated in TSBY medium at 37 °C and 200 rpm for 16 h (one-step cultivation) and the samples were cultivated in TSBY medium at 37 °C and 100 rpm in a two-step cultivation process (first 150 μL stock solutions in 30 mL TSBY; second 5 mL of the preculture diluted with 25 mL fresh medium). The *n*-butanol extracts were separated on NP with ethyl acetate−methanol−water (8:1.3:0.7, *V/V/V*).

growth performance. Hence, the pYES and pYAS bioassays were performed to study the presence of any active substances in the metabolite profiles of the different bacterial candidates. In their *n*-butanol extracts, no androgen-like metabolites were detected (Figure 5B). Some zones at hR_F 31 were slightly blue fluorescent in the pYAS bioautogram, however, these zones were already natively blue fluorescent before the bioassay application. The intensity of the zone at hR_F 31 was more pronounced in candidates 1 and 7 than in the other bacteria. This confirms the previously described faster metabolic rate of the cells.

A metabolite zone at hR_F 77 was detected in candidates 2 and 4 (Figure 5D). It indicated that these bacteria possess the possibility to form physiologically active metabolites under certain conditions. However, no active metabolite was detected in the strain stock solution 1, which could support and explain the postulated probiotic effects of this *B. subtilis* strain. Note that in and near the solvent front of the blank sample and of the candidates, estrogen-like substances were detected, which most likely derive from the soy meal in the TSBY medium. Soy meal contains flavonoids, which are known to exhibit phytoestrogenic activities. The comparison of these zones in the different bacterial candidates revealed that the candidates differently metabolized the flavonoids for their growth.

Furthermore, bioactive metabolites can have a positive effect on the health of animals. In the feed sample and the strain stock solutions 1 and 2, up to three luminescent zones were detectable (Figure 6B, hR_F 35, 60, and 78) in the *A. fischeri* bioautogram. The last two compound zones of a higher hR_F value were lipophilic, as both zones were visible (different transparency) in the *A. fischeri* bioautogram under white light illumination in the transmission mode (Figure 6C). The bioactive substances at hR_F 35 and 60 were detectable in all *Bacillus* candidates and the supplemented feed sample. The substance at hR_F 60 was identified as surfactin (via comparison with the respective standard on the HPTLC plate), which was proven to be present not only in strain 1, but also in the supplemented feed. The intensity of surfactin was more intense in the supplemented feed (one-step cultivation) than in the strain stock solution 1, which, however, was prepared as two-step cultivation (Figure 6B/C). The faster production of surfactin by strain 1 in a one-step instead of two-step cultivation (two-step cultivation, Figure S4) needs to be considered in this comparison. The one-step cultivation clearly

showed that strain 1 produced surfactin more rapidly and intensively than strain 2. The weak bioactive compound zone at hR_F 78 is only detectable in four strain stock solutions (1, 3, 5, and 7). This metabolite was not detected in the feed sample. Thus, the metabolism and the probiotic effect depend also on the duration time of still active cells in the intestine of the animals, fed with supplemented feed. Additionally, the feed ingredients could influence the metabolism of the bacteria. The magnitude of this influence depends on the investigated metabolites. Imaging HPTLC enabled the investigation of these influences to improve the understanding of the different metabolisms.

■ ASSOCIATED CONTENT

ⓢ Supporting Information

The Supporting Information is available free of charge at https://pubs.acs.org/doi/10.1021/acs.jafc.1c04811.

Characterization of metabolites produced by strain stock solutions 1 and 2; comparison of the HPLC chromatograms after elution of the digested and the non-digested zones; HPTLC chromatograms after derivatization of the eight different *Bacillus* candidates and feed premix Alterion NE, *A. fischeri* bioautogram of strain stock solution extracts and feed, HPTLC chromatograms after derivatization of the extracts of the undigested and digested *Bacillus* candidates 1−4, HPTLC chromatograms of the extracts of the pYES medium blank sample and *Bacillus* candidates 1−8, and of four dilutions of the commercial formulation Alterion NE (PDF)

■ AUTHOR INFORMATION

Corresponding Author

Gertrud E. Morlock − *Institute of Nutritional Science, Chair of Food Science, and Interdisciplinary Research Centre for Biosystems, Land Use and Nutrition, Justus Liebig University Giessen, Giessen 35392, Germany;* ◉ orcid.org/0000-0001-9406-0351; Phone: +49-641-9939141; Email: gertrud.morlock@uni-giessen.de; Fax: +49-641-99-39149

Authors

Stefanie Kruse − *Institute of Nutritional Science, Chair of Food Science, and Interdisciplinary Research Centre for*

PUBLICATION II

Biosystems, Land Use and Nutrition, Justus Liebig University Giessen, Giessen 35392, Germany

Francis Pierre − *Adisseo France S.A.S, Antony 92160, France*

Complete contact information is available at:
https://pubs.acs.org/10.1021/acs.jafc.1c04811

Author Contributions

S.K. contributed in conceptualization, methodology, experimental analysis, data analysis, and writing—original draft. F.P. contributed in resources and review—paper. G.E.M. contributed in conceptualization, methodology, supervision, resources, and writing—review and editing.

Notes

The authors declare no competing financial interest.

■ REFERENCES

(1) Choct, M. Managing gut health through nutrition. *Br. Poult. Sci.* **2009**, *50*, 9−15.

(2) Libby, D. A.; Schaible, P. J. Observations on growth responses to antibiotics and arsonic acids in poultry feeds. *Science* **1955**, *121*, 733−734.

(3) Dibner, J. J.; Richards, J. D. Antibiotic growth promoters in agriculture: history and mode of action. *Poultry Sci.* **2005**, *84*, 634−643.

(4) Castanon, J. I. R. History of the use of antibiotic as growth promoters in European poultry feeds. *Poultry Sci.* **2007**, *86*, 2466−2471.

(5) Al-Khalaifah, H. S. Benefits of probiotics and/or prebiotics for antibiotic-reduced poultry. *Poultry Sci.* **2018**, *97*, 3807−3815.

(6) Smith, M.; Do, T. N.; Gibson, J. S.; Jordan, D.; Cobbold, R. N.; Trott, D. J. Comparison of antimicrobial resistance phenotypes and genotypes in enterotoxigenic Escherichia coli isolated from Australian and Vietnamese pigs. *J Glob Antimicrob Resist.* **2014**, *2*, 162−167.

(7) Bedford, M. Removal of antibiotic growth promoters from poultry diets: implications and strategies to minimise subsequent problems. *Worlds Poultry Sci. J.* **2000**, *56*, 347−365.

(8) Official Journal of the European Union. Regulation (EC) No 1831/2003 of the European Parliament and of the Council of 22 September 2003 on additives for use in animal nutrition; Official Journal of the European Union, 2003; Vol. 268, pp 29−43. https://eur-lex.europa.eu/legal-content/EN/TXT/PDF/?uri=CELEX:32003R1831 (accessed on Sept 1 2021).

(9) FAO/WHO. Joint FAO/WHO Working Group Report on Drafting Guidelines for the Evaluation of Probiotics in Food; FAO/WHO: Canada, April 30 and May 1, 2002. www.who.int/foodsafety/fs_management/en/probiotic_guidelines.pdf (accessed on Sept 1 2021).

(10) Prieto, M. L.; O'Sullivan, L.; Tan, S. P.; McLoughlin, P.; Hughes, H.; O'Donovan, O.; Rea, M. C.; Kent, R. M.; Cassidy, J. P.; Gardiner, G. E.; Lawlor, P. G. Evaluation of the efficacy and safety of a marine-derived Bacillus strain for use as an in-feed probiotic for newly weaned pigs. *PloS One* **2014**, *9*, No. e88599.

(11) Dowarah, R.; Verma, A. K.; Agarwal, N. The use of Lactobacillus as an alternative of antibiotic growth promoters in pigs: A review. *Anim. Nutr.* **2017**, *3*, 1−6.

(12) Miyazaki, Y.; Yokota, H.; Takahashi, H.; Fukuda, M.; Kawakami, H.; Kamiya, S.; Hanawa, T. Effect of probiotic bacterial strains of Lactobacillus, Bifidobacterium, and Enterococcus on enteroaggregative Escherichia coli. *J. Infect. Chemother.* **2010**, *16*, 10−18.

(13) Trckova, M.; Faldyna, M.; Alexa, P.; Zajacova, Z. S.; Gopfert, E.; Kumprechtova, D.; Auclair, E.; D'Inca, R. The effects of live yeast Saccharomyces cerevisiae on postweaning diarrhea, immune response, and growth performance in weaned piglets. *J. Anim. Sci.* **2014**, *92*, 767−774.

(14) Mountzouris, K. C.; Tsirtsikos, P.; Kalamara, E.; Nitsch, S.; Schatzmayr, G.; Fegeros, K. Evaluation of the efficacy of a probiotic containing Lactobacillus, Bifidobacterium, Enterococcus, and Pediococcus strains in promoting broiler performance and modulating cecal microflora composition and metabolic activities. *Poultry Sci.* **2007**, *86*, 309−317.

(15) Awad, W. A.; Ghareeb, K.; Abdel-Raheem, S.; Böhm, J. Effects of dietary inclusion of probiotic and synbiotic on growth performance, organ weights, and intestinal histomorphology of broiler chickens. *Poultry Sci.* **2009**, *88*, 49−56.

(16) Gao, Z.; Wu, H.; Shi, L.; Zhang, X.; Sheng, R.; Yin, F.; Gooneratne, R. Study of Bacillus subtilis on growth performance, nutrition metabolism and intestinal microflora of 1 to 42 d broiler chickens. *Anim. Nutr.* **2017**, *3*, 109−113.

(17) Ross, R. P.; Desmond, C.; Fitzgerald, G. F.; Stanton, C. Overcoming the technological hurdles in the development of probiotic foods. *J. Appl. Microbiol.* **2005**, *98*, 1410−1417.

(18) Cutting, S. M. Bacillus probiotics. *Food Microbiol.* **2011**, *28*, 214−220.

(19) Surai, P. F.; Kochish, I. I.; Fisinin, V. I.; Kidd, M. T. Antioxidant Defence Systems and Oxidative Stress in Poultry Biology: An Update. *Antioxidants* **2019**, *8*, 235.

(20) Celi, P.; Gabai, G. Oxidant/Antioxidant Balance in Animal Nutrition and Health: The Role of Protein Oxidation. *Front. Vet. Sci.* **2015**, *2*, 48.

(21) Lykkesfeldt, J.; Svendsen, O. Oxidants and antioxidants in disease: oxidative stress in farm animals. *Vet. J.* **2007**, *173*, 502−511.

(22) Jacquier, V.; Nelson, A.; Jlali, M.; Rhayat, L.; Brinch, K. S.; Devillard, E. Bacillus subtilis 29784 induces a shift in broiler gut microbiome toward butyrate-producing bacteria and improves intestinal histomorphology and animal performance. *Poultry Sci.* **2019**, *98*, 2548−2554.

(23) Latorre, J. D.; Hernandez-Velasco, X.; Bielke, L. R.; Vicente, J. L.; Wolfenden, R.; Menconi, A.; Hargis, B. M.; Tellez, G. Evaluation of a Bacillus direct-fed microbial candidate on digesta viscosity, bacterial translocation, microbiota composition and bone mineralisation in broiler chickens fed on a rye-based diet. *Br. Poult. Sci.* **2015**, *56*, 723−732.

(24) Aljumaah, M. R.; Alkhulaifi, M. M.; Abudabos, A. M.; Aljumaah, R. S.; Alsaleh, A. N.; Stanley, D. Bacillus subtilis PB6 based probiotic supplementation plays a role in the recovery after the necrotic enteritis challenge. *PloS One* **2020**, *15*, 1−18.

(25) Panda, A. K.; Rao, S. V. R.; Raju, M. V. L. N.; Sunder, G. S. Effect of Butyric Acid on Performance, Gastrointestinal Tract Health and Carcass Characteristics in Broiler Chickens. *Asian-Australas. J. Anim. Sci.* **2009**, *22*, 1026−1031.

(26) Kruse, S.; Pierre, F.; Morlock, G. Imaging high-performance thin-layer chromatography as powerful tool to visualize metabolite profiles of eight Bacillus candidates upon cultivation and growth behavior. *J. Chromatogr. A* **2021**, *1640*, 461929.

(27) McDonnell, D. P.; Nawaz, Z.; Densmore, C.; Weigel, N. L.; Pham, T. A.; Clark, J. H.; O'Malley, B. W. High level expression of biologically active estrogen receptor in Saccharomyces cerevisiae. *J. Steroid Biochem.* **1991**, *39*, 291−297.

(28) McDonnell, D. P.; Nawaz, Z.; O'Malley, B. W. In situ distinction between steroid receptor binding and transactivation at a target gene. *Method Mol. Cell. Biol.* **1991**, *11*, 4350−4355.

(29) Purvis, I. J.; Chotai, D.; Dykes, C. W.; Lubahn, D. B.; French, F. S.; Wilson, E. M.; Hobden, A. N. An androgen-inducible expression system for Saccharomyces cerevisiae. *Gene* **1991**, *106*, 35−42.

(30) Klingelhöfer, I.; Morlock, G. E. Sharp-bounded zones link to the effect in planar chromatography-bioassay-mass spectrometry. *J. Chromatogr. A* **2014**, *1360*, 288−295.

(31) Klingelhöfer, I.; Morlock, G. E. Bioprofiling of Surface/ Wastewater and Bioquantitation of Discovered Endocrine-Active Compounds by Streamlined Direct Bioautography. *Anal. Chem.* **2015**, *87*, 11098−11104.

(32) Morlock, G. E.; Drotleff, L.; Brinkmann, S. Miniaturized all-in-one nanoGIT$^{+active}$ system for on-surface metabolization, separation and effect imaging. *Anal. Chim. Acta* **2021**, *1154*, 338307.

(33) Morlock, G. E.; Heil, J.; Inarejos-Garcia, A. M.; Maeder, J. Effect-Directed Profiling of Powdered Tea Extracts for Catechins, Theaflavins, Flavonols and Caffeine. *Antioxidants* **2021**, *10*, 117.

(34) Azadniya, E.; Morlock, G. E. Automated piezoelectric spraying of biological and enzymatic assays for effect-directed analysis of planar chromatograms. *J. Chromatogr. A* **2019**, *1602*, 458−466.

(35) Riegraf, C.; Reifferscheid, G.; Belkin, S.; Moscovici, L.; Shakibai, D.; Hollert, H.; Buchinger, S. Combination of yeast-based in vitro screens with high-performance thin-layer chromatography as a novel tool for the detection of hormonal and dioxin-like compounds. *Anal. Chim. Acta* **2019**, *1081*, 218−230.

(36) Kirchert, S.; Morlock, G. E. Orthogonal Hyphenation of Planar and Liquid Chromatography for Mass Spectrometry of Biomarkers out of the Bioassay Matrix (NP-HPTLC-UV/vis/FLD-Bioassay-RP/ IEX-HPLC-UV/vis-ESI-MS). *Anal. Chem.* **2020**, *92*, 9057−9064.

(37) Schreiner, T.; Morlock, G. E. Non-target bioanalytical eight-dimensional hyphenation including bioassay, heart-cut trapping, online desalting, orthogonal separations and mass spectrometry. *J. Chromatogr. A* **2021**, *1647*, 462154.

(38) Mehl, A.; Schwack, W.; Morlock, G. E. On-Surface Autosampling for Liquid Chromatography−Mass Spectrometry. *J. Chromatogr. A* **2021**, *1651*, 462334.

(39) Mehl, A.; Schmidt, L. J.; Schmidt, L.; Morlock, G. E. High-throughput planar solid-phase extraction coupled to orbitrap high-resolution mass spectrometry via the autoTLC-MS interface for screening of 66 multi-class antibiotic residues in food of animal origin. *Food Chem.* **2021**, *351*, 129211.

(40) Ma, Y.; Kong, Q.; Qin, C.; Chen, Y.; Chen, Y.; Lv, R.; Zhou, G. Identification of lipopeptides in Bacillus megaterium by two-step ultrafiltration and LC-ESI-MS/MS. *Amb. Express* **2016**, *6*, 79.

(41) Peypoux, F.; Bonmatin, J.-M.; Labbé, H.; Das, B. C.; Ptak, M.; Michel, G. Isolation and characterization of a new variant of surfactin, the Val7 surfactin. *Eur. J. Biochem.* **1991**, *202*, 101−106.

(42) Chen, X.-H.; Vater, J.; Piel, J.; Franke, P.; Scholz, R.; Schneider, K.; Koumoutsi, A.; Hitzeroth, G.; Grammel, N.; Strittmatter, A. W.; Gottschalk, G.; Süssmuth, R. D.; Borriss, R. Structural and functional characterization of three polyketide synthase gene clusters in Bacillus amyloliquefaciens FZB 42. *J. Bacteriol.* **2006**, *188*, 4024−4036.

(43) Razafindralambo, H.; Popineau, Y.; Deleu, M.; Hbid, C.; Jacques, P.; Thonart, P.; Paquot, M. Foaming Properties of Lipopeptides Produced by Bacillus subtilis : Effect of Lipid and Peptide Structural Attributes. *J. Agric. Food Chem.* **1998**, *46*, 911−916.

(44) Du, R.; Jiao, S.; Dai, Y.; An, J.; Lv, J.; Yan, X.; Wang, J.; Han, B. Probiotic Bacillus amyloliquefaciens C-1 Improves Growth Performance, Stimulates GH/IGF-1, and Regulates the Gut Microbiota of Growth-Retarded Beef Calves. *Front. Microbiol.* **2018**, *9*, 2006.

Supplementary Information

**Effects of the probiotic activity of *Bacillus subtilis* DSM 29784
in cultures and feeding stuff**

Stefanie Kruse[a], Francis Pierre[b], Gertrud Morlock[a,*]

[a]Chair of Food Science, Institute of Nutritional Science, and Interdisciplinary Research Centre
for Biosystems, Land Use and Nutrition, Justus Liebig University Giessen, Heinrich-Buff-Ring
26–32, 35392 Giessen, Germany

[b]Adisseo France S.A.S, Immeuble Anthony Parc 2, 10 Place du Général de Gaulle, 92160
Antony, France

*Corresponding authors: Prof. Dr. Gertrud Morlock, phone: +49-641-9939141; fax +49-641-
99-39149, email: gertrud.morlock@uni-giessen.de
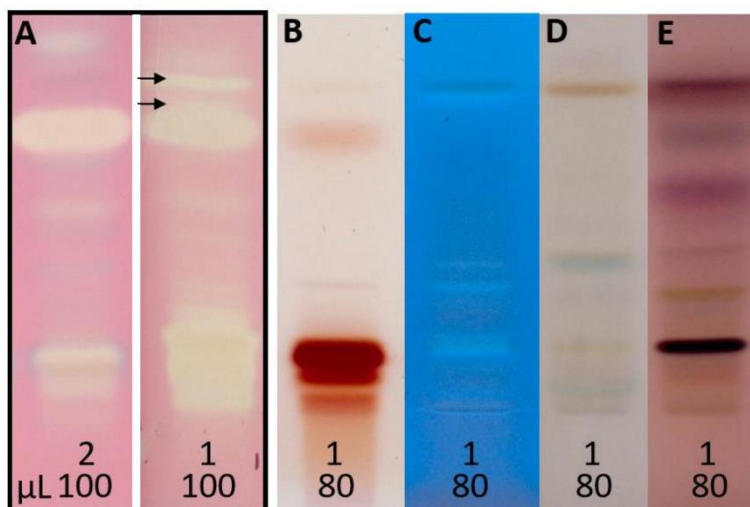
Table of Content

72

Figure S1 Characterization of metabolites produced by strain stock solutions **1** and **2** (80 µL/area each, *n*-butanol extracts): Chromatograms on HPTLC plates silica gel 60 with toluene – ethyl acetate – methanol – water – formic acid (12:17:8:2:1, *V/V/V/V/V*) detected via the DPPH˙ assay (A) and by derivatization with the ninhydrin (B), primuline (C), diphenylamine aniline (D) and anisaldehyde sulfuric acid (E) reagents, documented at white light illumination (A, C-E) and FLD 366 nm (B); strains were cultivated in TSBY medium at 100 rpm and 37 °C (150 mL stock solution in 30 mL TSBY medium, then 5 mL of the pre-culture in 25 mL fresh medium).
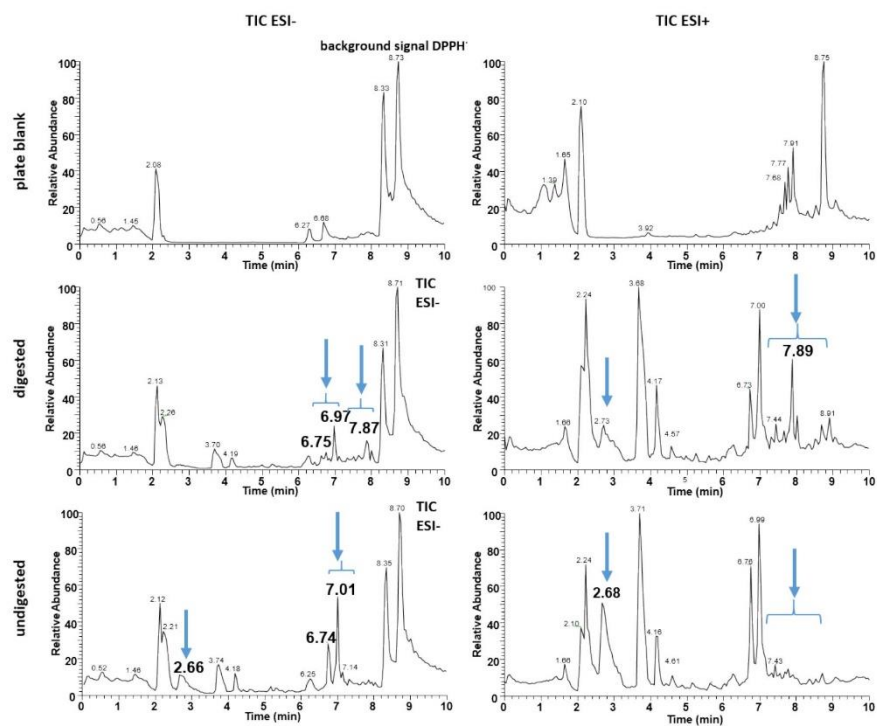
Figure S2 Comparison of the HPLC chromatograms after elution of the digested and the non-digested zones at hR$_F$ 28 directly out of the HPTLC−DPPH˙ autogram (*n*-butanol extracts of 100 μL/area each separated on NP plates with ethyl acetate − methanol 8:0.5, *V/V* up to 70 mm and then ethyl acetate − methanol − water 7:2:1, *V/V/V* up to 40 mm). The blue arrow indicates the changes in the metabolite profiles after digestion on the HPTLC plate.
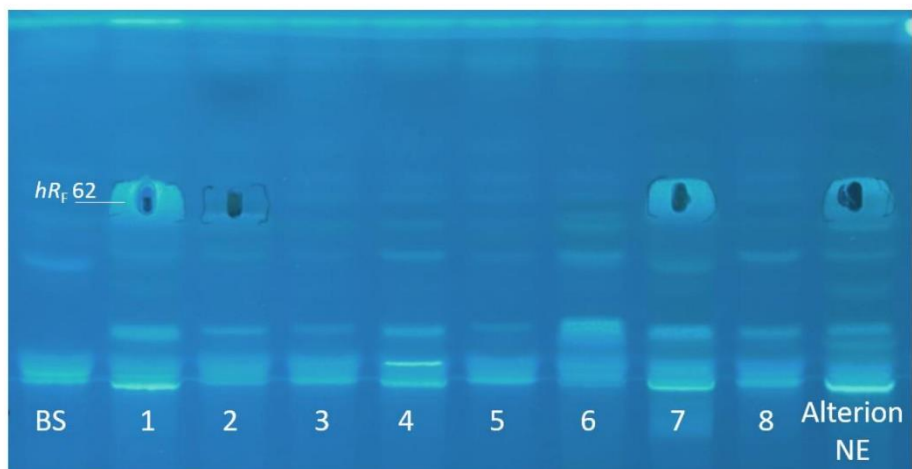
74

Figure S3 HPTLC chromatogram after derivatization with the primuline reagent at FLD 366 nm of the *n*-butanol extracts of the eight different *Bacillus* candidates **1–8** and the feed premix Alterion NE (100 µL/area each). The candidates were cultivated in TSBY at 37 °C and 200 rpm for 16 h and separated on NP with ethyl acetate – methanol – water (8.3:1.2:0.5, *V/V/V*). The zone at *hR*$_F$ 62 was directly heart-cut eluted and analyzed by UPLC−PDA−ESI-MS.
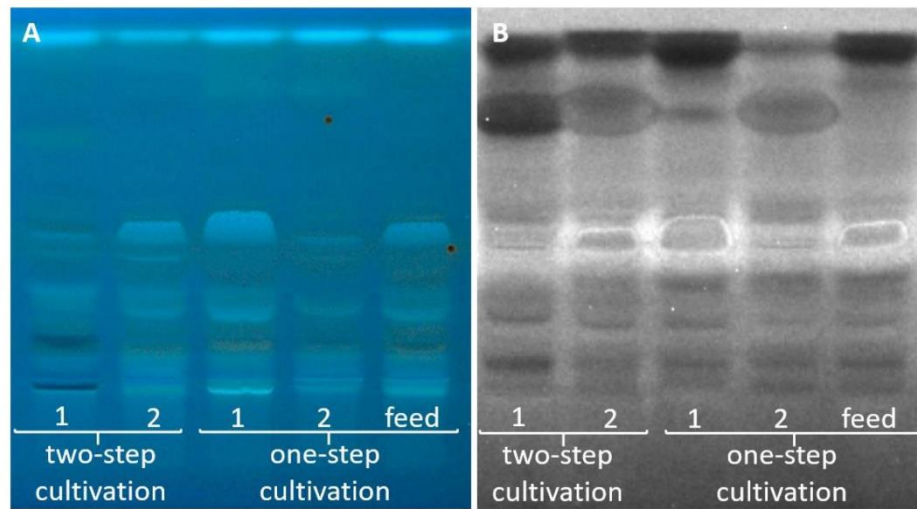
Figure S4 HPTLC chromatogram after derivatization with the primuline reagent at FLD 366 nm (A) and *A. fischeri* bioautogram (B) of the n-butanol extracts of the strain stock solutions **1** and **2** and the feed (each applied 100 µL/area) for different cultivation methods. For the one-step cultivation, 30 mL TSBY medium were inoculated with 150 µL of the stock solution cultivated at 200 rpm and 37 °C for 16 h. For the two-step cultivation, 30 mL TSBY medium were inoculated with 150 µL of the stock solutions and cultivated at 100 rpm and 37 °C for 16 h. Pre-culture (5 mL) was diluted with 25 mL fresh medium and cultivated using the same parameters for 24 h. The extracts were separated on NP with ethyl acetate – methanol – water (8.3:1.2:0.5, *V/V/V*).
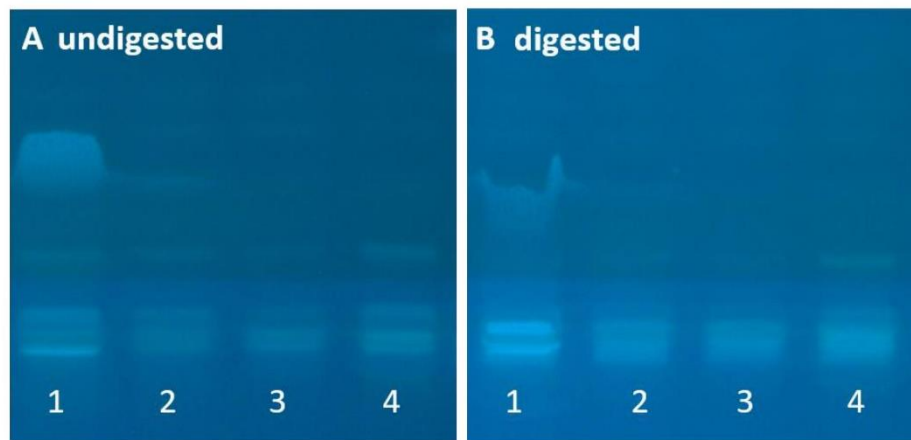
76

Figure S5 HPTLC chromatogramm after derivatization with the primuline reagent at FLD 366 nm of the *n*-butanol extracts of the undigested (A) and digested (B) *Bacillus* candidates **1**–**4** (100 µL/area each). The candidates were cultivated in TSBY at 37 °C and 200 rpm for 16 h and separated on NP with ethyl acetate – methanol – water (8.3:1.2:0.5, *V/V/V*).
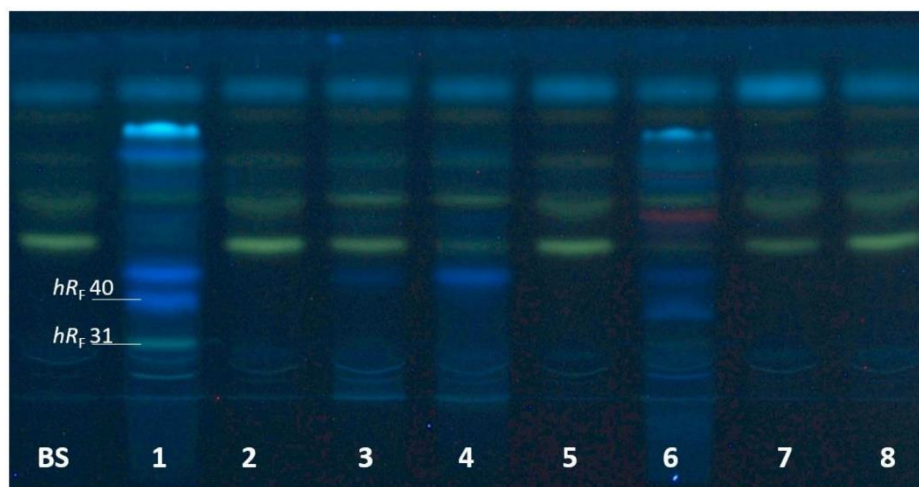
Figure S6 HPTLC chromatogram at FLD 366 nm of the *n*–butanol extracts of the pYES medium blank sample (BS) and *Bacillus* candidates **1**–**8** (200 µL/area each) after 20 h cultivation in pYES medium at a rotation speed of 100 rpm and a cultivation temperature of 37 °C. The extracts were separated with ethyl acetate – methanol – water (7.5:1.7:0.8, *V/V/V*).

S-9

78

Figure S7 HPTLC chromatogram at FLD 366 nm of the *n*-butanol extracts (200 µL/area) of four dilutions of the commercial formulation Alterion NE after a 23 h cultivation in pYES minimal medium at 37 °C and 100 rpm. After focusing with acetone and two times with methanol up to 20 mm, the extracts were developed with ethyl acetate – methanol – water (7.5:1.7:0.8, *V/V/V*) up to 70 mm.

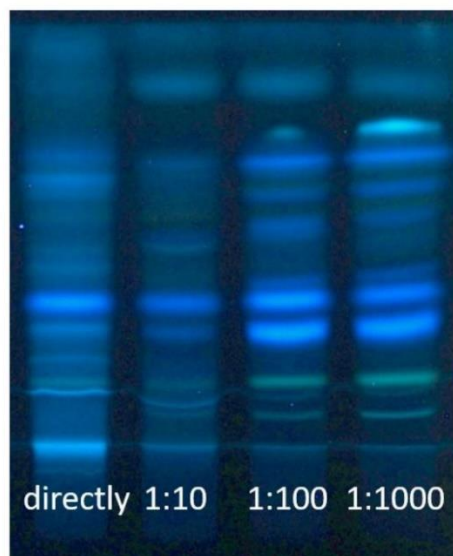## 5. Publication III

Metabolic profiling of bacterial co-cultures linked to predominant species identification.

Stefanie Kruse[a], Selina Becker[a], Francis Pierre[b], Gertrud E. Morlock[a,*]

[a]Chair of Food Science, Institute of Nutritional Science, and Interdisciplinary Research Centre for Biosystems, Land Use and Nutrition, Justus Liebig University Giessen, Heinrich-Buff-Ring 26-32, 35392 Giessen, Germany

[b]Adisseo France S.A.S, Immeuble Anthony Parc 2, 10 Place du Général de Gaulle, 92160 Antony, France

Submitted to

Journal of Chromatography A

81

1

2

3

4 **Metabolic profiling of bacterial co-cultures linked to**

5 **predominant species identification**

6

7

8 Stefanie Kruse[a], Selina Becker[a], Francis Pierre[b], Gertrud E. Morlock[a,*]

9

10

11

12 [a]Institute of Nutritional Science, Chair of Food Science, and Interdisciplinary Research Centre

13 for Biosystems, Land Use and Nutrition, Justus Liebig University Giessen, Heinrich-Buff-

14 Ring 26-32, 35392 Giessen, Germany

15 [b]Adisseo France S.A.S, Immeuble Anthony Parc 2, 10 Place du Général de Gaulle, 92160

16 Antony, France

17

18

19

20

21 *Corresponding authors: Prof. Dr. Gertrud Morlock, phone: +49-641-9939141; fax +49-641-

22 99-39149, email: gertrud.morlock@uni-giessen.de

82

23 **Abstract**

24 In animal production, the use of probiotic microorganisms has increased since the ban on

25 antibiotic growth promoters in 2006. The added microorganisms interact with the microbiome

26 of the animals, whereby the probiotic activity is not fully understood. Several microorganisms

27 of the genus *Bacillus* are already known for their probiotic activity and are applied as feed

28 supplements to increase the health status of the animals. They are thought to interact with

29 *Escherichia coli*, one of the most abundant bacteria in the animal gut. In biotechnological

30 applications, co-culturing enables the regulation of bacterial interaction or the production of

31 target metabolites. Imaging high-performance thin-layer chromatography (HPTLC) with

32 upstream cultivation was used to analyze the metabolic profiles of three axenic *Bacilli* cultures

33 compared to their co-cultures with *E. coli* DSM 18039. The comparative metabolite profiling

34 revealed the influence from inoculation, nutrients, microbiome, and bacterial interaction. The

35 additional hyphenation with planar antimicrobial assay detection revealed changes in the

36 activity profiles due to the presence of other microorganisms, especially in one commercially

37 available probiotic. This new application of imaging HPTLC enabled visualization of bacterial

38 metabolic interactions and detection of bioactive metabolites with evidence of the predominant

39 species in the co-culture through easy-to-understand images.

40 **Keywords** metabolic profiling, bacterial interaction, antibacterial assay, *Bacillus subtilis*,

41 *Escherichia coli*

2

83

1. Introduction

In nature, microbes only occur in the presence of other species, and the analysis of bacterial co-cultures is becoming increasingly important to study interaction between bacteria [1, 2] and the production of targeted metabolites [3, 4]. Specific diets were implemented in animal production, *e. g.*, to influence positively the gut microbiome, to improve the health status and to enhance the growth performance of the animals [5–8]. Different types of microorganisms such as *Bacilli* [9] or yeasts [10] were used as probiotic feed additives, *e. g.*, to support the gut microbiota [11–13], to inhibit the interactions with pathogens [12, 14], to increase the growth performance [13, 15], and to modulate the immune system [13, 16]. The probiotic effect is not fully understood, but it is assumed that the metabolites produced by probiotic strains influence positively the gut microbiome and support the intestinal health of animals. Several studies showed different effects of the same probiotic under changed conditions regarding animal age, antibiotic treatment, physical activity, and environment. It was assumed that all factors that influence the microbiome, also affect metabolite production and the probiotic effect. [17–19]

One of the Gram-positive *Bacillus* candidates studied here is known to have probiotic activity in poultry and was present in the intestines of the animals after administration [5, 20]. In contrast, the Gram-negative *E. coli* is one of the main microorganisms in the broiler gut but also known for potential diseases [21, 22]. Metabolic interactions between different bacteria depend on several conditions, such as the availability of resources (nutrients) or inoculation [23]. Therefore, the interaction between *Bacilli* and *E. coli* may change the metabolic profile. Several studies analyzed their interaction to identify specific effects, such as antimicrobial activity [24, 25], or to determine the reduction of pathogenic forms of *E. coli* in the animal gut [26].

Imaging high-performance thin-layer chromatography (HPTLC) was proven as an efficient and affordable tool [27, 28]. Recently, it was used to compare the metabolic profiles of axenic *Bacillus* cultures under the same analytical conditions [29] and to provide understanding of

3

69   their probiotic activity linked with differences in the metabolite profiles [30]. In the present

70   study, it was hypothesized that the presence of *E. coli* affects the metabolite formation of

71   *Bacilli*. In co-cultures, the interaction between different *Bacilli* and *E. coli* was studied at

72   different growth conditions. After upstream co-cultivation and extraction, the metabolite

73   profiles were analyzed by effect-directed imaging HPTLC. Three antimicrobial bioassays were

74   applied on-surface to detect antimicrobial compounds acting against Gram-positive and

75   Gram-negative bacteria. It allowed the side-by-side comparison of the biologically active

76   metabolite profiles of the axenic cultures with the co-cultures, their concerted interaction and

77   the identification of predominant species in the co-culture.

78   **2.   Materials and methods**

79   Chemicals and materials

80   The *Bacillus subtilis* (*B. s.*) were obtained from Novozymes, Bagsværd, Denmark. The *E. coli*

81   (DSM 18039) and Gram-negative marine *Aliivibrio fischeri* bacteria (DSM 7151, used for

82   bioautography) were provided by the Leibniz Institute, German Collection of Microorganisms

83   and Cell Cultures (DSMZ), Braunschweig, Germany. Gram-positive soil bacteria *Bacillus*

84   *subtilis* spore suspension (DSM 618, used for bioautography), tryptic soy broth (TSB), and

85   HPTLC plates silica gel 60 were purchased from Merck, Darmstadt, Germany. Lysogeny broth

86   (LB), primuline (≥99%), yeast extract (for use in microbial growth medium), D-glucose (Glc,

87   ≥99.5%), caffeine (≤100%, water-free), sodium chloride (NaCl, ≥99%), Ciprofloxacin

88   (≥98.0%), Grams iodine solution and Grams safranin solution (both for microscopy) were

89   purchased from Sigma-Aldrich Fluka, Steinheim, Germany. *n*-Butanol (HPLC grade) and

90   crystal violet were delivered by Acros Organics, Fair Lawn, NJ, USA. Methanol and acetone

91   (both HPLC grade) were purchased from VWR, Darmstadt, Germany. Ethyl acetate (≥99.8%)

92   was delivered by Th. Geyer, Renningen, Germany. Tetracycline hydrochloride (tetracycline,

93   reagent grade) was purchased from Serva Electrophoresis, Heidelberg, Germany.

94   Hydrochloric acid (HCl, 37%, purest), potassium chloride (KCl, ≥99%), potassium dihydrogen

4

95　phosphate (KH$_2$PO$_4$, ≥99%), magnesium chloride (MgCl$_2$, ≥98.5%), disodium hydrogen

96　phosphate (Na$_2$HPO$_4$, ≥99%), glycerol (86%, p.a.), 4-anisaldehyde (≥97.5%), 3-(4,5-

97　dimethylthiazolyl-2)-2,5-diphenyl-2H-tetrazolium bromide (MTT, ≥98%), sulfuric acid, toluene

98　(≥99%) and glacial acetic acid (both >98%) were obtained from Carl Roth, Karlsruhe,

99　Germany. Acetonitrile (≥99.9%, Honeywell Riedel-de Haen) and ethanol (≥99.8%, HPLC

100　grade) were obtained from Fisher Scientific, Schwerte, Germany. Bidistilled water was

101　prepared by a Destamat Bi 18E, Heraeus, Hanau, Germany.

102　Preparation of stock solutions

103　*Bacillu*s strains (**1**: *B. s.* 29784 commercially available as ALTERION® NE, ADISSEO France

104　SAS, France, **2**: *B. s.* MIC39 genetically similar up to 99.5%, **3**: *B. s.* ATCC 6633 genetically

105　similar up to 99.5%) were cultivated in TSB culture medium containing yeast (TSBY, 3% TSB

106　added to 1 L water with 0.6% yeast extract and adjusted to pH 6.2 with 2 M HCl solution) up

107　to an optical density (OD$_{660}$) of 1.4. The *E. coli* was cultivated in LB (20 g dried LB medium,

108　5 g NaCl and 1 g Glc, dissolved in bidistilled water, adjusted to pH 7, and filled up to 1 L) up

109　to OD$_{660}$ 1.4. To prepare stock solutions, each culture was 1:1 (*V/V*) mixed with 50% glycerol

110　and frozen at -80 °C.

111　Cultivation and extraction

112　The bacteria were cultivated in TSBY medium at 37 °C in a Labocult incubator (Servoprax,

113　Wesel, Germany) at a rotation speed of 175 rpm on an orbital shaker SM-30 (Edmund Bühler,

114　Bodelshausen, Germany). The different co-/cultivation processes used different cultivation

115　scenarios as specified (such as direct co-/cultivation, pre-cultivation of the bacteria, different

116　inoculation volumes, or different incubation times). After cultivation, each OD$_{660}$ was

117　determined with the M501 Single Beam Scanning UV/vis Spectrophotometer (CamSpec,

118　Garforth, UK). The cells were inspected by microscopy with crystal violet and Gram staining.

119　The cell suspension was centrifuged (centrifuge 5702, Eppendorf, Hamburg, Germany) at

120　3000 × *g* for 10 min. An aliquot (15 mL) of the cell-free supernatant was used for liquid-liquid

121　extraction with 5 mL *n*-butanol. The solution was vortexed (Vortex Genie 2 with multi-tube

5

122 holder, Scientific Industries, New York City, NY, USA) for 15 min at level 10 and subsequently

123 centrifuged at 3000 × g for 10 min. Each extract was transferred to an autosampler vial.

124 HPTLC−UV/vis/FLD method

125 On the HPTLC plate silica gel 60 (pre-washed two times with methanol – water 4:1, V/V), the

126 extracts (100 µL) were applied as 10 mm × 8 mm area (Automatic TLC Sampler 4, CAMAG,

127 Muttenz, Switzerland). The dosage speed was set to 600 nL/s and the syringe was rinsed

128 twice with methanol after each application. The area was focused once with acetone and two

129 times with methanol up to 20 mm (from plate bottom). The plate was developed with the

130 specified mobile phase up to a migration distance of 70 mm manually or after humidity control

131 (33% relative humidity via saturated $MgCl_2$ solution, Automatic Development Chamber 2,

132 CAMAG), then dried for 15 min and documented at vis, UV 254 nm, and FLD 366 nm (TLC

133 Visualizer, CAMAG).

134 Detection via derivatization

135 The HPTLC chromatogram was dipped (immersion time 2 s, immersion speed 3.5 cm/s,

136 Chromatogram Immersion Device 3, CAMAG) either in the primuline reagent (250 mg

137 primuline dissolved in 50 mL water and 200 mL acetone), dried in a stream of cold air

138 (hairdryer) for 1 min, and documented at FLD 366 nm, or in the anisaldehyde sulfuric acid

139 reagent (1.5 mL 4-anisaldehyde dissolved in a mixture of 210 mL methanol, 25 mL acetic acid,

140 and 13 mL sulfuric acid), heated at 110 °C (Plate Heater 3) for 10 min and documented at vis.

141 Detection via three planar antimicrobial bioassays

142 The HPTLC chromatogram was detected biologically via three different antimicrobial

143 bioassays. For the *A. fischeri* bioassay, bioluminescent Gram-negative *A. fischeri* were used

144 [31]. Briefly, the bacteria were cultivated at room temperature and 90 rpm overnight until they

145 exhibited brilliant bioluminescence (observed in a dark room upon shaking) The positive

146 control caffeine (1 µg/band; 1 mg/mL in methanol) was applied on the upper plate part. The

147 *A. fischeri* suspension was piezoelectrically sprayed (3.5 mL, blue nozzle, level 6, Derivatizer,

6

86

148 CAMAG) onto the plate. The bioluminescence (depicted as greyscale image) was monitored

149 for 30 min, whereby 10 bioautograms were recorded (exposure 100 s each, BioLuminizer 2,

150 CAMAG). For the *B. subtilis* bioassay, *B. s.* DSM 618 were used for the detection of Gram-

151 positive antimicrobial metabolites.[32] Briefly, the bacteria were cultivated overnight at 37 °C

152 and 90 rpm. The adjusted OD_{600} ranged 0.7–1.1. The positive control tetracycline (4, 8, and

153 12 ng/band; 1 µg/mL in ethanol) was applied on the upper plate part. The *B. s.* suspension

154 was piezoelectrically sprayed onto the plate (as mentioned but red nozzle) and incubated at

155 37 °C in a moistened polypropylene box (26.5 cm × 16 cm × 10 cm, ABM, Wolframs-

156 Eschenbach, Germany) for 2 h. After incubation, the 0.2% MTT substrate solution (0.1 g MTT

157 in 50 mL phosphate-buffered saline, containing 8 g/L NaCl, 0.2 g/L KCl, 1.4 g/L Na_2HPO_4,

158 0.2 g/L KH_2PO_4 in bidistilled water) was piezoelectrically sprayed onto the plate (0.5 mL; blue

159 nozzle, level 6, Derivatizer) and further incubated at 37 °C for 1 h. The plate was dried for

160 10 min at 50 °C (Plate Heater 3, CAMAG) and the chromatogram was documented at visible

161 light. For the *E. coli* bioassay, the *E. coli* DSM 18039 were used for the detection of Gram-

162 negative antimicrobial metabolites. The positive control ciprofloxacin (4 and 8 ng/band) was

163 applied on the upper plate part. The *E. coli* bioassay was performed analogously to the *B.*

164 *subtilis* bioassay, except that the first incubation step was extended by 1 h and the second

165 incubation by 2 h.

3. Results and discussion

167 Co-cultivation of two or more microorganisms is a challenging task, if all microorganisms are

168 to grow. Cultivation conditions were varied such that both microorganisms had the opportunity

169 to grow in the co-culture, but with different metabolic dominance (Table S1). Imaging HPTLC

170 was used to investigate and visualize the influence of *B. s.* and *E. coli* co-culturing on

171 metabolic profiles (Fig. 1). The method parameters (cultivation, extraction, and separation)

172 were varied to study any changes in the metabolite profile caused by specific metabolic

173 interactions in the co-culture.

7

174 *E. coli dominance in the co-culture*

175 The metabolic interaction between *B. s.* and *E. coli* was investigated in different cultivation

176 scenarios (Table S1, scenarios 1-4) of total dominance of *E. coli* in the co-culture. Only the

177 most important results are to be discussed. The generation time of the used *E. coli* is

178 approximately two times faster than the one of *B. s.* (20 min compared to 45 min). Therefore,

179 a higher inoculation volume of the *Bacillus* than *E. coli* stock solution (both in 25% glycerol,

180 OD_{660} 1.4) was necessary for the approximate growth of both microorganisms in the co-

181 culture. Despite the 10-fold higher inoculation with *Bacillus*, the cell number of *E. coli* was

182 significantly higher after 2 h due to their faster generation time. The bacteria were cultivated

183 overnight (Table S1, cultivation scenario 2, 175 rpm, 37 °C, 15 h). The Gram staining indicated

184 that both bacteria were present in the co-culture. The metabolites were extracted and imaging

185 HPTLC was performed. The UV/vis/FLD chromatograms showed that *E. coli* was the dominant

186 species in the co-culture. By derivatization with the primuline reagent (detection of lipophilic

187 metabolites), the metabolic profiles of the co-cultures were equivalent to the *E. coli* profile. In

188 the axenic *Bacillus* cultures, several metabolites were detectable, which were not present in

189 the co-cultures (Fig. S1a, hR_F 17, 21, 25, 44, 58). Thus, the used cultivation scenario led to

190 the overexpression of *E. coli*. However, despite the predominance of *E. coli*, the *Bacilli*

191 influenced their metabolic profile. In the presence of *Bacilli*, the *E. coli* is prevented to form

192 specific metabolites (Fig. 2, hR_F 68). In the gut of the animal, the presence of *Bacilli* could

193 protect the microbiome from the production of harmful substances of *E. coli*. Additionally,

194 imaging HPTLC indicated, that metabolites were only produced due to the interaction of both

195 microorganisms (Fig. 2, hR_F 57) or that the interaction promote the higher production of certain

196 metabolites (Fig. 2, hR_F 35). These aspects also influence the probiotic effect. The Gram-

197 negative *A. fischeri* bioassay (detection of antimicrobial substances as dark zones) showed

198 that the metabolite at hR_F 36 (Fig. S1b) was produced in a higher concentration in the co-

199 cultures due to the interaction. These results confirm that even at a low cell number, the *Bacilli*

200 exert an influence on the metabolism of *E. coli*. After application of two further antimicrobial

201 bioassays for detection, both the *B. subtilis* bioassay and the *E. coli* bioassay showed that

8

88

202   antimicrobial substances (Fig. 3, colorless zones on purple background) were formed in the

203   axenic cultures of the *Bacillus* strains (hR_F 18) and in *Bacillus* and *E. coli* co-culture (hR_F 95).

204   To exclude that the concentration of the metabolites within the extraction procedure influenced

205   the results, the extracts were diluted and analyzed again. The diluted samples also indicated

206   the detection of the antimicrobial substances in the axenic cultures (Fig. S2). However, the

207   effects on the plate are not exactly comparable to the effects in the gut. The assay only

208   indicates antimicrobial substances acting against Gram-negative bacteria and that their

209   interaction with microorganisms is relevant for the health of the animals. How these

210   metabolites interact with the microbiome, or whether the concentration is high enough to kill

211   dangerous bacteria such as *E. coli,* remains to be studied in more detail.

212   *Bacillus* dominance in the co-culture

213   The most interesting results related to the dominance of *Bacillus* in co-culture are discussed

214   as follows (Table S1, cultivation scenarios 5−11). A pre-cultivation of *Bacilli* was used to

215   induce their dominant growth in the co-cultures. An aliquot (1.5 mL) of the *Bacillus* pre-cultures

216   and the *E. coli* stock solutions (100 µL) were used for further cultivation of the axenic and co-

217   cultures. This procedure led to the dominance of *Bacillus* candidates in the co-cultures (Fig.

218   S3, Table S1, cultivation scenario 11). The metabolite at hR_F 39 was detected in all cultures

219   containing *Bacillus* (pre-, axenic- and co-culture), but was absent in the axenic *E. coli* culture.

220   Additionally, the time-dependent metabolite profiles of the *Bacillus* strains are documented.

221   The metabolite at hR_F 57 was detected in the pre-culture of strain 3 and main culture of strains

222   2 and 3, but was suppressed in both co-cultures. The metabolism of both candidates was

223   comparable, but faster in strain 3 under the given conditions (confirmed by another cultivation,

224   Fig. 4). The suppression of the metabolite in the co-cultures revealed an interaction of strains

225   2 and 3 with *E. coli*. The metabolite at hR_F 99 was also indicative of the dominance of *Bacillus*

226   in the co-culture (detected in the main and co-culture of strain 2, Fig. S3). Furthermore, the *A.*

227   *fischeri* bioautogram highlighted the interaction between *E. coli* and the probiotic *Bacillus*

228   strain. It showed antimicrobial substances acting against Gram-negative *A. fischeri* bacteria

9

229   as dark zones. An antimicrobial metabolite was detected at hR_F 22 in the pre-culture and main-

230   culture of the probiotic *Bacillus* strain 1, but not in the co-culture (Fig. 55a, Table S1, cultivation

231   scenario 11).The absence of the antimicrobial substance (hR_F 22) in the co-culture was

232   caused by the interaction of the probiotic strain 1 with *E. coli*. The metabolite only detectable

233   in the co-culture at hR_F 41 (Fig. 55b) also indicated the interaction of strain 1 with *E. coli*. The

234   presence of *E. coli* cells (even at low concentrations) affected the metabolic profiles of the

235   *Bacilli*, but the *A. fischeri* bioautogram showed that only the probiotic *Bacilli* strain 1 produced

236   metabolites that indicated antimicrobial activity against this Gram-negative microorganism.

237   The equivalence of *Bacilli* and *E. coli* in the co-cultures

238   Pre-cultivation of both microorganisms and further common cultivation led to an equivalent

239   metabolic activity of *E. coli* and *Bacillus* in the co-culture. Gram staining showed the presence

240   of both bacteria in the co-culture (Fig. 4, Table S1, cultivation scenarios 12 and 13), but

241   imaging HPTLC further showed equivalent dominant metabolic activity. The metabolite at hR_F

242   40 specified the presence of the *Bacillus* candidates (detected in all cultures containing

243   *Bacilli*), whereas the metabolite at hR_F 17 indicated the presence of *E. coli* (detected in all

244   cultures containing *E. coli*) by using the cultivation scenario 12. The results were confirmed

245   by Gram staining, whereby Gram-negative cells (*E. coli*) were stained red and Gram-positive

246   cells (*Bacillus*) were stained blue (Fig. 4a). The advantage of imaging HPTLC is the

247   visualization of the impact of co-culturing on the metabolite profiles. In the previous co-

248   cultivations, the Gram staining also indicated the presence of both species, but the dominance

249   or interaction of both species was only detected by imaging HPTLC due to metabolic pattern

250   recognition. For example, the probiotic *Bacillus* strain 1 exhibited a brownish zone (hR_F 25) in

251   the axenic cultures, which is usually also detected in the co-culture (Fig. S4a) when pre-

252   cultivation is only performed for the *Bacillus* strain. However, when the inoculation volume of

253   *E. coli* was increased in the pre-cultivation compared to the inoculation volume of the *Bacillus*

254   species, this zone was only detected in the axenic *Bacillus* culture (Fig. S4b). Interaction of

255   the microorganisms is only possible if both bacteria have had the opportunity to grow in the

10

90

256   co-cultures, but how the interaction affects metabolism also depends on the concentration.

257   Three sample types of the probiotic strain 1 were cultivated in parallel to determine the

258   influences of different concentrations on the metabolic profiles. The amount of dried spores

259   and the feed were selected to ensure cell viability under the selected cultivation conditions

260   (scenario 13), *i.e.* it is for the stock solution (OD_{660} 1.4), dried spores (contain 500 ng), and a

261   feed (containing 1.5 pg dried spores). The metabolic profiles of all pre-cultures and all axenic

262   cultures were comparable (Fig. S5). Due to the described different concentrations of the

263   probiotic strain 1 in the co-cultures the metabolic interactions and the metabolic profiles in the

264   co-cultures with *E. coli* changed. The metabolite at hR_F 99 is formed only in the co-culture of

265   *E. coli* with the stock solution and with the pure dried spores. In the co-culture with the feed,

266   the spores were less concentrated, which may have suppressed the formation of interacting

267   metabolites and led to the formation of metabolites produced by *E. coli* (hR_F 41). These results

268   suggest that the metabolic profiles of bacteria depend on several influencing factors and that

269   interactions within the microbiome seem to be an important factor.

270   **4. Conclusion**

271   The study demonstrated the advantages of imaging HPTLC for determining bacterial

272   interactions compared to Gram staining. The visualization enabled detection of the influence

273   of other microorganisms on the metabolite profile of axenic cultures and determined the

274   dominant species in bacterial co-cultures based on metabolic profiles and pattern recognition.

275   The results suggest that not only the health status and microbiome of the animals, but also

276   the used feed, in particular probiotic feed, influence the metabolism and metabolite production

277   of microorganisms. Studying the concerted bacterial interaction provides understanding why

278   certain bacteria exhibit probiotic activity in some animals and no activity was detected in

279   others. Imaging HPTLC with upstream co-cultivation and extraction of bacterial metabolites

280   helped to visualize the influences from nutrients, microbiome, and inoculation, on the

281   metabolic profile of the probiotic. These influences have already been known from our

282 previous studies, but can be investigated in more detail with this new co-cultivation method.

283 The outcome is useful to optimize industrial processes, such as the production of target

284 metabolites or the application of probiotics in animal nutrition.

285 **CrediT authorship contribution**

286 **SK**: Conceptualization, Methodology, Experimental Analysis, Data Analysis, Writing – Original

287 Draft. **SB**: Experimental Analysis, Review of paper. **FP:** Resources, Review of paper. **Gertrud**

288 **E. Morlock**: Conceptualization, Methodology, Supervision, Resources, Writing – Review and

289 Editing.

294 **Appendix A. Supplementary data**

295 Supplementary data to this article can be found online at…

12

93

References

1. Ravikrishnan A, Blank LM, Srivastava S, Raman K. Investigating metabolic interactions in a microbial co-culture through integrated modelling and experiments. Comput. Struct. Biotechnol. J. 2020; https://doi.org/10.1016/j.csbj.2020.03.019

2. Bertrand S, Bohni N, Schnee S, Schumpp O, Gindro K, Wolfender J-L. Metabolite induction via microorganism co-culture: a potential way to enhance chemical diversity for drug discovery. Biotechnol. Adv. 2014; https://doi.org/10.1016/j.biotechadv.2014.03.001

3. Zhang J, Luo W, Wang Z, Chen X, Lv P, Xu J. A novel strategy for D-psicose and lipase co-production using a co-culture system of engineered Bacillus subtilis and Escherichia coli and bioprocess analysis using metabolomics. Bioresour. Bioprocess. 2021; https://doi.org/10.1186/s40643-021-00429-8

4. S Hifnawy M, Hassan HM, Mohammed R, M Fouda M, Sayed AM, A Hamed A, F AbouZid S, Rateb ME, Alhadrami HA, Abdelmohsen UR. Induction of Antibacterial Metabolites by Co-Cultivation of Two Red-Sea-Sponge-Associated Actinomycetes Micromonospora sp. UR56 and Actinokinespora sp. EG49. Mar. Drugs. 2020; https://doi.org/10.3390/md18050243

5. Choi P, Rhayat L, Pinloche E, Devillard E, Paepe E de, Vanhaecke L, Haesebrouck F, Ducatelle R, van Immerseel F, Goossens E. Bacillus Subtilis 29784 as a Feed Additive for Broilers Shifts the Intestinal Microbial Composition and Supports the Production of Hypoxanthine and Nicotinic Acid. Animals. 2021; https://doi.org/10.3390/ani11051335

6. Awad WA, Ghareeb K, Abdel-Raheem S, Böhm J. Effects of dietary inclusion of probiotic and synbiotic on growth performance, organ weights, and intestinal histomorphology of broiler chickens. Poult. Sci. 2009; https://doi.org/10.3382/ps.2008-00244

7. Mountzouris KC, Tsirtsikos P, Kalamara E, Nitsch S, Schatzmayr G, Fegeros K. Evaluation of the efficacy of a probiotic containing Lactobacillus, Bifidobacterium, Enterococcus, and Pediococcus strains in promoting broiler performance and modulating cecal microflora composition and metabolic activities. Poult. Sci. 2007; https://doi.org/10.1093/ps/86.2.309

8. Gao Z, Wu H, Shi L, Zhang X, Sheng R, Yin F, Gooneratne R. Study of Bacillus subtilis on growth performance, nutrition metabolism and intestinal microflora of 1 to 42 d broiler chickens. Anim. Nutr. 2017; https://doi.org/10.1016/j.aninu.2017.02.002

9. Prieto ML, O'Sullivan L, Tan SP, McLoughlin P, Hughes H, O'Donovan O, Rea MC, Kent RM, Cassidy JP, Gardiner GE, Lawlor PG. Evaluation of the efficacy and safety of a marine-derived Bacillus strain for use as an in-feed probiotic for newly weaned pigs. PLoS One. 2014; https://doi.org/10.1371/journal.pone.0088599

13

94

333   10. Trckova M, Faldyna M, Alexa P, Sramkova Zajacova Z, Gopfert E, Kumprechtova D,
334   Auclair E, D'Inca R. The effects of live yeast Saccharomyces cerevisiae on postweaning
335   diarrhea, immune response, and growth performance in weaned piglets. J. Anim. Sci.
336   2014:767–774.

337   11. Neijat M, Habtewold J, Shirley RB, Welsher A, Barton J, Thiery P, Kiarie E. Bacillus
338   subtilis Strain DSM 29784 Modulates the Cecal Microbiome, Concentration of Short-
339   Chain Fatty Acids, and Apparent Retention of Dietary Components in Shaver White
340   Chickens during Grower, Developer, and Laying Phases. App. Environ. Microbiol. 2019;
341   https://doi.org/10.1128/AEM.00402-19.

342   12. Rodrigues DR, Briggs W, Duff A, Chasser K, Murugesan R, Pender C, Ramirez S,
343   Valenzuela L, Bielke LR. Comparative effectiveness of probiotic-based formulations on
344   cecal microbiota modulation in broilers. PLoS One. 2020;
345   https://doi.org/10.1371/journal.pone.0225871

346   13. Wang Y, Xu Y, Xu S, Yang J, Wang K, Zhan X. Bacillus subtilis DSM29784 Alleviates
347   Negative Effects on Growth Performance in Broilers by Improving the Intestinal Health
348   Under Necrotic Enteritis Challenge. Front. Microbiol. 2021;
349   https://doi.org/10.3389/fmicb.2021.723187

350   14. Yang JJ, Niu CC, Guo XH. Mixed culture models for predicting intestinal microbial
351   interactions between Escherichia coli and Lactobacillus in the presence of probiotic
352   Bacillus subtilis. Benef. Microbes. 2015; https://doi.org/10.3920/BM2015.0033

353   15. Neijat M, Shirley RB, Welsher A, Barton J, Thiery P, Kiarie E. Growth performance,
354   apparent retention of components, and excreta dry matter content in Shaver White
355   pullets (5 to 16 week of age) in response to dietary supplementation of graded levels of
356   a single strain Bacillus subtilis probiotic. Poult. Sci. 2019;
357   https://doi.org/10.3382/ps/pez080

358   16. Miyazaki Y, Kamiya S, Hanawa T, Fukuda M, Kawakami H, Takahashi H, Yokota H.
359   Effect of probiotic bacterial strains of Lactobacillus, Bifidobacterium, and Enterococcus
360   on enteroaggregative Escherichia coli. J. Infect. Chemother. 2010;
361   https://doi.org/10.1007/s10156-009-0007-2

362   17. Fernandes J, Su W, Rahat-Rozenbloom S, Wolever TMS, Comelli EM. Adiposity, gut
363   microbiota and faecal short chain fatty acids are linked in adult humans. Nutr. Diabetes.
364   2014; https://doi.org/10.1038/nutd.2014.23

365   18. Hou Q, Kwok L-Y, Zheng Y, Wang L, Guo Z, Zhang J, Huang W, Wang Y, Leng L, Li H,
366   Zhang H. Differential fecal microbiota are retained in broiler chicken lines divergently
367   selected for fatness traits. Sci. Rep. 2016; https://doi.org/10.1038/srep37376

14

368   19. Kers JG, Velkers FC, Fischer EAJ, Hermes GDA, Stegeman JA, Smidt H. Host and
369   Environmental Factors Affecting the Intestinal Microbiota in Chickens. Front. Microbiol.
370   2018; https://doi.org/10.3389/fmicb.2018.00235

371   20. Keerqin C, Rhayat L, Zhang Z-H, Gharib-Naseri K, Kheravii SK, Devillard E, Crowley
372   TM, Wu S-B. Probiotic Bacillus subtilis 29,784 improved weight gain and enhanced gut
373   health status of broilers under necrotic enteritis condition. Poult. Sci. 2021;
374   https://doi.org/10.1016/j.psj.2021.01.004

375   21. Paraskeuas V, Mountzouris KC. Broiler gut microbiota and expressions of gut barrier
376   genes affected by cereal type and phytogenic inclusion. Anim. Nutr. 2019;
377   https://doi.org/10.1016/j.aninu.2018.11.002

378   22. Yeoman CJ, Chia N, Jeraldo P, Sipos M, Goldenfeld ND, White BA. The microbiome of
379   the chicken gastrointestinal tract. Anim. Health Res. Rev. 2012;
380   https://doi.org/10.1017/S1466252312000138

381   23. Gao C-H, Cao H, Cai P, Sørensen SJ. The initial inoculation ratio regulates bacterial
382   coculture interactions and metabolic capacity. ISME J. 2021;
383   https://doi.org/10.1038/s41396-020-00751-7

384   24. Benitez L, Correa A, Daroit D, Brandelli A. Antimicrobial activity of Bacillus
385   amyloliquefaciens LBM 5006 is enhanced in the presence of Escherichia coli. Curr
386   Microbiol. 2011; https://doi.org/10.1007/s00284-010-9814-z

387   25. Grandchamp GM, Caro L, Shank EA. Pirated Siderophores Promote Sporulation in
388   Bacillus subtilis. App. Environ. Microbiol. 2017; https://doi.org/10.1128/AEM.03293-16

389   26. Guo M, Li M, Zhang C, Zhang X, Wu Y. Dietary Administration of the Bacillus subtilis
390   Enhances Immune Responses and Disease Resistance in Chickens. Front. Microbiol.
391   2020; https://doi.org/10.3389/fmicb.2020.01768

392   27. Morlock GE. High-performance thin-layer chromatography combined with effect-
393   directed assays and high-resolution mass spectrometry as an emerging hyphenated
394   technology: A tutorial review. Anal Chim Acta. 2021;
395   https://doi.org/10.1016/j.aca.2021.338644

396   28. Shen T, Morlock G, Zorn H. Production of cyathane type secondary metabolites by
397   submerged cultures of Hericium erinaceus and evaluation of their antibacterial activity
398   by direct bioautography. Fungal Biol Biotechnol. 2015; https://doi.org/10.1186/s40694-
399   015-0018-y

400   29. Kruse S, Pierre F, Morlock G. Imaging high-performance thin-layer chromatography as
401   powerful tool to visualize metabolite profiles of eight Bacillus candidates upon cultivation
402   and growth behavior. J. Chromatogr. A. 2021;
403   https://doi.org/10.1016/j.chroma.2021.461929

15

404 30. Kruse S, Pierre F, Morlock GE. Effects of the Probiotic Activity of Bacillus subtilis DSM
405   29784 in Cultures and Feeding Stuff. J. Agric. Food Chem. 2021;
406   https://doi.org/10.1021/acs.jafc.1c04811
407 31. Azadniya E, Morlock GE. Automated piezoelectric spraying of biological and enzymatic
408   assays for effect-directed analysis of planar chromatograms. J. Chromatogr. A. 2019;
409   https://doi.org/10.1016/j.chroma.2019.05.043
410 32. Jamshidi-Aidji M, Morlock GE. Bioprofiling of unknown antibiotics in herbal extracts:
411   Development of a streamlined direct bioautography using Bacillus subtilis linked to
412   mass spectrometry. J Chromatogr A. 2015;
413   https://doi.org/10.1016/j.chroma.2015.09.061
414
415

416   **Figure legends**

417   **Fig. 1** Schematic workflow for the metabolic profiling of bacterial co-cultures by imaging

418   HPTLC

419   **Fig. 2** HPTLC-vis chromatogram (separated on HPTLC plate silica gel 60 with ethyl

420   acetate – methanol – water 8:1.3:0.7, *V/V/V*) after derivatization with anisaldehyde sulfuric

421   acid reagent showing the profiles of the *n*-butanol bacterial metabolite extracts (100 µL each).

422   The *E. coli* (stock solution inoculation 30 µL) and the *B. s.* samples (stock solutions inoculation

423   100 µL) were cultivated in 30 mL TSBY at 37 °C and 175 rpm for 15 h.

424   **Fig. 3** HPTLC-vis chromatogram of bacterial (*B. subtilis* strains 1 and 2 as well as co-cultures

425   with *E. coli*) metabolite extracts (*n*-butanol, 100 µL each) separated on HPTLC plates silica

426   gel 60 with toluene – ethyl acetate – acetonitrile 2:2:1, V/V/V, and detected after the *E. coli*

427   bioassay as well as *B. subtilis* bioassay; *E. coli* (stock solution inoculation 30 µL) and *B.*

428   *subtilis* (stock solution inoculation 100 µL) bacteria were cultivated in 30 mL TSBY at 37 °C

429   and 175 rpm for 15 h.

430   **Fig. 4** Microscopy images of *E. coli* strain 1 and the respective co-culture after Gram staining

431   (A). HPTLC-vis chromatogram after derivatization with anisaldehyde sulfuric acid reagent

432   (separated on HPTLC plate silica gel 60 with toluene – ethyl acetate – acetonitrile 2:2:1,

433   *V/V/V*) showing the profiles of the *n*-butanol bacterial metabolite extracts (100 µL each). The

434   *B. s.* and *E. coli* strain stock solutions (inoculation 50 µL) were pre-cultivated in 30 mL TSBY

435   at 37 °C and 175 rpm for 15.5 h. An aliquot of the *B. s.* (1.0 mL) and of the *E. coli* (0.5 mL)

436   pre-cultures were added to fresh TSBY medium (total volume 20 mL) and cultivated at 37 °C

437   and 175 rpm for 4.5 h

438   **Fig. 5** *A. fischeri* bioluminescent bioautogram (A, after 30 min depicted as grey scale image)

439   and HPTLC chromatogram at FLD 366 nm (B) of *n*-butanol bacterial metabolite extracts

440   (100 µL each). The *B. s.* strain stock solutions (inoculation 50 µL) were pre-cultivated in 30 mL

441   TSBY at 37 °C and 175 rpm for 15.5 h. An aliquot (1.5 mL) of the pre-cultures and 100 µL *E.*
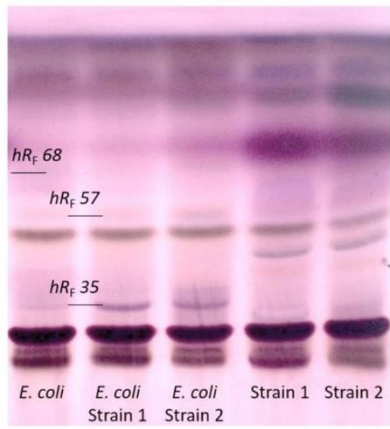
442   *coli* strain stock solutions were added to fresh TSBY medium (total volume 20 mL) and

443   cultivated at 37 °C and 175 rpm for 4.5 h. The extracts were separated with *n*-

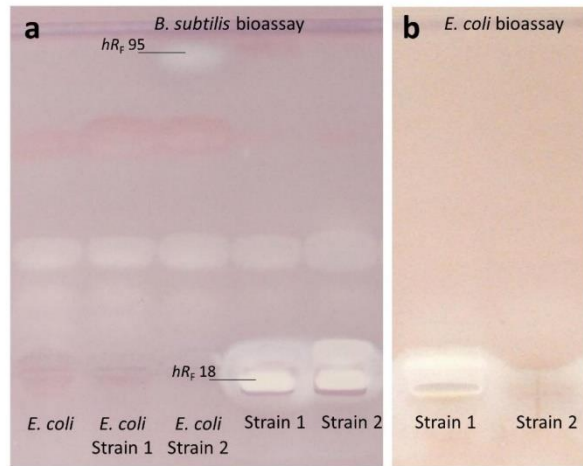444   butanol – diisopropyl ether (1:1, *V/V*) to detect antimicrobial metabolites.
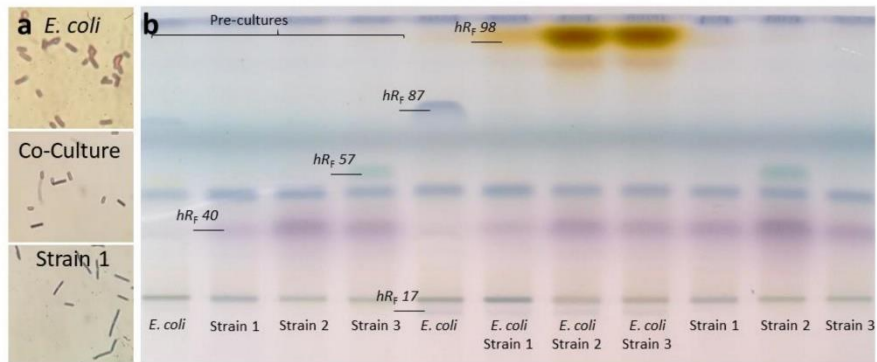
445

18

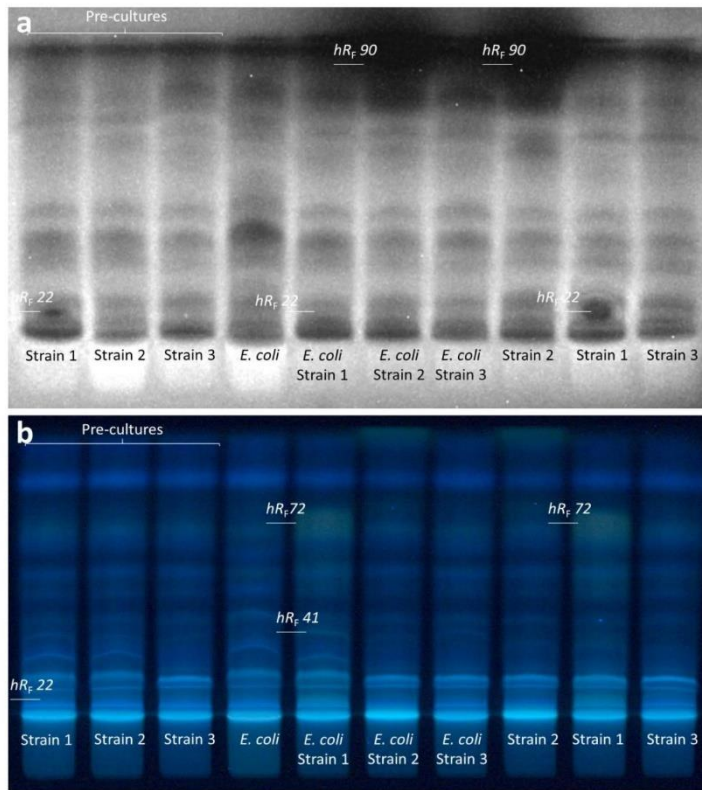98

446

447 **Fig. 1**

19
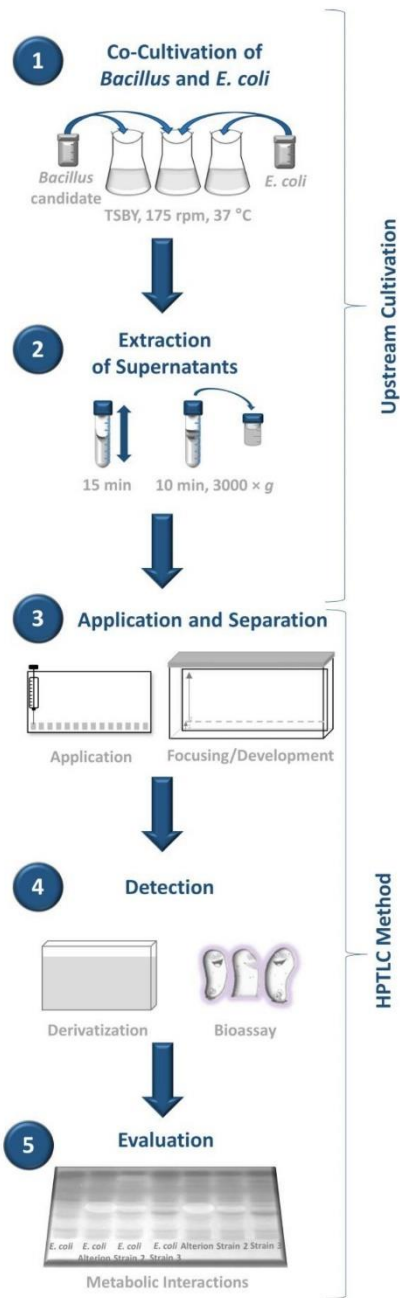
448

449 **Fig. 2**

450

451 **Fig. 3**

452
453 **Fig. 4**
454

455

456   **Fig. 5**

PUBLICATION III

105

Supplementary Information

Metabolic profiling of bacterial co-cultures linked to the predominant species identification

Stefanie Kruse[a], Selina Becker[a] Francis Pierre[b], Gertrud Morlock[a,*]

[a]Institute of Nutritional Science, Chair of Food Science, and Interdisciplinary Research Centre for Biosystems, Land Use and Nutrition, Justus Liebig University Giessen, Heinrich-Buff-Ring 26–32, 35392 Giessen, Germany

[b]Adisseo France S.A.S, Immeuble Anthony Parc 2, 10 Place du Général de Gaulle, 92160 Antony, France

*Corresponding authors: Prof. Dr. Gertrud Morlock, phone: +49-641-9939141; fax +49-641-99-39149, email: gertrud.morlock@uni-giessen.de

1

Table of Content

2

106

50 µL) and the *B. subtilis* samples (stock solution inoculation 100 µL, feed 1 mL of 1:10 dilution feed, dried spores 1 mL of 1:10000 dilution) were pre-cultivated at 37 °C and 175 rpm in 30 mL TSBY for 15.5 h. Aliquots of the *Bacillus* pre-cultures (1.5 mL) and *E. coli* pre-culture (1 mL) were added to the fresh TSBY medium (total volume 20 mL) and cultivated at 37 °C and 175 rpm for 4.5 h.

3

Table S1 Optimization of cultivation scenarios 1−13 to indicate bacterial growth and metabolic activity in co-cultures of *B. subtilis* and *E. coli*

	Pre-cultivation	Main cultivation
	Pre-cultivation	**Main cultivation**
	E. coli **dominance in the co-culture**	
1	-	100 µL *Bacillus* + 30 µL *E. coli* in 30 mL TSBY 37 °C, 175 rpm, 17 h
2	-	100 µL *Bacillus* + 10 µL *E. coli* in 30 mL TSBY 37 °C, 175 rpm, 15 h
3	-	50 µL *Bacillus* + 15 µL *E. coli* in 30 mL TSBY 37 °C, 175 rpm, 14 h
4	-	50 µL *Bacillus*, 15 µL *E. coli* (in 30 mL TSBY, 37 °C 175 rpm, 15.5 h
	Bacillus **dominance in the co-culture**	
5	50 µL *Bacillus* in 30 mL TSBY, 37 °C 175 rpm, 15h	5 mL *Bacillus* pre culture + 15 µL *E. coli* in 15 mL TSBY 37 °C, 175 rpm, 3.5 h
6	50 µL *Bacillus* in 30 mL TSBY, 37 °C 175 rpm, 15h	3 mL *Bacillus* pre culture + 15 µL *E. coli* in 15 mL TSBY 37 °C, 175 rpm, 4h in centrifuge tubes
7	50 µL *Bacillus* in 30 mL TSBY, 37 °C 175 rpm, 15h	3 mL *Bacillus* pre culture + 50 µL *E. coli* in 15 mL TSBY 37 °C, 175 rpm, 4h in centrifuge tubes
8	50 µL *Bacillus* in 30 mL TSBY, 37 °C 175 rpm, 15h	3 mL *Bacillus* pre culture + 50 µL *E. coli* in 15 mL TSBY 37 °C, 175 rpm, 6h in centrifuge tubes
9	50 µL *Bacillus* in 30 mL TSBY, 37 °C 175 rpm, 15h	3 mL *Bacillus* pre culture + 50 µL *E. coli* in 15 mL TSBY 37 °C, 175 rpm, 4h
10	50 µL *Bacillus* in 30 mL TSBY, 37 °C 175 rpm, 15h	3 mL *Bacillus* pre culture + 100 µL *E. coli* in 15 mL TSBY 37 °C, 175 rpm, 4.5h
11	50 µL *Bacillus* in 30 mL TSBY, 37 °C 175 rpm, 15.5h	1.5 mL *Bacillus* pre culture + 100 µL *E. coli* in 20 mL TSBY 37 °C, 175 rpm, 4.5h
	Equivalence of *Bacilli* **and** *E. coli* **in the co-culture**	
12	50 µL *Bacillus*, 50 µL *E. coli* in 30 mL TSBY, 37 °C 175 rpm, 15.5h	1 mL *Bacillus* pre culture + 0.5 mL *E. coli* pre-culture in 20 mL TSBY 37 °C, 175 rpm, 4h
13	50 µL *Bacillus*, 50 µL *E. coli* in 30 mL TSBY, 37 °C 175 rpm, 15.5h	1.5 mL *Bacillus* pre culture + 1 mL *E. coli* pre-culture in 20 mL TSBY 37 °C, 175 rpm, 4.5h

4

Fig. S1 HPTLC chromatograms of bacterial (*B. subtilis* strains 1 and 2 as well as co-cultures with *E. coli*, 100 µL each) metabolite extracts (*n*-butanol and ethyl acetate) on HPTLC plates silica gel 60 separated with ethyl acetate – methanol – water 8:1.3:0.7, V/V/V, detected at FLD 366 nm after derivatization with the primuline reagent (a) as well as bioluminescence image (depicted as greyscale image) after the *A. fischeri* bioassay (b); cultivations were performed using scenarios 2 (a) and 3 (b) in Table S1.

5
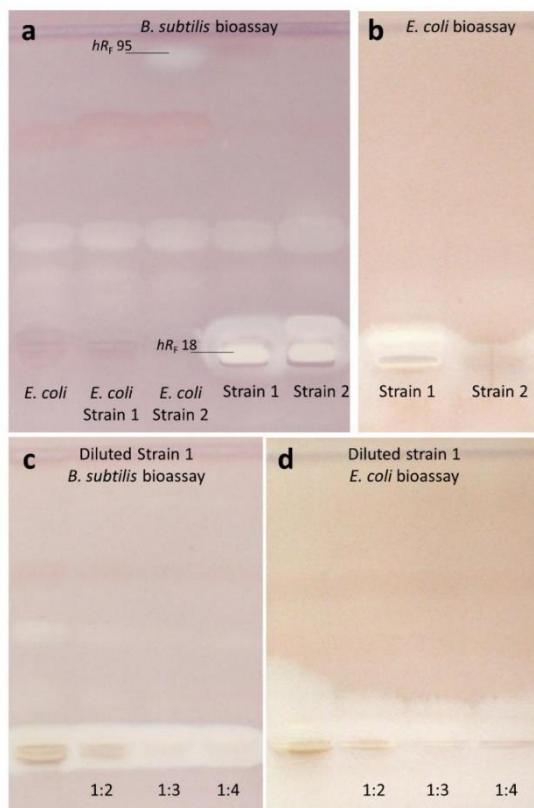
Fig. S2 HPTLC−vis chromatogram of undiluted (a, b) and diluted (c, d) bacterial (*B. subtilis* strains 1 and 2 as well as co-cultures with *E. coli*) metabolite extracts (*n*-butanol, 100 µL each) separated on HPTLC plates silica gel 60 with toluene – ethyl acetate – acetonitrile 2:2:1, *V/V/V*, and detected after the *E. coli* bioassay as well as *B. subtilis bioassay*; *E. coli* (stock solution inoculation 30 µL) and *B. subtilis* (stock solution inoculation 100 µL) bacteria were cultivated in 30 mL TSBY at 37 °C and 175 rpm for 15 h.
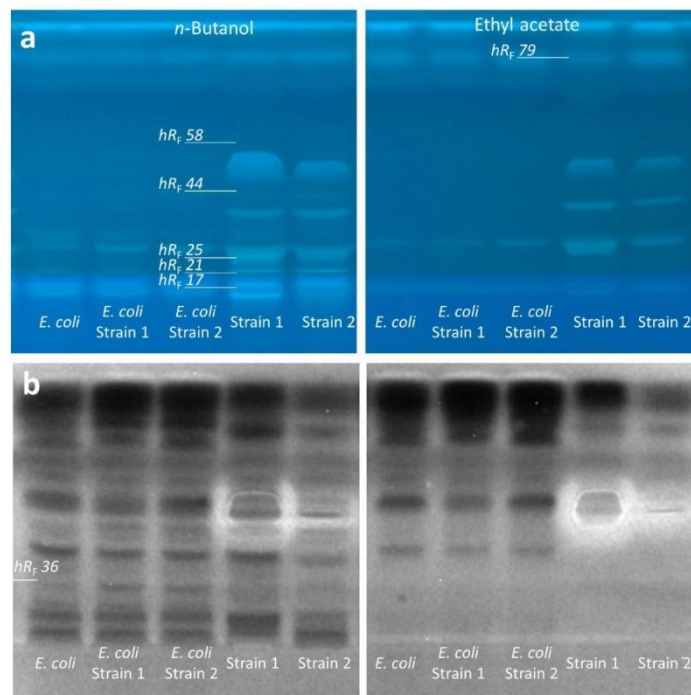
6
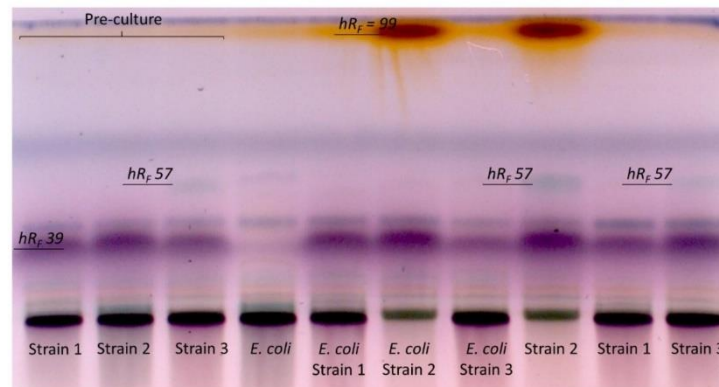
Fig. S3 HPTLC−vis chromatogram of bacterial (*B. subtilis* strains 1−3 as well as co-cultures with *E. coli*) metabolite extracts (*n*-butanol, each 100 µL) separated on HPTLC plates silica gel 60 with toluene – ethyl acetate – acetonitrile 2:2:1, *V/V/V*, and detected after derivatization with the anisaldehyde sulfuric acid reagent. The *B. subtilis* strain stock solutions (inoculation 50 µL) were pre-cultivated at 37 °C and 175 rpm in 30 mL TSBY for 15.5 h. An aliquot (1.5 mL) of these pre-cultures and 100 µL *E. coli* strain stock solutions were added to fresh TSBY medium (total volume 20 mL) and cultivated at 37 °C and 175 rpm for 4.5 h.
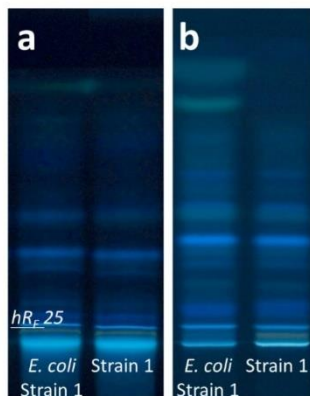
Fig. S4 HPTLC−FLD chromatograms separated on HPTLC plates silica gel 60 with ethyl acetate – acetonitrile 1:1, *V*/*V*, and detected at 366 nm of bacterial (*B. subtilis* strain 1 as well as co-culture with *E. coli*) metabolite extracts (*n*-butanol, each 100 µL). The *B. subtilis* (for b, also *E. coli*) strain stock solutions (inoculation 50 µL) were pre-cultivated at 37 °C and 175 rpm in 30 mL TSBY for 15.5 h. Therefore, 1.5 mL *B. subtilis* pre-cultures and 100 µL *E. coli* strain stock solutions (a) as well as 1 mL of the *E. coli* pre-culture (b) were added to fresh TSBY medium (total volume 20 mL) and cultivated at 37 °C and 175 rpm for 4.5 h.

8
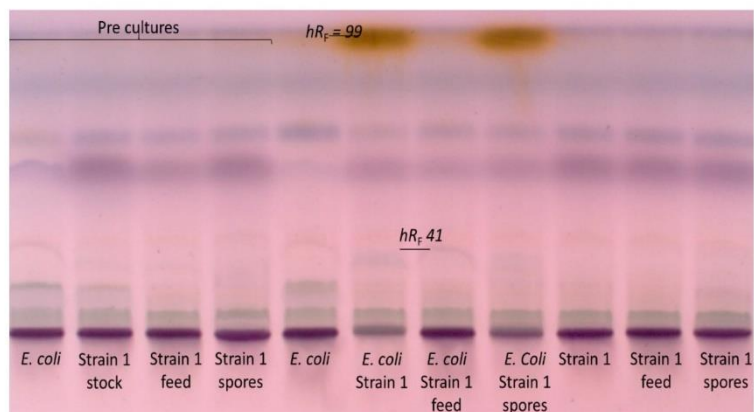
Fig. S5 HPTLC−vis chromatogram of bacterial (as stock solution, in feed, added as spores) metabolite extracts (*n*-butanol, each 100 µL) separated on HPTLC plates silica gel 60 with ethyl acetate − acetonitrile 1:1, *V/V,* and detected after derivatization with anisaldehyde sulfuric acid reagent. The *E. coli* (inoculation 50 µL) and the *B. subtilis* samples (stock solution inoculation 100 µL, feed 1 mL of 1:10 dilution feed, dried spores 1 mL of 1:10000 dilution) were pre-cultivated at 37 °C and 175 rpm in 30 mL TSBY for 15.5 h. Aliquots of the *Bacillus* pre-cultures (1.5 mL) and *E. coli* pre-culture (1 mL) were added to the fresh TSBY medium (total volume 20 mL) and cultivated at 37 °C and 175 rpm for 4.5 h.

9

6. Publication IV

Bacillus subtilis spores in probiotic feed quantified via bacterial metabolite using planar chromatography

Stefanie Kruse[a], Mareike Schenk[a], Francis Pierre[b], Gertrud E. Morlock[a,*]

[a]Chair of Food Science, Institute of Nutritional Science, and Interdisciplinary Research Centre for Biosystems, Land Use and Nutrition, Justus Liebig University Giessen, Heinrich-Buff-Ring 26-32, 35392 Giessen, Germany

[b]Adisseo France S.A.S, Immeuble Anthony Parc 2, 10 Place du Général de Gaulle, 92160 Antony, France

1

2

3

4 **_Bacillus subtilis_ spores in probiotic feed quantified via**

5 **bacterial metabolite using planar chromatography**

6

7

8 Stefanie Kruse[a], Mareike Schenk[a], Francis Pierre[b], Gertrud E. Morlock[a,*]

9

10

11

12 [a]Chair of Food Science, Institute of Nutritional Science, and Interdisciplinary Research Centre

13 for Biosystems, Land Use and Nutrition, Justus Liebig University Giessen, Heinrich-Buff-

14 Ring 26-32, 35392 Giessen, Germany

15 [b]Adisseo France S.A.S, Immeuble Anthony Parc 2, 10 Place du Général de Gaulle, 92160

16 Antony, France

17

18

19

20

21 *Corresponding authors: Prof. Dr. Gertrud Morlock, phone: +49-641-9939141; fax +49-641-

22 99-39149, email: gertrud.morlock@uni-giessen.de

Abstract

Interest in probiotics in animal production has increased due to the European ban on antibiotic growth promoters in 2006. *Bacillus subtilis* DSM 29784 (*B. s.* 29784) is one such probiotic feed additive used in poultry. Cell counting has been the most common analytical tool for counting cells in feed, besides flow cytometry and quantitative polymerase chain reaction. However, quantification of the active probiotic in feed is challenging, since results are influenced by cultivation conditions, viable but non-culturable bacteria and the high contents of feed ingredients. This study presents the first quantitative analysis of a metabolite generated by *B. s.* 29784 spores in feed to draw conclusions on the amount of active dried spores in the feed. Thus, it is the first quantification of active probiotic bacteria at the trace level in feed based on metabolite production but not cell counting. To generate the calibration standards, solutions with different amounts of dried *B. s.* 29784 spores were cultured under the same conditions as the feed sample, ensuring independence from growth performance. Upstream cultivation, metabolite extraction and high-performance thin-layer chromatography analysis were proven to be highly reliable and reproducible. The repeatability of the method (RSD 1.9%) and the recovery (111% ± 21% in feed additive matrix, 96% ± 13% in ionized feed matrix) were excellent. The variations during cultivation occurred due to the complex spore germination process and presence of other microbes in the feed. This new procedure, detecting only those cells that produced the metabolite of interest, has several advantages as it takes into account bacterial viability, cultivation conditions, spore germination process, growth behavior and the influence of the nutrient-rich feed matrix. It truly reflects the activity of the probiotic in the feed product, allows side-by-side comparison of characteristic metabolite patterns and nutrient consumptions to understand the metabolism of dried spores in matrix.

Keywords Metabolite quantification, *Bacillus subtilis* DSM 29784, HPTLC, high-performance thin-layer chromatography, Profiling, Pattern recognition

2

118

1. Introduction

The European Union banned the usage of antibiotic growth promoters in animal production in 2006 [1]. As an efficacious alternative, probiotics are available to sustain the health status of animals and increase animal production [2]. Different species of the genus *Bacillus* are already known for a probiotic effect [3,4]. *Bacillus subtilis* DSM 29784 (*B. s.* 29784) is one of these probiotics. The positive effects were demonstrated in different studies and the efficiency was also performed *in vivo* [5–9]. To be authorized as a feed additive for poultry application, probiotics must follow the requirements set down in the regulation (EC) No. 429/2008 [10]. The identification and quantification of an individual probiotic are necessary to determine the efficacy, and thus, to assign the benefits of the feed additive. Up to now different quantification methods were reported to determine bacterial concentrations in commercial products, *i.e.* cell counting [11], optical density, flow cytometry [12] and quantitative polymerase chain reaction (qPCR) [12,13]. The European standard EN 15784:2009 has to be applied for the official control of probiotics (microorganisms) used in animal feeds. Therein, cell counting as the most common method for counting *Bacilli* species is described. *Bacilli* spores (capable of germination) used as feed additives should be counted with this methodology. The heat-resistant spores are treated for 10 min at 80 °C, causing other vegetative cells to die. After plate cultivation, the *Bacilli* colonies are counted, known to be user-dependend, and reported as colony forming units (CFU). Only plates containing more than 30 and not more than 300 putative *Bacilli* are taken into account. This plate restriction to the middle range is unclear and appears to be based on arbitrary criteria. The cultivation time is flexible (*e.g.*, 16−24 h). The influence of bacterial viability, cultivation conditions, spore germination process, growth behavior and feed matrix is not considered in the CFU value obtained. Furthermore, flow cytometry enabled the detection of probiotic bacteria in complex matrices [14]. The benefit compared to cell counting is that the biological state of the cells can be determined. Damaged or quiescent cells, which were viable but non-culturable, are detected and excluded, avoiding errors in quantification [15]. Species-specific qPCR analysis of probiotic bacteria was more

3

76 accurate compared to cell counting [13] because the cell number depends on the quantity of

77 a nucleic acid target. However, it requires the use of expensive reagents and extensive sample

78 preparation (deoxyribonucleic acid of the target organism must be released from the cell body

79 requiring a chemical and/or physical cell lysis step). All these quantitative methods are

80 appropriate research tools to count the cell number of the probiotic in the feed, but none of

81 them considers the influence of the individual germination process of the spores, the growth

82 behavior in the feed and the cultivation conditions. Therefore, current quantitative methods do

83 not provide results that truly reflect probiotic activity in feed products. Since the activity of

84 probiotic feed additives and respective feed products is touted as an important benefit but is

85 not yet measured in routine quality control, new methods are imperative.

86 So far, the effect of probiotics has not been fully understood and it was suggested that the

87 effect may also depend on the metabolites generated by the microorganism [16]. High-

88 performance thin-layer chromatography (HPTLC) could be a helpful tool with regard to

89 metabolite profiling. The influence of cultivation parameters on the growth performance and

90 metabolite profile of the probiotic *Bacilli* was proven in a first study [17]. In a second study,

91 multi-imaging and effect-directed assay detection were used as strong features of HPTLC to

92 visualize metabolite patterns depending on cultivation conditions, which improved the

93 understanding of the probiotic effect [18]. In this third study, it was hypothesized whether

94 quantitative HPTLC can be used to determine via a selective metabolite the amount of active

95 dried spores of *B. s.* 29784 in feed, using a calibration based on biologically produced

96 metabolite reference levels. Reproducible cultivation would be prerequisite for using as

97 calibration standards the cultures containing different amounts of added spores that produce

98 the metabolite of interest for linear calibration. Such an attempt is in marked contrast to former

99 studies, in which HPTLC was used to quantify bacterial metabolites via external calibration

100 using different levels of a chemical reference solution [19−21]. The procedure intended to be

101 developed would have several advantages as it takes into account bacterial viability,

102 cultivation conditions, spore germination process, growth behavior and the influence of the

4

120

103 nutrient-rich feed matrix. Its performance needs to be proven with regard to linearity,

104 selectivity, limit of quantification (LOQ), precision, recovery, and robustness.

105 **2. Materials and methods**

106 2.1 Chemicals and materials

107 Tryptic soy broth (TSB), HPTLC plates silica gel 60 and syringe filters of polytetrafluoro-

108 ethylene (PTFE), polyvinylidenchloride (PVDF) and mixed cellulose ester (CME), all <2 µm,

109 as well as PTFE (0.45 µm) were purchased from Merck, Darmstadt, Germany. Folded filter

110 595 ½ was obtained by GE Healthcare Whatman, Solingen, Germany. n–Butanol (HPLC

111 grade) was delivered by Acros Organics, Fair Lawn, NJ, USA. Yeast extract (for use in

112 microbial growth medium), D–glucose (Glc, ≥99.5%), yeast nitrogen base without amino acids

113 (for molecular biology), aniline (≥99.5%) and diphenylamine (≥99%) were purchased from

114 Sigma Aldrich, Steinheim, Germany. Sodium chloride (NaCl, ≥99%) was obtained from Fluka,

115 Buchs, Switzerland. Methanol and acetone (both HPLC grade) were purchased from VWR,

116 Darmstadt, Germany. Hydrochloric acid (37%, purest), potassium chloride (KCl, ≥99%),

117 potassium dihydrogen phosphate (KH_2PO_4, ≥99%), magnesium chloride (≥98.5%), and

118 disodium hydrogen phosphate (Na_2HPO_4, ≥99%) were obtained from Carl Roth, Karlsruhe,

119 Germany. Ethyl acetate (≥99.8%) and o–phosphoric acid (85%) were delivered by Th. Geyer,

120 Renningen, Germany. Bidistilled water was prepared by a Destamat Bi 18E, Heraeus, Hanau,

121 Germany. The dried spores of $B.$ $s.$ 29784 (ALTERION® NE) and the matrix compounds

122 (sodium aluminosilicate, calcium carbonate and sucrose) used for the commercial formulation

123 were obtained by Novozymes, Bagsværd, Denmark. The feed sample with and without feed

124 additive at 10 g t^{-1} (0.001 W%) was obtained from Adisseo France SAS, Antony, France.

125 2.2 Method development

126 First the influence of culture medium was proven. A complex TSB culture medium containing

127 Yeast (TSBY, 3% TSB added to 1 L water with 0.6% yeast extract and adjusted to pH 6.2 with

128 2 M hydrochloric acid solution) and a minimal culture medium (sterile solution of 10 g Glc and

5

129 6.8 g yeast nitrogen base without amino acids in 100 mL water added to 800 mL autoclaved

130 double distilled water and 100 mL sterile amino acid solution) [22,23] were tested for a

131 quantitative growth behavior of the spores.

132 Next, the influence of the feed matrix on the metabolite formation was studied. Different

133 amounts of feed additive were added directly to 30 mL culture media (Table S1A). To

134 compensate the influence of the feed matrix, spore standard solution was added according to

135 the standard addition method and tested. The same amount of a feed sample (50 mg) was

136 suspended in 10 mL phosphate-buffered saline (PBS; NaCl 8.0 g L^{-1}, KCl 0.2 g L^{-1}, Na_2HPO_4

137 1.15 g L^{-1}, KH_2PO_4 0.2 g L^{-1} in water) and diluted 1:10 again with PBS. An aliquot of the dilution

138 (1 mL) was added to each culture of the standard levels with increasing amounts of the dried

139 spores (Table S1B). Additionally, the matrix influence was reduced by filtration of 10 mL of the

140 feed additive and feed suspension, both 1:10 diluted in PBS, using different filters (folded filter

141 4–7 µm, sterile syringe filter <2 µm of PTFE, PVDF, CME and 0.45 µm of PTFE). The filtrate

142 (1 mL) or the backwashed cells (absorbed on the syringe filter material and then backwashed

143 with 5 mL of PBS) were used for the cultivation process.

144 Stability of the spore stock solution was investigated. A stock solution of dried spores of

145 *B. s.* 29784 was prepared (5 mg mL^{-1}) in PBS. This spore stock solution (5 mg mL^{-1}) was used

146 directly and after storage at −20 °C for 24 h for the preparation of the $1:10^8$ diluted spore

147 standard solution (50 pg mL^{-1}). After cultivation, the cells were examined with the microscope,

148 extracted with *n*-butanol and analyzed by HPTLC. The microscopy image and HPTLC

149 chromatogram of the fresh stock solution were compared to the stored one.

150 The cultivation process was studied in an incubation room considering linearity and recovery

151 (Table S1C and S1F without matrix). The pre-incubation at room temperature (used by

152 cultivation in the Labocult incubator) was omitted. The dried *B. s.* spores (50 mg ± 2 mg) and

153 the feed (50 mg ± 2 mg) were suspended in PBS (5 mg mL $^{-1}$), diluted with PBS (Table S1C

154 and S1F without matrix), cultivated (at 37 °C, at 175 rpm for 12.5 h) in parallel and the

155 calculated amount of dried spores were compared.

6

122

156

157   2.3 Final method

158   2.3.1 Cultivation and extraction

159   Each feed sample was prepared in PBS (5 mg mL^{-1}) and diluted 1:10 with PBS. A stock

160   solution of dried spores of *B. s.* 29784 was prepared (5 mg mL^{-1}) in PBS and diluted 1:10^8 with

161   PBS. Different amounts of the diluted stock solution (0.5–3.0 mL, corresponding to 25–150 pg

162   of dried spores) as well as the diluted feed sample (1.0 mL) were added to 30-mL TSBY

163   culture medium. Different volumes (1.0–2.5 mL) of autoclaved bidistilled water were added to

164   adapt the volume for each culture to 33-mL (spore standard solutions S1–S4, Table S1C).

165   The samples were pre-incubated at room temperature at 175 rpm (orbital shaker SM-30,

166   Edmund Bühler, Bodelshausen, Germany) for 4 h and further cultivated at 37 °C (Labocult

167   incubator, Servoprax, Wesel, Germany) at 175 rpm for 10.5 h. The temperature was proven

168   and measured with a laser thermometer (Laserliner ThermoSpot, Umarex GmbH & Co. KG,

169   Arnsberg, Germany). After cultivation, the OD_{660} was measured with the M501 Single Beam

170   Scanning UV/Vis Spectrophotometer (CamSpec, Garforth, UK) and the cell suspension was

171   centrifuged with the centrifuge 5702 (Eppendorf, Hamburg, Germany) at 3000 × *g* for 10 min.

172   An aliquot (15 mL) of the cell-free supernatant was used for the liquid-liquid extraction. As

173   described [17], *n*–butanol (5 mL) was added to the supernatant (1:3, *V*/*V*) and shaken with a

174   vortex shaker at level 10 for 15 min. After extraction, the samples were centrifuged at 3000 × *g*

175   for 10 min and each *n*–butanol phase was transferred in an autosampler vial.

176   2.3.2 HPTLC method

177   The *n*-butanol extracts (100 µL) were applied as area (10 mm × 8 mm) on an HPTLC plate

178   (prewashed two times with methanol – water, 4:1 *V*/*V*) with the Automatic TLC Sampler 4

179   (CAMAG, Muttenz, Switzerland). The dosage speed was set to 600 nL s^{-1} and the syringe was

180   rinsed twice with methanol after each application. The area was focused once with acetone

181   and two times with methanol up to 20 mm from the lower end of the plate. After activation of

182   the plate surface with a saturated solution of magnesium chloride (33% relative humidity) for

7

183   10 min, the development was performed with ethyl acetate – methanol – water (8:1.3:0.7

184   *V/V/V*) up to a migration distance of 70 mm with Automatic Development Chamber 2

185   (CAMAG). The chromatogram was immersed for 2 s (speed 3.5 cm s^{-1}) in the diphenylamine

186   aniline *o*-phosphoric acid reagent (2 g diphenylamine in 100 mL *i*-propanol and 2 mL aniline

187   in 100 mL *i*-propanol mixed 1:1, *V/V*, plus 20 mL *o*-phosphoric acid 85%) and dried. The

188   absorbance was measured at 645 nm with the TLC Scanner 4 (CAMAG).

189   2.4 Method validation

190   2.4.1. Working range and LOQ

191   The cultivation, extraction and HPTLC method were performed as described (Table S1C). For

192   the determination of a mean LOQ (*n* = 3), the intensity of the metabolite at hR_F 68 on the track

193   of the lowest spore standard solution (S1, 25 pg dried spores in the 33-mL culture) was

194   repeatedly compared to the intensity of the baseline noise (same peak width and same hR_F

195   value) on a blank track. The signal-to-noise ratio (S/N) was calculated to be ≥10, although the

196   intensity of the metabolite and thus the LOQ depended on the individual growth behavior of

197   the cells.

198   2.4.2 Selectivity

199   The spore standard solution 2 (S2, 50 pg dried spores in the 30-mL culture) and the

200   corresponding amount of matrix compounds from the feed additive (5 ng, Table S1D) were

201   each threefold cultivated (*n* = 3), extracted and subjected to the HPTLC analysis (100 µL

202   each). The metabolite signals at hR_F 68 of S2 extracts were compared to those of the matrix

203   of the feed additive. The selectivity towards the matrix compounds, the used solvents and the

204   culture media was given when no substances were detected at the hR_F of the metabolite. The

205   same procedure was performed with the corresponding amount of a feed matrix (500 µg,

206   Table S1E).

207   2.4.3 Precision

8

124

208   The repeatability (residual standard deviation RSD, $n = 6$) of the metabolite signals at hR_F 68

209   was calculated for the HPTLC method (physico-chemical repeatability) as well as for the

210   cultivation process (biological repeatability). The same S1 extract was applied six times and

211   analyzed by HPTLC to study the repeatability of the HPTLC method. Six cultures of S2

212   (comparable preparation to the feed sample, Table S1C) were prepared, simultaneously

213   cultivated, extracted and analyzed by HPTLC to study the repeatability of the cultivation

214   process.

215   2.4.4 Recovery

216   Six cultures of S2 were prepared, of which feed additive matrix (500 ng, Table S1F) was added

217   to three. The samples were cultivated, extracted and analyzed by HPTLC. The mean values

218   of the metabolite signals at hR_F 68 were calculated for the three cultures ($n = 3$) either with or

219   without matrix. Analogously, the recovery in the ionized feed matrix (treated with ionizing

220   radiation to protect it from potential pathogenic microorganisms) was investigated (Table

221   S1G). Each two S2 cultures with and without feed blank matrix were prepared, and as a

222   reference, two feed blank matrix cultures. All six cultures were extracted and analyzed by

223   HPTLC. The respective mean values of the metabolite signals at hR_F 68 were calculated for

224   the S2 cultures with and without feed blank matrix ($n = 2$). The recovery was determined as

225   quotient of respective mean values times 100. The recovery measurement in the feed was

226   repeated by adding the individual ionized feed matrix (total of two different matrices) to five

227   S2 cultures and one S2 culture was cultivated without any matrix components. The recovery

228   was determined for each culture, related to the S2 culture without matrix components (each

229   $n = 5$).

230   2.4.5 Robustness

231   The cultivation time of dried spores in the feed was extended by 30 min to simulate a varied

232   cultivation time. The extraction and HPTLC method were performed as described. To

233   investigate the stability, the n-butanol extracts were stored at room temperature (3.5 h, 7 h

234   and 24 h) and at -20 °C (3.5 h, 7 h, 24 h, 3 weeks and 8 weeks) and analyzed by HPTLC.

9

235 **3. Results and discussion**

236 This study presents the first quantitative analysis of a metabolite generated by *B. s.* 29784

237 spores in feed to draw conclusions on the amount of active dried spores in feed. In our

238 previous study [17], an intensive and selective metabolite was detected in the probiotic *Bacilli*,

239 which were used to evaluate the validity of imaging HPTLC as quantitative method of bacterial

240 metabolite production. Furthermore, *n*-butanol was proven to be highly suited for extraction

241 and thus selected [17]. Compared to the less significant analysis by cell counting, the new

242 method has to cope with the following aspects to provide results that truly reflect the probiotic

243 activity in the feed product. Firstly, the specified amount of dried spores in feed was present

244 at the trace level in the low $\mu g\ kg^{-1}$ range. Secondly, the germination process of the spores

245 and growth behavior during cultivation was strongly influenced by the feed ingredients. Thirdly,

246 increasing the amount of spores added needed to correlate with increased cell numbers

247 (OD_{660}) along with increased metabolite production, and thus, increased signal intensities in

248 the HPTLC chromatogram. Fourthly, the cultivation process, as well as the preparation of the

249 standard solutions of the dried *B. s.* 29784 spores and the feed samples, should be performed

250 as simply as possible to provide a rapid and economical procedure suited for routine product

251 control.

252 3.1 Method development

253 Two different cultivation media were evaluated for reproducible germination and quantitative

254 growth of the dried spores. A nutrient-rich complex medium, such as the TSBY medium, and

255 a minimal medium that provided only the minimum of nutrients for cell growth were used.

256 Initially, the feed additive was added directly to both culture media to allow easy handling for

257 cultivation. Compared to other *Bacilli,* the probiotic was assumed to better adapt to the minimal

258 medium [17], but after cultivation a reproducible growth of the cells was not possible. Different

259 inoculation volumes of a feed additive standard solution (diluted) were added to the minimal

260 medium to analyze the reproducible growth performance of the spores, but the fluctuations in

261 the OD_{660} were too high for a quantitative method (Fig. S1). An influence of the feed additive

262   matrix compounds on the growth reproducibility was excluded due to the hundredfold dilution

263   of the feed additive with PBS. In contrast, the TSBY medium provided faster growth of cells

264   and an increased cell number with increasing amounts of the added non-diluted feed additive.

265   Furthermore, analysis of the metabolite of interest at hR_F 68 was not impaired by the high

266   matrix load from the TSBY medium and zone resolution remained sufficient in the HPTLC

267   chromatogram (Fig. S2, no interferences in the blank sample BS in the region of the blue

268   marked zone). Consequently, the complex TSBY medium had to be used for cultivation to

269   achieve quantification of the metabolite in *B. s.* 29784. To simplify the method, firstly the feed

270   additive was added directly to the 30-mL culture. A linear working range was established

271   between 50–350 mg, but higher quantities led to signal saturation and flattening of the curve

272   (Fig. S2). By using higher amounts of the dried spores, the cells achieved a growth phase, in

273   which the nutrients were consumed and the metabolite at hR_F 68 was not produced further.

274   To apply this procedure to the feed, a feed sample (containing the feed additive) was added

275   directly to the cultures and analyzed with regard to cell growth and metabolite production. The

276   feed ingredients had a substantial influence on the cultivation process, *i.e.* faster germination

277   and growth of the vegetative cells were observed, and the achievement of quantitative results

278   was impaired. Calibration according to the standard addition method (feed additive added to

279   feed followed by upstream cultivation) was tested to compensate the influence of the feed

280   matrix components. However, the growth behavior in the culture, in which the feed additive

281   (containing *B. s.* 29784, sodium aluminosilicate, calcium carbonate and sucrose) was added

282   to the feed, was different compared to the culture of the mere feed additive. The growth

283   behavior changed due to the presence of additional nutrients in the feed. Thus, for the

284   quantification of active dried spores in feeds, the influence of the feed matrix had to be

285   reduced. Different filtration modes were tested to reduce these influences. A tenfold dilution

286   (in PBS) of the culture containing the feed spiked with different levels of the *B. s.* 29784 spores

287   and the filtration of this suspension through a sterile syringe filter, followed by backwashing of

288   the cells, led to a well-fitted calibration curve (R 0.9986, RSD 2.8%). A decrease in the nutrient

289   content and an increase in the production of the metabolite at hR_F 68 were achieved. However,

11

290   using this procedure, the syringe filter clogged at higher amounts of the feed additive or feed

291   samples.

292   As the dilution of the feed was necessary to minimize the influence of the feed matrix on the

293   growth behavior, metabolite standards (by upstream cultivation) were prepared by adding

294   different volumes of the hundred millionfold diluted *B. s.* 29784 in the tenfold diluted feed

295   sample according to the standard addition method. However, the correlation coefficient of the

296   calibration function was still not reliable (R of 0.8400, RSD 18.3%). The lack in a linear

297   correlation was explained by the spores originally present in the feed along with the added

298   spores, and thus exponential growth of the cells (Fig. S3). Next, different concentrations of

299   cultivated dried spores of *B. s.* 29784, generating the metabolite at different levels, were used

300   as calibration standard solutions (without feed). As before, the feed sample was cultured 1:10

301   diluted in PBS. The dilution of the feed also resulted in a dilution of the standard solution

302   spiked with *B. s.* 29784 spores. According to the manufacturer specification, the concentration

303   of the feed additive in the feed is 10 g t^{-1} (0.001 W%), which is equal to an amount of 3 mg t^{-1}

304   dried *B. s.* 29784 spores, and thus after dilution, dried spores were present in the low pg range

305   in the culture. This required a small amount of dried spores (25−150 pg) in the standard

306   solutions. A high dilution was necessary which could increase the variances of the results

307   obtained. The simultaneous cultivation of feed samples and standard solutions under the

308   same conditions helped to compensate for influences on growth performance from cultivation

309   or environmental conditions. Additionally, the germination period of the spores in the standard

310   solutions was comparable to that in the feed sample. All this was precondition for the

311   calculation of the amount of active probiotic bacteria in the feed, leading to the developed

312   method (Fig. 1).

313   Usual feed samples are weighed in the gram range. Using lower sample amounts and

314   volumes (Table S1), such as 50 mg instead of 1 g, the working process was much easier

315   under the laminar flow cabinet for routine analysis, since centrifuge tubes (instead of

316   autoclaved larger bottles) could be used for the dilution steps. In addition, a 20-fold volume of

317   autoclaved PBS buffer was saved (only 190 mL instead of 2100 mL of the autoclaved PBS

318 was needed, if calculated for 10 samples). However, the smaller weigh-in of the feed sample

319 could influence the result within the cultivation process when the probiotic is not

320 homogeneously mixed in the feed. To ensure that the smaller amount did not influence the

321 result, the low amount was cultivated in parallel to a 20-fold amount of the feed. The same

322 results for the amount of dried spores were achieved (Fig. 2), proving that the weighed amount

323 did not influence the calculated amount of dried spores in the feed. Thus, the homogeneous

324 distribution of the spores in the feed was confirmed.

325 Instead of incubation in the Labocult incubator, the cultivation was studied in an incubation

326 room at 37 °C and 175 rpm to reduce the influence coming from a variation of the cultivation

327 temperature. Within the cultivation process, the temperature was constant. However, for

328 different days, a fluctuation up to ± 3 °C was observed. The pre-incubation at room

329 temperature was omitted and the cultivation was prolonged to 12.5 h. The extraction and

330 HPTLC method was performed as described. The linear regression achieved (Table S1C; R

331 of 0.96–0.99; RSD of 6.1–10.4%) was good and the feed sample result was in the same range

332 as determined using the Labocult incubator (3.3). However, precision and recovery were

333 significantly worsened. The germination of spores is a complex process with different

334 morphological changes and can be described in two different phases – germination and

335 outgrowth. In the literature, the germination processes of individual spores were demonstrated

336 to be different under the same conditions. Spores were in the outgrowth, whereas others were

337 still in the germination phase [26,27]. The individual germination process is also evident for

338 *B. s.* 29784 [28]. The pre-incubation of the cultures using the Labocult incubator did reduce

339 the variations between the individual spores in these two phases. After the 4 h pre-incubation,

340 most spores had reached the outgrowth and the growth performance of the cells was more

341 constant. This outcome proved that pre-incubation is crucial for successful validation.

342

343 3.2 Method validation

344 The validation was performed according to the International Council for Harmonisation of

345 Technical Requirements Quality guidelines 2 (ICH Q2). The validation of the method included

13

346   linearity, selectivity, LOQ, precision, recovery, and robustness (Fig S4). As usual in HPTLC

347   analysis, the calculated sample result for the metabolite of interest at hR_F 68 (and not the

348   detected peak area) was used for inter day and inter plate data analysis. For intra plate

349   analysis the detected peak area was used. The stock solution (5 mg mL^{-1}) of the dried

350   *B. s.* 29784 was prepared freshly for each cultivation process because a significant change in

351   cell performance was observed by microscopy after freezing and re-culturing of the spores.

352   The cells tended to form aggregates faster (Fig. S5, which hindered the nutrient supply for the

353   enclosed cells. Although such differences were not detected in the HPTLC chromatogram, it

354   was recommended to prepare stock solution freshly.

355   3.2.1 Linearity and LOQ

356   Preparing the spore standard solutions that generate the metabolite of interest (hR_F 68) during

357   the cultivation, the high dilution (1: 10^8) of the spore stock solution (from 5 mg mL^{-1} to

358   50 pg mL^{-1}) was necessary to match the low concentration of the spores in the feed. The

359   linearity for four spore standard solution levels (25, 50, 100 and 150 pg dried *B. s.* 29784 in

360   33-mL feed culture, Table S1) was investigated six times. The cells in the cultures started to

361   grow well, while for standard solutions with higher amounts of the dried spores, cell adhesion,

362   exponential growth of the cells and metabolite degradation were observed, which impaired

363   linearity. The correlation coefficients of six regressions ranged between 0.94 and 0.99 with

364   precisions (RSD) of the calibration curves of 4–16% (Fig. 3). These performance data were

365   acceptable for the detection of the generated metabolite of interest via cultivated *B. s.* 29784

366   spores at the trace level. The variation of the cell growth behavior and resulting metabolite

367   production was explained by the high dilution (small amounts are prone to variations in the

368   cultivation process), by different temperatures (up to ± 3 °C), solar radiation and humidities,

369   and by the fact that the spores had to germinate before the growth phase started, whereby

370   the spore germination of isogenic populations can be heterogenic [24,25] (Fig. S6).

371   3.2.2 Selectivity

372   The culture medium as well as the matrices of the feed additive and the feed were analyzed

373 with regard to interfering signals. The corresponding amounts of the two matrices in a 50 mg

374 feed sample were calculated. The feed sample (50 mg) was suspended in 10 mL PBS, diluted

375 1:10 in PBS, and 1 mL of this dilution was added to the cultures. This corresponded to 500 µg

376 of the feed sample in the culture and was considered equal to the feed matrix. The

377 concentration of feed additive in the feed is 10 g t^{-1}, converted to the 500 µg feed in the culture,

378 this corresponds to 5 ng of feed additive based on the feed additive matrix. The cultivation of

379 the two matrix samples and a culture medium sample was performed analogously to the

380 previous cultivation in the feed. The respective *n*-butanol extracts were analyzed along with

381 solvent blanks (PBS and *n*-butanol). The HPTLC-Vis chromatogram and the densitogram at

382 645 nm showed no interferences at hR_F 68 in the feed additive matrix and solvent blanks (Fig.

383 S7A/B), which confirmed method selectivity. In comparison, a weak interference was observed

384 in the non-ionized feed matrix at hR_F 68 (Fig. S7C/D). In the non-sterile feed matrix, cells were

385 present, which also produced the analyzed metabolite, however, the low signal had no

386 pronounced influence on the quantification of dried spores in the feed (compare recovery,

387 blank feed also indicated interferences Fig. S9). But as long as an unspecific metabolite is

388 used for the quantification, it is better the feed matrix should be ionized, before the addition of

389 *B. s.* 29874 spores and the quantification has to be performed directly afterward, to minimize

390 the influence of environmental microflora.

391 3.2.3 Repeatability

392 The physico-chemical repeatability (RSD, *n* = 6) of the determination of the metabolite at

393 hR_F 68 was 1.9% for the same S1 extract applied six times. This result indicated the very good

394 repeatability of the HPTLC method (Fig. S8). The repeatability of the cultivation process was

395 studied for six individual cultures of S2 prepared comparably to the feed sample and cultivated

396 simultaneously. In the Labocult incubator, the temperature fluctuated up to ± 1.5 °C between

397 the cultures and up to ± 3 °C between different cultivations. The individual growth and the

398 resulting metabolite intensity at hR_F 68 led to a mean repeatability (RSD, *n* = 6) of 12% (ranged

399 7.8%–13.9%, Fig. 4). The repeatability of the cultivation process showed 6-fold higher

15

400   fluctuations, depending on the individual growth behavior of the spores than that of the HPTLC

401   method. The repeatability (RSD, $n = 6$) of the cultivation of feed (500 µg feed mL^{-1}) calculated

402   via the produced metabolite in the simultaneously cultivated spore standard solutions was

403   14%.

404   3.2.4 Recovery

405   The recovery experiments were performed in three matrices, *i.e.* in feed additive and two feeds

406   (Fig. 5, Fig. S9 and Fig. S10). The recovery was proven and calculated via the mean value of

407   the metabolite signal intensity at hR_F 68 of three S2 solutions and three S2 solutions with the

408   feed additive matrix. Small variations between the cultures were visible in the HPTLC

409   chromatogram. These variations could be explained by the growth performance of the spores

410   and the high dilution of the S2 solutions. However, the matrix of the feed additive had no

411   influence on the growth behavior of the cells. The recovery was calculated to be 111% ± 21%

412   ($n = 3$). The repeatability of 21% was comparable to that of the previously reported feed

413   cultivation (14% in 3.2.3.). Thus, no influence of the feed additive matrix on the cultivation of

414   the feed samples was detected (Fig. 5). Also, the ionized feed matrix had no influence on the

415   growth behavior of the cells. In the cultures, which contained only the matrix compounds, a

416   few cells were detected. These cells also produced the metabolite at hR_F 68, but the HPTLC

417   signal intensity was negligible and had no influence on the quantification of *B. s.* 29784 spores

418   in the feed. For example, the metabolite intensity in the S2 cultures was comparable to the S2

419   culture with the matrix, proving that the contribution to the signal was negligible. In addition,

420   the recovery was performed in an ionized feed matrix, so that the environmental microflora

421   does not influence the results. The recovery in the ionized feed matrix was 90% ± 22 (Fig. 5).

422   The variations in the signal intensity could be explained by the individual germination of spores

423   in the different cultures [26,27] and were comparable to the variation in the feed additive

424   matrix. The repeated recovery test in two different ionized feed matrices indicated comparable

425   results (Fig. S10, all $n = 5$; feed matrix 1: 96% ± 13%, 95% ± 13% feed matrix 2: 85% ± 10%).

426   This results concluded that the matrices of the feed additive and the feed had no substantial

16

132

427   influence on the growth behavior of the cells. In the ionized feed matrix, cells of the

428   environmental microflora were present and formed the analyzed metabolite (Fig. S9), but an

429   acceptable recovery was achieved. Compared to the cell counting, the side-by-side

430   comparison of blank feed samples to spore standards and feed samples is a significant

431   advantage of the newly developed method because the influence of each matrix compound

432   on the growth behavior of the cells can be assessed.

433   3.2.5 Robustness

434   Variations in the cultivation time and stability of the *n*-butanol extract were studied for analysis

435   of a feed sample. The influence of a cultivation time extended by 30 min was investigated,

436   resulting in a poor calibration performance (correlation coefficient R of 0.94 and precision RSD

437   of 18%) of the metabolite of interest. The calculated mean amount of the dried spores in the

438   feed (168 pg mg^{-1} feed) was below the analyzed feed samples (180–250 pg mg^{-1} feed, as in

439   3.3), which revealed the high influence of the cultivation time on the result. Next, stability of

440   the *n*-butanol extract was proven stored at room temperature (3.5 h, 7 h and 24 h) and at -

441   20 °C (3.5 h, 7 h, 24 h, 3 weeks and 8 weeks). The HPTLC procedure was performed and

442   stability was given for storage at room temperature up to 24 h, whereas stored frozen, it was

443   stable for 3 weeks. A minor difference between the metabolite intensity of the individual

444   measurements was observed, but a comparable correlation coefficient, precision and amount

445   of dried spores in the feed were obtained. After eight weeks, the correlation coefficient and

446   precision were worse, and a higher amount of dried spores was calculated. The *n*–butanol

447   extracts were stable over 24 h at room temperature and over three weeks at −20 °C. These

448   results indicated that the extracts were stable at room temperature over 24 h and frozen over

449   three weeks but not over eight weeks. The difference in signal intensity was due to the different

450   implementations (Fig. S11).

451

452   3.3 Probiotic feed sample analysis

453   With regard to sample throughput in the industrial application, the analysis of 15 samples in

17

454   parallel took 5 h after cultivation (OD, microscopy, centrifugation, extraction and HPTLC

455   analysis), which is 20 min per sample. Respective consumption costs were 0.7 Euro per

456   sample. The developed bioanalytical method was therefore cost- and time-saving.

457   Finally, the validated method was applied to commercially available non-ionized feed

458   containing the probiotic *B. s.* 29784. Non-ionized feed means that other microorganisms can

459   be present in the feed. The obtained mean amount of the dried spores in the feed was

460   212 µg kg^{-1} ± 14% (*n* = 6; ranged 180–250 pg mg^{-1} feed). In comparison, the theoretical trace

461   amount of added dried spores according to the manufacturer information was calculated to be

462   3 µg kg^{-1}. The 70-fold higher value was plausible because the microflora environment of the

463   non-ionized feed sample does influence the result. The exponential growth of microbes in

464   feeds more dramatically increases the outcome (metabolite production) compared to

465   chemistry alone. The used metabolite is highly selective for the probiotic *B. s.* 29784 strain,

466   but genetically very similar *Bacilli* could also produce this metabolite, explaining increased

467   results. But, the specification of the probiotic *Bacilli* is a manufacturer information. The cell

468   counting only indicated the CFU/g and not the actual amount of dried spores present in the

469   feed. Thus, higher amounts of dried *B. s.* 29784 spores in the feed are possible. Hence, if the

470   developed method will be performed with a specific (not only selective) metabolite, the results

471   will gain in accuracy. Neverthless, identifying a distinct metabolite of a probiotic, this method

472   leads to results that truly reflect the activity in the probiotic feed product. Taking into account

473   that the analysis of the biologically produced metabolite was performed at the trace level in

474   the feed matrix , comparatively accurate results were obtained. In contrast, results from the

475   commonly used cell counting are not as convincing, since the results depend on the user,

476   protocol (plates preselected according to arbitrary criteria, and unspecific cultivation time of

477   16−24 h), bacterial viability, cultivation conditions, spore germination process, growth behavior

478   and feed matrix.

479

18

134

135

4. Conclusions

The developed and validated method allowed the calculation of the amount of active dried spores in the feed that produced the metabolite of interest. To the best of our knowledge, this was the first time that the amount of probiotic bacteria was quantified based on their metabolite production rather than by cell counting. The good performance of the streamlined method (20 min per sample analysis, 0.7 Euro per sample) was proven by excellent validation data obtained for repeatability and recovery in feed additive matrix and ionized feed matrix. Yet, variations occurred during the cultivation process due to the complex germination process of the spores and the presence of other microbes in non-ionized feed. Compared to the non-specific and non-selective quantification by cell counting, providing a number of CFU, this new method showed clear advantages. The quantification by imaging HPTLC led to more accurate results, as only the metabolic active cells were considered and analyzed under standardized conditions. In the feed production process, a specific amount of dried spores is added to the feed and the actual activity depends on growth conditions. Neither is reflected in the measured number of CFU during cell counting. For the latter, feed samples were cultivated over an unspecific time of 16−24 h and plates with less than 30 CFU and more than 300 CFU were arbitrarily excluded from the result calculation. In contrast, the new method used a defined incubation time, took into account the influence of cultivation parameters on cell growth behavior at each cultivation and referred to probiotic-generated standards. Additionally, the side-by-side comparison of metabolite profiles and nutrient consumption is helpful for understanding of the calculated results. The nutrients in the culture medium of the feed sample should decrease in the same way, compared to the nutrients in the spore standard solutions. If not, the feed matrix could have affected the growth behavior of the cells. This is additional important information for evaluation of the probiotic feed that is not obtained by cell counting. Furthermore, cell counting only indicates whether any cells are present. The reported CFU says nothing about the amount of active dried spores in the feed. Thus, also more spores could be present in the feed. In the future, when a specific metabolite is identified in a probiotic,

19

507 only the cultivation parameters need to be optimized to generate a linear calibration function,

508 and this developed method including sample preparation can be used for quantification of the

509 probiotic in the feed.

510 **CrediT authorship contribution**

511 **Stefanie Kruse**: Conceptualization, Methodology, Experimental Analysis, Data Analysis,

512 Writing – Original Draft. **Mareike Schenk**: Experimental Analysis. **Francis Pierre**: Resources,

513 Paper Review. **Gertrud E. Morlock**: Conceptualization, Methodology, Supervision,

514 Resources, Writing – Review and Editing.

515 **Declaration of competing interest**

516 The authors declare that they have no known competing financial interests or personal

517 relationships that could have appeared to influence the work reported in this paper.

518 **Acknowledgments**

519 Instrumentation was partially funded by the Deutsche Forschungsgemeinschaft (DFG,

520 German Research Foundation) – INST 162/471-1 FUGG; INST 162/536-1 FUGG.

521 **Appendix A. Supplementary data**

522 Supplementary data to this article can be found online at…

20

References

[1] The European Parlament And Of The CouncilL, Regulation (EC) No 1831/2003 of the European Parlament and of the CouncilL of 22 September 2003 on additives for use in animal nutrition: L 268/29, 2003.

[2] R. Dowarah, A.K. Verma, N. Agarwal, The use of Lactobacillus as an alternative of antibiotic growth promoters in pigs: A review, Anim. Nutr. 3 (2017) 1–6.

[3] S. Mingmongkolchai, W. Panbangred, Bacillus probiotics: an alternative to antibiotics for livestock production, J. Appl. Microbiol. 124 (2018) 1334–1346.

[4] S. Mazkour, S.S. Shekarforoush, S. Basiri, S. Nazifi, A. Yektaseresht, M. Honarmand, Effects of two probiotic spores of Bacillus species on hematological, biochemical, and inflammatory parameters in Salmonella Typhimurium infected rats, Sci. Rep. 10 (2020) 8035.

[5] V. Jacquier, A. Nelson, M. Jlali, L. Rhayat, K.S. Brinch, E. Devillard, Bacillus subtilis 29784 induces a shift in broiler gut microbiome toward butyrate-producing bacteria and improves intestinal histomorphology and animal performance, Poult. Sci. 98 (2019) 2548–2554.

[6] C. Keerqin, L. Rhayat, Z.-H. Zhang, K. Gharib-Naseri, S.K. Kheravii, E. Devillard, T.M. Crowley, S.-B. Wu, Probiotic Bacillus subtilis 29,784 improved weight gain and enhanced gut health status of broilers under necrotic enteritis condition, Poult. Sci. 100 (2021) 100981.

[7] M. Neijat, J. Habtewold, R.B. Shirley, A. Welsher, J. Barton, P. Thiery, E. Kiarie, Bacillus subtilis Strain DSM 29784 Modulates the Cecal Microbiome, Concentration of Short-Chain Fatty Acids, and Apparent Retention of Dietary Components in Shaver White Chickens during Grower, Developer, and Laying Phases, Appl. Environ. Microbiol. 85 (2019).

[8] L. Rhayat, M. Maresca, C. Nicoletti, J. Perrier, K.S. Brinch, S. Christian, E. Devillard, E. Eckhardt, Effect of Bacillus subtilis Strains on Intestinal Barrier Function and Inflammatory Response, Front. Immunol. 10 (2019) 564.

21

551 [9] Y. Wang, C. Heng, X. Zhou, G. Cao, L. Jiang, J. Wang, K. Li, D. Wang, X. Zhan,

552 Supplemental Bacillus subtilis DSM 29784 and enzymes, alone or in combination, as

553 alternatives for antibiotics to improve growth performance, digestive enzyme activity,

554 anti-oxidative status, immune response and the intestinal barrier of broiler chickens,

555 Br. J. Nutr. 125 (2021) 494–507.

556 [10] The European Parlament And Of The CouncilL, Commission Regulation (EC) No

557 429/2008 of 25 April 2008 on detailed rules for the implementation of Regulation (EC)

558 No 1831/2003 of the EuropeanParliament and of the Council as regards the

559 preparation and the presentation of applications and theassessment and the

560 authorisation of feed additives: L 133/1, 2008.

561 [11] R.S. Breed, W.D. Dotterrer, The Number of Colonies Allowable on Satisfactory Agar

562 Plates, J. Bacteriol. 1 (1916) 321–331.

563 [12] J. Gorsuch, D. LeSaint, J. VanderKelen, D. Buckman, C.L. Kitts, A comparison of

564 methods for enumerating bacteria in direct fed microbials for animal feed, Journal of

565 microbiological methods 160 (2019) 124–129.

566 [13] C. Davis, Enumeration of probiotic strains: Review of culture-dependent and alter-

567 native techniques to quantify viable bacteria, J. Microbiol. Methods 103 (2014) 9–17.

568 [14] L. Michelutti, M. Bulfoni, E. Nencioni, A novel pharmaceutical approach for the

569 analytical validation of probiotic bacterial count by flow cytometry, J. Microbiol.

570 Methods 170 (2020) 105834.

571 [15] C. Chiron, T.A. Tompkins, P. Burguière, Flow cytometry: a versatile technology for

572 specific quantification and viability assessment of micro-organisms in multistrain

573 probiotic products, J. Appl. Microbiol. 124 (2018) 572–584.

574 [16] P. Choi, L. Rhayat, E. Pinloche, E. Devillard, E. de Paepe, L. Vanhaecke, F.

575 Haesebrouck, R. Ducatelle, F. van Immerseel, E. Goossens, Bacillus Subtilis 29784 as

576 a Feed Additive for Broilers Shifts the Intestinal Microbial Composition and Supports

577 the Production of Hypoxanthine and Nicotinic Acid, Animals 11 (2021).

22

138

578 [17] S. Kruse, F. Pierre, G. Morlock, Imaging high-performance thin-layer chromatography
579 as powerful tool to visualize metabolite profiles of eight Bacillus candidates upon
580 cultivation and growth behavior, J. Chromatogr. A 1640 (2021) 461929.

581 [18] S. Kruse, F. Pierre, G.E. Morlock, Effects of the Probiotic Activity of Bacillus subtilis
582 DSM 29784 in Cultures and Feeding Stuff, J. Agric. Food Chem. 69 (2021) 11272–
583 11281.

584 [19] M. Geissler, C. Oellig, K. Moss, W. Schwack, M. Henkel, R. Hausmann, High-
585 performance thin-layer chromatography (HPTLC) for the simultaneous quantification of
586 the cyclic lipopeptides Surfactin, Iturin A and Fengycin in culture samples of *Bacillus*
587 species, J. Chromatogr. B 1044–1045 (2017) 214–224.

588 [20] M. Jamshidi-Aidji, G.E. Morlock, Fast equivalency estimation of unknown enzyme
589 inhibitors in situ the effect-directed fingerprint, shown for *Bacillus* lipopeptide extracts,
590 Anal. Chem. 90 (2018) 14260–1426

591 [21] M. Jamshidi-Aidji, I. Dimkić, P. Ristivojević, S. Stanković, G.E. Morlock, Effect-directed
592 screening of Bacillus lipopeptide extracts via hyphenated high-performance thin-layer
593 chromatography, J. Chromatogr. A 1605 (2019) 460366

594 [22] I. Klingelhöfer, G.E. Morlock, Bioprofiling of Surface/Wastewater and Bioquantitation of
595 Discovered Endocrine-Active Compounds by Streamlined Direct Bioautography, Anal.
596 Chem. 87 (2015) 11098–11104.

597 [23] E.J. Routledge, J.P. Sumpter, Estrogenic activity of surfactants and some of their
598 degradation products assessed using a recombinant yeast screen, Environ Toxicol
599 Chem 15 (1996) 241–248.

600 [24] L. Peng, de Chen, P. Setlow, Y. Li, Elastic and inelastic light scattering from single
601 bacterial spores in an optical trap allows the monitoring of spore germination
602 dynamics, Anal. Chem. 81 (2009) 4035–4042.

603 [25] P. Zhang, W. Garner, X. Yi, J. Yu, Y. Li, P. Setlow, Factors affecting variability in time
604 between addition of nutrient germinants and rapid dipicolinic acid release during
605 germination of spores of Bacillus species, J. Bacteriol. 192 (2010) 3608–3619.

23

139

606   [26]   B. Setlow, J. Yu, Y.-Q. Li, P. Setlow, Analysis of the germination kinetics of individual

607   Bacillus subtilis spores treated with hydrogen peroxide or sodium hypochlorite, Lett.

608   Appl. Microbiol. 57 (2013) 259–265.

609   [27]   de Chen, S.-S. Huang, Y. Li, Real-time detection of kinetic germination and

610   heterogeneity of single Bacillus spores by laser tweezers Raman spectroscopy, Anal.

611   Chem. 78 (2006) 6936–6941.

612   [28]   A. Moal, Devillard Estelle, K. Siedelmann Brinch, Visualising germination and activity

613   of Bacillus subtilis in broilers, International Poultry Production 28 (2020) 14–15.

614

24

140

Figure legends

Fig. 1 Schematic workflow for the metabolite quantification in the probiotic feed additve *B. s.* 29784 by imaging HPTLC.

Fig. 2 Method development – Influence of the feed matrix: Baffle flasks of spore standard solution S1–S4 and the feed sample (non-ionized feed pellets containing Alterion at 10 g t^{-1}) with two different weighings after cultivation (A) and the corresponding microscopy images (B). HPTLC-Vis chromatogram after derivatization with diphenylamine aniline *o*-phosphoric acid reagent of the *n*-butanol extracts and the corresponding absorbance measurement at 645 nm (C). The linear regression and deviation of the calibration process are demonstrated (D). Evaluation was performed of the blue-marked zone.

Fig. 3 Method validation – Linearity: Baffled flasks of spore standard solutions S1–S4 and the feed sample (non-ionized feed pellets containing 10 g t^{-1} Alterion) after cultivation (A) and the corresponding microscopy images (B). HPTLC-Vis chromatogram after derivatization with diphenylamine aniline *o*-phosphoric acid reagent of the *n*-butanol extracts and the corresponding absorbance measurement at 645 nm (C). The linear regression and deviation of the calibration process are demonstrated (D), evaluated via the blue-marked zone.

Fig. 4 Method validation – Repeatability: Post-cultivation image of baffled flasks 1–6 used for determination of the repeatability (n = 6), exemplarily, of the cultivation of spore standard solution S2, corresponding to 50 pg dried spores of *B. s.* 29784 (A). HPTLC-Vis chromatogram after derivatization with diphenylamine aniline *o*-phosphoric acid reagent of the *n*-butanol extracts of each culture supernatant (B) and the corresponding deviations (C). The produced metabolite at *hR*$_F$ 68 is marked blue.

Fig. 5 Method validation – Recovery: Baffled flasks of the three spore standard solutions S2 with and without the feed additive matrix (A) after cultivation and the corresponding microscopy images (B). HPTLC-Vis chromatogram after derivatization with diphenylamine aniline *o*-phosphoric acid reagent of the *n*-butanol extracts and the corresponding absorbance measurement at 645 nm (C). The deviation between the individual cultures is given (D). Evaluation was performed of the blue-marked zone.
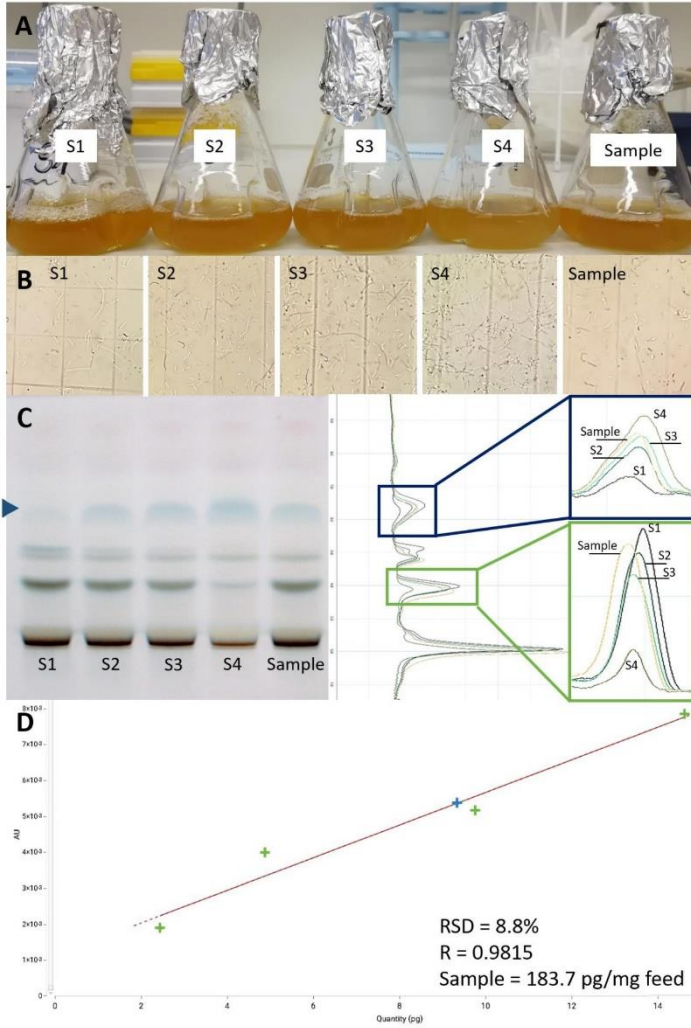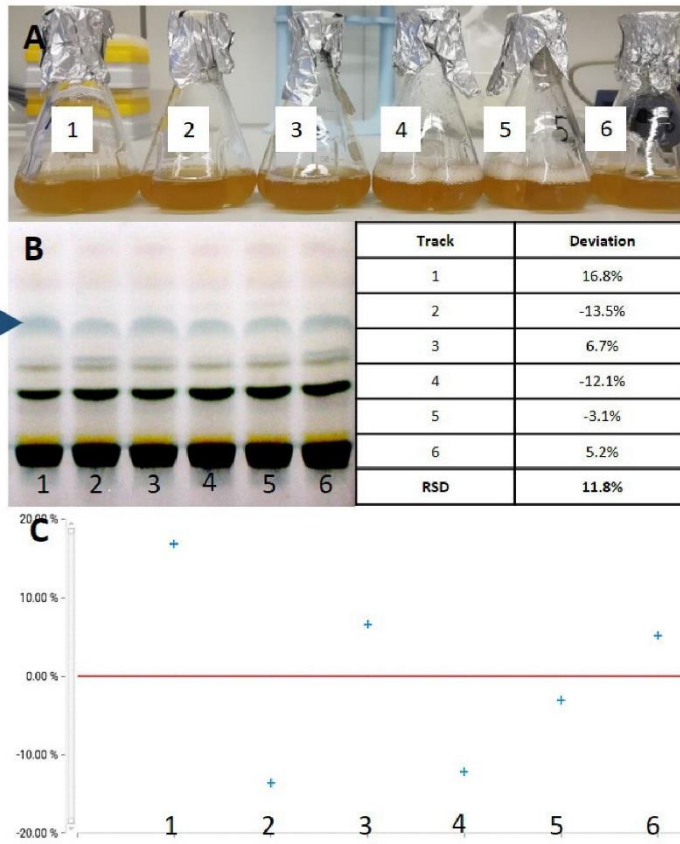
25

643

Fig. 1

142
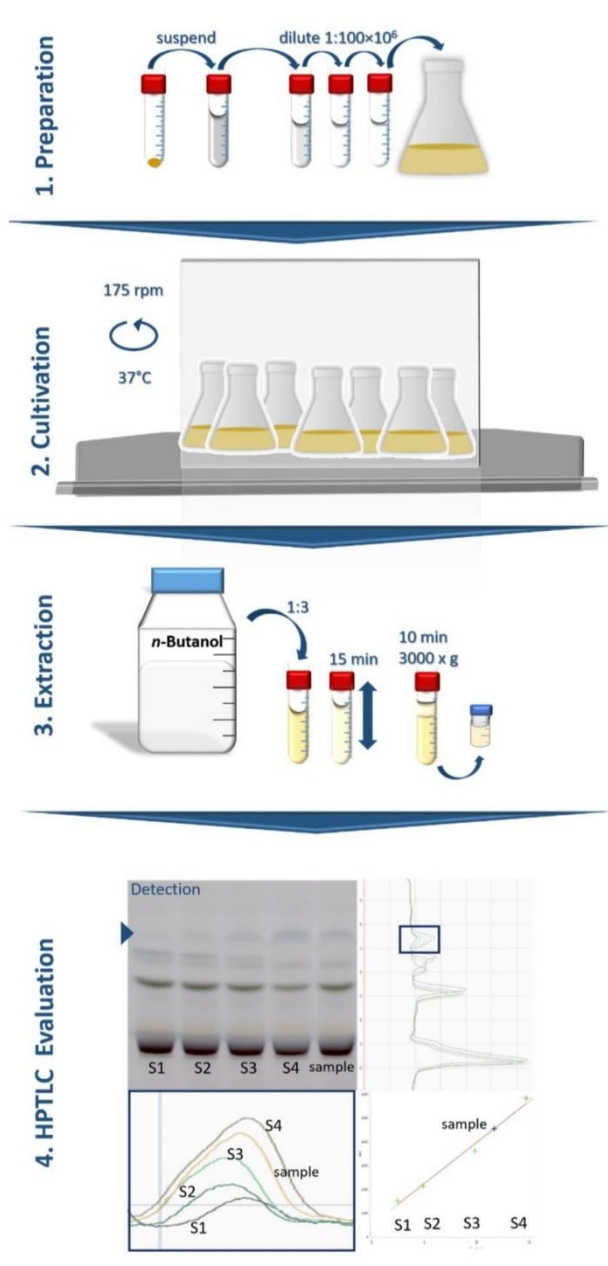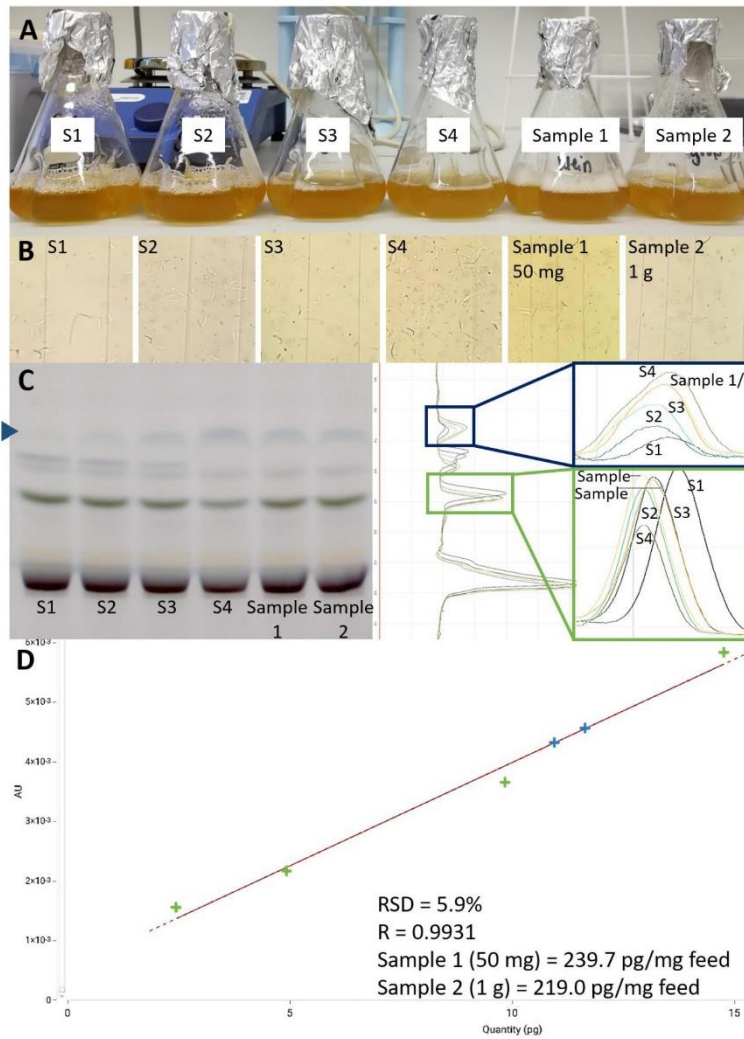
647   Fig. 2

648

649

650

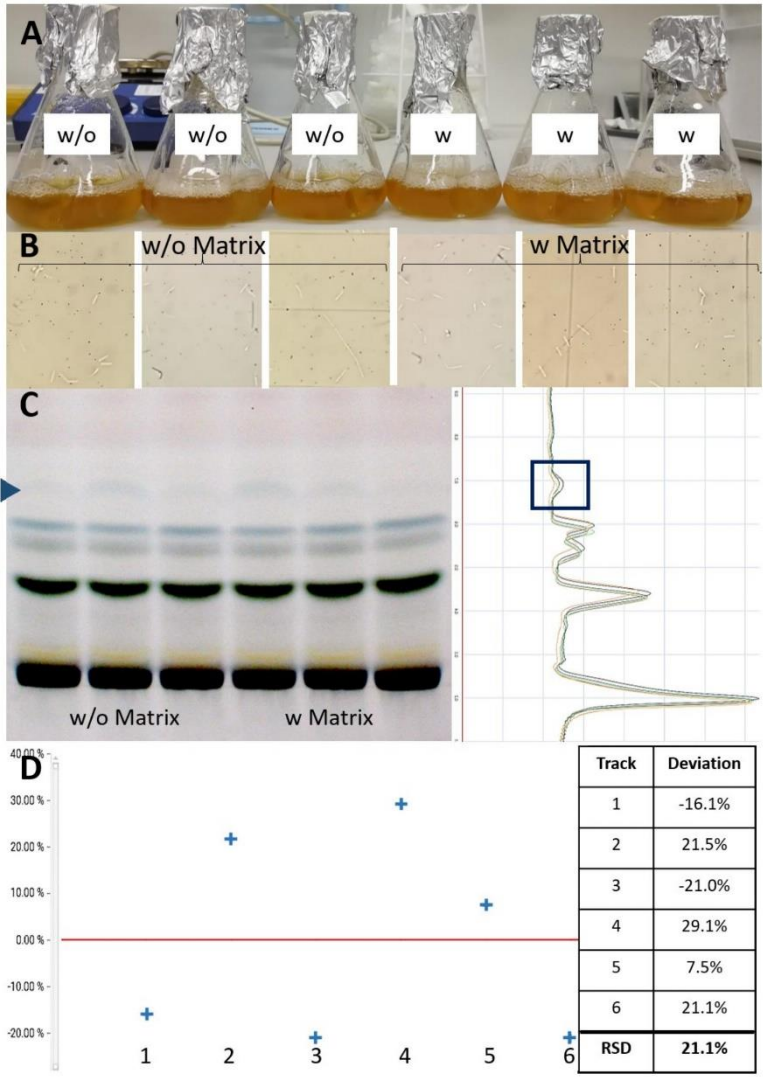651   Fig. 3

Track	Deviation
1	16.8%
2	-13.5%
3	6.7%
4	-12.1%
5	-3.1%
6	5.2%
RSD	11.8%

652

653

654   Fig. 4

29

655

656

657

658   Fig. 5

147

Supplementary Information

Bacillus subtilis spores in probiotic feed quantified via bacterial metabolite using planar chromatography

Stefanie Kruse[a], Mareike Schenk[a] Francis Pierre[b], Gertrud Morlock[a,*]

[a]Chair of Food Science, Institute of Nutritional Science, and Interdisciplinary Research Centre for Biosystems, Land Use and Nutrition, Justus Liebig University Giessen, Heinrich-Buff-Ring 26–32, 35392 Giessen, Germany

[b]Adisseo France S.A.S, Immeuble Anthony Parc 2, 10 Place du Général de Gaulle, 92160 Antony, France

*Corresponding authors: Prof. Dr. Gertrud Morlock, phone: +49-641-9939141; fax +49-641-99-39149, email: gertrud.morlock@uni-giessen.de

1

Table of Content

2

148

3

Table S1 Template for the preparation of cultures for the different validation experiments.

	Culture	Standard (dried *B. s.* 29784 spores)		Sample (feed)	Additive Matrix	Feed Matrix	Auto-claved bidest. water	TSBY
Method development								
A		Polynomial	Linear	-	-	-	-	30 mL
		Feed additive (added directly) [mg]						
	S1	50	50					
	S2	250	150					
	S3	500	250					
	S4	750	350					
	S5	1000	-					
B	S0	0.0 mL		1.0 mL			3.0 mL	30 mL
	S1	0.5 mL		1.0 mL			2.5 mL	
	S2	1.0 mL		1.0 mL			2.0 mL	
	S3	2.0 mL		1.0 mL			1.0 mL	
	S4	3.0 mL		1.0 mL			-	
Method validation (C: final method)								
	Preparation	50 mg suspended (10 mL PBS) diluted $1{:}10^8$	50 mg suspended (10 mL PBS) diluted 1:10	50 mg suspended (10 mL PBS) diluted 1:10000	50 mg suspended (10 mL PBS) diluted 1:10		30 mL
C (Linearity, working range, LOQ)	S1	0.5 mL				3.0 mL	30 mL
	S2	1.0 mL				2.5 mL	
	S3	2.0 mL				2.0 mL	
	S4	3.0 mL				1.0 mL	
	Feed sample	-	1.0 mL			2.0 mL	
D (Selectivity)	S2	1.0 mL (3x)		-			30 mL
	Additive Matrix	-		1.0 mL (3x)			
E (Selectivity)	S2	1.0 mL (3x)			-		30 mL
	Feed Matrix	-			1.0 mL (3x)		
F (Recovery)	S2	1.0 mL (3x)		-		1.0 mL	30 mL
	Additive Matrix	1.0 mL (3x)		1.0 mL (3x)		-	
G (Recovery)	S2	1.0 mL (2x)			-		30 mL
	Feed Matrix	1.0 mL (2x)			1.0 mL (2x)		
		-			1.0 mL (2x)		
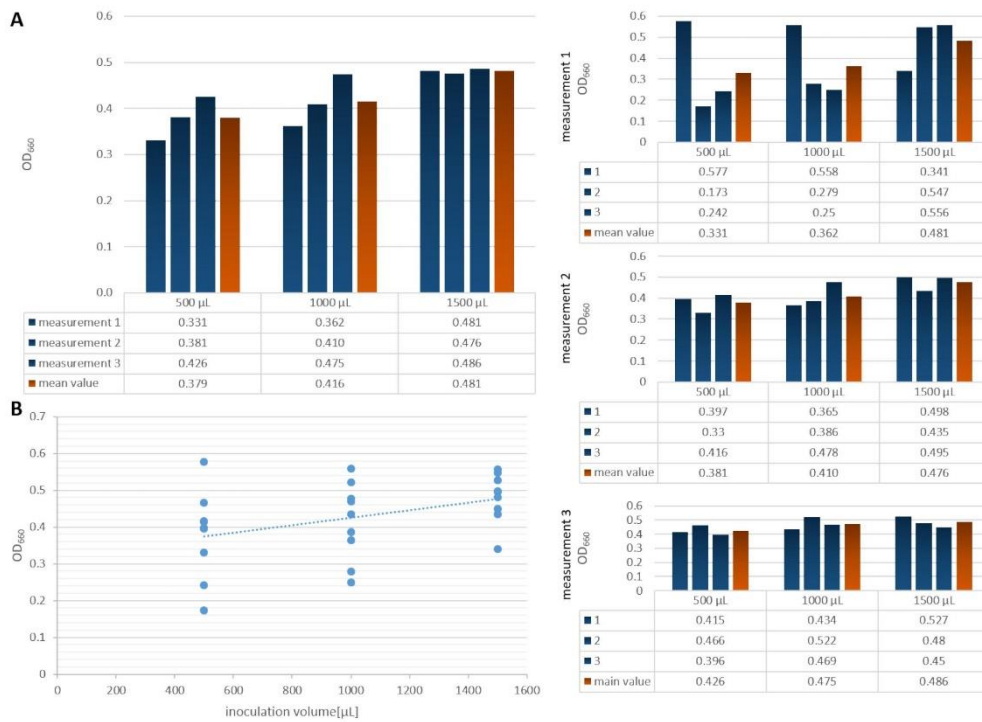
Fig. S1 Method development – Influence of culture media: Mean of mean OD_{660} ($n = 3$) of three threefold OD_{660} determinations of cultures of a 1:100 with PBS diluted *B. s.* 29784 feed additive at three inoculation volumes of 500 µL, 1000 µL and 1500 µL (A). Scatter plot showing the deviation of the nine individually measured OD_{660} values from the mean OD_{660} marked as dotted line (B).

5

Fig. S2 Method development – Working range: HPTLC-Vis chromatogram after derivatization with diphenylamine aniline *o*-phosphoric acid reagent of the *n*-butanol extracts of the supernatant of dried spores of a blank sample (BS) and *B. s.* 29784 as standard solutions S1–S5, corresponding to 50–1000 mg of the additive (A) and the corresponding polynomial regression (B). The produced metabolite at hR_F 68 is marked blue.

6

152
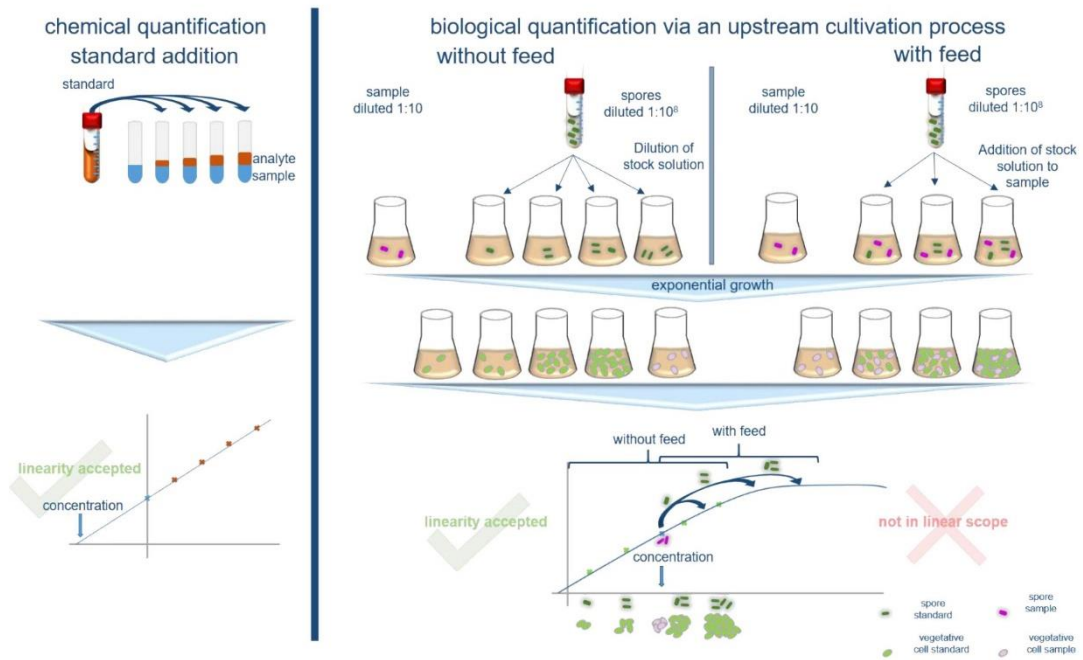
Fig. S3 Simplified comparison of chemical and biological quantification methods.

7

153
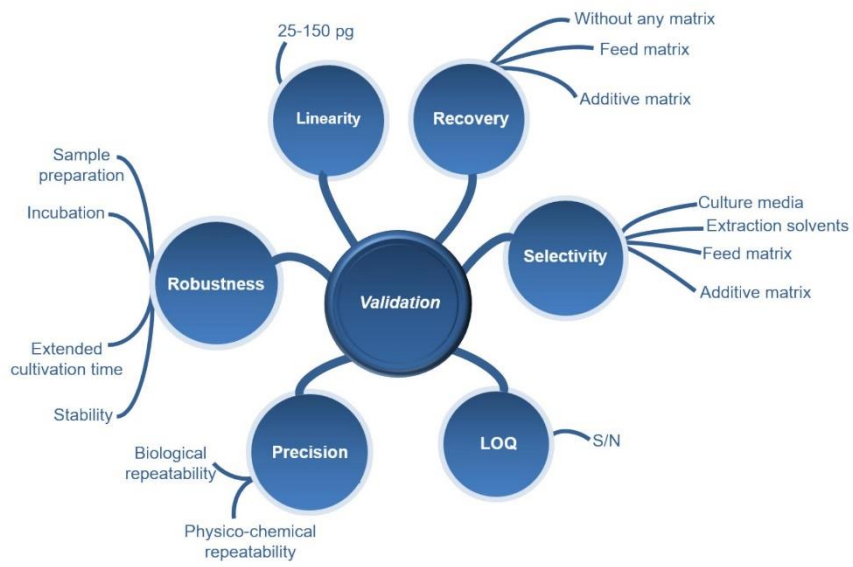
Fig. S4 Analyzed parameters of the validation process.

155

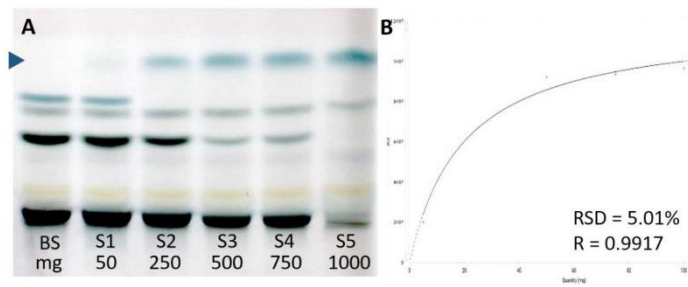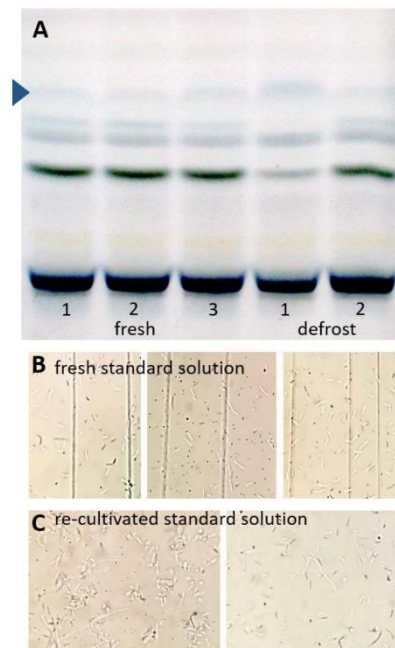**Fig. S5** Method development – Stability spore stock solution: HPTLC-Vis chromatogram after derivatization with diphenylamine aniline *o*-phosphoric acid reagent of the *n*-butanol extracts of standard solution and the corresponding microscopy images of the fresh cultivated spores (B) and re-cultivation of the frozen stock solutions (C).

9
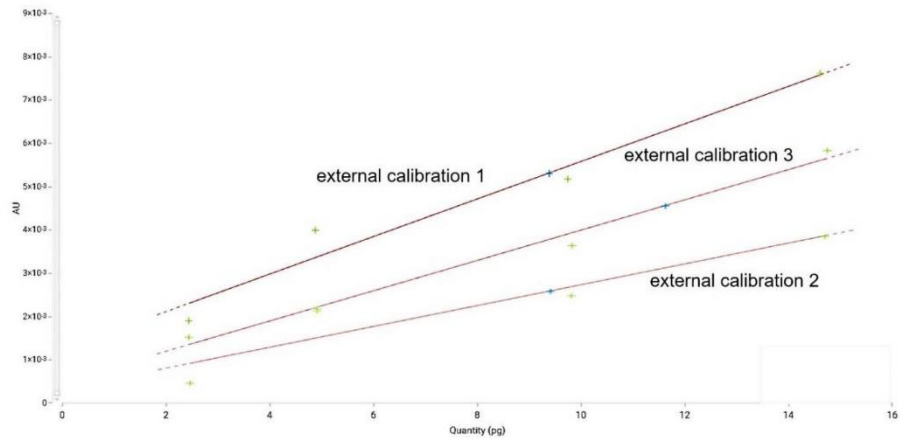
Fig. S6 Method validation – Variation of cell growth behavior: Linear regression of three individual external calibration within different cultivation processes (green cross: signal of *B. s.* 29784 standard solutions, blue cross: signal of the non-ionized feed pellet sample with Alterion 10 g t^{-1}).

10

156
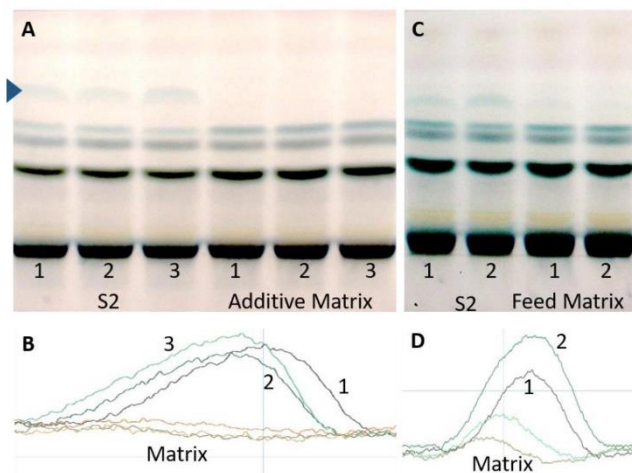
Fig. S7 Method validation – Selectivity: HPTLC chromatogram at white light illumination after derivatization with diphenylamine aniline *o*-phosphoric acid reagent of the *n*-butanol extracts (A, C) and the corresponding scan at 645 nm (B, D) of standard S2 compared to the additive matrix (A, B) as well as to a specific feed matrix (C, D). Evaluation was performed of the blue-marked zone. The measured absorbance cannot be used for an inter day comparison, due to the independent growth behavior of the cells.
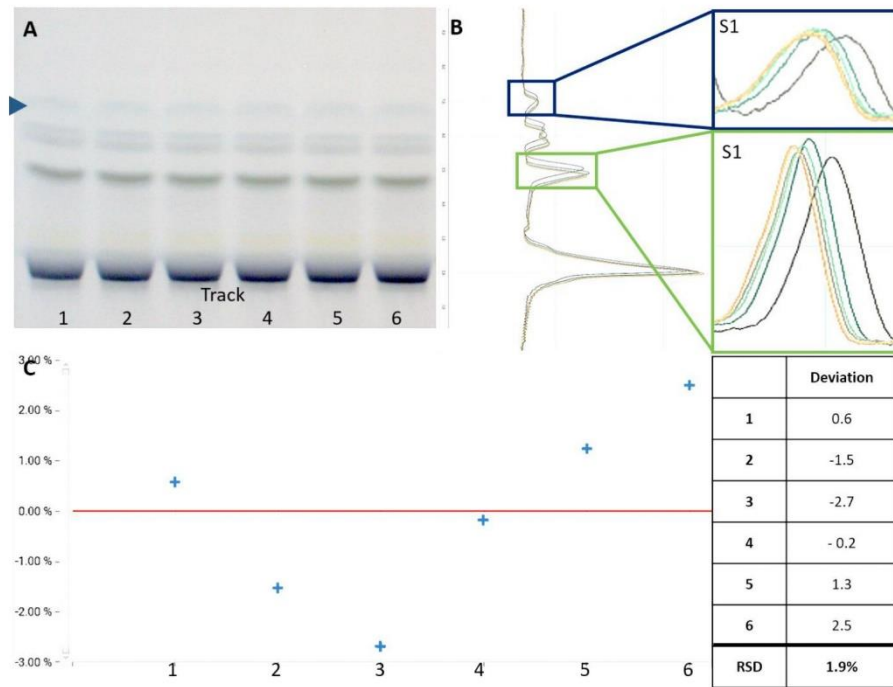
Fig. S8 Method validation – Repeatability: HPTLC-Vis chromatogram after derivatization with diphenylamine aniline *o*-phosphoric acid reagent of the sixfold applied S1 *n*-butanol extract (A) and the corresponding absorbance measurement at 645 nm (B). The deviation of the marked metabolite between the individual applications is demonstrated (C).

12
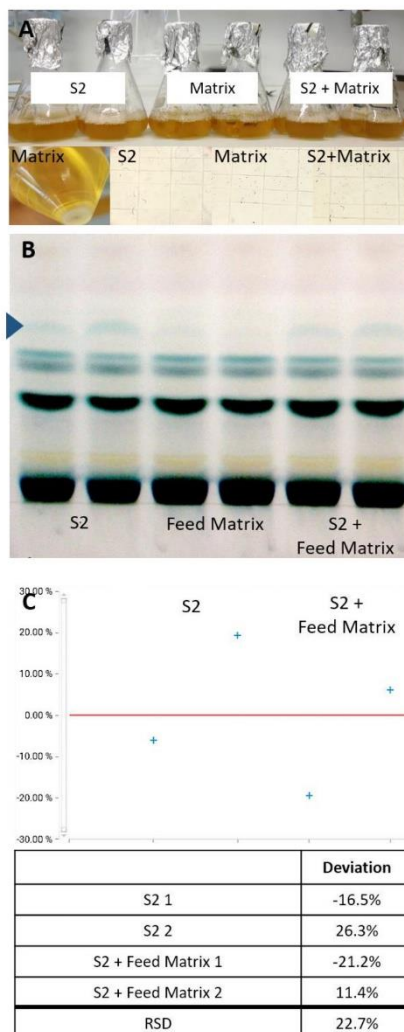
Fig. S9 Method validation – Recovery: Baffled flasks of standard solution S2, feed matrix and both together as S2 in feed blank matrix (A) and the corresponding microscope images. HPTLC-Vis chromatogram after derivatization with diphenylamine aniline o-phosphoric acid reagent of the n-butanol extracts and the deviation of the blue-marked metabolite signal intensity at hR_F 68 (C).

13
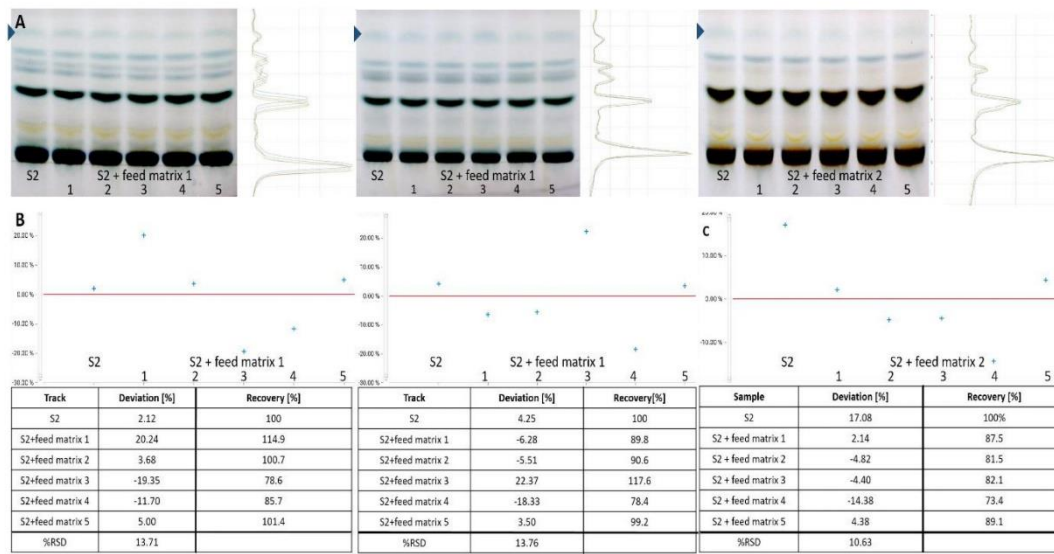
Fig. S10 Method validation – Recovery: HPTLC-Vis chromatogram after derivatization with diphenylamine aniline *o*-phosphoric acid reagent of the *n*-butanol extracts (A) and deviation of the blue-marked metabolite signal intensity at hR_F 68 as well as the calculated recovery related to S2 without matrix components (B).

14
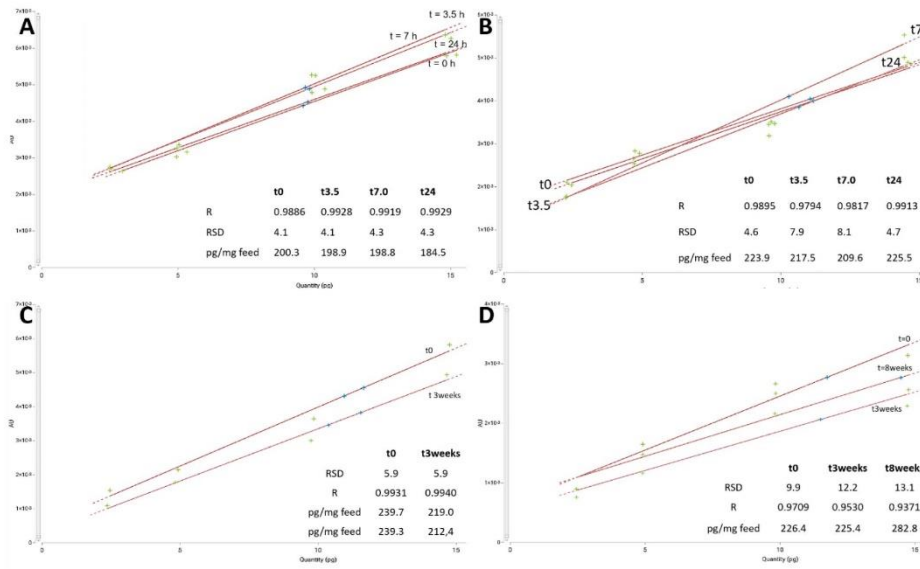
Fig. S11 Method validation – Stability of *n*-butanol extracts after 3.5 h, 7.0 h and 24 h at room temperature (A, B) and of frozen extracts after 3 and 8 weeks (C, D): Comparison of the linear regression, the deviation and the calculated amount of dried spores in the feed (blue cross) of four individual calibrations via the *B. s.* 29784 standard solutions S1−S4 (green cross).

15

Publication IV

7. Publication V

Strain-specific quantification of probiotic *Bacillus subtilis* DSM 29784 in feed by imaging high-performance thin-layer chromatography

Stefanie Kruse[a], Selina Becker[a], Francis Pierre[b], Gertrud E. Morlock[a,*]

[a]Chair of Food Science, Institute of Nutritional Science, and Interdisciplinary Research Centre for Biosystems, Land Use and Nutrition, Justus Liebig University Giessen, Heinrich-Buff-Ring 26-32, 35392 Giessen, Germany

[b]Adisseo France S.A.S, Immeuble Anthony Parc 2, 10 Place du Général de Gaulle, 92160 Antony, France

Publication V

165

1

2

3

Strain-specific quantification of probiotic *Bacillus subtilis* DSM 29784 in feed by imaging high-performance thin-layer chromatography

7

8

Stefanie Kruse[a], Selina Becker[a], Francis Pierre[b], Gertrud E. Morlock[a,*]

10

11

12

[a]Institute of Nutritional Science, Chair of Food Science, and Interdisciplinary Research Centre for Biosystems, Land Use and Nutrition, Justus Liebig University Giessen, Heinrich-Buff-Ring 26-32, 35392 Giessen, Germany

[b]Adisseo France S.A.S, Immeuble Anthony Parc 2, 10 Place du Général de Gaulle, 92160 Antony, France

18

19

20

21

*Corresponding author: Prof. Dr. Gertrud Morlock, phone: +49-641-9939141; fax +49-641-99-39149, email: gertrud.morlock@uni-giessen.de

Abstract

The European Union has banned the use of antibiotic growth promoters in animal production, which has led to increased use of probiotic microorganisms. These feed additives result in higher costs for farmers, which is why the demand for a quality control system to quantify probiotics in feeds has increased in recent years. Imaging high-performance thin-layer chromatography (HPTLC) was proven to be a robust method for determining the probiotic *Bacillus subtilis* DSM 29784 strain based on the production of bacterial metabolites and thus characteristic metabolite pattern. To quantify the probiotic microorganism in feed, identification of a strain-specific metabolite not produced by genetically very similar bacteria is necessary. Compared to five bacteria with high genetic similarity, a strain-specific metabolite was formed in the probiotic bacteria by a two-step cultivation procedure. Antimicrobial properties were found for this metabolite, which is indicative of probiotic activity, among other properties. The hyphenation of normal-phase HPTLC and reversed-phase high-performance liquid chromatography with diode array detection and high-resolution mass spectrometry allowed the preliminary assignment of this strain-specific metabolite to the molecular formula $C_{35}H_{44}N_6O_2$ (580.3527 Da). This metabolite was used for the quantification of probiotic active cells in the feed. Data on selectivity, linearity, detection limit, recovery and precision have shown good performance of the method.

Keywords probiotic feed additive, bacterial profiling, bacteria differentiation, bacterial pattern recognition, planar chromatography, validation

2

166

1. Introduction

In the animal production sector, antibiotic growth promoters were banned in the European Union in 2006 [1], due to increasing antibiotic resistance in humans. Probiotics seem to be a promising substitute, which is why scientific research on probiotics has increased over the past decade. In 2016, Adisseo and Novozymes launched the probiotic feed additive based on the strain *Bacillus subtilis* DSM 29784 (*B. s.* 29784). The probiotic bacterium was selected from 900 potential candidates and fulfilled all safety, functionality, and technological requirements of the European Regulation (EC) No. 1831/2003. The beneficial effects of probiotics are not fully understood, but a positive impact of *B. s.* 29784 has been reported in recent years. The application of this probiotic increased the body weight gain and growth performance of shaver white pullets [2], broilers [3], and Tom turkeys [4]. In addition, improved feed conversion and interaction of the probiotic with the microbiome, resulting in a change of the microbial composition in the animal gut, have been reported. [5–9] Depending on the age of the animals, physical activity, environmental or antibiotic conditions, probiotic treatment can help reverse an imbalanced microbiome and prevent microbial dysbiosis. [10–12] In addition, after supplementation with *B. s.* 29784, positive-acting metabolites, *e.g.,* butyrate and linoleic acid, were produced in higher proportions and microvilli elongation was observed. [7,9]

These results confirm the positive effects of the probiotic strain *B. s.* 29784. However, developing a quality control system to quantify the probiotic *B. s.* 29784 in feed is challenging. Cell counting is the most valid method for the detection of probiotic cells in feed. [13] The official requirements are described in the European standard EN 15784:2009. [14] Briefly, a portion of the feed is suspended in phosphate-buffered saline (PBS), homogenized, and heat-treated at 80 °C for 10 min. Through this treatment, all vegetative cells should die. The suspension is decimally diluted, plated on tryptic soy agar, and incubated at 37 °C for up to 16–24 h. All plates with colony counts between 30–300 are counted and colony-forming units (CFU) per gram feed are calculated. Flow cytometry [15] or strain-specific quantitative polymerase chain reaction (qPCR) [16] are also used for quantification. [17] Still drawbacks

3

71   are either the non-specificity of the methods and the calculation error by counting other

72   bacteria than *B. s.* 29784, or for more specific methods (qPCR), the expensive reagents

73   required.

74   Imaging high-performance thin-layer chromatography (HPTLC) was proven as an efficient

75   tool for characterization of the probiotic effect of *B. s. 29784* via characteristic metabolite

76   patterns [18,19] and quantification of bacterial metabolites via an upstream cultivation process

77   [20]. This new approach highlighted several advantages over the usually performed cell

78   counting. The use of spore-containing standard solutions to establish a calibration function of

79   a formed metabolite allowed the influence of cultivation conditions on the growth performance

80   to be taken into account. The standardized conditions enabled a robust quantification of the

81   formed bacterial metabolites in feed with excellent performance data for a biological method.

82   In this study, a strain-specific metabolite was found and used for strain-specific quantification

83   of the probiotic microorganism in feed. The cultivation parameters were optimized for

84   formation of this strain-specific metabolite. The recently reported HPTLC method with an

85   upstream cultivation process [20] was optimized for quantification of this strain-specific

86   metabolite in feed. The strain-specific metabolite was characterized by high-performance

87   liquid chromatography diode array detection heated electrospray ionization high-resolution

88   mass spectrometry (HPLC−DAD−HESI-HRMS).

2. Materials and methods

2.1. Chemicals and materials

91   Tryptic soy broth (TSB) and HPTLC silica gel 60 plates were purchased from Merck,

92   Darmstadt, Germany. *n*−Butanol (HPLC grade) was delivered by Acros Organics, Fair Lawn,

93   NJ, USA. Sodium chloride (NaCl, ≥99%), yeast extract (for use in microbial growth medium),

94   primuline (≥99%), diphenylamine (≥99%), ninhydrin (≥99%), aniline (≥99.5%), and

95   pancreatin from porcine pancreas (8 × USP specifications) were purchased from Fluka

96   Sigma-Aldrich, Steinheim, Germany. Methanol and acetone (both HPLC grade) were

4

97 purchased from VWR, Darmstadt, Germany. Hydrochloric acid (37%, purest), potassium

98 chloride (KCl, ≥99%), potassium dihydrogen phosphate (KH₂PO₄, ≥99%), disodium hydrogen

99 phosphate (Na₂HPO₄, ≥99%), 4-anisaldehyde (≥97.5%), glycerol (86%, Rotipuran) and

100 sulfuric acid (96%) were obtained from Carl Roth, Karlsruhe, Germany. Ethyl acetate (≥99.8%)

101 was delivered by Th. Geyer, Renningen, Germany. Bidistilled water was prepared by a

102 Destamat Bi 18E, Heraeus, Hanau, Germany. The preparation of the culture medium for

103 bioluminescent *Aliivibrio fischeri* bacteria (DSM-7151, German Collection of Microorganisms

104 and Cell Cultures, Berlin, Germany), is described elsewhere.[21] The dried spores of *B. s.*

105 29784 and the matrix compounds (sodium aluminosilicate, calcium carbonate, and sucrose)

106 used for the commercial feed additive formulation (ALTERION®NE, 0.03 *W*%) as well as, the

107 feed sample without and with ALTERION®NE at 10 g t⁻¹ (0.001 *W*%) was obtained from

108 Adisseo France SAS, Antony, France.

109 *2.2. Optimization of the upstream cultivation process*

110 Dried spores of *B. s.* 29784 (50 mg) were suspended in 10 mL PBS (NaCl 8.0 g/L, KCl

111 0.2 g/L, Na₂HPO₄ 1.15 g/L, KH₂PO₄ 0.2 g/L in water), providing the spore stock solution at

112 5 mg/mL, and diluted further up to 1:10⁸ with PBS to a final concentration of 50 pg/mL.

113 Different aliquots (0.1–3 mL, specified in each optimization, Table S1) of the diluted spore

114 stock solution were added to 30 mL TSBY and the volume of each culture was adjusted to

115 33 mL with autoclaved bidistilled water. The incubation time (3.5–5.5 h, Table S1) for the

116 second cultivation step was studied to receive a linear working range with an increasing

117 metabolite intensity.

118 *2.3. Cultivation and HPTLC method for detection of the strain-specific metabolite*

119 Six different *Bacillus* strains (**1**: probiotic strain *B. s.* 29784, **2**: MIC39 strain genetically

120 similar up to 99.5%, **3**: ATCC 6633 strain genetically similar up to 99.4%, and **4**: not identified

121 strain, genetically similar up to 98.4%, **5**: *Bacillus licheniformis* strain SB3114, **6**: *Bacillus*

122 *pumilus* strain SB3839) were cultivated in parallel. Bacterial glycerol stock solutions were

5

123   prepared by using 500 µL bacterial culture adjusted to OD_{660} 1.4 (measured with M501 Single

124   Beam Scanning UV/visible Spectrophotometer, CamSpec, Garforth, UK), added to 500 µL

125   50% glycerol and frozen by −80 °C. For the pre-cultures, 50 µL bacterial glycerol stock

126   solution was inoculated in 30 mL tryptic soy broth containing yeast (TSBY; 3% added to 1 L

127   water with 0.6% yeast extract, adjusted to pH 6.2 with 2 M hydrochloric acid solution). The

128   culture samples were shaken at room temperature and 175 rpm (orbital shaker SM-30,

129   Edmund Bühler, Bodelshausen, Germany) for 5.5 h and cultivated further at 37 °C in Labocult

130   incubator (Servoprax, Wesel, Germany) for 11.5 h. For each strain, an aliquot (1.5 mL) of the

131   pre-cultures was used, added to 18.5 mL fresh TSBY, and cultivated further at 175 rpm and

132   37 °C for 4 h. The cell suspension was centrifuged (centrifuge 5702, Eppendorf, Hamburg,

133   Germany) at 3000 × g for 10 min, and the cell-free supernatant (15 mL) was used for liquid-

134   liquid extraction of the metabolites with n-butanol 3:1, V/V.

135   HPTLC instruments (CAMAG, Muttenz, Switzerland, if not stated otherwise) were controlled

136   by visionCATS software (version 3.1.21109.3, CAMAG). The n-butanol extracts (100 µL) were

137   applied (as area, 8 mm × 10 mm) on an HPTLC plate (pre-washed two times with methanol-

138   water, 4:1 V/V). The dosage speed was set to 600 nL/s and the syringe was rinsed twice with

139   methanol after each application (Automatic TLC Sampler 4). The area was focused once with

140   acetone and two times with methanol up to 20 mm from the lower end of the plate. The plate

141   was developed with acetonitrile – ethyl acetate – acetone (2:1:1, $V/V/V$; Twin-Trough

142   Chamber), dried with a hairdryer for 2 min, and documented at FLD 366 nm (TLC Visualizer

143   2). The UV spectrum (200–400 nm) of the strain-specific metabolite was measured to obtain

144   the maximal absorbance wavelength of 366 nm (TLC Scanner 4).

145   *2.4.   Chemical derivatization*

146   The HPTLC chromatogram was dipped in each derivatization reagent with the same

147   parameters (immersion time 2 s, immersion speed 3.5 cm/s, Chromatogram Immersion

148   Device 3). For the detection of lipophilic substances, the plate was immersed into the primuline

149   reagent (250 mg primuline in 50 mL water and 200 mL acetone), followed by drying in a cold

6

150 stream of air (hairdryer) for 1 min. The ninhydrin reagent (500 mg ninhydrin in 230 mL ethanol

151 and 20 mL acetic acid) was used for the detection of amines or amino acids. For the detection

152 of sugars, the diphenylamine aniline *o*-phosphoric acid reagent (2 g diphenylamine in 100 mL

153 *i*-propanol and 2 mL aniline in 100 mL *i*-propanol, mixed 1:1, *V/V*, dropwise addition of 20 mL

154 *o*-phosphoric acid, 85%) and for natural products, the anisaldehyde sulfuric acid reagent

155 (1.5 mL 4-anisaldehyde in a mixture of 210 mL methanol, 25 mL acetic acid, and 13 mL

156 sulfuric acid) were used. The later three plates were heated at 110 °C (Plate Heater III) for

157 10 min.

158 *2.5. Simulated static intestinal phase digestion*

159 The simulated on-surface digestion of the extract was performed as described [19]. Briefly,

160 the *n*-butanol extracts were area-applied on an HPTLC plate and oversprayed with the

161 pancreatic enzyme solution. The plate was transferred into a moistened polypropylene KIS

162 box (26.5 cm × 16 cm × 10 cm, ABM, Wolframs-Eschenbach, Germany), incubated at 37 °C

163 in an oven (Memmert, Schwabach, Germany) for 1 h, dried for 20 min (Automatic Developing

164 Chamber 2) and subjected to the HPTLC analysis as described.

165 *2.6. A. fischeri and B. subtilis bioassays*

166 Caffeine (1 µg/band; 1 mg/mL in methanol) was applied as positive control on the upper

167 part of the plate for the *A. fischeri* bioassay. An aliquot (3.5 mL) of an overnight cultivated (at

168 room temperature and 100 rpm) bacterial suspension was piezoelectrically sprayed onto the

169 plate (blue nozzle, level 6, Derivatizer). Over a 30-min period, 10 bioautograms were recorded

170 (exposure time 100 s, BioLuminizer 2). Antimicrobial substances were detected as dark

171 zones, indicating the impairment of the bioluminescence, depicted as grey-scale image.[21]

172 For the *B. subtilis* bioassay, tetracycline (3 µL/band; 0.005 mg/mL in ethanol) was applied

173 as positive control on the upper edge of the plate. An aliquot (3.5 mL) of an overnight culture

174 (90 µL bacterial solution in 20 mL 2.3% Müller-Hinton broth at 37 °C and 100 rpm, optical

175 density of 1 at 600 nm) was sprayed (red nozzle, level 6) on the plate. The plate was

7

176   transferred into a moistened polypropylene KIS box (same as before) and incubated at 37 °C

177   in an oven (Memmert, Schwabach, Germany) for 2 h. The chromatogram was sprayed with

178   500 µL 3-(4,5-dimethylthiazol-2-yl)-2,5-diphenyltetrazolium bromide solution and incubated at

179   37 °C for 1 h, followed by drying (50 °C, 10 min, Plate Heater III). Antimicrobial substances

180   were detected at white light illumination as colorless bands on a purple background.

181   *2.7. Tentative assignment of the strain-specific metabolite by HPLC-DAD-HESI-HRMS*

182   The characteristic zone on the normal-phase HPTLC plate was transferred via the

183   automated elution head-based interface [22,23] connected to an reversed-phase RP-MS

184   column (100 mm x 2.1 mm, 2.6-µm spherical solid core RP18e particles of 8 nm porous size,

185   Thermo Scientific, Bellefonte, PA, United States) and detected by DAD (wavelength scan

186   200–400 nm, and selected wavelengths of 240, 280 and 320 nm) as well as by Q Exactive

187   Plus Hybrid Quadrupole-Orbitrap Mass Spectrometer (Thermo Fisher Scientific).[24]

188   *2.8. Method performance*

189   The tests for selectivity, linearity, limit of quantification (LOQ), precision, and recovery were

190   performed according to the latest biological quantification via upstream cultivation of a

191   bacterial metabolite in feed. [20] The optimized cultivation parameters (Table S1, scenario 8,

192   framed red), metabolite extraction and HPTLC analysis were performed as described. The

193   respective preparation of the culture, depending on the validation parameter, is described in

194   detail (Table S2). For studying selectivity, a spore standard solution (5 mg/mL dried

195   *B. s.* 29784, diluted $1:10^8$ with PBS) and a sample only containing the corresponding amount

196   of feed matrix (5 mg/L diluted 1:10 with PBS) were prepared and cultivated (Table S2A). The

197   absorbance (measured at 366 nm) of the produced metabolite at hR_F 38 was compared to the

198   signal at the same intensity in the feed matrix. Selectivity towards feed matrix, culture medium,

199   and used solvents was acceptable, when no signal was measured in the feed matrix sample

200   at the hR_F value of the analyzed metabolite. For determination of linearity, different volumes

201   of the spore standard solution (S1–S4, 0.1–2.2 mL, corresponding to 5–110 pg) were added

8

202 to 30 mL TSBY and filled up to 33 mL (add 0.8–2.9 mL) with autoclaved bidistilled water (Table

203 S2B). For linearity R and RSD were calculated based on the metabolite intensity (at hR_F 38)

204 of each spore standard solution on the HPTLC chromatogram. LOQ was determined by the

205 deviation of the metabolite intensity (hR_F 38) in S1 (5 pg spores in culture, Table S2B) from

206 the baseline noise intensity in the blank at the same hR_F value. A signal-to-noise (S/N) ratio

207 of ≥10 is expected for LOQ (Table S3). The physico-chemical repeatability ($RSD, n = 6$) of the

208 HPTLC method was analyzed (Table S2B) via the metabolite intensity at hR_F 38 in the same

209 S1 spore standard solution. The recovery of the metabolite at hR_F 38 was determined with

210 and without feed matrix. Six cultures of S2 were prepared. To five of them, a diluted feed

211 matrix (50 mg suspended in 10 mL PBS and diluted 1:10 in PBS, Table S2C) was added and

212 all samples were cultivated in parallel. For probiotic feed sample analysis, the feed sample

213 was suspended in PBS (5 mg/mL) and diluted 1:10 with PBS. An aliquot (0.5 mL) was added

214 to 30 mL TSBY and filled up with autoclaved bidistilled water to 33 mL (Table S2D).

215 **3. Results and discussion**

216 *3.1. Detection of the strain-specific metabolite*

217 The metabolic profiles of different *Bacillus* strains were analyzed under changing cultivation

218 and extraction conditions by imaging HPTLC, leading to a better understanding of the probiotic

219 activity in previous studies. [18,19] Also the metabolic interactions of *Bacillus* with *E. coli* were

220 studied, whereby a brown zone was observed in the probiotic *Bacillus* strain 1 in the

221 HPTLC−FLD chromatogram at 366 nm. [25] The detection of this metabolite was investigated

222 in more detail. All genetically similar *Bacillus* strains were cultivated in parallel, followed by

223 metabolite extraction and HPTLC analysis. In the HPTLC−FLD chromatogram, an intensive

224 brown zone (hR_F 38) was only detected in the main culture of strain 1 (Figure 1A). The whole

225 procedure was reproduced ($n = 3$), and the specificity of this metabolite for the probiotic strain

226 1 was confirmed. The specificity was also proven by the comparison of the UV absorbance

227 spectra (200–400 nm) of respective metabolites at hR_F 38 of strains 1 and 2. The spectra were

9

228   not comparable, which confirmed the strain-specific differentiation (Figure 1C). The metabolite

229   of strain 1 absorbed between 325 nm and 400 nm and showed its absorbance maximum at

230   366 nm. This underlined that the metabolite at hR_F 38 was only present in strain 1. For further

231   evidence of metabolite specificity, all strains were densitometrically recorded at 366 nm

232   (Figure 1D). The peak signal at hR_F 38 was only detected in strain 1. The chromatogram at

233   FLD 366 nm, the comparison of the absorbance spectra (200–400 nm) and the measured

234   absorbance at 366 nm (Figure 1) confirmed the specificity of this metabolite for the probiotic

235   strain 1 under the given conditions.

236   For characterization of this metabolite, several chemical derivatizations were performed

237   (Figure S1A–F). The strain-specific metabolite was detectable via the ninhydrin (amine

238   moiety), diphenylamine aniline (saccharide moiety), and anisaldehyde sulfuric acid reagents

239   (universally detecting organic compounds). However, analysis with methanolic sulfuric acid

240   (Figure S1F) proved that detection was caused by the acidity of the reagents and did not

241   necessarily indicate a saccharide or amine moiety. In addition, biological assays (*A. fischeri*

242   and *B. subtilis* bioassays) were performed to detect antimicrobial substances (Figure S1G/H).

243   Antimicrobial metabolites could protect the animal gut from, *e.g.,* Gram-negative *E. coli* or

244   Gram-positive *Clostridium perfringens* infections. Gram-positive antimicrobial metabolites

245   were detected as white zones on a purple background, whereas Gram-negative antimicrobial

246   metabolites were detected as dark zones on a grey background (bioluminescence depicted

247   as greyscale image). The strain-specific metabolite at hR_F 38 was detectable in both

248   bioassays.

249   Moreover, the simulated static intestinal phase digestion by pancreatic enzymes caused a

250   conversion of the strain-specific metabolite. In the digested sample, the metabolite was not

251   detectable anymore, so the metabolite was digested (Figure S1I). Trypsin (selective

252   cleavage of peptide bonds), chymotrypsin (hydrolysis of proteins or peptides), amylases

253   (hydrolysis of starch), and lipases (hydrolysis of fats) are present in the used porcine

254   pancreatin. Thus, the strain-specific metabolite may contain a peptide or lipid or carbohydrate

255   moiety, which could be metabolized by enzymes in the animal gut. In the non-digested pattern,

256 the brown zone was not so clearly visible than in the other derivatization patterns (Figure

257 S10I), since the incubation at 37 °C for 1 h caused diffusion of the metabolite. Furthermore,

258 the metabolite seemed to be slightly volatile, and the influence of its volatility was investigated

259 in detail. The gas phase formed during plate development and the subsequent plate drying

260 had a significant influence on its sharpness. The same samples were applied on comparable

261 plates and separated using a large (20 cm × 10 cm, high impact of the gas phase) and small

262 developing chamber (10 cm× 10 cm, less impact of the gas phase). The larger the developing

263 chamber, the larger the gaseous space in the glass tank, which resulted in a higher diffusion

264 of the strain-specific metabolite on the plate (Figure S2A). This observation showed that a

265 small gas phase space is advantageous for separation. Additionally, subsequent plate drying

266 should be as short as possible (2 min). Prolonged drying favored the evaporation of the

267 metabolite (Figure S2B).

268 *3.2. Tentative assignment of the strain-specific metabolite by HPLC-DAD-HESI-MS*

269   The strain-specific metabolite (hR_F 38) was transferred via the automated elution head-

270 based interface [23] to an RP-HPLC column for additional separation and detected by DAD–

271 HESI-HRMS. The HPLC–DAD chromatogram (Figure 2A) indicated four different peaks. To

272 identify among these the retention time of the strain-specific metabolite in strain 1, the

273 measured on-surface absorbance spectrum in strain 1 at hR_F 38 (Figure 2B) was compared

274 with the HPLC–DAD spectrum of the four different peaks (Figure 2C). The spectrum of peak

275 4 (retention time 7.8 min) was comparable and tentatively assigned to the strain-specific

276 metabolite (Figure 2A) with the molecular formula $C_{35}H_{44}N_6O_2$, based on the negative and

277 positive HESI-HRMS spectra and the formed adducts with a mass error <3 ppm (Figure 3A).

278 Despite the two-dimensional separation (HPTLC and HPLC), a variety of weaker HRMS

279 signals were observed especially in the positive ion mode, explained by the wide range of

280 metabolites produced by the spores and nutrient-rich culture medium (Figure 3B).

281 Nevertheless, the HRMS/MS signals could be assigned to fragment formulas of the precursor

282 ion. Still structure elucidation by nuclear magnetic resonance spectroscopy would be

283 necessary, however, needs further dedicated studies.

3.3. Method optimization (upstream cultivation process)

285 The proof-of-principle of quantification of selective *B. s.* 29784 metabolites in feed by

286 imaging HPTLC with upstream cultivation of spore standard solutions has been described

287 recently. [20] For quantification of this strain-specific metabolite, the cultivation conditions had

288 to be optimized to obtain a linear working range. For the formation of the strain-specific

289 metabolite in stock solution, feed and dried spores, a two-step cultivation procedure was

290 required (Figure 1B). The metabolite was found to be consumed at higher concentrations.

291 Considering the strain-specific metabolite in the spore standard solutions S1–S3, excellent

292 linearity was obtained, but a decreased metabolite intensity of S4 indicated its starting

293 consumption by the cells. In different cultivation tests (Table S1), the spore concentration

294 (from 150 pg to 5 pg) and cultivation time (from 5.5 h to 4 h in the second cultivation step)

295 were reduced to prevent the consumption of the strain-specific metabolite and ensure a

296 quantitative growth behavior of the cells (with increasing amount of dried spores, increased

297 cell number, metabolite production and signal intensity).

3.4. Method performance

299 Validation of the method for quantification of probiotic active cells in feed has already been

300 performed via selective *B. s.* 29784 metabolites produced by imaging HPTLC with upstream

301 cultivation of spore standard solutions. [20] Therefore, full validation via a specific metabolite

302 is not required. Nevertheless, selectivity, linearity, LOQ, precision, and recovery were studied

303 using the optimized cultivation conditions (Table S1, scenario 8, framed red) for formation of

304 the strain-specific metabolite (hR_F 38). In the HPTLC−FLD chromatogram and UV-absorbance

305 densitogram, no interfering signals were detected in the feed matrix, which confirmed

306 selectivity towards feed matrix, TSBY culture medium and solvents used (Figure S3). For

307 linearity, acceptable results were obtained (Figure 4, *R* of 0.96, *RSD* of 14%), given the

308 included upstream cultivation of spore standard solutions. The optimization of the cultivation

309 process resulted in a reduction of the cell number and thus produced metabolites.

310 Nevertheless, the brown metabolite zone provided still sufficient signal intensity in the

311 HPTLC−FLD chromatogram and UV-absorbance densitogram (Figure 4). For LOQ, an S/N

312 value of 15 (Table S3) was obtained for the strain-specific metabolite (hR_F 38) in the spore

313 standard solution S1 (5 pg spores in culture, Table S2B). For repeatability, a precision of *RSD*

314 5.2% was obtained for the lowest intensity of the strain-specific metabolite produced in the

315 spore standard solution S1. For recovery in the feed matrix, the spore standard solution S2

316 (40 pg spores in culture) was added to 500 µg feed matrix in the 33-mL culture. A recovery of

317 90% ± 22% was achieved. The individual growth behavior of the cells varied comparably (*RSD*

318 of 22%) [20], which proved that the results were not influenced by the feed matrix. Finally, a

319 probiotic feed sample was analyzed repeatedly, and the calculated mean amount of dried

320 spores in the feed was 216 pg/mg (175 and 258 pg/mg). In a former study, the amount of dried

321 spores was calculated based on the formation of a selective (non-specific) metabolite of the

322 probiotic and a similar mean result of 212 pg/mg (180–250 pg/mg, *n* = 6 [20]) was obtained.

323 The difference between the two mean contents obtained via a strain-specific *versus* selective

324 quantification method was 4 pg/mg (2%). This was in good agreement.

325 The amount of active dried spores in ALTERION®NE (0.03 *W*%) added to the feed (0.001

326 *W*%) was 3 pg/mg according to the manufacturer information. Thus, a 70-fold higher amount

327 was obtained. The higher amount was explained by quantification at the trace level and due

328 to the exponential growth of cells and thus exponential formation of metabolites. Nevertheless,

329 the question arose to what extent the specificity of the metabolite formed can be claimed,

330 despite the comparison to genetically very similar strains (up to 99.5%). Other *Bacilli* not

331 studied here might also produce this metabolite and explain actually higher amounts of

332 *B. s.* 29784 spores present in the feed. However, compared to the status quo of cell counting,

333 this new method was advantageous, since several factors of influence on quantification of

334 probiotic spores were taken into account, such as spore germination process, viability and

335 metabolic activity of cells, cultivation conditions, and high feed matrix content. Furthermore

13

336 despite the high matrix load and metabolite content of the n-butanol extracts, the tentative

337 assignment of the strain-specific metabolite to the molecular formula $C_{35}H_{44}N_6O_2$ was

338 successful due to the comparison of the HRMS/MS spectra with the HPTLC absorbance

339 spectra and HPLC−DAD chromatogram.

340 **4. Conclusions**

341   A strain-specific metabolite, tentatively assigned to the molecular formula $C_{35}H_{44}N_6O_2$, was

342 identified in the metabolic profile of the probiotic strain *B. s.* 29784 in comparison to five other

343 profiles of up to 99.5% genetically similar bacteria. Only two-step cultivation of the probiotic

344 strain *B. s.* 29784 led to the production of the strain-specific metabolite. This clearly showed

345 the influence of cultivation parameters on bacterial metabolite profiles and the importance of

346 standardization of cultivation parameters. This metabolite produced via an upstream

347 cultivation process was used for analysis and calculation of the probiotic active bacterial

348 spores added as feed additive and supposed to be actively present in the feed. The selectivity,

349 linearity, LOQ, repeatability, and recovery of the new method including a biological cultivation

350 were very convincing. The quantification of probiotic dried bacterial spores in feed via the

351 strain-specific metabolite led to comparable results to a recently reported quantification via a

352 selective metabolite. This highlighted the reproducibility of the method in quantifying the

353 amount of dried spores in feeds via formation of different metabolites. Although the calculated

354 amount was 70-fold higher compared to the manufacturer information, the results of the

355 developed method was found to be more reliable, as the specificity for the probiotic strain

356 *B. s.* 29784 was clearly given and only active probiotic cells were taken into account. Both

357 criteria are important for a probiotic claim and underline the developed methodology. A 70-

358 fold difference can be explained by the exponential formation of metabolites at the trace level.

359 Compared to the status quo of cell counting, this new quantification method via a strain-

360 specific metabolite takes newly into account the spore germination process, viability and

361 metabolic activity of cells, cultivation conditions, and high feed matrix content.

14

179

362 CrediT authorship contribution

363 **Stefanie Kruse**: Conceptualization, Methodology, Experimental Analysis, Data Analysis,

364 Writing – Original Draft. **Selina Becker**: Experimental Analysis. **Francis Pierre**: Resources,

365 Review. **Gertrud E. Morlock**: Conceptualization, Methodology, Supervision, Resources,

366 Writing – Review, and Editing.

367 Declaration of competing interest

370 Acknowledgments

375 Appendix A. Supplementary data

376 Supplementary data to this article can be found online at…

15

References

[1] The European Parliament And Of The Council, Regulation (EC) No 1831/2003 of the European Parlament and of the Council of 22 September 2003 on additives for use in animal nutrition: L 268/29, 2003.

[2] M. Neijat, R.B. Shirley, A. Welsher, J. Barton, P. Thiery, E. Kiarie, Growth performance, apparent retention of components, and excreta dry matter content in Shaver White pullets (5 to 16 week of age) in response to dietary supplementation of graded levels of a single strain *Bacillus subtilis* probiotic, Poult. Sci. 98 (2019) 3777–3786. https://doi.org/10.3382/ps/pez080.

[3] L. Rhayat, V. Jacquier, K.S. Brinch, P. Nielsen, A. Nelson, P.-A. Geraert, E. Devillard, *Bacillus subtilis* strain specificity affects performance improvement in broilers, Poult. Sci. 96 (2017) 2274–2280. https://doi.org/10.3382/ps/pex018.

[4] M. Mohammadigheisar, R.B. Shirley, J. Barton, A. Welsher, P. Thiery, E. Kiarie, Growth performance and gastrointestinal responses in heavy Tom turkeys fed antibiotic free corn-soybean meal diets supplemented with multiple doses of a single strain *Bacillus subtilis* probiotic (DSM29784)1, Poult. Sci. 98 (2019) 5541–5550. https://doi.org/10.3382/ps/pez305.

[5] C. Keerqin, L. Rhayat, Z.-H. Zhang, K. Gharib-Naseri, S.K. Kheravii, E. Devillard, T.M. Crowley, S.-B. Wu, Probiotic *Bacillus subtilis* 29,784 improved weight gain and enhanced gut health status of broilers under necrotic enteritis condition, Poult. Sci. 100 (2021) 100981. https://doi.org/10.1016/j.psj.2021.01.004.

[6] P. Choi, L. Rhayat, E. Pinloche, E. Devillard, E. de Paepe, L. Vanhaecke, F. Haesebrouck, R. Ducatelle, F. van Immerseel, E. Goossens, *Bacillus Subtilis* 29784 as a Feed Additive for Broilers Shifts the Intestinal Microbial Composition and Supports the Production of Hypoxanthine and Nicotinic Acid, Animals 11 (2021). https://doi.org/10.3390/ani11051335.

[7] M. Neijat, J. Habtewold, R.B. Shirley, A. Welsher, J. Barton, P. Thiery, E. Kiarie, *Bacillus subtilis* Strain DSM 29784 Modulates the Cecal Microbiome, Concentration of

16

180

405   Short-Chain Fatty Acids, and Apparent Retention of Dietary Components in Shaver

406   White Chickens during Grower, Developer, and Laying Phases, Appl. Environ.

407   Microbiol. 85 (2019). https://doi.org/10.1128/AEM.00402-19.

408   [8] Y. Wang, C. Heng, X. Zhou, G. Cao, L. Jiang, J. Wang, K. Li, D. Wang, X. Zhan,

409   Supplemental *Bacillus subtilis* DSM 29784 and enzymes, alone or in combination, as

410   alternatives for antibiotics to improve growth performance, digestive enzyme activity,

411   anti-oxidative status, immune response and the intestinal barrier of broiler chickens, Br.

412   J. Nutr. 125 (2021) 494–507. https://doi.org/10.1017/S0007114520002755.

413   [9] V. Jacquier, A. Nelson, M. Jlali, L. Rhayat, K.S. Brinch, E. Devillard, *Bacillus subtilis*

414   29784 induces a shift in broiler gut microbiome toward butyrate-producing bacteria and

415   improves intestinal histomorphology and animal performance, Poult. Sci 98 (2019)

416   2548–2554. https://doi.org/10.3382/ps/pey602.

417   [10] D. Stanley, M.S. Geier, R.J. Hughes, S.E. Denman, R.J. Moore, Highly Variable

418   Microbiota Development in the Chicken Gastrointestinal Tract, PLoS One 8 (2013)

419   e84290. https://doi.org/10.1371/journal.pone.0084290.

420   [11] Q. Hou, L.-Y. Kwok, Y. Zheng, L. Wang, Z. Guo, J. Zhang, W. Huang, Y. Wang, L.

421   Leng, H. Li, H. Zhang, Differential fecal microbiota are retained in broiler chicken lines

422   divergently selected for fatness traits, Sci. Rep. 6 (2016) 37376.

423   https://doi.org/10.1038/srep37376.

424   [12] J. Fernandes, W. Su, S. Rahat-Rozenbloom, T.M.S. Wolever, E.M. Comelli, Adiposity,

425   gut microbiota and faecal short chain fatty acids are linked in adult humans, Nut.

426   Diabetes 4 (2014) e121. https://doi.org/10.1038/nutd.2014.23.

427   [13] R.S. Breed, W.D. Dotterrer, The Number of Colonies Allowable on Satisfactory Agar

428   Plates, J. Bacteriol. 1 (1916) 321–331. https://doi.org/10.1128/jb.1.3.321-331.1916.

429   [14] European Commission, Animal Feeding Stuffs - Isolation And Enumeration Of

430   Presumptive Bacillus Spp: EN 15784, 2009.

431   [15] C. Chiron, T.A. Tompkins, P. Burguière, Flow cytometry: a versatile technology for

432   specific quantification and viability assessment of micro-organisms in multistrain

17

433   probiotic products, J. Appl. Microbiol. 124 (2018) 572–584.

434   https://doi.org/10.1111/jam.13666.

435   [16] V.A. Sattler, M. Mohnl, V. Klose, Development of a strain-specific real-time PCR assay

436   for enumeration of a probiotic Lactobacillus reuteri in chicken feed and intestine, PLoS

437   One 9 (2014) e90208. https://doi.org/10.1371/journal.pone.0090208.

438   [17] J. Gorsuch, D. LeSaint, J. VanderKelen, D. Buckman, C.L. Kitts, A comparison of

439   methods for enumerating bacteria in direct fed microbials for animal feed, J. Microbiol.

440   Methods 160 (2019) 124–129. https://doi.org/10.1016/j.mimet.2019.04.003.

441   [18] S. Kruse, F. Pierre, G. Morlock, Imaging high-performance thin-layer chromatography

442   as powerful tool to visualize metabolite profiles of eight Bacillus candidates upon

443   cultivation and growth behavior, J. Chromatogr. A 1640 (2021) 461929.

444   https://doi.org/10.1016/j.chroma.2021.461929.

445   [19] S. Kruse, F. Pierre, G.E. Morlock, Effects of the Probiotic Activity of Bacillus subtilis

446   DSM 29784 in Cultures and Feeding Stuff, J. Agric. Food Chem. 69 (2021) 11272–

447   11281. https://doi.org/10.1021/acs.jafc.1c04811.

448   [20] S. Kruse, M. Schenk, F. Pierre, G.E. Morlock, *Bacillus subtilis* spores in probiotic feed

449   quantified via bacterial metabolite using planar chromatography, In submission 2022.

450   [21] European Committee for Standardization, Water Quality - Determination of the

451   Inhibitory Effect of Water Samples on the Light Emission of Vibrio Fischeri

452   (Luminescent Bacteria Test): Part 1: Method Using Freshly Prepared Bacteria, 2007.

453   [22] T.T. Häbe, G.E. Morlock, Open-source add-on kit for automation of zone elution in

454   planar chromatography, RCM 34 (2020) e8631. https://doi.org/10.1002/rcm.8631.

455   [23] A. Mehl, W. Schwack, G.E. Morlock, On-surface autosampling for liquid

456   chromatography-mass spectrometry, J. Chromatogr. A 1651 (2021) 462334.

457   https://doi.org/10.1016/j.chroma.2021.462334.

458   [24] T. Schreiner, N.M. Eggerstorfer, G.E. Morlock, Effects of gastrointestinal digestion on

459   the bioactivity of convenience tomato products examined by ten-dimensional

460   hyphenation, In submission 2022.

18

182

183

461   [25] S. Kruse, S. Becker, F. Pierre, G.E. Morlock, Metabolic profiling of bacterial co-cultures

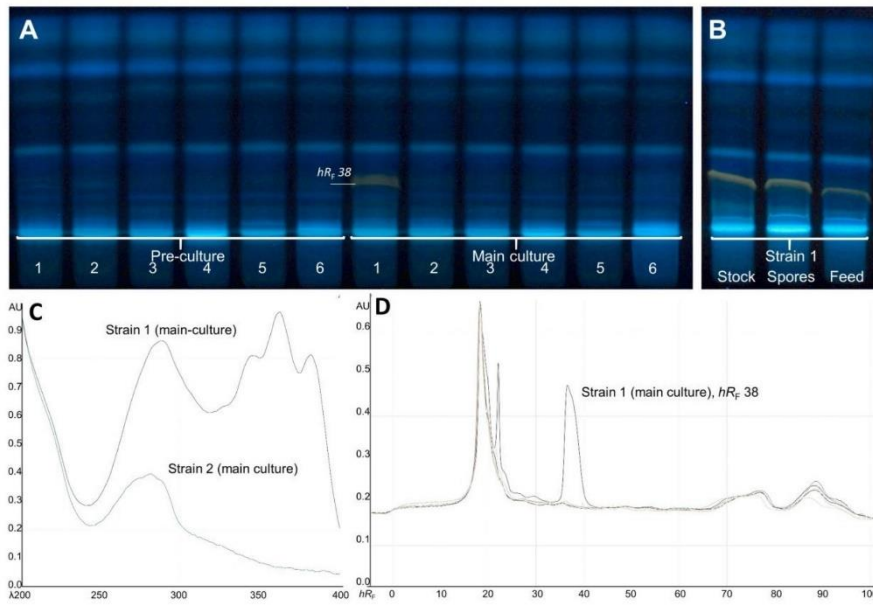462   with link to the dominant species identification, In submission 2022.

463

19

Figure legends

Figure 1 Specificity of the developed method: the metabolite at hR_F 38 was specific for the probiotic strain 1, as evident in the HPTLC chromatogram at FLD 366 nm of *n*-butanol extracts of *Bacillus* strains 1–6 in the pre-culture and main culture (A) and strain 1 cultivated as stock solution, dried spores and feed containing the spores (B), 100 μL/area each, separated on HPTLC silica gel 60 plates with acetonitrile – ethyl acetate – acetone 2:1:1 (*V/V/V*). UV spectra (C, 200–400 nm) recorded at hR_F 38 of strain 1 in the main culture, in comparison to strain 2, and overlaid UV-absorbance densitograms of all 6 strains at 366 nm (D), showing clearly the specificity of strain 1.

Figure 2 Assignment of the strain-specific metabolite: HPTLC−HPLC−DAD−HESI-HRMS chromatogram of the four peaks eluting from the strain-specific metabolite zone at hR_F 38 on the HPTLC plate (A), HPTLC–UV absorbance spectra (200–400 nm) at hR_F 38 in strain 1, in comparison to strain 2 (B), and HPLC-DAD spectra of the four peaks 1–4 (C), assigning peak 4 to the strain-specific metabolite zone.

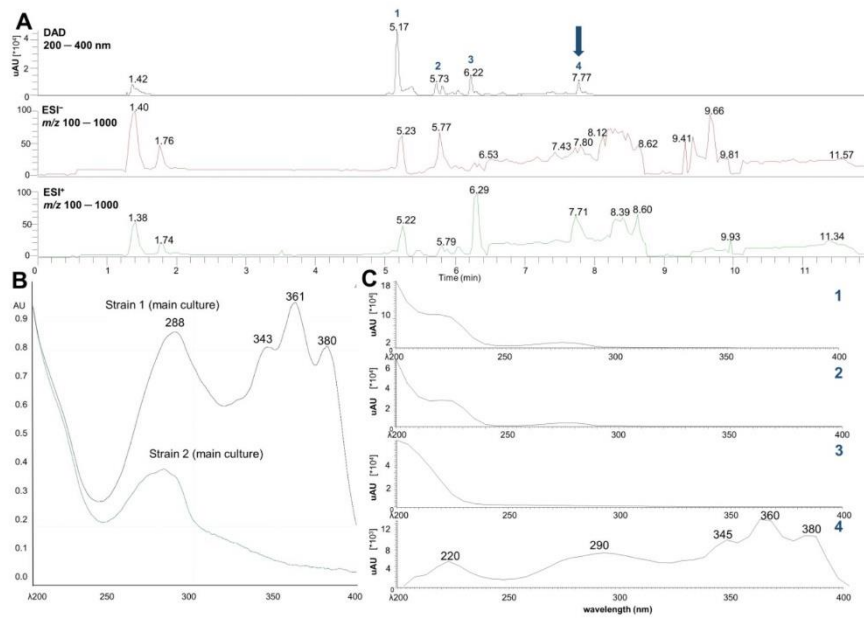**Figure 3** Tentative assignment of the molecular formula: HPTLC−HPLC−DAD−HESI-HRMS mass spectra in the positive and negative ionization mode of the strain-specific molecule with a neutral mass of 580.3527 Da (A) and respective MS/MS mass spectra providing fragments for confirmation (B).

Figure 4 Linearity of the developed method: HPTLC–FLD chromatogram at 366 nm of *n*-butanol extracts of blank, feed and upstream cultivated spore standard solutions S1–S4, corresponding to 5–110 pg of dried spores in culture (A, white mark: strain-specific metabolite zone) and respective overlaid UV-absorbance densitograms at 366 nm (B, region of interest) as well as linear regression based on the strain-specific metabolite response (C).
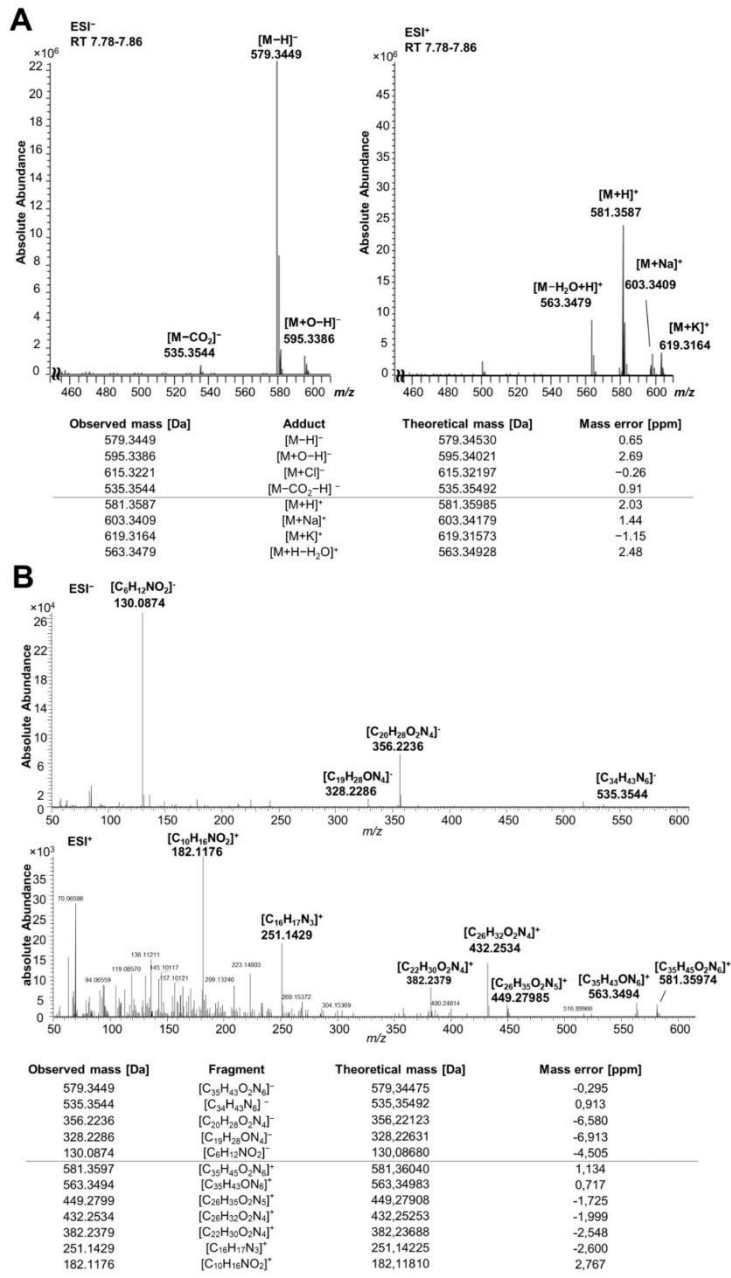
20

184

185

487

488 **Figure 1**

21

489

Figure 2

A

Observed mass [Da]	Adduct	Theoretical mass [Da]	Mass error [ppm]
579.3449	[M−H]⁻	579.34530	0.65
595.3386	[M+O−H]⁻	595.34021	2.69
615.3221	[M+Cl]⁻	615.32197	−0.26
535.3544	[M−CO₂−H]⁻	535.35492	0.91
581.3587	[M+H]⁺	581.35985	2.03
603.3409	[M+Na]⁺	603.34179	1.44
619.3164	[M+K]⁺	619.31573	−1.15
563.3479	[M+H−H₂O]⁺	563.34928	2.48

B

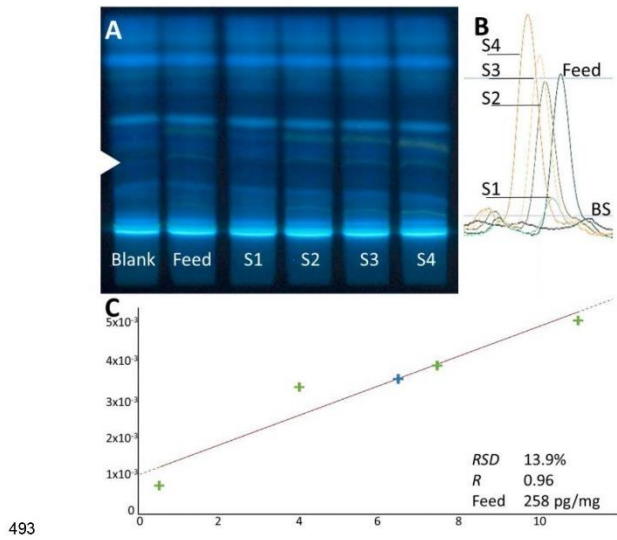| Observed mass [Da]	Fragment	Theoretical mass [Da]	Mass error [ppm]
579.3449	[C₃₅H₄₃O₂N₆]⁻	579,34475	-0,295
535.3544	[C₃₄H₄₃N₆]⁻	535,35492	0,913
356.2236	[C₂₀H₂₈O₂N₄]⁻	356,22123	-6,580
328.2286	[C₁₉H₂₈ON₄]⁻	328,22631	-6,913
130.0874	[C₆H₁₂NO₂]⁻	130,08680	-4,505
581.3597	[C₃₅H₄₅O₂N₆]⁺	581,36040	1,134
563.3494	[C₃₅H₄₃ON₆]⁺	563,34983	0,717
449.2799	[C₂₆H₃₅O₂N₅]⁺	449,27908	-1,725
432.2534	[C₂₆H₃₂O₂N₄]⁺	432,25253	-1,999
382.2379	[C₂₂H₃₀O₂N₄]⁺	382,23688	-2,548
251.1429	[C₁₆H₁₇N₃]⁺	251,14225	-2,600
182.1176	[C₁₀H₁₆NO₂]⁺	182,11810	2,767

491

492 **Figure 3**

23

187

493

494   **Figure 4**

Supplementary information

Strain-specific quantification of probiotic *Bacillus subtilis* DSM 29784 in feed by imaging high-performance thin-layer chromatography

Stefanie Kruse[a], Mareike Schenk[a], Francis Pierre[b], Gertrud E. Morlock[a,*]

[a]Institute of Nutritional Science, Chair of Food Science, and Interdisciplinary Research Centre for Biosystems, Land Use and Nutrition, Justus Liebig University Giessen, Heinrich-Buff-Ring 26-32, 35392 Giessen, Germany

[b]Adisseo France S.A.S, Immeuble Anthony Parc 2, 10 Place du Général de Gaulle, 92160 Antony, France

*Corresponding author: Prof. Dr. Gertrud Morlock, phone: +49-641-9939141; fax +49-641-99-39149, email: gertrud.morlock@uni-giessen.de

Table of Content

Table S1 Optimization of the cultivation process. The spore concentration and the cultivation time (second cultivation step) were optimized to achieve a linear working range.

Optimization	1	2	3	4	5	6	7	8
Cultivation step 1 (in 30 mL TSBY)								
Dilution standard stock solution	$1:10^8$							
Standard added to culture [mL] S1 S2 S3 S4	0.5 1.0 2.0 3.0	0.5 1.0 2.0 3.0	0.6 1.2 1.8 2.4	0.2 0.8 1.4 2.0	0.2 0.8 1.4 2.0	0.5 1.0 2.0 3.0	0.2 0.9 1.6 2.3	0.1 0.8 1.5 2.2
Dilution sample	1:10							
Sample added to culture [mL]	1.0	1.0	1.0	0.5	0.5	1.0	0.5	0.5
Incubation	4.5 h at room temperature and 175 rpm 11.5 h at 37 °C and 175 rpm							
Cultivation step 2 (in 20 mL TSBY)								
Volume pre-culture	1.5 mL							
Incubation	at 37 °C and 175 rpm							
Cultivation time [h]	5.5	4.5	4.5	4.5	3.5	3.5	3.5	4.0

Table S2 Template for the preparation of cultures for the different performance experiments.

	Culture		Standard Solution	Sample (feed) Solution	Feed Matrix	Autoclaved Bidistilled Water	TSBY
	Preparation		50 mg suspended (10 mL PBS), diluted 1:10^8	50 mg suspended (10 mL PBS) diluted 1:10	50 mg suspended (10 mL PBS) diluted 1:10		
A	Selectivity	S1 Matrix	0.1 mL (3x) -	-	- 0.5 mL (3x)	2.9 mL 2.5 mL-	30 mL
B	Linearity, working, range, LOQ	S1 S2 S3 S4	0.1 mL 0.8 mL 1.5 mL 2.2 mL		-	2.9 mL 2.2 mL 1.5 mL 0.8 mL	30 mL
C	Recovery	S2 Matrix	0.8 mL (1x) 0.8 mL (5x)	-	- 0.5 mL (5x)	2.2 mL 1.7 mL	30 mL
D	Feed analysis	Feed	-	0.5 mL		2.5 mL	30 mL

193

Table S3 Calculation of the S/N ratio.

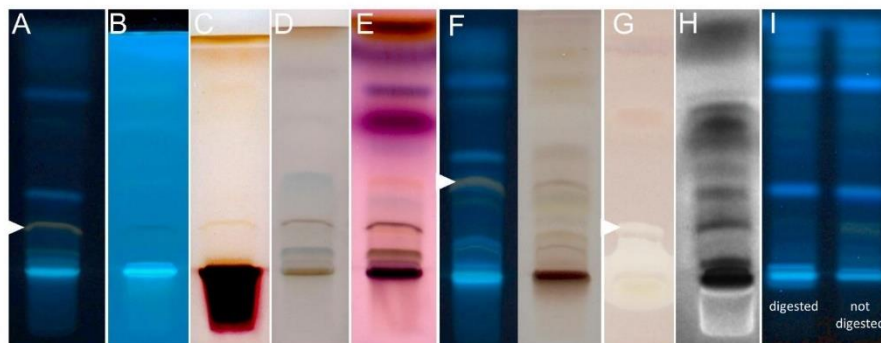|	
$R_{F\ End} - R_{F\ Start}$ feed matrix	0.053
$R_{F\ End} - R_{F\ Start}$ S1	0.053
Area blank sample [AU]	0.00005
Area S1 [AU]	0.00075
S/N	**15**

Figure S1 Characterization of the metabolite at *hR*_F *38* marked (A, FLD 366 nm) in strain 1 (100 µL *n*-butanol extract) separated on HPTLC plate silica gel 60 with acetonitrile – ethyl acetate – acetone 2:1:1, *V*/*V*/*V*: detection of lipophilic substances (B, primuline reagent, FLD 366 nm), amines and amino acids (C, ninhydrin reagent, Vis), saccharides (D, diphenylamine aniline phosphoric acid reagent, Vis), organic compounds (E, anisaldehyde sulfuric acid reagent, Vis; F, methanolic sulfuric acid, Vis; native FLD 366 nm image in comparison; located at a higher *hR*_F due to different plate activity) as well as antimicrobial substances against Gram-positive (G, *B. subtilis* bioassay, Vis) and Gram-negative bacteria (H, *A. fischeri* bioassay, luminescence), and the digestion by pancreatin (I, compared to the undigested extract, FLD 366 nm).
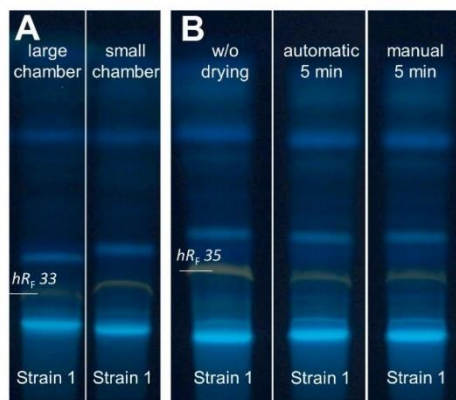
195

Figure S2 Influence of the metabolite volatility on the signal intensity: HPTLC−FLD chromatograms at 366 nm of *n*-butanol extracts of strain 1 (100 μL each) after the two step cultivation, separated with acetonitrile – ethyl acetate – acetone (2:1:1, *V/V/V*) in a small *versus* large developing chamber (A) and by using different drying processes (B) to indicate the influence on the marked metabolite.
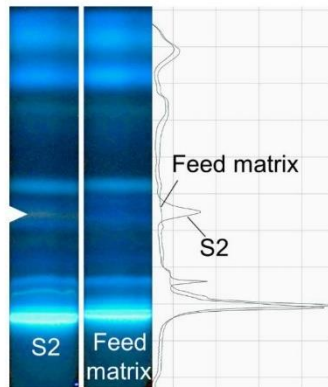
Figure S3 Method performance − selectivity: HPTLC−FLD chromatograms at 366 nm of the spore standard solution S2 and the feed matrix as well as both absorbance densitograms measured at 366 nm.

8. Summary

In animal production, AGP were used for several decades to improve animal growth and FCRs as well as to reduce morbidity and mortality of the animals. However, in 2006, the European Union banned the use of several AGPs due to the increased antibiotic resistance of infectious human pathogens. Probiotics seem to be an effective alternative to replace growth-promoting agents but up to now their mode of action is not fully understood. Imaging HPTLC with upstream cultivation proved to be an excellent method to characterize the metabolic profiles of the probiotic *B. s.* 29784, compared to those of genetically similar bacteria. Due to the various detection capabilities, the method enabled a better understanding of the probiotic effect. Special characteristics in the metabolic profile of the probiotic, such as the production of bioactive or antimicrobial metabolites, were described and a target metabolite, such as the lipopeptide surfactin, was identified. In the animal gut, the probiotic bacteria interacts with several other bacteria that could affect the metabolic profile of probiotics. Imaging HPTLC with upstream cultivation of bacteria in a co-culture proved the influence of this interaction by inoculation of *E. coli* (common pathogen) together with the probiotic. The results explain the sometimes contradictory observations of different probiotics in industrial use and the need for controlled conditions for the application of probiotics. In industrial quality control, cell counting is the most common method to determine the cell number of probiotics in feed. However, the results only describe the number of CFU/kg in the feed and do not determine the amount of probiotic spores. In the last decades, scientists in the field of probiotic research assumed that specific metabolites of the probiotic are responsible for the positive effect. Based on imaging HPTLC, a new method was developed to quantify spores of the probiotic in feed based on a non-specific metabolite. The validation of this method showed excellent results. Thus, imaging HPTLC offers the possibility of precise and accurate quantification of spores in feeds. Furthermore, in the probiotic *B. s.* 29784 a specific metabolite was detected (tested against high genetically similar bacteria) under the analyzed cultivation condition. For specific quantification of the probiotic in feed, the new developed and validated HPTLC method was adapted to this metabolite. In conclusion imaging HPTLC can be used to characterize bacterial metabolic profiles, such as probiotics, monitor bacterial interactions, and quantify the amount of probiotic spores in feed.

Summary

9. Zusammenfassung

In der Tierproduktion werden seit Jahrzehnten antibiotische Wachstumsförderer eingesetzt, um das Wachstum der Tiere als auch deren Futterverwertung zu verbessern und die Morbidität sowie Mortalität der Tiere zu verringern. Aufgrund der zunehmenden Antibiotikaresistenz von Humanpathogenen, wurde der Einsatz dieser Wachstumsförderer 2006 in der Europäischen Union verboten. Im Laufe der Zeit erwiesen sich Probiotika als eine hervorragende Alternative, doch bis heute sind ihre genauen Wirkmechanismen noch nicht vollständig geklärt. Die bildgebende HPTLC mit vorgeschalteter Kultivierung erwies sich als eine hervorragende Methode, um die Stoffwechselprofile handelsüblicher Probiotika mit denen von genetisch sehr ähnlichen Bakterien zu vergleichen. Die Methode ermöglichte durch die vielseitigen Detektionsmöglichkeiten ein besseres Verständnis potentieller probiotischer Wirkungen. Besondere Merkmale im Stoffwechselprofil des Probiotikums, wie die Produktion von bioaktiven oder antimikrobiellen Metaboliten, wurden detektiert und Zielmetabolite, wie das Lipopeptid Surfactin, konnten identifiziert werden. Im Darm der Tiere interagieren Probiotika mit verschiedenen Bakterien, wodurch ihr Stoffwechselprofil beeinflusst werden könnte. Mit Hilfe der bildgebenden HPTLC und einer vorgelagerten Kultivierung von Bakterien in einer Ko-Kultur, konnte der Einfluss der Interaktion von *E. coli* (häufiger Erreger) mit dem Probiotikum auf das metabolische Profil gezeigt werden. Diese Ergebnisse erklären die zum Teil konträren Beobachtungen verschiedener Probiotika im industriellen Einsatz und die Notwendigkeit kontrollierter Anwendungsbedingungen.

In der industriellen Qualitätskontrolle wird die Zellzählung als gängigste Methode zur Bestimmung der Zellzahl der Probiotika in Futtermitteln verwendet. Die Ergebnisse beschreiben jdeoch nur die Anzahl der koloniebildenden Einheiten (KBE/kg) im Futter und bestimmen nicht die Menge an vorhandenden probiotisch Sporen. Seit dem letzten Jahrzehnt gehen Wissenschaftler auf dem Gebiet der Probiotikaforschung davon aus, dass spezifische Metaboliten der verwendeten Mikrooganismen für die probiotische Wirkung verantwortlich sind. Auf Grundlage der bildgebenden HPTLC wurde eine Methode zur Quantifizierung der probiotischen Sporen im Futtermittel anhand eines unspezifischen Metaboliten entwickelt. Die Validierung dieser Methode zeigte exzellente Ergebnisse. Somit bietet die bildgebende HPTLC die Möglichkeit einer präzisen und genauen

Zusammenfassung

Quantifizierung von Sporen in Futtermitteln. Bei Verwendung bestimmter Kultivierungsbedingungen konnte in dem Probiotikum *B. s.* 29784 (getestet gegen genetisch sehr ähnliche Bakterien) ein spezifischer Metabolit nachgewiesen werden. Zur spezifischen Quantifizierung des Probiotikums in Futtermitteln wurde die neu entwickelte und validierte HPTLC-Methode an diesen Metaboliten angepasst. Zusammenfassend lässt sich sagen, dass die bildgebende HPTLC zur Charakterisierung bakterieller Stoffwechselprofile, von z. B. Probiotika, zur Überwachung bakterieller Interaktionen und zur Quantifizierung probiotischer Sporen im Futtermittel verwendet werden kann.